

BEYOND THE STANDARD MODEL: DARK MESONS AND CUSTODIAL
SYMMETRY

by

TOM TONG

A DISSERTATION

Presented to the Department of Physics
and the Graduate School of the University of Oregon
in partial fulfillment of the requirements
for the degree of
Doctor of Philosophy

June 2020

DISSERTATION APPROVAL PAGE

Student: Tom Tong

Title: Beyond the Standard Model: Dark Mesons and Custodial Symmetry

This dissertation has been accepted and approved in partial fulfillment of the requirements for the Doctor of Philosophy degree in the Department of Physics by:

Dr. Timothy Cohen	Chair
Dr. Graham D. Kribs	Advisor
Dr. Laura Jeanty	Core Member
Dr. Boris Botvinnik	Institutional Representative

and

Dr. Kate Mondloch	Interim Vice Provost and Dean of the Graduate School
-------------------	---

Original approval signatures are on file with the University of Oregon Graduate School.

Degree awarded June 2020

© 2020 Tom Tong
All rights reserved.

DISSERTATION ABSTRACT

Tom Tong

Doctor of Philosophy

Department of Physics

June 2020

Title: Beyond the Standard Model: Dark Mesons and Custodial Symmetry

We describe our investigations on possible new physics beyond the Standard Model that reveal their connections with custodial symmetry.

First, we consider several strongly-coupled dark sectors with fermions that transform under the electroweak group. We construct the non-linear sigma model describing the dark pions and match the ultraviolet theory onto a low energy effective theory that provides the leading interactions of the lightest dark pions with the Standard Model. We uncover two distinct classes of effective theories: “Gaugephilic” and “Gaugephobic”.

Second, we demonstrate such a dark sector could be accessible to current searches by studying the production and decay of dark mesons at the LHC. Dark pions can be pair-produced and decay in one of two distinct ways: “gaugephilic” or “gaugephobic”. We recast a vast set of existing LHC searches to determine the current constraints on the dark meson. We find the relative insensitivity of LHC searches, especially at 13 TeV, can be blamed mainly on their penchant for high mass objects or large missing energy. Future dedicated searches would undoubtedly improve sensitivity.

Finally, we consider custodially-symmetric UV physics, mapping their effects onto higher-dimensional operators in a custodial basis. This basis explicitly identifies the global $SU(2)_R$ symmetries of the Higgs and flavor sector with custodial preserving and violating operators. Custodially symmetric UV physics that contributes purely to oblique corrections at leading matching order leads to the electroweak observable $\rho = 1$ at tree-level. Nevertheless, such UV physics can also generate non-oblique corrections, and thus $\rho \neq 1$ is insufficient to claim custodial violation. We therefore identify a set of observables that are able to capture the leading tree-level effects of integrating out a custodially-symmetric UV sector. We illustrate our results with four examples: a heavy singlet scalar; a heavy Z' transforming under $U(1)_{B-L}$; heavy W' 's and Z' 's transforming under $SU(2)_L \times SU(2)_R \times U(1)_{B-L}$; and a heavy W'_L coupling purely to left-handed fields. These examples demonstrate that our observables could be used to “fingerprint” custodial symmetry of UV physics.

This dissertation consists of previously published and unpublished co-authored material.

CURRICULUM VITAE

NAME OF AUTHOR: Tom Tong

GRADUATE AND UNDERGRADUATE SCHOOLS ATTENDED:

University of Oregon, Eugene, Oregon, USA
Ball State University, Muncie, Indiana, USA

DEGREES AWARDED:

Doctor of Philosophy in Physics, 2020, University of Oregon
Master of Arts in Mathematics, 2014, Ball State University
Bachelor of Science in Physics, 2012, Ball State University

AREAS OF SPECIAL INTEREST:

Particle Physics
Cosmology
Astrophysics

PROFESSIONAL EXPERIENCE:

Graduate Research Assistant, University of Oregon, 2016-2020
Graduate Employee, University of Oregon, 2014-2019

GRANTS, AWARDS AND HONORS:

UO Dissertation Research Fellowship, University of Oregon, 2019
Graduate Qualifying Exam Award, University of Oregon, 2015
Outstanding Graduate Assistant, Ball State University, 2014

PUBLICATIONS:

G. Kribs, A. Martin, X. Lu, T. Tong, “Fingerprints of UV symmetries utilizing a custodial basis of SMEFT”, In preparation.

G. Kribs, A. Martin, T. Tong, “Dark mesons at the LHC”, JHEP, 07:133, 2019, arXiv: 1809.10184.

G. Kribs, A. Martin, T. Tong, “Effective theories of dark mesons with custodial symmetry”, JHEP, 08:020, 2019, arXiv: 1809.10183.

ACKNOWLEDGEMENTS

I am deeply indebted to the following people for my PhD experience, and for the joy of life with which I shall remember.

For her unlimited love and support, my mother, Yuqi Lu;

for planting the seed of curiosity about the world and nature, my father, Weigang Tong;

for her unwavering understanding and unbreakable trust in me, and a bond that is eternal, my wife, Yvonne Bao;

for his especially generous help paving my way to graduate school, Hanspeter Fischer;

for an uncountable set of enlightenment and for helping me grow better both as a physicist and a person, Timothy Cohen;

for readily extending his guidance and collaboration in my research, Adam Martin;

for lending me all the wisdom of knowledge and benefit of experience, Bryan Ostdiek;

for a pedagogical education from a living textbook that was always hot and ready whenever I need it, Xiaochuan Lu;

for conversations of indelible lessons and inspiration, Spencer Chang;

for all the warm encouragement in those times I feel cold, Tien-tien Yu;

for wondrous courses and discussions that shed a light penetrating the impenetrable, James Isenberg;

for a creative and eye-opening course in phenomenology, Stephanie Majewski;

for impressing in me what does it mean by practicing experiment, Laura Jeanty;

for entertaining and instructive discussions, Dave Soper, Nilendra Deshpande, Ben Farr, Marat Freytsis, Dietrich Belitz, John Toner and my fellow Oregon physics students;

for educative experiences and lots of fun, Paddy Fox, Roni Harnik, Bogdan Dobrescu, David Curtin;

for irreplaceable guidance on my writing of this dissertation, Nirmal Raj;

for revealing the meaning of life to me once more, Nima Arkani-Hamed;

and Graham Kribs, for all of the above added together, and a torch illuminating the path that extends to infinity.

TABLE OF CONTENTS

Chapter	Page
I. INTRODUCTION	1
Effective theories of dark mesons	3
Collider phenomenology of dark mesons	6
SMEFT with custodial symmetry	10
Outline	15
II. EFFECTIVE THEORIES OF DARK MESONS	16
Defining the dark sector	16
Custodial SU(2)	18
Effective Interactions of Dark Pions	22
Dark Pion Triplet interactions in custodial preserving strong sectors	22
Two-Higgs Doublet Models	25
Neutral Dark Pion Decay to Diphotons	26
Two-flavor theories	27
Two-flavor chiral theory	28
Two-flavor vector-like theories	33
Four-flavor theories	37
Mixing with the Higgs and Goldstones	43
Dark Pion Couplings to the SM	44
Dark Sector Custodial Violation	46

Chapter	Page
III.LHC PHENOMENOLOGY OF DARK MESONS	49
Phenomenological Description of Dark Mesons	49
Dark Mesons in $SU(2)$ Triplet Representations	50
Kinetic Mixing of ρ_D with SM	51
Dark Pion Decay to SM	54
Constraints from single production	59
ρ_D constraints	61
Constraints on the dark pion coupling to SM	65
Resonant Dark Pion Pair-Production at LHC	68
Searching for taus	71
Generic multilepton searches	74
Same sign lepton searches	78
Additional searches	83
IV.SMEFT WITH CUSTODIAL SYMMETRY	87
$SU(2)$ Symmetries of the Standard Model	87
The Custodial Basis	89
Notation and Definitions	89
The Custodial Basis of (ν) SMEFT Operators	91
Recovering SMEFT from ν SMEFT	95
Flavor Indices of the Wilson Coefficients	95
Observables of Custodial Symmetry in (ν) SMEFT	96
Observables in the SM	97
Observables in the SMEFT	98

Chapter	Page
Observables in the Custodial Basis	100
EOM Redundancies	102
Implications of EOM Redundancies for our Observables	104
Observables of UV Theories with Custodial Symmetry	106
Singlet scalar extension	107
Z' associated with a $U(1)_{B-L}$ symmetry	108
Heavy W 's and Z 's from a UV theory with $SU(2)_L \times$ $SU(2)_R \times U(1)_{B-L}$	110
A Heavy W'_L Gauge Boson	116
Custodial Symmetry vis-a-vis Flavor Symmetry	121
Experimental Measurements of our Observables	122
Tables of Operators, Coefficients, and Translations	124
V. CONCLUSIONS	130
Effective Theories of Dark Mesons	130
LHC Phenomenology of Dark Mesons	132
SMEFT with Custodial Symmetry	134
APPENDICES	
A. EFFECTIVE THEORIES OF DARK MESON	139
Gaugephobic 2HDMs	139
B. SMEFT WITH CUSTODIAL SYMMETRY	145
Details of Mapping onto Observables	145
Hadronic Observables	150

Chapter	Page
Tree-level Dim-6 Operators	153
EOM Equivalence Example	156
ν SM Predictions	158
Correction in Warsaw Basis	159
Correction in the Alternative Basis	160

LIST OF FIGURES

Figure	Page
<p>1. The left panel shows the production cross section at $\sqrt{s} = 13$ TeV for the dark vector mesons. The blue and orange lines depict whether the vector mesons are $SU(2)_L$ or $SU(2)_R$ symmetric and kinetically mix with the appropriate standard model gauge bosons. The middle and right panels show the subsequent branching ratio for the ρ_D depending on whether or not it can decay to the π_D. The red lines denote decays to quark anti-quark pairs, and the dashed line indicates the top quark. The purple lines show leptonic decays.</p>	53
<p>2. Branching ratios of the charged pions</p>	57
<p>3. Branching ratios of the neutral pions</p>	58
<p>4. Constraints on the kinetic mixing between the the SM and ρ_D^0 (times the leptonic branching fraction of ρ_D^0) from the non-observation of a dilepton resonance near m_{ρ_D}. The black line is the model-independent limit. To illustrate the impact of this bound on the model space, we have superimposed the predicted $\epsilon^2 \times \text{BR}(\rho_D^0 \rightarrow \ell^+ \ell^-)$ for the $SU(2)_L$ model, varying the number of colors between 2 to 16. On the right, the 2-body decay $\rho_D^0 \rightarrow \pi_d^+ \pi_d^-$ is kinematically forbidden, leading to strong constraints: $m_{\rho_D} > 1.5\text{-}2.5$ TeV. On the left, the 2-body decay $\rho_D^0 \rightarrow \pi_d^+ \pi_d^-$ is open, and we see that when $N_D \lesssim 4$, there is no constraint from resonant ρ_D^0 production and decay to dileptons.</p>	63
<p>5. Constraints on the value of $1/v_\pi$ as a function of the dark pion mass. Precise measurements of the top quark exclude regions above the red line. The green, blue, and orange lines come from collider searches for heavy Higgs particles (mainly in 2HDM). Lastly, the brown and pink dashed lines are not constraints, but show at what point the phenomenology changes. Below these lines, the pions start to travel an appreciable distance in the detector, either leading to displaced vertices or disappearing tracks. The lower of these lines are around the scale when the particles leave the detector either as missing energy or look like stable charged particles.</p>	66

Figure	Page
6. Summary of the dark meson exclusions for the benchmark scenarios and values of the π_D and ρ_D masses. The scenarios are labeled by the type of kinetic mixing, the ratio of the dark pion to dark rho mass $\eta = m_{\pi_D}/m_{\rho_D}$, and the relative strength of the fermionic versus bosonic dark pion decay modes. All of the dark pions decay promptly. The top line indicates the bound on ρ_D^0 inferred from recasting the latest dilepton bounds and interpreted in terms of m_{π_D} . The next five lines (in black) show the π_D mass bound from the most constraining 8 and 13 TeV searches we could find. The union of the exclusions from all of the searches is shown in the last line.	70
7. Cut flow for the search for hadronically decaying taus, optimized for electroweak production of supersymmetric particles [1]. The efficiency is much larger for the $\eta = 0.25$ benchmarks than the $\eta = 0.45$ models because the larger ρ_D mass leads to more energetic π_D . This increase in efficiency is offset by the decrease in resonant production cross section.	73
8. Exclusions from the ATLAS search for supersymmetry in final states with tau leptons [1]. The dark mesons on the lighter side of our spectrum predominately decay to taus, and the cross sections are large. The $SU(2)_L$ type models are excluded if $m_{\pi_D} \lesssim 180$ GeV while the $SU(2)_R$ models limits are around 130 GeV. This is the only search which limits the $SU(2)_R$ models where the ρ_D can decay to $\pi_D\pi_D$	75
9. Expected signal cross section in two different signal regions of the ATLAS multilepton search [2] as a function of dark pion mass. . . .	76
10. Out of the 144 signal regions defined in Ref. [2], 16 regions constrain some portion of the dark meson parameter space. The mass ranges which are colored are excluded. The gaugephilic models have larger branching ratios to Zh and Wh than the gaugephobic models, which leads to greater search efficiency and larger bounds.	77

11. Out of the 192 signal regions defined in the CMS multilepton search [3], 8 regions constrain some part of the dark meson parameter space. The excluded mass ranges are colored according to the denoted signal region. The regions labeled SR3 and SR4 regions contain either 3 or 4 leptons, respectively. The L or H denotes whether the scalar sum of the p_T of the selected jets is less than 200 GeV or greater than 200 GeV. While there are different cuts concerning the number of b -jets or taus, all of the constraining regions require either $E_T^{\text{miss}} < 50$ GeV or $50 \text{ GeV} < E_T^{\text{miss}} \leq 100$ GeV. 79
12. Signal regions of ATLAS searches for three leptons or same sign leptons which have sensitivity to our benchmarks. The left panel shows the limits from the 8 TeV analysis [4] and the right panel has the limits for the 13 TeV analysis [5]. The 8 TeV analysis has bounds to the largest values of m_{π_D} for all of the 8 and 13 TeV analysis which we studied. The 13 TeV search does not do as well because the focus of the analysis shifted to search for higher mass objects. 81

LIST OF TABLES

Table	Page
1. Two-flavor fermion content of the chiral theory.	28
2. Two-flavor fermion content of $SU(2)_L$ and $SU(2)_R$ vector-like theories. . .	33
3. Four-flavor, custodially-symmetric dark sector fermion content.	38
4. Benchmark models and parameters used in our study. Note that the gaugephilic case only occurs for the $SU(2)_L$ model, as discussed in Sec. III in the text.	61
5. Phenomenological regions for collider signatures. The charged and neutral current columns show the SM particles for the dominant branching ratios.	69
6. Possible search strategies which seem like they should set bounds, but have limited-to-no sensitivity.	84
7. Recovering SMEFT from ν SMEFT: the left (right) column shows the constraints on the Wilson coefficients in Warsaw (custodial) basis.	95
8. Custodial invariants outside of Warsaw basis that yield custodial violating operators in Warsaw basis upon using H and ψ EOM redundancies.	105
9. Fermion charges Y_Z under the Z' gauge interaction.	109
.1. ν SMEFT dim-6 baryon-preserving operators in Warsaw basis. In addition to the $76 = 42 + (17 + \text{h.c.})$ SMEFT operators, there are $25 = 7 + (9 + \text{h.c.})$ new operators involving right-handed neutrinos ν , which are colored in brown.	125

Table	Page
.2. ν SMEFT dim-6 baryon-preserving operators in our custodial basis. Operators are colored black (custodial preserving), blue (custodial violating), red (quark isospin violating), or green (lepton isospin violating). For example, O^+ is custodial preserving while O^- is custodial violating, since the former involves P_+ while the latter involves P_- . The notation O^{-} implies the operator violates both quark and lepton isospin. See text for details.	126
.3. A dictionary of the custodial basis in terms of Warsaw basis. The color scheme is the same as given in Table .1 and Table .2.	127
.4. A translation dictionary from the Warsaw basis Wilson Coefficients C_i to Custodial basis Wilson Coefficients a_i	128
.5. A translation dictionary from the Custodial basis Wilson Coefficients a_i to Warsaw basis Wilson Coefficients C_i	129

CHAPTER I

INTRODUCTION

The discovery of a Higgs-like boson at the Large Hadron Collider in 2012 is a profound milestone. As the final missing piece, it completed the Standard Model of particle physics and made it a reliable model to both explain and predict virtually all of the microscopic physical phenomena known to us. Nevertheless, the Standard Model cannot be the whole story. We list several well-established observational and experimental facts below as motivations for new physics beyond the Standard to attempt to explain the mysteries.

- Dark matter. There is vast evidence that roughly 80% of the matter content of the universe does not interact through electromagnetism, the strong force, or the weak force, hence dark matter. From the large scale structure formation of our universe, we believe dark matter is massive and “cold” in the sense that its primordial velocity dispersion is small. And from the fact that no evidence of dark matter decay has been observed so far, it must be stable on at least a cosmological timescale. According to these properties, the Standard Model provides us no particle candidate. (And while primordial black holes are a theoretical possibility, even this explanation is highly constrained [6].)
- Neutrino mass. Current measurements [7] assert that at least two neutrino species have non-zero masses. These results directly contradict the (conventional) definition of the Standard Model, which treat neutrinos as massless particles. Neutrino masses can be incorporated in a ν -extended Standard Model but this requires new interactions and/or fields that is an extension of the Standard Model.

There is also a mysterious matter-antimatter asymmetry. The fact that almost all of the baryonic content in our observable universe is matter instead of antimatter suggests that something distinguished baryons and antibaryons in the early universe. Long ago Sakharov recognized that mechanisms of baryogenesis require baryon number violation, C and CP violation, with interactions out of thermal equilibrium [8]. However, the size of the imbalance is several orders of magnitude larger when compared to the known sources of CP-violation in the Standard Model that could have possibly produced the asymmetry while still satisfying current experimental constraints [9]. Baryogenesis, therefore, may very likely require novel mechanisms from new physics beyond the Standard Model to provide an adequate explanation.

In addition to these evidences, the Standard Model also contains other theoretical puzzles within its own framework, such as the hierarchy problem and the strong-CP problem. Very often, the proposed solutions to these problems, such as supersymmetry and the axion, also involve new physics beyond the Standard Model.

Two primary methods are used in the search of BSM physics. One is to look for new particles. The other is to look for new or modified interactions of known particles.¹ Both methods have been utilized by our studies described in this dissertation, using effective field theory. Effective field theory is a common tool used in particle physics and other areas of physics. It is defined by particle content and symmetries with a cutoff scale; higher dimensional operators account for integrating out particles that are not able to be produced directly at low energies. By matching an ultraviolet full theory model onto an effective field theory description of the physical system of interest, it connects the ultraviolet theory to an infrared theory that only

¹These are not necessarily independent searches although they can probe different energy scales of new physics.

contains the degrees of freedom relevant to the infrared regime [10]. This is a trade-off between staying agnostic to the complete ultraviolet theory and having the theory we use being valid to arbitrarily high energy scales.

In this dissertation, we first implement an effective theory approach to consider beyond the Standard Model scenarios of strongly-coupled new physics that provides a novel explanation to dark matter. Then we explore the potential of a discovery of such dark mesons both at the current LHC experiments and in the near future. Finally, we treat the Standard Model itself as an effective theory (SMEFT), and then investigate the theoretical and phenomenological implications of matching UV theories that satisfy custodial symmetry within a new basis that we construct for this purpose: the custodial basis of ν SMEFT (SMEFT with right-handed neutrinos). To be specific, the definition of custodial symmetry in our study states that UV physics is said to be “custodial symmetric” when an $SU(2)_R$ global symmetry is preserved by all UV interactions with the Higgs sector of the SM.

Effective theories of dark mesons

The Chapter II of this dissertation describes our studies into the effective theories of dark mesons, particularly with those preserving custodial symmetry. We consider extensions of the Standard Model that incorporate a new, strongly-coupled, confining gauge theory with fermion representations that transform under the electroweak group. The notion of a new sector of fields transforming under a new, strongly-coupled, confining group is a fascinating possibility for physics beyond the Standard Model. All of the new sector’s scales are either natural (the new confinement scale) or technically natural (new fermion masses), and so such a scenario is, at a minimum, no worse off than the Standard Model in terms of naturalness.

From a theoretical point of view, there are a wide variety of uses of a new, strongly-coupled, confining group. One use is to at least partially break electroweak symmetry dynamically, such as bosonic technicolor [11, 12, 13, 14, 15, 16, 17, 18, 19] and the closely related ideas on strongly-coupled induced electroweak symmetry breaking [20, 21, 22, 23, 24, 25, 26, 27, 28, 29, 30]. Composite Higgs theories also posit a new strongly-coupled sector in which at least an entire Higgs doublet emerges in the low energy effective theory (the literature is far too vast to survey, for a review see e.g., [31]). There is also an interesting connection to the relaxation of the electroweak scale [32] using a new strongly-coupled sector, e.g., [32, 33, 29, 34, 30].

Another use is to simply characterize generic strongly-coupled-like signals as targets for LHC and future colliders. Vector-like confinement [35] pioneered this study in the context of vector-like fermions that transform under part of the SM group as well as under a new, strongly-coupled group with scales near or above the electroweak scale. Further explorations into the phenomenology and especially the meson sector included [36, 37, 38, 39, 40, 41, 42, 43, 44, 45, 30, 46]. In theories with somewhat lower confinement scales, the new sector may lead to invisible showers and related phenomena [47, 48, 49, 50, 51, 52, 53], displaced signals [54, 55] and potentially intriguing spectroscopy [56, 57, 58]. Spectacular “quirky” signals can arise in theories with a very low confinement scale [59, 60]. The latter theories may also lead to a high multiplicity of soft particles that are tricky to observe [61, 62, 63].

The difficulty with strongly-coupled physics is that it is strongly-coupled, implying the breakdown in perturbative calculation and the significance of non-perturbative effects. However, many years ago Kilic, Okui, and Sundrum pioneered the study of a new strongly-coupled sector’s phenomenology for collider physics [35]. Their insight was to determine the leading interactions of an effective theory of

pseudo-Nambu Goldstone (pNGB) mesons with vector mesons (both composite and fundamental). They were motivated by imagining QCD scaled up to weak scale energies, except, and here is the key point, their BSM fermion masses were taken to be purely vector-like. We generalize vector-like confinement by permitting specific interactions between the strong sector fermions and the Standard Model. In some models, these interactions are renormalizable Yukawa couplings of the dark sector fermions with the Higgs of the SM. In others that do not permit Yukawa couplings, we also consider higher dimensional operators (that also involve the Higgs sector in some way). These interactions lead to dark pion decay. And, what is distinct in the vector-like theories we consider is that there is no axial anomaly contribution to neutral dark pion decay. We use a non-linear sigma model (NLSM) to describe the pNGB mesons, which we carry out in detail. Equally important, the fact that we break the flavor symmetries of the strong sector with Higgs interactions necessarily locks the strong sector flavor symmetries to the $O(4) \cong SU(2)_L \times SU(2)_R$ global symmetry of the Higgs potential. As a result, the strong sector fields can be grouped into multiplets of this symmetry, with different assignments possessing qualitatively different phenomenology.

Needless to say, the biggest motivation for such a strongly-coupled theory is that dark matter can emerge as a composite meson or baryon, often with an automatic accidental symmetry that protects against its decay. Since the early days of technicolor there was a possibility of dark matter emerging as technibaryons [64, 65, 66, 67, 68, 69, 70]. There is now a growing literature that has studied strongly-coupled dark matter as dark pions [71, 72, 73, 74, 75, 76, 40, 77, 78, 79, 80, 81, 82, 83, 56, 84, 85, 86, 87], dark quarkonia-like states [88, 36, 89, 90], as well as dark baryons and related candidates [91, 92, 93, 71, 94, 36, 95, 96, 97, 75, 98, 99, 100, 101, 102, 78,

103, 104, 42, 105, 106, 107, 108, 109, 110, 111, 112, 113, 114, 115, 116] (for a review, see [117]).

Collider phenomenology of dark mesons

In Chapter III of this dissertation, we studied the collider phenomenology of the dark meson theories and its signatures for a potential discovery at the LHC. The dark sector model that is of particular interest to us is Stealth Dark Matter [106]. In this theory, there is a new, strongly-coupled “dark sector” that consists of vector-like fermions that transform under both the new “dark group” group as well as the electroweak part of the SM, and crucially, also permit Higgs interactions. Others have also pursued dark sectors with vector-like fermions that permit Higgs interactions for a variety of purposes [81, 33, 118, 115, 30].

One might think a dark meson sector whose low energy effective theory is a set of scalars with electroweak quantum numbers has already been fully (or mostly) covered by the wide range of existing search strategies. This is simply *not* the case. We find that a dark vector meson could be as light as about 300 GeV, something that, at first glance, seems hard to believe given the multi-TeV bounds on new Z' bosons from LHC data. The dark vector meson can mediate dark pion pair production (just like $\rho \rightarrow \pi\pi$ in QCD), and in some models, the bounds on the dark pion mass could be as small as 130 GeV. Clearly, the LHC easily has the energy to produce these states, and so it really comes down to finding search strategies that maximize sensitivity. We believe substantial improvements are possible, providing impetus and breathing new life into LHC searches in the hundreds of GeV regime.

The dark meson sector of the Stealth Dark Matter theory has several intriguing properties due to the accidental symmetries of the model. Like vector-like confinement

[35] the dark sector is free of constraints from precision electroweak observables and Higgs coupling measurements so long as the vector-like mass is dominant. Unlike vector-like confinement, however, the Higgs interactions break the global (species) symmetries of the dark sector, permitting dark pions to decay into SM states. Provided the vector-like masses are smaller than $\sim 4\pi f$, where f is the scale of the new strong interaction, we can organize the states using chiral perturbation theory. In this study we focus on the most phenomenologically relevant states: the (lightest) triplet of pseudoscalar pions π_D^a and the heavier triplet of vector mesons ρ_D^a [119]. The scales of the theory, as we will see, are comparable to or somewhat larger than the electroweak scale.

The presence of a $SU(2)$ dark flavor symmetry arises from global symmetries of the ultraviolet strongly-coupled sector. For example, a strongly-coupled sector that contains two flavors of dark fermions with identical (current) masses has a global $SU(2) \times SU(2)$ symmetry that is broken by the condensate to a $SU(2)$ dark flavor symmetry [120]. This is just like QCD with its two light flavors of quarks with nearly equal (current) masses. In Ref. [120], we demonstrate strongly-coupled theories where the $SU(2)$ dark flavor symmetry can be identified as an exact custodial symmetry of the dark sector. That is, the Higgs multiplet interacts with the dark flavors such that the $SO(3) \sim SU(2)_c$ is not further broken by the dark sector. Consequently, the dark sector's meson degrees of freedom can be categorized in custodial symmetric representations. Again considering the example of theories with two flavors of dark fermions, the meson sector contains dark pions and one set of dark vector mesons in a triplet representation of the $SU(2)$ dark flavor symmetry. Unlike QCD, however, the vector-like nature of the dark sector permits two possibilities for gauging the global flavor symmetry: the entire $SU(2)$ could be gauged (the $SU(2)_L$ weak interaction)

or just the $U(1)$ (as in $U(1)_B$ hypercharge).² This leads to two distinct low energy effective theories of dark mesons:

$$\begin{aligned} SU(2)_L \text{ model : } & \quad SU(2)_{\text{global flavor}} \leftrightarrow SU(2)_L \\ SU(2)_R \text{ model : } & \quad SU(2)_{\text{global flavor}} \leftrightarrow SU(2)_R \end{aligned} \tag{1.1}$$

In the latter case, obviously only the $U(1)$ subgroup is gauged, but since we assume the dark sector respects the full global $SU(2)$, we'll refer to this as the $SU(2)_R$ model.

In the meson sector the dark pion states can be pair-produced, either via Drell-Yan or resonantly via mixing of the ρ with SM electroweak gauge bosons. The dark pion decays can be categorized into two distinct possibilities: “gaugephobic”, when $\pi_D \rightarrow f\bar{f}$ dominates; or “gaugephilic”, when $\pi \rightarrow W + h, Z + h$ dominates once kinematically open. The decay $\pi_D^0 \rightarrow \gamma\gamma$ is highly suppressed due to the dark flavor symmetry [120]. For a wide range of parameters, the interaction between single dark pions and the SM is small enough to make single pion production phenomenologically irrelevant, and yet, the interaction can be easily large enough that the dark pions decay *promptly* back to SM states. We also briefly comment on the possibility that dark pions are sufficiently long-lived so as to modify their phenomenological signature.

Dark mesons are therefore an example of new physics that must be pair produced with \sim weak strength and decay back to multiple SM particles (only). The combination of a relatively low production cross section and complex final states with no BSM sources of missing energy can lead to weak LHC constraints. We perform a detailed breakdown of which LHC searches could potentially set bounds on dark mesons. For the searches with potential sensitivity, we recast the searches and estimate the bounds for some benchmark dark meson scenarios. For the searches

²It is also possible that there is some mixture between $SU(2)_L$ and $SU(2)_R$, but this requires more than just a single triplet of dark pions and dark vector mesons. More details can be found in Ref. [120].

that fail, we identify why. This latter step is useful as we find many 13 TeV analysis are insensitive to dark mesons because their cut thresholds are too high.

One lesson we have learned from our investigation of dark mesons is that custodial symmetry has the potential of constraining certain kinds of theories and their corresponding phenomenology. Regarding the two types of dark meson decay patterns, i.e. “gaugephilic” and “gaugephobic”, custodial symmetry was demonstrated to be of critical importance. For example, in the 2-flavor vector-like theory, by imposing custodial symmetry on the dark sector, we found that the leading higher dimensional operators that are responsible for the π - f - f decay first appeared at dimension-7. Meanwhile, those dimension-7 operators with respect to π - V - h are forbidden by the custodial symmetry. The leading custodial preserving π - V - h operators first appear at dimension-9. As a result, the coefficient of the π - V - h interaction is *suppressed* relative to the π - f - f interaction by two extra powers of the heavy cutoff mass scale of the EFT. Thus, dark pions preferentially interact with (and ultimately decay primarily to) SM fermions – these theories are gaugephobic – in two-flavor, vector-like, custodially-preserving dark sector theories.

Another such example we have studied during the investigation was the Two-Higgs-Doublet-Model (2HDM) [120]. Although a general 2HDM model does not necessarily preserve custodial symmetry, the amount of custodial violation is nevertheless proportional to $(g')^2$ and the electroweak VEV v^2 , but is also suppressed by the mass scale of the heavy Higgs state m_A^2 . As a result, one can say that the 2HDM becomes custodially symmetric when $m_A \gg v$. Moreover, it is also well-known that the decays of 2HDM heavy states to gauge bosons are suppressed by two extra

powers of m_A compared to that of fermions. In other words, they are gaugephobic [121].

From these two brief examples we see that, custodial symmetry is capable of affecting the leading interactions of BSM sectors with the Higgs sector of the SM. This effect will further determine the decay branching fraction of that BSM sector, and may well be testable in the LHC physics.

SMEFT with custodial symmetry

The goal of this project is to elaborate on the connection between the potential unknown new physics at a high energy scale (the ultraviolet, or UV physics scale) and custodial symmetry in a model-independent manner. For new physics that is sufficiently heavy, it can be integrated out, resulting in contributions to higher dimensional operators of the Standard Model Effective Field Theory (SMEFT). Chapter IV of this dissertation covers our recent effort of a systematic investigation on this topic.

The SMEFT is a consistent effective theory generalization of the Standard Model constructed from a series of higher dimensional operators that use the same building blocks and obey the same gauge symmetries as the Standard Model. In other words, these higher dimensional operators are $SU(3)_C \times SU(2)_L \times U(1)_Y$ invariants constructed out of the Standard Model fields.

Following these assumptions, the SMEFT is defined as [122]

$$\mathcal{L}_{SMEFT} = \mathcal{L}_{SM} + \mathcal{L}^{(5)} + \mathcal{L}^{(6)} + \mathcal{L}^{(7)} + \dots, \quad \mathcal{L}^{(d)} = \sum_{i=1}^{n_d} \frac{C_i^{(d)}}{\Lambda^{d-4}} O_i^{(d)} \quad \text{for } d > 4. \quad (1.2)$$

The dimension- d operators $O_i^{(d)}$ are suppressed by $d - 4$ powers of the cutoff scale Λ , and the $C_i^{(d)}$ are the Wilson coefficients. The number of non-redundant operators in

$\mathcal{L}^{(5)}$, $\mathcal{L}^{(6)}$, $\mathcal{L}^{(7)}$ and $\mathcal{L}^{(8)}$ is known [123]. Furthermore, general algorithms to determine operator bases at higher orders have been thoroughly studied [123, 122, 124].

The basic idea of SMEFT is perfectly well-aligned with the goal of our investigation:

- It is generally model-independent as long as the new physics is heavy. Hence it does not overly rely on the existence of a particular UV-completion.
- It can be truncated to arbitrary desired dimension and generate a well-defined set of operators.
- It can incorporate global symmetries we wish to impose with a relatively simple implementation.

Nevertheless, the number of higher dimensional operators in SMEFT increases exponentially with dimension. For practical reasons, in this study, we restrict to higher dimensional operators up to dimension-6. Any possible further investigation involving operators at dimension-7 or higher will depend on these results obtained at dimension-6, and is outside the scope of this dissertation.

Classifying the general form of these operators has had a long history [125, 126]. The ‘Warsaw’ basis [127], for instance, provides a non-redundant parameterization of the set of all dimension-six (dim-6) operators. Other operator bases, e.g. SILH basis [128] can be related through integration-by-parts (IBP) and equations-of-motion (EOM) redundancies [129]. A systematic classification and counting of SMEFT operators has been recently achieved using the Hilbert series technique [130, 131, 132, 133, 134] up to dim-8 and beyond [135, 136, 123, 124].

The number of operators grows rapidly with the dimension [123]. At dim-6, SMEFT contains 3045 operators [137, 123], assuming all of the global symmetries

of the Standard Model are broken. This has led to simplifications of SMEFT by focusing on a more restricted set of operators. For instance, a subset of operators that preserves part of the global symmetries of the SM, such as baryon number. Or a subset of operators restricted to just one generation [138], just bosonic operators [139, 140] and related “universal” theories [141, 142, 143].

It is also possible that integrating out ultraviolet (UV) physics does not result in any additional violation of global symmetries that are not already violated in the SM. There are two distinct possibilities: 1) UV physics is *invariant* under the global symmetries, or, 2) UV physics *minimally* violates the global symmetries. Uncovering UV physics that is invariant under the SM global symmetries will be our main focus, and includes a wealth of possibilities, as we will see below. This is a presumption about the form of the UV physics, not of the EFT, similar in spirit to Universal Theories [141, 142, 143]. Alternatively, UV physics that minimally violates the global symmetries is presumed to have global symmetry-violating couplings proportional to the same couplings that violate those symmetries in the SM. A well-known example is minimal flavor violation (MFV) [144], in which the full ensemble of flavor violating higher dimensional operators are presumed to exist but with coefficients proportional to the flavor-violating Yukawa couplings of the SM.

The focus of Chapter IV is to uncover the “fingerprint” of custodial symmetric UV physics in low energy precision observables. Many theories beyond the Standard Model utilize custodial symmetry in order to avoid the strong bounds from experiment on custodial violation, including originally technicolor [145] (for a review [146]) as well as composite Higgs, e.g., [147, 148, 149, 150, 128] little Higgs theories [151, 152, 153, 154, 155] dark matter theories [156, 120, 157], etc. We re-emphasize our definition

that UV physics is said to be “custodial symmetric” when an $SU(2)_R$ global symmetry is preserved by all UV interactions with the Higgs sector of the SM.

In order to study the impact of custodial symmetric UV physics onto precision observables, we need to identify the various ways in which higher dimensional operators can violate custodial symmetry. This is not as simple as it sounds. For example, in the SM the Yukawa couplings simultaneously break all $SU(2)_R$ symmetries [the custodial $SU(2)$ of the Higgs sector as well as $SU(2)$ isospin in the flavor sector]. By contrast, these symmetries can be separately violated by different operators in SMEFT. This impacts the predictions of low energy observables – which is a good thing! – since it means we have ways to fingerprint the symmetry structure of the UV physics. In order to study the impact of UV physics with custodial symmetry on SMEFT, we re-write all interactions with $SU(2)_R$ invariance (and $SU(2)_R$ breaking) manifest. When this is done for all but the lepton sector, we call this the “custodial basis” for SMEFT. When the $SU(2)_R$ symmetry is formally extended also to lepton sector, we include right-handed neutrinos enlarging SMEFT to ν SMEFT, and then are able to construct the custodial basis for ν SMEFT.

The explicit violation of $SU(2)_R$ in the SM could easily make it difficult to disentangle the UV preservation of custodial symmetry from the SM-induced violation of custodial symmetry. This subject has a long history. The ρ parameter [158]

$$\rho = \frac{m_W^2}{m_Z^2 c_\theta^2} \quad (1.3)$$

was proposed as an observable that was designed to distinguish between custodial symmetric and custodial violating UV physics. Common lore is that is sufficient to establish custodial symmetry violation beyond the SM. For instance, in theories with new scalars transforming under $SU(2)_L \times U(1)_Y$ in representations other than $\mathbf{2}_{1/2}$ tree-level deviations from 1 are possible, e.g. [7]. More precisely, it is well-known

that new physics contributions that are purely oblique at leading matching order implies $\rho \neq 1$ at tree-level is in one-to-one correspondence with custodial violation of the UV physics (e.g., [159]). However, for general UV physics, there can be non-oblique contributions to electroweak precision observables that is still nevertheless custodial symmetric, and this leads to $\rho \neq 1$ at tree-level [160, 161]. If we wish to unambiguously discern the custodial symmetric structure of UV physics imprint on (ν) SMEFT, we must account for these contributions. One of the main results of our paper is to determine the *correlated* predictions of custodial symmetric physics on a set of low energy observables. So while ρ by itself is insufficient to “fingerprint” custodial symmetry in UV physics, when combined with other observables including several Z and W partial widths, we find the correlated predictions that unambiguously signal the UV physics that was integrated out does not violate custodial symmetry at tree-level.

There is a critical issue we must tackle in order to identify the pattern of correlated predictions of observables. Integrating out custodial symmetric UV physics generates custodial symmetric operators, but not necessarily in our custodial basis of (ν) SMEFT. (Predictions for physical observables are, of course, basis-independent.) Ordinarily one simply utilizes integration-by-parts (IBP) and equation of motion (EOM) redundancies to rewrite the UV generated operator(s) in terms of whatever basis one prefers, in our case, our custodial basis of (ν) SMEFT. However, the EOM redundancy is incomplete – custodial symmetric operators can be traded for custodial violating operators proportional to the SM violation of custodial symmetry. This is simply because the EFT does not respect custodial symmetry, even if the integrated-out UV physics does. This could have sunk any chance to recover correlated predictions. Our central result is that we have identified observables that remain

faithful to fingerprinting custodial symmetric UV physics at tree-level and do not suffer from the EOM ambiguity. By contrast, other observables that one might naively have assumed could have provided discriminating power about the UV physics are ultimately subject to the EOM ambiguity. For instance, the absence of certain custodial violating operators, such as $\psi^2 H^3$, might have been a sign of custodial symmetric UV physics, but these can be generated at tree-level proportional to the SM violation of custodial symmetry, and so are not obviously useful discriminators.

Outline

The theme of this dissertation is the impact of custodial symmetry with regard to beyond the Standard Model theories of dark matter and new physics in general. In detail, Chapter II discusses effective theories of dark mesons, with a deeper perspective on those preserving custodial symmetry; Chapter III investigates, in light of the current LHC searches done by ATLAS and CMS, the collider phenomenology of the dark meson theories and its signatures for a potential discovery at the LHC. The dark sector model that is of particular interest to us is Stealth Dark Matter; Chapter IV discusses observable fingerprints of extensions to the Standard Model Effective Theory integrated out from custodial symmetric UV theories, with right-handed neutrinos included.

Chapter II contains previously published material co-authored with G. D. Kribs, A. Martin; Chapter III contains previously published material co-authored with G. D. Kribs, A. Martin and B. Ostdiek; Chapter IV contains unpublished material co-authored with G. D. Kribs, X. Lu and A. Martin.

CHAPTER II

EFFECTIVE THEORIES OF DARK MESONS

In this chapter, we describe our study on the effective theories of dark mesons. The structure of this chapter is as follows. First (Sec. II), we briefly remind the reader of the ingredients in the type of strong sector we want to consider. Next, in Sec. II we discuss custodial $SU(2)$ of the Higgs sector, emphasizing the role of hypercharge and the difference between up-type and down-type fermion Yukawa couplings that act as the spurions for custodial $SU(2)$ violation. This will greatly assist us in understanding and classifying the dynamics of dark mesons in the set of theories we consider. In Sec. II, we discuss two-flavor theories, one chiral and two vector-like scenarios. Understanding the dynamics of these relatively simple theories provides a warmup to theories with more flavors. Next we consider vector-like four-flavor theories, that are the smallest field content that permit vector-like masses and Higgs interactions at the renormalizable level. The model was first proposed in [106, 107] where baryonic sector of these theories was extensively studied since the lightest baryon is a viable dark matter candidate. Our main goal is to determine the dark pion interactions with the SM, and to understand the results in terms of limits when two of the flavors are decoupled and the theory reduces to just a two-flavor theory with higher dimensional interactions. Finally, to emphasize the role of custodial $SU(2)$, we discuss a vector-like two-flavor theories where custodial symmetry is violated, and the consequences for the dark pion decays. In Appendix A, we review the case of a general two-Higgs doublet model and the “gaugephobic” decays of its A^0, H^\pm states.

Defining the dark sector

Throughout this paper, we will refer to the new strong sector as the “dark” sector. It consists of a strongly-coupled “dark gauge group” $SU(N_D)$ with its own

“dark confinement scale”, and “dark fermions” or “dark flavors” that transform under the dark group as well as the electroweak part of the Standard Model. Below the dark confinement scale, the effective theory description of the composites includes “dark baryons” and “dark mesons”; the latter breaking up into “dark vector mesons” and “dark pions”. Despite the naming convention, we emphasize that the new states are certainly not “dark” to collider experiments [162].

When describing the fermionic content of the dark sector (in the UV), we will work entirely with left-handed fields, meaning $(1/2, 0)$ under the Lorentz group. We will distinguish between theories by the number of dark fermion flavors, where each flavor corresponds to one (two-component) fermion in the fundamental of the dark color group and one anti-fundamental. We will generically refer to dark color fundamentals as F , and anti-fundamental as \hat{F} . Throughout this paper, we will assume that all dark fermions are inert under SM $SU(3)_c$ while at least some of them interact electroweakly. Other references that have pursued dark sectors transforming under $SU(3)_c$ can be found in [35, 74, 163].

In the absence of other interactions, the symmetry of the dark sector is $SU(N_{fund}) \times SU(N_{anti})$. Turning on electroweak interactions, some of these flavor symmetries are explicitly broken. The majority of the dark sectors we’ll study are vector-like, which – in terms of two-component fermions – implies that if F_i is a fundamental of dark color and transforms under EW representation G , then the theory also includes a dark-color anti-fundamental \hat{F}_j also residing in EW representation G . This charge assignment permits mass terms of the form $M_{ij}F_i\hat{F}_j$. In addition, we can form dimension > 3 operators connecting dark fermions with the Higgs boson. Interactions with the Higgs force us to connect flavor symmetries of the fermionic sector with the $O(4) \cong SU(2)_L \times SU(2)_R$ global symmetry Higgs potential. If F are

EW doublets and \hat{F} are EW singlets, then the interactions take a form familiar from SM Yukawas, $yF\hat{F}\mathcal{H}$. For other representations of F, \hat{F} , the interactions only come about at the non-renormalizable level, e.g., $F\hat{F}H^\dagger H/\Lambda$.

Once we cross below the dark confining scale, the low energy effective theory is described in terms of the composite mesons and baryons of this sector. Provided that the vector-like dark fermion masses are $< 4\pi f$, the leading interactions of the dark pions can be determined using non-linear sigma model language analogous to the real pions of QCD. Confinement spontaneously breaks the chiral symmetry of the dark fermions down to the diagonal subgroup: $SU(N_{fund}) \times SU(N_{anti}) \rightarrow SU(N)_V$, with the dark pion multiplets falling into representations of $SU(N)_V$. Whether or not $SU(N)_V$ is gauged and how it connects with the Higgs potential symmetries depends on the setup. In the IR, interactions between dark fermions and Higgses become interactions between the dark pions and the Higgs. For example, the two examples used above become $tr(\Sigma\mathcal{H}^\dagger) + h.c.$ and $\text{Tr}(\Sigma\mathcal{H}^\dagger\mathcal{H} + h.c.)$ respectively, where Σ is the NLSM field.

At this point it is useful to distinguish between the dark sectors that we consider in this paper and early proposals for dynamical electroweak symmetry breaking (technicolor). Simply put, in the extension we consider, we *assume* there is a Higgs doublet in the low energy effective theory that acquires an electroweak breaking vev that is responsible for (most) of electroweak symmetry breaking in the Standard Model.

Custodial SU(2)

A critical part of the classification of effective theories of dark mesons is whether custodial $SU(2)$ is preserved or violated by the dark sector dynamics. Custodial

$SU(2)$ is the residual accidental global symmetry of the Higgs multiplet after it acquires an expectation value, $O(4) \cong SU(2)_L \times SU(2)_R \rightarrow O(3) \cong SU(2)_C$.

Custodial $SU(2)$ arises automatically once the matter content and interactions are (at least formally) promoted to become $SU(2)_L \times SU(2)_R$ invariant. We will use the terminology $SU(2)_L$, $SU(2)_R$ frequently in this paper and emphasize that this will always refer to internal symmetries of the theory and never to Lorentz symmetry. It will become very convenient to utilize a manifestly $SU(2)_C$ symmetric formalism for writing interactions of the dark sector with the Higgs multiplet. The basic notions are well-known, though not necessarily exploited in the ways that we will be doing. A manifestly custodially $SU(2)_C$ symmetric formalism promotes $U(1)_Y$ to $SU(2)_R$, where only the t_3 generator of $SU(2)_R$ is gauged.

To establish notation, the Higgs doublet of the Standard Model

$$H = \begin{pmatrix} G^+ \\ (v + h + iG^0)/\sqrt{2} \end{pmatrix}, \quad (2.1)$$

can be re-expressed in terms of a $(\mathbf{2}, \mathbf{2})$ bifundamental scalar field under $SU(2)_L \times SU(2)_R$ as

$$\mathcal{H}_{i_L i_R} = \frac{1}{\sqrt{2}} \begin{pmatrix} (v + h - iG^0)/\sqrt{2} & G^+ \\ -G^- & (v + h + iG^0)/\sqrt{2} \end{pmatrix}. \quad (2.2)$$

In principle, all custodially-symmetric interactions can be written in terms of powers of \mathcal{H} , and suitable $SU(2)_L$ and $SU(2)_R$ contractions. The notation becomes much more compact when we utilize the definition

$$\mathcal{H}_{i_R i_L}^\dagger \equiv \epsilon_{i_R j_R} \epsilon_{i_L j_L} \mathcal{H}_{i_L i_R} \quad (2.3)$$

which matches the naive complex conjugation and transpose of the 2×2 matrix definition in Eq. (2.2). In this form, the Standard Model Higgs potential becomes

simply

$$V = m_H^2 \text{Tr } \mathcal{H}^\dagger \mathcal{H} + \frac{\lambda}{4} (\text{Tr } \mathcal{H}^\dagger \mathcal{H})^2. \quad (2.4)$$

The absence of any explicit t_R^3 signals the absence of any explicit custodial symmetry violation. When the Higgs gets a vev and $SU(2)_L \times SU(2)_R$ breaks to the diagonal $SU(2)_C$, the original $(\mathbf{2}, \mathbf{2})$ of Higgs states decomposes into a singlet (radial mode) plus a triplet (Goldstones) of the diagonal $SU(2)_C$.

The full covariant derivative for the Higgs multiplet, Eq. (2.2), does not respect $SU(2)_R$ due to gauging hypercharge, i.e., just the t_R^3 generator is gauged. This is straightforwardly handled by writing the covariant derivative as

$$D_\mu \mathcal{H}_{i_L i_R} = \partial_\mu \mathcal{H}_{i_L i_R} - ig W_\mu^a (t_L^a \mathcal{H})_{i_L i_R} - ig' B_\mu (\mathcal{H} t_R^3)_{i_L i_R} \quad (2.5)$$

making kinetic term of the bi-doublet \mathcal{H} :

$$\text{Tr } D_\mu \mathcal{H}^\dagger D^\mu \mathcal{H}. \quad (2.6)$$

The explicit t_R^3 can be thought of as $2Yt_R^3$, where the Higgs doublet $H_{Y=1/2}$ and its complex conjugate $H_{Y=-1/2}^*$ are embedded as the two components of an $SU(2)_R$ doublet. In the limit $g'Y \rightarrow 0$, the last term of Eq. (2.5) vanishes, restoring the full $SU(2)_R$ global symmetry. In this way, we see that $g'Yt_R^3$ acts as a spurion for custodial $SU(2)$ violation. One could instead promote $B_\mu t_R^3 \rightarrow W_R^a t_R^a$, formally gauging the full $SU(2)_R$ symmetry. In this case, we would need an explicit $SU(2)_R$ -breaking mass term in order to remove the $W_R^{1,2}$ gauge bosons and recover the Standard Model. Moreover, as is well-known from left-right models, an additional $U(1)$ is required to obtain the correct hypercharge of the left-handed and right-handed quarks and leptons (e.g., for a review, see [164]).

Yukawa couplings are another source of custodial breaking. In terms of the usual Higgs doublet H , the up and down Yukawa couplings are

$$y_{ij}^u Q_{Li} \epsilon H u_{Rj} + y_{ij}^d Q_{Li} H^\dagger d_{Rj} + h.c. \quad (2.7)$$

Grouping $Q_{Ri} = \{u_i^c, d_i^c\}$ together, we can rewrite the up and down quark Yukawas in terms of \mathcal{H} as

$$y_{ij}^u Q_{Li} \mathcal{H} P_u Q_{Rj} + y_{ij}^d Q_{Li} \mathcal{H} P_d Q_{Rj} + h.c. \quad (2.8)$$

where $P_{u,d} = (\mathbf{1}_R \mp 2t_R^3)/2$ are matrices in $SU(2)_R$ space that project out the up-type or down-type right-handed fermion. In fact, it is useful to rewrite Eq. (2.8) as the sum of a custodial symmetric Yukawa plus a custodial violating term:

$$\mathcal{L}_{\text{Yuk}} = \mathcal{Y}_{ij}^C Q_{Li} \mathcal{H} \frac{\mathbf{1}_R}{2} Q_{Rj} + \mathcal{Y}_{ij}^\phi Q_{Li} \mathcal{H} t_R^3 Q_{Rj} + h.c. \quad (2.9)$$

where

$$\begin{aligned} \mathcal{Y}_{ij}^C &= y_{ij}^u + y_{ij}^d \\ \mathcal{Y}_{ij}^\phi &= y_{ij}^u - y_{ij}^d. \end{aligned} \quad (2.10)$$

There is no loss of generality from the SM, i.e., \mathcal{Y}_{ij}^C and \mathcal{Y}_{ij}^ϕ are independent matrices. In the special case where $y_{ij}^u = y_{ij}^d$ and thus $\mathcal{Y}_{ij}^\phi = 0$, the Yukawa couplings are custodially symmetric. Later in the paper when we write higher dimensional operators involving the SM fermions, we will always assume a form of minimal flavor-violation (MFV) where operators involving $Q_{Li} \mathcal{H} (\mathbf{1}_R/2) Q_{Rj}$ are accompanied by \mathcal{Y}_{ij}^C and operators involving $Q_{Li} \mathcal{H} t_R^3 Q_{Rj}$ are accompanied by \mathcal{Y}_{ij}^ϕ .

Looking beyond the SM, we will use the same logic we applied to SM Yukawas when writing down interactions between the dark fermions and the Higgs. Specifically, in addition to grouping dark fermions into multiplets of (gauged) $SU(2)_W \equiv SU(2)_L$, we also assign them to multiplets of $SU(2)_R$ then classify interactions in $SU(2)_L \times SU(2)_R$ language. Put another way, interactions among the SM Higgs multiplet

and dark fermions break the combination of the $SU(2)_R$ Higgs potential symmetry and the $SU(N_{fund})$ (or $SU(N_{anti})$) flavor symmetries of the dark fermions down to a common $SU(2)$, which we relabel as $SU(2)_R$. New custodial violating breaking interactions/spurions must be proportional to t_R^3 , as that is the only choice consistent with gauging $SU(2)_L$ and the t^3 generator $[U(1)_Y]$ of $SU(2)_R$ [165]. Thus, in $SU(2)_L \times SU(2)_R$ language, strong sectors that respect custodial symmetry contain no terms with explicit t_R^3 , while a generic custodial violating dark sector can have one or more such terms.¹

Effective Interactions of Dark Pions

The dark sectors of greatest interest to us in this paper preserve custodial $SU(2)$, so all deviations from exact custodial symmetry can be traced to $g'Y$ or the differences among SM Yukawas. Consequently, dark pions transform in representations of $SU(2)_L \times SU(2)_R$. Once the Higgs gets a vacuum expectation, these pions will break up into multiplets of custodial $SU(2)$. The smallest, and therefore lightest, non-trivial $SU(2)_C$ representation the pions can fill is the triplet. Heavier dark pions in larger representations are possible, as are higher spin composites such spin-1 dark rho mesons. In general, these states rapidly decay into the lightest dark pions. While this is certainly highly relevant for phenomenology [35, 162], it the lightest dark pion decays that are the main concern for this paper.

Dark Pion Triplet interactions in custodial preserving strong sectors.

Suppose we have an $SU(2)_C$ triplet of dark pions π^a , that we have already motivated as arising in a wide class of interesting class of dark sector theories, and we wish to understand its interactions. The most phenomenologically relevant interactions to

¹Additionally, dark sector theories with $SU(2)_L$ multiplets with hypercharge, as well as $SU(2)_R$ multiplets with hypercharge not proportional to t_R^3 , require an additional $U(1)_X$. We do not consider such theories in this paper.

determine are those with a single dark pion since they will govern decays. As we will show below, single pion interactions can be understood from symmetry considerations alone.

First, let's consider a “toy” Standard Model that is fully $SU(2)_L \times SU(2)_R$ symmetric – meaning we set $g' = 0$ and $\mathcal{Y}_{ij}^{\mathcal{C}} = 0$, in the presence of a dark sector that produces a (custodially symmetric) triplet of dark pions. In this limit, the $\{u^c, d^c\}$ quarks of the SM can be written in terms of a $SU(2)_R$ doublet as in Eq. (2.8) and the $SU(2)_W$ gauge bosons lie in a $SU(2)_L$ triplet. When EWSB occurs, $SU(2)_L \times SU(2)_R \rightarrow SU(2)_C$, so we can reclassify all fields into $SU(2)_C$ multiplets and form invariants from them. Contracting π^a with $SU(2)_C$ triplets formed from SM fields, the lowest dimension operators involving a single dark pion are:

$$\mathcal{Y}_{ij}^C \left(\frac{v}{v_\pi} \right) \pi^a (Q_{Li} t^a Q_{Rj}) + \xi g \left(\frac{v}{v_\pi} \right) W_\mu^a \left(h \overleftrightarrow{\partial}^\mu \pi^a \right), \quad (2.11)$$

where t^a are the generators of $SU(2)_C$. (A similar expression for the first term is also present for the leptons of the SM.) As both terms require electroweak symmetry breaking, they must be proportional to the mass of the SM fields. Therefore, we need another dimensionful parameter v_π to balance dimensions. For the fermion terms, we have assumed the flavor structure obeys minimal flavor violation with a (lowest order) coefficient of \mathcal{Y}_{ij}^C . The factor ξ parameterizes the relative strength between the interactions of pions with fermions versus the gauge/Higgs sector. We will explore the size and origin of v_π and ξ in specific theories shortly. The presence of the Higgs boson in the second term is also easy to motivate. While $W_\mu^a \partial_\mu \pi^a$ is custodially symmetric, by itself this is a mixing involving longitudinal W^a and would indicate that we have not properly gauge fixed. Hence, we need to add a $SU(2)_C$ singlet, and h is the option with the lowest dimension in the broken phase of the SM.

One might wonder how ξ could be different from unity, given what we have described thus far. When dark pions transform in representations that are larger than a triplet, there is a possibility of dark pion–Higgs boson mixing. For example, dark pions in the complex representation $(\mathbf{2}, \mathbf{2})$ under $SU(2)_L \times SU(2)_R$ contain a “Higgs-like” dark pion state ($SU(2)_C$ singlet) that can – and generically does – mix with the SM ($SU(2)_C$ singlet) Higgs boson. This implies additional contributions to the gauge/Higgs boson/dark pion interactions arise from the covariant derivative of the dark pions. These interactions turn out to be *critical* to understanding the phenomenology of models with more than two flavors of dark fermions.

Let’s now re-introduce the custodial $SU(2)$ violation in the SM. This involves the difference between up and down Yukawas,

$$\mathcal{Y}_{ij}^{\mathcal{C}} \left(\frac{v}{v_\pi} \right) \pi^a (Q_{Li} t^a t_R^3 Q_{Rj}) \quad (2.12)$$

as well as $g' \neq 0$,

$$\xi g' \left(\frac{v}{v_\pi} \right) B_\mu \left(h \overleftrightarrow{\partial}^\mu \pi^0 \right). \quad (2.13)$$

With these terms, the simple lagrangian Eq. (2.11) becomes somewhat more complicated. If we focus our attention on just one generation of quarks, and convert from two-component fermions to four-component notation, the effective lagrangian for dark pion decay becomes:

$$\begin{aligned} \mathcal{L}_{\text{decay}} = & \frac{\sqrt{2}}{v_\pi} \left[\pi_D^+ \bar{\psi}_u (m_d P_R - m_u P_L) \psi_d + \pi_D^- \bar{\psi}_d (m_d P_L - m_u P_R) \psi_u \right. \\ & \left. + \frac{i}{\sqrt{2}} \pi_D^0 (m_u \bar{\psi}_u \gamma_5 \psi_u - m_d \bar{\psi}_d \gamma_5 \psi_d) \right] \\ & - \xi \frac{m_W}{v_\pi} \left[(W_\mu^- h \overleftrightarrow{\partial}^\mu \pi_D^+) + (W_\mu^+ h \overleftrightarrow{\partial}^\mu \pi_D^-) + \frac{1}{\cos \theta_W} (Z_\mu h \overleftrightarrow{\partial}^\mu \pi_D^0) \right] \end{aligned} \quad (2.14)$$

The effective theories of dark mesons that we consider below will give specific predictions for these couplings. We find two qualitatively distinct possibilities:

$$\begin{array}{l} \xi \sim 1 \quad \text{“gaugephilic”} \\ \xi \ll 1 \quad \text{“gaugephobic”} \end{array} \quad (2.15)$$

Equation (2.14), which has been argued purely from custodial symmetry and assumptions about the most relevant connections between the dark sector and the SM, is our first main result. The main purpose of the rest of this paper is to determine how dark pion interactions in different dark sector theories with (or without) custodial $SU(2)_C$ map into Eq. (2.14) and, especially, whether they fall into the gaugephilic or gaugephobic category.

Before jumping head first into strongly-coupled dark sectors, the interactions of a custodial $SU(2)$ triplet given in Eq. (2.14) are perhaps most familiar from two-Higgs doublet models. We take a brief look at this in the next section, leaving a detailed discussion to Appendix A.

Two-Higgs Doublet Models. As a point of reference, it is helpful to consider the couplings of (H^\pm, A^0) in two-Higgs doublet models (2HDMs). The couplings to the fermions are model-dependent; for illustration here let’s consider the so-called Type I 2HDM where the fermions couple to just one Higgs doublet as that is the 2HDM setup that most closely resembles the our dark pion theories. In Type I 2HDM theory, one obtains [166]

$$\frac{1}{v_\pi} = \frac{1}{v} \cot \beta$$

where we have neglected the CKM mixing for the charged Higgs couplings. For the gauge/Higgs sector,

$$\frac{\xi}{v_\pi} = \frac{1}{v} \cos(\beta - \alpha)$$

Here, $\cot \beta$ is the usual ratio of the expectation values in two Higgs doublets. In the decoupling limit, the coupling to gauge/Higgs boson is well-known to scale as [121]

$$|\cos(\beta - \alpha)| \sim \frac{v^2}{m_A^2}. \quad (2.16)$$

Since the coupling of fermions does not have a similar scaling, we see that 2HDMs are gaugephobic regardless of the Type of 2HDM.

There is an interesting story about utilizing the custodially-symmetric basis for 2HDMs. In the decoupling limit a 2HDM becomes custodially symmetric, and the decays of its heavy states (H^\pm, A^0) to SM particles in this limit are gaugephobic. Details are presented in Appendix A.

Neutral Dark Pion Decay to Diphotons. Finally, it is interesting to discuss the coupling of π^0 to $\gamma\gamma$. The usual axial anomaly contribution to this decay mode, $\pi^0 F_{\mu\nu} \tilde{F}^{\mu\nu} / f$, whose leading contribution is proportional to $\text{Tr } Q^2 t_a^3$ [where t_a^3 is the generator of the axial $U(1)$] is conspicuously absent from Eq. (2.14). The reason for this is that in a dark sector where the $SU(N)_V$, preserved by strong interactions, is an exact symmetry, this contribution must vanish. For example, in a two-flavor dark sector, invariance under an exact $SU(2)_V$ would enforce the two flavors of dark fermion masses are equal. Gauging the full $SU(2)_V$ [as in $SU(2)_L$] or just the t^3 subgroup [as in $U(1)_Y$] implies the dark fermion electric charges are equal and opposite. In this case, $\text{Tr } Q^2 t_a^3$ vanishes, as do higher order $\pi_D^0 \gamma\gamma$ operators proportional to the differences of dark fermion masses.

Nevertheless, there is a very small, residual contribution to $\pi_D^0 \rightarrow \gamma\gamma$, due to the interactions with the SM in Eq. (2.14). That is, even though custodial $SU(2)$ is preserved by the dark sector interactions with the SM, the SM itself violates custodial $SU(2)$. The dark pion interactions with the SM fermion axial current generate a one-loop suppressed π_D^0 - γ - γ coupling proportional to $m_f / (16\pi^2 v_\pi)$. We can calculate the

amplitude for the rate by borrowing the standard results for A^0 decay in two-Higgs doublet models [167] and suitably substituting couplings:

$$\mathcal{A}(\pi_D^0 \rightarrow \gamma\gamma) = \sum_f \frac{\alpha}{4\pi} N_c Q_f^2 \left(\frac{m_f}{v_\pi} \right) \sqrt{\tau_f} f(\tau_f) \quad (2.17)$$

where N_c is the number of colors, Q_f is the electric charge, $\tau_f = 4m_f^2/m_\pi^2$, and

$$f(\tau) = \begin{cases} \arcsin^2 \frac{1}{\sqrt{\tau}} & \tau \geq 1 \\ -\frac{1}{4} \left[\log \frac{1+\sqrt{1-\tau}}{1-\sqrt{1-\tau}} - i\pi \right]^2 & \tau < 1. \end{cases} \quad (2.18)$$

In the limit $\tau \ll 1$,

$$f(\tau) \rightarrow -(1/4)[\log(4/\tau) - i\pi]^2, \quad (2.19)$$

and thus we see an additional suppression of the π_D^0 decay amplitude of roughly $\sqrt{\tau_f} = 2m_f/m_{\pi_D}$ when $m_{\pi_D} \gg m_f$ (neglecting the τ dependence of the log). Hence, while there is π_D^0 decay to $\gamma\gamma$ due to the custodial $SU(2)$ breaking in the SM, the decay rate is suppressed by roughly $\alpha^2/(16\pi^2) \times (4m_f^2/m_{\pi_D}^2)$ that is $\simeq 10^{-6} \times m_f^2/m_{\pi_D}^2$ smaller than the direct decay to fermions. This is so small as to be phenomenologically irrelevant.

Two-flavor theories

The simplest anomaly-free dark sector theories that we consider have two flavors of dark fermions. We refer to the dark color fundamentals as F_i and anti-fundamentals as \hat{F}_i transforming under $SU(N_D)$ with flavor index $i = 1, 2$. The global symmetry of the flavors is $SU(2)_{\text{fund}} \times SU(2)_{\text{anti}}$. Once we include interactions between the dark fermions and the Higgs multiplet, we will be forced to connect the fermion flavor symmetries to the $SU(2)_L \times SU(2)_R$ symmetry of the Higgs potential. This connection can be made in a few different ways, two vector-like and one chiral. In the vector-like assignments, both F_i and \hat{F}_i must be doublets of the same $SU(2)$ – either $SU(2)_L$ or $SU(2)_R$, while in the chiral assignment, F and \hat{F} transform under

different $SU(2)$ s.² However, in all of these cases, $SU(2)_{\text{fund}} \times SU(2)_{\text{anti}}$ is broken to the diagonal $SU(2)_V$ by strong dynamics, just as in two-flavor QCD. Also just like QCD, the dark pions form a triplet of the diagonal $SU(2)_V$, which ultimately becomes (π^+, π^0, π^-) after electroweak breaking down to just $U(1)_{\text{em}}$. This is the custodial $SU(2)$ symmetric triplet that we discussed in the previous section.

Prior to electroweak breaking scale, all three pions π^\pm, π^0 are stable. Once electroweak symmetry is broken, electromagnetic corrections split the multiplets by [168]

$$m_{\pi^\pm}^2 - m_{\pi^0}^2 = \frac{(3 \ln 2)}{2\pi} \alpha m_\rho^2 \quad (2.20)$$

where α is the electroweak coupling constant, and m_ρ is the mass of the vector resonances of the dark sector. This mass splitting allows the weak decay of $\pi^\pm \rightarrow \pi^0 \bar{f}' f$. Whether this decay is competitive (or not) with direct decays $\pi \rightarrow \text{SM}$ will depend on the π -SM-SM coupling strength proportional to $1/v_\pi$ in the effective theory.

We now consider each of these theories in turn.

Field	$(SU(N_D), SU(2)_L, SU(2)_R)$
F	$(\mathbf{N}, \mathbf{2}, \mathbf{1})$
\hat{F}	$(\bar{\mathbf{N}}, \mathbf{1}, \mathbf{2})$

Table 1. Two-flavor fermion content of the chiral theory.

Two-flavor chiral theory. The two-flavor chiral theory contains the matter content in Table 1. $SU(2)_L$ is embedded as $SU(2)_{\text{fund}}$ while $U(1)_Y$ is the t^3 generator of $SU(2)_{\text{anti}}$. Confinement breaks the global symmetry to $SU(2)_V$, of which only the gauged $U(1)_{\text{em}}$ survives.

²Anomaly cancellation requires N_D to be even for the chiral case.

Identifying the flavor symmetries $SU(2)_{fund}, SU(2)_{anti}$ with $SU(2)_L, SU(2)_R$ respectively, we can write a Yukawa interaction between the Higgs bi-doublet and the dark fermions

$$\mathcal{Y}_{\text{Yuk}} = y F \mathcal{H} \hat{F} + h.c., \quad (2.21)$$

Once the Higgs acquires a vev, this will give gives equal contributions to the masses of the “up-type” and “down-type” dark fermions. In the absence of a fundamental Higgs, this theory is minimal technicolor. Including the Higgs (and Yukawa coupling), the two-flavor chiral theory dynamics “induces” electroweak symmetry breaking even when the Higgs multiplet (mass)² is positive. This theory is better known as bosonic technicolor [11, 12] or strongly-coupled induced electroweak symmetry breaking [20, 21].

Now that we have established how dark fermions transform under $SU(2)_L \times SU(2)_R$ we can consider a more general set of interactions that arise with higher dimensional operators. These terms can involve more Higgs fields, derivatives, SM quarks and/or leptons. Examples at dimension-6 include:

$$c_{6A} \frac{(F \hat{F})(Q_L \hat{Q}_R)}{\Lambda^2}, c_{6B} \frac{(F^\dagger \bar{\sigma}^\mu F)(\mathcal{H} D_\mu \mathcal{H})}{\Lambda^2}, c_{6C} \frac{(F^\dagger \bar{\sigma}^\mu t_L^a F)(\mathcal{H} t_L^a D_\mu \mathcal{H})}{\Lambda^2}, \dots \quad (2.22)$$

where t_L^a are the generators of $SU(2)_L$ that pick out the triplet combination of the two doublets. We will use t_L^a and the $SU(2)_R$ counterpart t_R^a throughout this paper.

The translation to the NLSM involves

$$F \hat{F} \rightarrow 4\pi f^3 \Sigma, \quad \Sigma = \exp \left[i \frac{2\pi^a t^a}{f} \right]. \quad (2.23)$$

The covariant derivative acts on Σ identically to the Higgs bi-doublet, Eq. (2.5), leading to interactions of the dark pions with the electroweak gauge bosons. While there is a systematic way to transmute interactions between a strong, chiral symmetry breaking sector and external fields into interactions involving pNGBs [169, 170], we

do not need the full machinery since we are interested in the additional (higher dimensional) terms in the dark sector chiral lagrangian that, after expanding Σ , involve a single power of π^a . This criteria selects out operators whose dark sector components are i.) Lorentz invariant, as we want operators with π_D , not $\partial_\mu\pi_D$, and ii.) that transform non-trivially under $SU(2)_C$ – as discussed in Sec. II, the dark pion decay terms involve connecting $SU(2)_C$ triplets in the strong sector with SM $SU(2)_C$ triplets. In the chiral case, these criteria tell us to ignore operators containing $F^\dagger\bar{\sigma}^\mu F$ (inert under $SU(2)_C$ and not a Lorentz invariant) in favor of operators containing $F\hat{F}$.

Performing the translation to pNGB form and focusing on the most relevant interactions between the dark fermions and the Higgs/SM, the theory becomes

$$\begin{aligned} \mathcal{L} = & \frac{f^2}{4}\text{Tr}(D_\mu\Sigma)^\dagger D^\mu\Sigma \\ & + 4\pi f^3 y \text{Tr}(\mathcal{H}\Sigma^\dagger + h.c.) + \text{higher dimensional terms}. \end{aligned} \quad (2.24)$$

Here Σ contains the triplet of dark pions, and “higher dimensional” here refers to operators such as Eq. (2.22) that are non-renormalizable when written in the UV, in terms of the underlying dark fermions. In this model the higher dimensional operators are subdominant (and so we can ignore them for now), but as we will see in later sections, in other models they are vital to connect the dark sector to the SM.

With the pNGB description of the theory in hand, we can now work out how these Σ interactions map into interactions among dark pions to SM fields in Eq. (2.14). The term linear in Σ expresses the explicit chiral symmetry breaking that arises from the Yukawa interactions. Expanding the linear term out to quadratic order in the dark pion fields,

$$4\pi f^3 y \text{Tr}(\mathcal{H}\Sigma^\dagger + h.c.) \supset 8\pi f^2 y G^a \pi^a + 4\pi f y v \pi^a \pi^a, \quad (2.25)$$

we see the dark pions acquire masses $m_\pi^2 = 8\pi f y v$ and mixing between the would-be Goldstones of the Higgs doublet and the triplet of dark pion fields. The Goldstone-dark pion mixing is independent of a , as it should be given the custodially-symmetric origin of the Yukawa couplings.

Defining the physical pions and Goldstones as

$$\begin{pmatrix} G_{\text{phys}}^a \\ \pi_{\text{phys}}^a \end{pmatrix} = V \begin{pmatrix} G^a \\ \pi^a \end{pmatrix} \quad (2.26)$$

where the mixing angle is determined by diagonalizing the mass matrix

$$M_{\text{diag}}^2 = V M^2 V^T \quad (2.27)$$

with

$$M^2 = \begin{pmatrix} 8\pi f^3 y/v & 8\pi f^2 y \\ 8\pi f^2 y & 8\pi f y v \end{pmatrix}, \quad V = \begin{pmatrix} c_\theta & -s_\theta \\ s_\theta & c_\theta \end{pmatrix} \quad (2.28)$$

and $\theta = \arctan(f/v)$ is the mixing angle. The nonzero entry for Goldstone part of the mass matrix ($G^a G^a$) arises after minimizing the Higgs potential to include the contributions from the dark sector (see [24] for details). Inserting the diagonalized eigenstates back into the Lagrangian leads to a shift of the electroweak vev

$$v^2 + f^2 = v_{246}^2 \simeq (246 \text{ GeV})^2. \quad (2.29)$$

This leads to well-known corrections to Higgs couplings [24]. For our purposes, the couplings of the physical pions to $\bar{f}f$, Zh and $\bar{f}'f$, Wh become

$$\begin{aligned} (\pi_{\text{phys}}^\pm \partial_\mu h - h \partial_\mu \pi_{\text{phys}}^\pm) W^{\mu, \mp} &: \frac{M_W}{v} s_\theta \\ (\pi_{\text{phys}}^0 \partial_\mu h - h \partial_\mu \pi_{\text{phys}}^0) Z^\mu &: \frac{M_Z}{v} s_\theta \\ \pi_{\text{phys}}^\pm \bar{f}' f &: \sqrt{2} \left(\frac{m_{f'}}{v} P_L - \frac{m_f}{v} P_R \right) (2T_3^f) s_\theta \\ \pi_{\text{phys}}^0 \bar{f} f &: i \left(\frac{m_f}{v} \gamma_5 \right) (2T_3^f) s_\theta \end{aligned} \quad (2.30)$$

where $2T_3^f = \pm 1$ is the isospin of the fermion. The mixing angle is

$$s_\theta = \frac{f}{v_{246}}. \quad (2.31)$$

We see that custodially-symmetric two-flavor chiral theories have couplings to fermions and gauge bosons that are parametrically comparable – $M_{W,Z}$ versus m_f .

From the couplings we can identify

$$\frac{1}{v_\pi} \simeq \frac{1}{v} \times \left(\frac{f}{v_{246}} \right), \quad \xi = 1 \quad (2.32)$$

so the couplings are “gaugephilic” according to Eq. (2.14). While this provides an excellent example of “gaugephilic” dark pion interactions, there is no way to formally separate the Goldstone/pion mixing from the dark pion mass itself – both are proportional to the Yukawa coupling y . Consequently, there is no limit where the mixing between the Goldstone and the dark pion can be taken small while simultaneously holding the dark pion mass fixed.

We should emphasize that in the two-flavor chiral model we arrive at Eq. (2.14) through the mixing of the dark pions with the triplet of Goldstone bosons. This mixing was possible only because of the Yukawa term, which is the only allowed renormalizable coupling. Had we included the higher dimensional terms in the chiral lagrangian, we would find that they can still be parameterized by the effective lagrangian Eq. (2.14). In two-flavor vector-like models, which we explore next, the dark pion–Goldstone mixing is not present, however we will still recover Eq. (2.14).

Finally, the absence of π^0 - γ - γ coupling critically relied on the renormalizable coupling between the dark sector and the SM, Eq. (2.21), being custodially symmetric. If there had been an explicit custodial violation of the dark sector with Higgs multiplet, e.g., $y^\psi F\mathcal{H}t_R^3\hat{F}$, the pions would acquire different masses as well as different

mixings with the Goldstones. This would re-introduce $\pi^0 \rightarrow \gamma\gamma$ and a more detailed calculation would be needed to determine the branching fractions of π^0 .

Two-flavor vector-like theories. Vector-like confinement [35] popularized the possibility that a new strong sector contains fermions in vector-like representations so that contributions to electroweak precision corrections are negligible, and (bare) vector-like masses for the dark fermions are allowed. There are two versions of two-flavor vector-like theories, shown in Table 2, depending on whether the dark fermions transform under just $SU(2)_L$ or just $SU(2)_R$. We will refer to these as the “ $SU(2)_L$ model” and “ $SU(2)_R$ model”, respectively.

$SU(2)_L$ model		$SU(2)_R$ model	
Field	$(SU(N_D), SU(2)_L, SU(2)_R)$	Field	$(SU(N_D), SU(2)_L, SU(2)_R)$
F	$(\mathbf{N}, \mathbf{2}, \mathbf{1})$	F	$(\mathbf{N}, \mathbf{1}, \mathbf{2})$
\hat{F}	$(\overline{\mathbf{N}}, \mathbf{2}, \mathbf{1})$	\hat{F}	$(\overline{\mathbf{N}}, \mathbf{1}, \mathbf{2})$

Table 2. Two-flavor fermion content of $SU(2)_L$ and $SU(2)_R$ vector-like theories.

Vector-like theories permit dark fermion masses,

$$\mathcal{L}_{\text{mass}} = MF\hat{F} + h.c.. \quad (2.33)$$

The global $SU(2)_{\text{fund}} \times SU(2)_{\text{anti}}$ symmetries are broken to $SU(2)_V$ that is identified either with the fully gauged $SU(2)_L$ or $SU(2)_R$ (with, as usual, just $U(1)_Y$ gauged).

Now we begin to add interactions between the dark fermions and the SM fields, working in a $SU(2)_L \times SU(2)_R$ invariant manner. Unlike the two-flavor chiral model, in the vector-like models we cannot write a renormalizable interaction between F, \hat{F} and \mathcal{H} . To write down interactions between the Higgs and the dark fermions, we need to consider higher dimensional operators. Both the $SU(2)_L$ and $SU(2)_R$ vector-like

models theories allow the “singlet” contribution at dimension-5

$$c_{5M} \frac{(F\hat{F})\text{Tr } \mathcal{H}^\dagger \mathcal{H}}{\Lambda} + h.c. \quad (2.34)$$

The $(F\hat{F})$ part and the $\text{Tr } \mathcal{H}^\dagger \mathcal{H}$ are singlets that are separately invariant under their respective global symmetries. After electroweak symmetry breaking, this operator leads to a $\sim v^2/\Lambda$ contribution to the dark fermion masses but does not influence their decays. This is because the first non-zero interactions arising from expanding out Eq. (2.34) must contain a singlet, i.e., at least two dark pions.

Hence, to find an operator contributing to dark pion decay we need to go beyond dimension-5. We seek a non-singlet contraction of F and \hat{F} . In the case of the $SU(2)_L$ model, this is $Ft_L^a \hat{F}$. In the case of the $SU(2)_R$ model, invariance under the full $SU(2)_R$ allows just $Ft_R^a \hat{F}$. Of course given that just $U(1)_Y$ is gauged, the term $Ft_R^3 \hat{F}$ is gauge-invariant but not $SU(2)_R$ invariant. If we insist that the dark sector preserves custodial $SU(2)$, this combination is forbidden.

In the Standard Model, there are no dimension-3 operators of the form $Qt_L^a Q'$ since, of course, the SM fermions transform under a chiral representation of the electroweak group. By dimension-4 we can write, e.g., $QLt_L^a \mathcal{H} \hat{Q}_R$, which can be combined with the $Ft_{L,R}^a \hat{F}$ from the dark sector to obtain dimension-7 operators including:

$$\begin{aligned} SU(2)_L \text{ model : } \quad \mathcal{L} &= \mathcal{Y}_{ij}^C \frac{(Ft_L^a \hat{F})(Q_{Li} t_L^a \mathcal{H} \frac{1}{2} \hat{Q}_{Rj})}{\Lambda^3} + \mathcal{Y}_{ij}^\phi \frac{(Ft_L^a \hat{F})(Q_{Li} t_L^a \mathcal{H} t_R^3 \hat{Q}_{Rj})}{\Lambda^3}, \\ SU(2)_R \text{ model : } \quad \mathcal{L} &= \mathcal{Y}_{ij}^C \frac{(Ft_R^a \hat{F})(Q_{Li} \mathcal{H} t_R^a \hat{Q}_{Rj})}{\Lambda^3} + \mathcal{Y}_{ij}^\phi \frac{(Ft_R^a \hat{F})(Q_{Li} \mathcal{H} t_R^a t_R^3 \hat{Q}_{Rj})}{\Lambda^3} \end{aligned} \quad (2.35)$$

As we discussed in Sec. II, we have included the SM Yukawa couplings as coefficients to these operators in order to maintain minimal flavor violation.

Focusing on just one generation of SM fermions, these dimension-7 operators become

$$\begin{aligned}
SU(2)_L \text{ model : } \quad \mathcal{L} &= c_{7f} \frac{(Ft_L^a \hat{F})(Q_L t_L^a \mathcal{H} Y_{ud} \hat{Q}_R)}{\Lambda^3}, \\
SU(2)_R \text{ model : } \quad \mathcal{L} &= c_{7f} \frac{(Ft_R^a \hat{F})(Q_L \mathcal{H} t_R^a Y_{ud} \hat{Q}_R)}{\Lambda^3}.
\end{aligned} \tag{2.36}$$

where Y_{ud} is a 2×2 matrix in $SU(2)_R$ space with the form $Y_{ud} = (y_u + y_d)\mathbf{1}_R/2 + (y_u - y_d)t_R^3$. After electroweak symmetry breaking, this operator mixes $(Ft_{L,R}^a \hat{F})$ with a triplet combination of SM fermions $(y_d u_L d_R^c, y_u u_L u_L^c - y_d d_L d_L^c, y_u d_L u_L^c)$. Passing to the non-linear sigma model formalism, the dimension-7 operator becomes

$$\begin{aligned}
SU(2)_L \text{ model : } \quad \mathcal{L} &= c_{7f} \frac{4\pi f^3}{\Lambda^3} (\text{Tr} \Sigma_L t_L^a) Q_L t_L^a \mathcal{H} Y_{ud} \hat{Q}_R \\
SU(2)_R \text{ model : } \quad \mathcal{L} &= c_{7f} \frac{4\pi f^3}{\Lambda^3} (\text{Tr} \Sigma_R t_R^a) Q_L \mathcal{H} t_R^a Y_{ud} \hat{Q}_R,
\end{aligned} \tag{2.37}$$

where $\Sigma_{L,R}$ is in terms of the $SU(2)_{L,R}$ generators, $\Sigma_{L,R} = \exp[i2\pi^a t_{L,R}^a/f]$. Notice that Σ_L transforms as an adjoint under the $SU(2)_V$ [that is fully gauged as $SU(2)_L$], hence the combination $\text{Tr} \Sigma_L t_L^a$ expands to π^a/f to leading order in π^a . Using this expansion, we obtain the interactions:

$$\begin{aligned}
\pi_{\text{phys}}^\pm \bar{f}' f : \quad & \sqrt{2} (m_{f'} P_L - m_f P_R) (2T_3^f) \times (c_{7f} \frac{\sqrt{2}\pi f^2}{\Lambda^3}) \\
\pi_{\text{phys}}^0 \bar{f} f : \quad & i (m_f \gamma_5) (2T_3^f) \times (c_{7f} \frac{\sqrt{2}\pi f^2}{\Lambda^3})
\end{aligned} \tag{2.38}$$

From this we can identify

$$\frac{1}{v_\pi} = c_{7f} \frac{\sqrt{2}\pi f^2}{\Lambda^3} \tag{2.39}$$

Notice that the interactions are otherwise identical regardless of whether the underlying theory is $SU(2)_L$ or $SU(2)_R$.

If we extend the effective theory to even higher dimension operators, we encounter operators involving the triplet combination $Ft_{L,R}^a \hat{F}$ with the Higgs multiplet. The lowest dimension operator involving $Ft_{L,R}^a \hat{F}$ and custodially symmetric contractions

of powers of \mathcal{H} occurs at dimension-9:

$$\begin{aligned}
SU(2)_L \text{ model : } \quad \mathcal{L} &= c_{9C} \epsilon_{abc} \delta_{de} \frac{(F t_L^a \hat{F}) \text{Tr} [(D_\mu \mathcal{H})^\dagger t_L^b (D^\mu \mathcal{H}) t_R^d \mathcal{H}^\dagger t_L^c \mathcal{H} t_R^e]}{\Lambda^5} \\
SU(2)_R \text{ model : } \quad \mathcal{L} &= c_{9C} \epsilon_{abc} \delta_{de} \frac{(F t_R^a \hat{F}) \text{Tr} [(D_\mu \mathcal{H})^\dagger t_L^d (D^\mu \mathcal{H}) t_R^b \mathcal{H}^\dagger t_L^e \mathcal{H} t_R^c]}{\Lambda^5} \quad (2.40)
\end{aligned}$$

Passing to the low energy effective theory, the non-linear sigma model acquires the same kinetic and mass terms as in Eq. (2.83) with an interaction term

$$\begin{aligned}
SU(2)_L \text{ model : } \quad \mathcal{L} &= c_{9C} \frac{4\pi f^3}{\Lambda^5} \epsilon_{abc} \delta_{de} \text{Tr} [\Sigma_L t_L^a] \text{Tr} [(D_\mu \mathcal{H})^\dagger t_L^b (D^\mu \mathcal{H}) t_R^d \mathcal{H}^\dagger t_L^c \mathcal{H} t_R^e] \\
SU(2)_R \text{ model : } \quad \mathcal{L} &= c_{9C} \frac{4\pi f^3}{\Lambda^5} \epsilon_{abc} \delta_{de} \text{Tr} [\Sigma_R t_R^a] \text{Tr} [(D_\mu \mathcal{H})^\dagger t_L^d (D^\mu \mathcal{H}) t_R^b \mathcal{H}^\dagger t_L^e \mathcal{H} t_R^c]
\end{aligned}$$

where $\Sigma_{L,R}$ is as before. Expanding the interaction in unitary gauge to leading order in π^a we obtain:

$$\mathcal{L} = c_{9C} \frac{\pi f^2}{16\Lambda^5} (v+h)^3 \left[g W_\mu^\mp (\pi^\pm \partial^\mu h - h \partial^\mu \pi^\pm) + \sqrt{g^2 + g'^2} Z_\mu (\pi^0 \partial^\mu h - h \partial^\mu \pi^0) \right] \quad (2.42)$$

and thus the couplings are

$$\begin{aligned}
(\pi_{\text{phys}}^\pm \partial_\mu h - h \partial_\mu \pi_{\text{phys}}^\pm) W^{\mu,\mp} : \quad & M_W \times \left(c_{9C} \frac{\pi f^2}{\Lambda^3} \right) \times \left(\frac{v^2}{8\Lambda^2} \right) \\
(\pi_{\text{phys}}^0 \partial_\mu h - h \partial_\mu \pi_{\text{phys}}^0) Z^\mu : \quad & M_Z \times \left(c_{9C} \frac{\pi f^2}{\Lambda^3} \right) \times \left(\frac{v^2}{8\Lambda^2} \right) \quad (2.43)
\end{aligned}$$

Compare to the fermion couplings, we then obtain

$$\frac{1}{v_\pi} = c_{7f} \frac{\sqrt{2}\pi f^2}{\Lambda^3}, \quad \xi = \left(\frac{c_{9C}}{c_{7f}} \right) \times \left(\frac{v^2}{8\sqrt{2}\Lambda^2} \right). \quad (2.44)$$

The single dark pion interactions with the Standard Model can be precisely characterized by the effective lagrangian Eq. (2.14). Unlike the two-flavor chiral model, in the vector-like models there is no Goldstone/dark pion mixing connecting the dark sector with the Standard Model. Instead, this is fully characterized by the higher dimensional interactions that, by assumption, preserve custodial $SU(2)$.

Notice also that the coefficient of the π - V - h interaction is *suppressed* relative to the π - f - f interaction by an amount $\xi \propto v^2/\Lambda^2$. In this particular model, the suppression arises because custodial symmetry demanded that operators involving the Higgs multiplets appear at a dimension that is *two powers* higher than that for SM fermions. Thus, dark pions preferentially interact with (and ultimately decay primarily to) SM fermions – these theories are gaugephobic – in two-flavor, vector-like, custodially-preserving dark sector theories.

Four-flavor theories

The main disadvantage to limiting ourselves to two flavors of fermions is that we are forced to choose between either having chiral masses or vector-like masses for fermions at the renormalizable level. With four flavors, we can engineer the electroweak quantum numbers to permit both vector-like and chiral masses, governed by Lagrangian parameters that are fully adjustable.

Large chiral masses with small vector-like masses will tend to cause the dark sector to substantially break electroweak symmetry (and violate bounds from the S parameter as well as Higgs coupling measurements). Therefore, we focus on the opposite case – the parameter space where the dark sector fermion masses are *mostly* vector-like with small chiral masses where $yv/M \ll 1$. In this way, these theories are automatically safe from electroweak precision constraints and Higgs coupling measurements. Yet, the presence of both vector-like and small chiral masses in general means that the dark sector flavor symmetries are broken to $SU(2)_L \times SU(2)_R \times U(1)_{\text{dark baryon}}$. The existence of baryons stabilized by the accidental $U(1)_{\text{dark baryon}}$ was exploited by the Stealth Dark Matter model [106]. In that theory, with $N(\geq 4, \text{even})$, the lightest baryon was shown to be a viable dark

Field	$(SU(N_D), SU(2)_L, SU(2)_R)$
F_L	$(\mathbf{N}, \mathbf{2}, \mathbf{1})$
\hat{F}_L	$(\overline{\mathbf{N}}, \mathbf{2}, \mathbf{1})$
F_R	$(\mathbf{N}, \mathbf{1}, \mathbf{2})$
\hat{F}_R	$(\overline{\mathbf{N}}, \mathbf{1}, \mathbf{2})$

Table 3. Four-flavor, custodially-symmetric dark sector fermion content.

matter candidate. In this paper, we focus solely on the mesons of the dark sector that was of only peripheral interest in the dark matter papers.

The field content of our prototype four-flavor, custodially-symmetric theory is given in Table 3. At dimension-3, the vector-like masses for the dark fermions are

$$\mathcal{L} = M_{12}F_L\hat{F}_L + M_{34}F_R\hat{F}_R + h.c.. \quad (2.45)$$

At dimension-4, the chiral masses for the dark fermions are

$$\mathcal{L} = y_{14}F_L\mathcal{H}\hat{F}_R + y_{23}\hat{F}_L\mathcal{H}F_R + h.c.. \quad (2.46)$$

With fully general M_{12} , M_{34} , y_{14} , y_{23} , and the gauging of $SU(2)_L \times U(1)_Y$, we see that vector-like and chiral masses arise at the renormalizable level, unlike the case of the two-flavor theories.³ We could also include higher dimensional operators that we considered earlier in Sec. II. But like the two-flavor chiral theory, we anticipate the renormalizable interactions with the SM Higgs sector above will dominate over the higher dimensional ones, and so we won't consider them further in this section.

³We have switched notation $(F_1, F_2, F_3, F_4) \rightarrow (F_L, \hat{F}_L, F_R, \hat{F}_R)$ but retained the same mass and Yukawa coupling parameter names as Ref. [106].

After electroweak symmetry breaking, the mass matrix for the dark fermions can be written in a fully Higgs field-dependent way as

$$\mathcal{L}_{\text{mass}} = - \begin{pmatrix} F_L^u & -iF_L^d & F_R^u & -iF_R^d \end{pmatrix} \mathcal{M} \begin{pmatrix} \hat{F}_L^d \\ -i\hat{F}_L^u \\ \hat{F}_R^d \\ -i\hat{F}_R^u \end{pmatrix} + h.c., \quad (2.47)$$

where

$$\mathcal{M} = \begin{pmatrix} M_{12} & 0 & \frac{y_{23}(-iG^0+h+v)}{\sqrt{2}} & -iy_{23}G^+ \\ 0 & M_{11} & -iy_{23}G^- & \frac{y_{23}(iG^0+h+v)}{\sqrt{2}} \\ \frac{y_{14}(iG^0+h+v)}{\sqrt{2}} & iy_{14}G^+ & M_{34} & 0 \\ iy_{14}G^- & \frac{y_{14}(-iG^0+h+v)}{\sqrt{2}} & 0 & M_{34} \end{pmatrix} \quad (2.48)$$

The field-independent mass terms break up into two 2×2 mass matrices – one for the $Q = +1/2$ fermions and one for the $Q = -1/2$ fermions that are identical due to custodial symmetry. It is very convenient to rewrite $y_{14} = y(1 + \epsilon)$ and $y_{23} = y(1 - \epsilon)$ since, as we will see, contributions to electroweak precision observables is proportional to $(\epsilon y)^2$. Using this parameterization, the 2×2 mass matrices are

$$M_u = M_d = \begin{pmatrix} M_{12} & y(1 - \epsilon)v/\sqrt{2} \\ y(1 + \epsilon)v/\sqrt{2} & M_{34} \end{pmatrix}. \quad (2.49)$$

The mass matrix can be diagonalized by a biunitary transformation involving

$$\begin{aligned} \tan 2\theta_1 &= -\frac{\sqrt{2}yv(\Delta\epsilon - M)}{2\Delta M + \epsilon y^2 v^2} \\ \tan 2\theta_2 &= \frac{\sqrt{2}yv(\Delta\epsilon + M)}{2\Delta M - \epsilon y^2 v^2} \end{aligned} \quad (2.50)$$

where $M \equiv (M_{12} + M_{34})/2$, $\Delta \equiv (M_{34} - M_{12})/2$, and θ_1 (θ_2) diagonalizes $M_u M_u^T$ ($M_d^T M_d$). The diagonalized fermion masses are

$$m_{1,2} = M \mp \sqrt{\Delta^2 + \frac{y^2(1 - \epsilon^2)v^2}{2}}. \quad (2.51)$$

We can use these results to rotate Eq. (2.47) into the mass basis. The field-independent parts of the mass matrix are, of course, fully diagonalized. But the field-dependent ones are not. We need the field-dependence to determine the dark pion / Goldstone mixing.

Passing to the non-linear sigma model, we use

$$\Sigma = \exp \left[\frac{2i\pi^a t_{15}^a}{f} \right], \quad (2.52)$$

where the π^a are in the adjoint representation of $SU(4)_V$. Decomposing π^a into multiplets of $SU(2)_L \times SU(2)_R$, we have

$$\mathbf{15} \rightarrow (\mathbf{3}, \mathbf{1}) \oplus (\mathbf{2}, \mathbf{2})_a \oplus (\mathbf{2}, \mathbf{2})_b \oplus (\mathbf{1}, \mathbf{3}) \oplus (\mathbf{1}, \mathbf{1}), \quad (2.53)$$

where a and b are two separate bi-doublets. After rotating into the mass eigenstates of the dark mesons, we have

$$\Sigma = \exp \left[\frac{i}{f} \begin{pmatrix} \pi_1^0 + \frac{\eta}{\sqrt{2}} & \sqrt{2}\pi_1^+ & K_A^0 & -\sqrt{2}K_B^+ \\ \sqrt{2}\pi_1^- & -\pi_1^0 + \frac{\eta}{\sqrt{2}} & -\sqrt{2}K_A^- & K_B^0 \\ \bar{K}_A^0 & -\sqrt{2}K_A^+ & \pi_2^0 - \frac{\eta}{\sqrt{2}} & \sqrt{2}\pi_2^+ \\ -\sqrt{2}K_B^- & \bar{K}_B^0 & \sqrt{2}\pi_2^- & -\pi_2^0 - \frac{\eta}{\sqrt{2}} \end{pmatrix} \right] \quad (2.54)$$

where we use $\pi_{1,2}$ to denote the dark pions transforming as $(\mathbf{3}, \mathbf{1})$ and $(\mathbf{1}, \mathbf{3})$, $K_{A,B}$ to denote the “dark kaons” that are in $(\mathbf{2}, \mathbf{2})$ representations, and η to denote the “dark eta” singlet.

The lowest dimension terms in the NLSM lagrangian are:

$$\mathcal{L}_\chi = \frac{f^2}{4} \text{Tr}(D_\mu \Sigma (D^\mu \Sigma)^\dagger) + 4\pi c_D f^3 \text{Tr}(L \mathcal{M} R^\dagger \Sigma^\dagger + h.c.), \quad (2.55)$$

where c_D is an $\mathcal{O}(1)$ coefficient from the strong dynamics. As we discussed in Sec. II, these terms are sufficient to capture the leading interactions of the dark pions, and in particular, will allow us to characterize the single dark pion interactions with the SM that lead to dark pion decay. The mixing matrices are formed from the angles

Eq. (2.50)

$$\mathcal{L} = \begin{pmatrix} \cos \theta_1 & 0 & -\sin \theta_1 & 0 \\ 0 & \cos \theta_1 & 0 & -\sin \theta_1 \\ \sin \theta_1 & 0 & \cos \theta_1 & 0 \\ 0 & \sin \theta_1 & 0 & \cos \theta_1 \end{pmatrix} \quad (2.56)$$

$$\mathcal{R} = \begin{pmatrix} \cos \theta_2 & 0 & -\sin \theta_2 & 0 \\ 0 & \cos \theta_2 & 0 & -\sin \theta_2 \\ \sin \theta_2 & 0 & \cos \theta_2 & 0 \\ 0 & \sin \theta_2 & 0 & \cos \theta_2 \end{pmatrix}. \quad (2.57)$$

In the field-independent limit,

$$\mathcal{L}\mathcal{M}\mathcal{R}^\dagger = \begin{pmatrix} m_1 & 0 & 0 & 0 \\ 0 & m_1 & 0 & 0 \\ 0 & 0 & m_2 & 0 \\ 0 & 0 & 0 & m_2 \end{pmatrix}, \quad (2.58)$$

and so the dark pion masses are

$$m_{\pi_1} = 4\pi c_D f(2m_1) \quad (2.59)$$

$$m_K = 4\pi c_D f(m_1 + m_2) \quad (2.60)$$

$$m_{\pi_2} = 4\pi c_D f(2m_2). \quad (2.61)$$

Finally, the covariant derivative for Σ involves the weak currents

$$D_\mu \Sigma = \partial_\mu \Sigma - i g W_\mu^\alpha (j_\alpha^V + j_\alpha^A) \Sigma - i g' B_\mu (j_Y^V + j_Y^A) \Sigma \quad (2.62)$$

where it is convenient to express the vector and axial currents explicitly

$$j_\alpha^{V,A} = \mathcal{L}^\dagger t^\alpha \mathcal{L} \pm \mathcal{R}^\dagger t^\alpha \mathcal{R} \quad (\alpha = 1 \dots 3) \quad (2.63)$$

$$j_Y^{V,A} = \mathcal{L}^\dagger t^{15} \mathcal{L} \pm \mathcal{R}^\dagger t^{15} \mathcal{R}. \quad (2.64)$$

Expanding the covariant derivatives to extract only the non-derivative contributions – the mass terms for W^μ and Z^μ – we find the contributions of the dark sector to electroweak symmetry breaking for two flavors:

$$v_{246}^2 = v^2 \left(1 + \frac{\epsilon^2 y^2 f^2}{M^2} + \dots \right). \quad (2.65)$$

Here we have written the leading result in a small ϵ expansion. Obviously the correction from the dark sector, $\epsilon^2 y^2 f^2 / M^2$, should be small to avoid constraints from the electroweak precision observables as well as Higgs coupling measurements. In particular, the dark sector's contribution to the S parameter can be estimated [106] utilizing QCD and large N_D ,

$$S \sim \frac{1}{6\pi} N_F N_D \left(\frac{\epsilon y f}{M} \right)^2 \simeq 0.1 \frac{N_F}{4} \frac{N_D}{4} \left(\frac{\epsilon y}{0.3} \right)^2 \left(\frac{f}{M} \right)^2 \quad (2.66)$$

Since $M < 4\pi f$ for the NLSM effective theory to be valid, in general we need $|\epsilon y|$ small to ensure the dark sector condensate is aligned nearly (but not completely) in an electroweak preserving direction.

While Eq. (2.65) is reminiscent of Eq. (2.29) in the two-flavor chiral case, there are some crucial differences. In Eq. (2.29), we could not take f – the EWSB contribution from the strong sector – to be arbitrarily small without making the dark pions dangerously light. As a result, there is a minimum f that we can take, and therefore a minimum deviation in Higgs coupling and precision electroweak observables, see Ref. [24]. In the four flavor case, we have more freedom. The fact that the fermions are vector-like means we can take f (more correctly yf) as small as we like without worrying about m_{π_D} . This allows us to explore a parameter space where the renormalizable coupling between the Higgs and the dark sector has negligible role on EWSB yet still acts as a portal for the dark pions to decay through.

Mixing with the Higgs and Goldstones. We have chosen a basis for our dark pions such that they do not acquire an expectation value. This is evident by expanding the linear term, Eq. (2.55), where one finds no terms linear in the dark pion fields, i.e., contributions of the form $\mathcal{L} \subset (\text{constant})\pi$ are absent.

There are, however, dark pion mixing terms with both the Higgs field h and (prior to gauge-fixing) the Higgs Goldstone fields G^\pm, G^0 . Disentangling the mixing among the Higgs and dark pion fields is somewhat involved, and in full generality would need to be done numerically. In the following, we have calculated the mixing to leading order in ϵy , where we can obtain analytic expressions. Since we know ϵy must in general be small to ensure electroweak symmetry breaking occurs mostly from the fundamental Higgs field, this is a good choice of an expansion parameter.

One unique combination of the dark pion fields mixes with the Higgs boson h ,

$$4\pi c_D f^3 \text{Tr} (\mathcal{L} \mathcal{M} \mathcal{R}^\dagger \Sigma^\dagger + h.c.) \subset 4\sqrt{2}\pi c_D \epsilon y f^2 h \text{Im}(K_A^0 + K_B^0). \quad (2.67)$$

This will turn out to be *critical* to understand the effective couplings of the lightest dark pions to the SM gauge sector.

The dark pions also mix with the Higgs Goldstones,

$$4\pi c_D f^3 \text{Tr} (\mathcal{L} \mathcal{M} \mathcal{R}^\dagger \Sigma^\dagger + h.c.) \subset \frac{8\pi c_D f^2 \epsilon y}{M} \left[\left(G^- (s_m (2m_1 \pi_1^+ - 2m_2 \pi_2^+) + c_m (m_1 + m_2) (K_A^+ - K_B^+)) + h.c. \right) + G^0 (s_m (2m_1 \pi_1^0 - 2m_2 \pi_2^0) + c_m (m_1 + m_2) \text{Re}(K_A^0 - K_B^0)) \right], \quad (2.68)$$

where

$$s_m \equiv \sin \theta_m \equiv \frac{\sqrt{2} y v}{\sqrt{2(yv)^2 + 4\Delta^2}} \quad (2.69)$$

$$c_m \equiv \cos \theta_m \equiv \frac{2\Delta}{\sqrt{2(yv)^2 + 4\Delta^2}}, \quad (2.70)$$

are mixing angles among combinations of the dark pions. The dark pion / Goldstone mass mixing can be perturbatively diagonalized to leading order in ϵy ,

$$G_{\text{phys}}^{\pm,0} = G^{\pm,0} + \frac{\epsilon y f}{M} (s_m (\pi_1^{\pm,0} - \pi_2^{\pm,0}) + c_m \text{Re}(K_A - K_B)) \quad (2.71)$$

$$\pi_{1,\text{phys}}^{\pm,0} = \pi_1^{\pm,0} + \frac{\epsilon y f}{M} s_m G^{\pm,0} \quad (2.72)$$

$$\pi_{2,\text{phys}}^{\pm,0} = \pi_2^{\pm,0} - \frac{\epsilon y f}{M} s_m G^{\pm,0} \quad (2.73)$$

$$\frac{\text{Re}(K_{A,\text{phys}}^{\pm,0} - K_{B,\text{phys}}^{\pm,0})}{\sqrt{2}} = \frac{\text{Re}(K_A^{\pm,0} - K_B^{\pm,0})}{\sqrt{2}} + \frac{\epsilon y f}{M} c_m G^{\pm,0} \quad (2.74)$$

$$\frac{\text{Re}(K_{A,\text{phys}}^{\pm,0} + K_{B,\text{phys}}^{\pm,0})}{\sqrt{2}} = \frac{\text{Re}(K_A^{\pm,0} + K_B^{\pm,0})}{\sqrt{2}}. \quad (2.75)$$

In addition, diagonalizing the Higgs boson / dark pion mixing one obtains

$$h_{\text{phys}} = h - \frac{\epsilon y f m_K}{M} \frac{\text{Im}(K_A^0 + K_B^0)}{m_h^2 - m_K^2} \quad (2.76)$$

$$\text{Im}(K_{A,\text{phys}}^0 + K_{B,\text{phys}}^0) = \text{Im}(K_A^0 + K_B^0) + \frac{\epsilon y f m_K}{M} \frac{h}{m_h^2 - m_K^2} \quad (2.77)$$

where m_K is given by Eq. (2.60).

Dark Pion Couplings to the SM. We now calculate the couplings of dark pions to the gauge sector of the Standard Model. These couplings arise when the interaction eigenstates (G , π , K) are rotated into the physical states (G_{phys} , π_{phys} , K_{phys}). Gauge-fixing in unitary gauge removes all terms involving G_{phys} , leaving just the interactions with the “physical” (mass eigenstate) dark pions.

It is clear from Eqs. (2.51) that a non-zero Yukawa coupling necessarily splits the fermion masses, and thus there is always some (possibly small) mass hierarchy between π_1 , K , and π_2 (and η), see Eqs. (2.59)–(2.61). While it is straightforward to calculate the couplings of all of the dark pions to the Standard Model, here we focus only on the lightest pions. For instance, strong decays of $\pi_{\text{heavy}}, K \rightarrow \pi_{\text{light}} + X$ are expected to be rapid so long as the dark pion mass differences are large enough that phase space does not severely limit their rates.

The two-pion interactions with the SM gauge sector take the form

$$W^{\mu,\mp} (\pi_{\text{phys}}^{\pm} \partial_{\mu} \pi_{\text{phys}}^0 - \pi_{\text{phys}}^0 \partial_{\mu} \pi_{\text{phys}}^{\pm}) : = g \frac{1 + c_m}{2}. \quad (2.78)$$

Several limits are interesting. First, for $\Delta > 0$ and $\Delta \gg yv$, then $c_m \simeq 1$, and so the coupling of the dark pions to the gauge bosons becomes $\simeq g$ – exactly the coupling expected for three $SU(2)_L$ -triplets to interact via the $SU(2)$ anti-symmetric tensor contraction. This is not surprising – in this limit the lightest pions are a nearly exactly an $SU(2)_L$ triplet with only $(yv)/\Delta$ -suppressed mixings into the other dark pions.

Next consider $\Delta < 0$, while still $|\Delta| \gg yv$. Now $c_m \simeq -1$, and the coupling of the dark pions to the gauge bosons becomes $\simeq 0$. This is again unsurprising – in this limit the lightest pions are a nearly exact $SU(2)_R$ triplet that does not couple with $SU(2)_L$ gauge bosons.

Finally, when $\Delta \ll yv$ (and thus $c_m \simeq 0$) the splittings among the dark pions are dominated by electroweak symmetry breaking contributions. In this case, the would-be $SU(2)_L$ triplet and $SU(2)_R$ triplets are fully mixed, and each share an approximately $g/2$ coupling to $SU(2)_L$ gauge bosons.

Single pion interactions with one gauge boson and one Higgs boson are the most interesting (and most relevant for pion decay). We obtain:

$$\begin{aligned} (\pi_{\text{phys}}^{\pm} \partial_{\mu} h - h \partial_{\mu} \pi_{\text{phys}}^{\pm}) W^{\mu,\mp} : & \quad \frac{M_W}{v} \times \left(\sqrt{2} c_D \epsilon y s_m \frac{4\pi f^2}{m_K^2} \right) \times \left(\frac{m_h^2}{m_K^2 - m_h^2} \right) \\ (\pi_{\text{phys}}^0 \partial_{\mu} h - h \partial_{\mu} \pi_{\text{phys}}^0) Z^{\mu} : & \quad \frac{M_Z}{v} \times \left(\sqrt{2} c_D \epsilon y s_m \frac{4\pi f^2}{m_K^2} \right) \times \left(\frac{m_h^2}{m_K^2 - m_h^2} \right) \\ \pi_{\text{phys}}^{\pm} \bar{f}' f : & \quad \sqrt{2} \left(\frac{m_{f'}}{v} P_L - \frac{m_f}{v} P_R \right) (2T_3^f) \times \left(\sqrt{2} c_D \epsilon y s_m \frac{4\pi f^2}{m_K^2} \right) \\ \pi_{\text{phys}}^0 \bar{f} f : & \quad i \left(\frac{m_f}{v} \gamma_5 \right) (2T_3^f) \times \left(\sqrt{2} c_D \epsilon y s_m \frac{4\pi f^2}{m_K^2} \right) \end{aligned} \quad (2.79)$$

From these expressions, we can identify

$$\frac{1}{v_{\pi}} = \frac{1}{v} \times \left(\sqrt{2} c_D \epsilon y s_m \frac{4\pi f^2}{m_K^2} \right), \quad \xi = \frac{m_h^2}{m_K^2 - m_h^2} \quad (2.80)$$

This is the main result for the four-flavor theory. We find that the pion interactions with the gauge bosons and Higgs boson are suppressed relative to the fermion couplings by a factor $m_h^2/(m_K^2 - m_h^2)$ that becomes roughly m_h^2/m_K^2 for larger dark kaon masses. This relative suppression in gauge/Higgs boson couplings to the fermion couplings is exactly what happened in the two-flavor, custodially-symmetric model.

The four-flavor model is, essentially, one ultraviolet completion of the two-flavor theory with higher-dimensional operators that are both custodially symmetric and minimal flavor violating. The dimension-7 operators that lead to interactions with the fermions are matched at $\Lambda^3 = 4\pi f m_K^2$; the dimension-9 operator that leads to the interactions with the gauge bosons and Higgs boson is matched at $\Lambda^5 = 4\pi f^3 m_K^2$; with the coefficient $c_{9C} \propto \lambda_h$ the quartic coupling of the Higgs sector.

Dark Sector Custodial Violation

We have focused on dark sectors that preserve custodial $SU(2)$. In practice this means that renormalizable and higher dimensional operators involving dark fermions do not involve explicit t_R^3 – this only appears from the custodially violating SM spurions proportional to $g'Y$ or \mathcal{Y}_{ij}^ϕ .

Naturally, it is interesting to consider what happens when explicit t_R^3 is introduced. In the $SU(2)_R$ model, this is possible already at the renormalizable level. One can include $M'Ft_R^3\hat{F}$ in addition to $MF\hat{F}$. This is equivalent to simply writing different dark fermion masses for the $Y = +1/2$ and $Y = -1/2$ states under $U(1)_Y$.

In the $SU(2)_L$ model, gauge invariance forbids a dimension-3 term violating custodial $SU(2)$. At dimension-5 there is an interaction:

$$\mathcal{L} = c_{5V} \frac{(F_1 t_L^a F_2) \text{Tr } \mathcal{H}^\dagger t_L^a \mathcal{H} t_R^3}{\Lambda} \quad (2.81)$$

that violates custodial $SU(2)$. With two Higgs bifundamentals, the group contractions are

$$(\mathbf{2}_L, \mathbf{2}_R) \otimes (\mathbf{2}_L, \mathbf{2}_R) = (\mathbf{1}_L, \mathbf{1}_R) \oplus (\mathbf{3}_L, \mathbf{3}_R) \quad (2.82)$$

where the surviving combinations are precisely those in Eqs. (2.34),(2.81). (The would-be $(\mathbf{3}_L, \mathbf{1}_R)$ or $(\mathbf{1}_L, \mathbf{3}_R)$ involves $\text{Tr } \mathcal{H}^\dagger t_{L,R}^a \mathcal{H}$ that simply vanishes.) The only way we can write a gauge-invariant term of the form Eq. (2.81) is to use t_R^3 of $SU(2)_R$, and hence is custodially violating.

The low energy effective theory including higher dimensional operators up to $\mathcal{O}(v^2/\Lambda)$ can again be described by a non-linear sigma model,

$$\begin{aligned} \mathcal{L} = & \frac{f^2}{4} \text{Tr} (D_\mu \Sigma)^\dagger D^\mu \Sigma + 4\pi f^3 \left(M + c_{5M} \frac{v^2}{\Lambda} \right) \text{Tr} (\Sigma^\dagger + h.c.) \\ & + c_{5V} \frac{4\pi f^3}{\Lambda} \text{Tr} (\Sigma_L t_L^a) \text{Tr} (\mathcal{H}^\dagger t_L^a \mathcal{H} t_R^3 + h.c.) \end{aligned} \quad (2.83)$$

Expanding the non-linear sigma model up to $\mathcal{O}(\pi^2)$, we obtain

$$\mathcal{L} = \text{Tr} D_\mu \pi^a D^\mu \pi^a - \frac{1}{2} m_\pi^2 \pi^a \pi^a - c_{5V} \frac{4\pi f^2}{\Lambda} H^\dagger \pi^a t_L^a H \quad (2.84)$$

where $m_\pi^2 = 4\pi f(M + \mathcal{O}(v^2/\Lambda))$, and we have written the single pion – Higgs interaction in the more familiar form using Higgs doublet notation. This Lagrangian is precisely that of a “crappy triplet model”⁴, e.g. [171]. That is, the two-flavor $SU(2)_L$ dark sector with a dimension-5 custodially-violating interaction with the SM Higgs sector provides an ultraviolet completion of the SM extended to include a real triplet. Higher order terms in the chiral Lagrangian lead to the usual pion self-interactions as well as interactions of multiple pions with Higgs fields.

In this theory, we see that the dark pion interactions with the SM arise at a comparatively low dimension operator, Eq. (2.81). The explicit custodial violation

⁴“Crappy” in the sense that the linear term for π^a causes it to acquire a custodially-violating vev.

causes the dark pions to acquire a “triplet” vev

$$v_T \equiv \langle \pi^a \rangle \sim c_{5V} \frac{fv^2}{\Lambda M}. \quad (2.85)$$

Obviously this is highly constrained by electroweak precision data. Nevertheless, following Ref. [171] one can proceed as usual, shift to the new vacuum, and extract the effective interactions from Eq. (2.84). The result is that there is a neutral singlet that mixes with the Higgs boson and a charged scalar that mixes with the charged Higgs Goldstones. Diagonalizing these interactions leads to

$$\begin{pmatrix} G_{\text{phys}}^\pm \\ \pi_{\text{phys}}^\pm \end{pmatrix} = \begin{pmatrix} \cos \delta & \sin \delta \\ -\sin \delta & \cos \delta \end{pmatrix} \begin{pmatrix} G^\pm \\ \pi^\pm \end{pmatrix} \quad (2.86)$$

where $\sin \delta \sim v_T / \sqrt{v^2 + v_T^2}$. The interactions of the charged dark pions are obtained by replacing G^+ with π_{phys}^\pm . Just like in the two-flavor chiral model, this leads to gaugephilic branching ratios. However, unlike the two-flavor chiral model, there is no neutral dark pion / neutral Goldstone mixing.

CHAPTER III

LHC PHENOMENOLOGY OF DARK MESONS

In Chapter II we discussed dark sectors whose (ultraviolet) strongly-coupled sector preserves a $SU(2)$ dark flavor symmetry. These theories are mapped into a low energy effective theory that provides the leading interactions of the dark mesons with the Standard Model. In this chapter we further investigate the collider phenomenology of dark mesons. The structure of this chapter is as follows. In Sec. III we introduce our phenomenological dark meson model and its relevant parameters. This model description is broken up into three parts: the strong sector, kinetic mixing, and π_D decay. Using this setup, we explore the constraints on dark meson parameter space. Sec. III is devoted to constraints from single ρ_D production, while we explore constraints from π_D pair production in Sec. III. We step through the details of the searches that provide constraints and provide insight into why other searches fail to. Finally, we present our conclusions in Sec. V.

Phenomenological Description of Dark Mesons

The dark meson interactions will be described below using a phenomenological lagrangian. The core philosophy was formulated in “vector-like confinement” [35, 37], and our discussion of resonant production of dark pions through a dark rho parallels theirs. The key distinction between our formulation and vector-like confinement is the presence of Higgs interactions among the dark fermions which breaks enough of the dark flavor symmetries to allow dark pions to decay. In the language of vector-like confinement, all species symmetries are broken by Higgs interactions in the dark sector (either Yukawa couplings or higher-dimensional interactions).

Dark Mesons in $SU(2)$ Triplet Representations. The lagrangian can be written as

$$\mathcal{L} = \mathcal{L}_{\text{strong}} + \mathcal{L}_{\text{kinetic mixing}} + \mathcal{L}_{\text{decay}}. \quad (3.1)$$

The first contribution contains the meson sector of the theory as it arises from the strongly-coupled dark sector:

$$\mathcal{L}_{\text{strong}} = -\frac{1}{4}\rho_{D\mu\nu}^a\rho_D^{a\mu\nu} - \frac{m_{\rho_D}^2}{2}\rho_{D\mu}^a\rho_D^{a\mu} \quad (3.2)$$

$$+ \frac{1}{2}(D_\mu\pi_D^a)^\dagger(D^\mu\pi_D^a) - \frac{1}{2}m_{\pi_D}^2\pi_D^a\pi_D^a \quad (3.3)$$

$$- g_{\rho_D\pi_D\pi_D}f^{abc}\rho_{D\mu}^a\pi_D^bD^\mu\pi_D^c, \quad (3.4)$$

It contains the kinetic terms of the vector (ρ_D) and pseudoscalar (π_D) mesons, mass terms, and the interactions among these mesons. As we indicated in the introduction, the mesons fill out representations of the $SU(2)$ dark flavor symmetry, and the meson self-interactions respect the $SU(2)$ dark flavor symmetry. Throughout all of these expressions, we have assumed that the dark sector contains (at least) one set of dark pions and (at least) one set of dark vector mesons in the triplet representation of the $SU(2)$ dark flavor symmetry. Hence the $a = 1, 2, 3$ index attached to π_D^a and ρ_D^a .¹ We will only consider the phenomenological consequences of the lightest triplet dark vector meson (ρ_D^a) and the lightest triplet dark pion (π_D^a).

The coupling between the ρ_D and π_D is show in Eq. (3.4). This is the analogue of $g_{\rho\pi\pi}$ in QCD. In the $SU(2)_R$ model, the full set of $SU(2)_R$ -symmetric interactions are present, though in practice only the $\rho_D^0\pi_D^+\pi_D^-$ interaction is phenomenologically relevant since only ρ_D^0 talks to SM fermions via kinetic mixing (see Sec. III). The NDA estimate of the coupling strength is given by

$$g_{\rho_D\pi_D\pi_D} \approx \frac{4\pi}{\sqrt{N_D}}. \quad (3.5)$$

¹We use ρ_D^3 and ρ_D^0 interchangeably.

Kinetic Mixing of ρ_D with SM. The second term of Eq. (3.1) contains the kinetic mixing of the dark rhos and the electroweak gauge bosons:

$$\mathcal{L}_{\text{kinetic mixing}} = -\frac{\epsilon}{2}\rho_{D\mu\nu}^a F^{a\mu\nu} = \begin{cases} -\frac{\epsilon}{2}\rho_{D\mu\nu}^a W^{a\mu\nu} & SU(2)_L \text{ model} \\ -\frac{\epsilon'}{2}\rho_{D\mu\nu}^0 B^{\mu\nu} & SU(2)_R \text{ model} \end{cases} \quad (3.6)$$

This provides the main ‘‘portal’’ from the Standard Model into the dark sector. There are two cases we detail below: $F^{a\mu\nu}$ identified with $W^{a\mu\nu}$ (the $SU(2)_L$ model), and $F^{a\mu\nu}$ identified with $\delta^{a0}B^{\mu\nu}$ (the $SU(2)_R$ model).

In each of the models defined by Eq. (1.1), all or part of the $SU(2)$ dark flavor symmetry is gauged. In $SU(2)_L$ model, the triplet of global $SU(2)$ is identified as a triplet of the gauged electroweak $SU(2)_L$ group. In the $SU(2)_R$ model, the triplet of global $SU(2)$ is identified as a triplet of the would-be gauged electroweak $SU(2)_R$ group, had the entire $SU(2)_R$ been gauged. Of course the entire $SU(2)_R$ is not gauged – just the $U(1)_B$ subgroup. After electroweak symmetry breaking, $SU(2)_L \times U(1)_B \rightarrow U(1)_{\text{em}}$, the triplet of vector and pseudoscalar mesons of the $SU(2)_L$ and $SU(2)_R$ models have the same electric charges, $Q = (+1, 0, -1)$.

In both models, we use naive dimensional analysis (NDA) to estimate the size of the kinetic mixing:

$$\begin{aligned} \epsilon &\approx \frac{\sqrt{N_D}}{4\pi}g, & SU(2)_L \text{ model} \\ \epsilon' &\approx \frac{\sqrt{N_D}}{4\pi}g' & SU(2)_R \text{ model,} \end{aligned} \quad (3.7)$$

strictly valid for a large number of colors N_D of the confining dark gauge group.

Diagonalizing the kinetic terms leads to a field redefinition of

$$\begin{aligned} W_\mu^a &\rightarrow W_\mu^a - \epsilon \rho_{D\mu}^a & SU(2)_L \text{ model} \\ B_\mu &\rightarrow B_\mu - \epsilon' \rho_{D\mu}^0 & SU(2)_R \text{ model,} \end{aligned} \quad (3.8)$$

at leading order in ϵ . This leads to a ρ_D interaction with the SM fermions with a coupling strength proportional to g^2 or g'^2 ,

$$\mathcal{L}_{\rho_D f \bar{f}} = \begin{cases} \epsilon g \bar{f}_i \bar{\sigma}^{\mu t_{ij}^a} \rho_{D\mu}^a f_j & SU(2)_L \text{ model} \\ \epsilon' Y_f g' \bar{f} \bar{\sigma}^\mu \rho_{D\mu}^0 f & SU(2)_R \text{ model,} \end{cases} \quad (3.9)$$

where $f_{i,j}$ are left-handed SM fermions in the $SU(2)_L$ model, while f are any SM fermions with hypercharge Y_f in the $SU(2)_R$ model.

The difference between the two models is mainly in the kinetic mixing. In the $SU(2)_L$ model, the entire triplet of ρ_D^a mixes with the triplet of W^a bosons. In the $SU(2)_R$ model, only the neutral component of the triplet, ρ_D^0 , mixes with the hypercharge gauge boson. Additionally, the kinetic mixing ϵ has one power of the gauge coupling: g in the $SU(2)_L$ model; g' in the $SU(2)_R$ model. Here we emphasize that while the difference between $g/g' \simeq 2$ may seem small or trivial, $pp \rightarrow \rho$ production is proportional to $3g^4$ in the $SU(2)_L$ model (compared with g'^4 in the $SU(2)_R$ model), and so this leads to a significant difference in the production rates of ρ_D 's in the two models.

Neglecting mass differences among states within the triplets, the strong sector is thus described by three parameters:

$$m_{\pi_D}, m_{\rho_D}, N_D \quad \text{or equivalently} \quad m_{\pi_D}, \eta \equiv \frac{m_{\pi_D}}{m_{\rho_D}}, N_D. \quad (3.10)$$

As our canonical example that we use throughout this paper, we have taken $N_D = 4$ in the bulk of our results below. This choice was motivated by the Stealth Dark Matter model [106]; the phenomenology is broadly similar so long as the number of colors is not excessive. We quantify this in detail below.

Additionally, we will often replace one of the dark meson mass parameters for the ratio $\eta = m_{\pi_D}/m_{\rho_D}$. This ratio is important because it governs how the ρ_D can

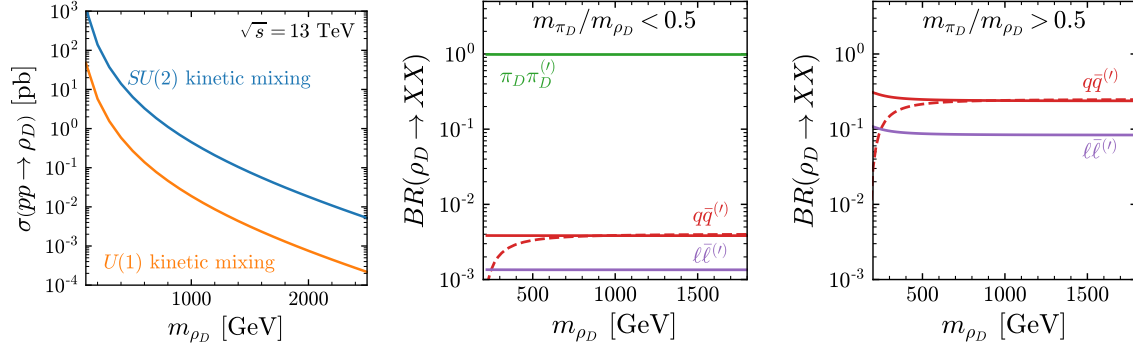


Figure 1. The left panel shows the production cross section at $\sqrt{s} = 13$ TeV for the dark vector mesons. The blue and orange lines depict whether the vector mesons are $SU(2)_L$ or $SU(2)_R$ symmetric and kinetically mix with the appropriate standard model gauge bosons. The middle and right panels show the subsequent branching ratio for the ρ_D depending on whether or not it can decay to the π_D . The red lines denote decays to quark anti-quark pairs, and the dashed line indicates the top quark. The purple lines show leptonic decays.

decay. Specifically, if $\eta < 0.5$, ρ_D can decay to a pair of dark pions, while if $\eta > 0.5$ the dark rhos must decay directly back to SM particles. As we will see, the latter case is strongly constrained by limits from Z', W' searches. From now on, we will label our dark meson models by the type of kinetic mixing and the ratio of dark meson masses, i.e.,

$$\begin{aligned}
 SU(2)_L^\eta &: \quad \epsilon = g\sqrt{N_D}/(4\pi), \quad \epsilon' = 0 \\
 SU(2)_R^\eta &: \quad \epsilon = 0, \quad \epsilon' = g'\sqrt{N_D}/(4\pi)
 \end{aligned}$$

Having specified N_D , the production cross section for ρ_D is completely determined for both models as shown in the left-side plot in Fig. 1. Figure 1 also shows the ρ_D branching ratios for two different η values: as expected, if $\eta < 0.5$ (middle panel) then the interaction strength and form of the $\rho_D\pi_D\pi_D$ interaction make $\rho_D \rightarrow \pi_D\pi_D$. On the other hand, if the π_D are too heavy ($\eta > 0.5$, right plot), the ρ_D decay back through kinetic mixing and the branching ratios are simply determined by the SM color factors.

In focusing on the two models, we are ignoring scenarios where the $SU(2)_L \times U(1)_Y$ properties of the ρ_D [and π_D] are not well defined. Generally, large mixing can only happen in scenarios where the strong sector plays a large role in electroweak breaking and therefore faces constraints from Higgs coupling measurements and precision electroweak tests. In terms of ρ_D phenomenology, having well defined $SU(2)_L \times U(1)_Y$ properties means that the $\rho_D \rightarrow V\pi_D$ ($V = \text{SM electroweak boson}$) decay modes are always small.

We would be remiss to not point out that the $SU(2)_R$ model involving a dark $U(1)$ vector boson mixing between the hypercharge is ubiquitous in the literature of simple dark sectors as “dark photons” (e.g., for a review [172]). While most of this literature focuses on (much) lighter dark photons, for simple dark photon models with a dark photon mass at or above the electroweak scale, we can map this toy model onto a special case of our strongly-coupled dark sector. The mapping utilizes the $SU(2)_R$ model with: $\eta > 0.5$ (so that the dark vector boson can decay only into SM states), m_{SM}/v_π small (so that single production of dark pions is negligible), and the number of dark colors N_D chosen to obtain a kinetic mixing ϵ' . Even with these parameter choices, our strongly-coupled dark sector obviously has differences from the simple toy models. One is that the kinetic mixing is at most one-loop suppressed. Another is that there is relationship between the smallness of the kinetic mixing, the number of dark colors, and the relative size of self-interactions of the dark mesons. While it would be interesting to map out this space more fully, this is beyond the scope of this paper.

Dark Pion Decay to SM. Finally, dark pion decay. This is the main subject of our companion paper [120]. There we show that strongly-coupled models with custodially-symmetric Higgs interactions among the dark fermions leads to a

low energy effective theory in which dark pions interact with the SM through:

$$\begin{aligned} \mathcal{L}_{decay} = & \frac{\sqrt{2}}{v_\pi} \left[\pi_D^+ \bar{\psi}_u (m_d P_R - m_u P_L) \psi_d + \pi_D^- \bar{\psi}_d (m_d P_L - m_u P_R) \psi_u \right. \\ & \left. + \frac{i}{\sqrt{2}} \pi_D^0 (m_u \bar{\psi}_u \gamma_5 \psi_u - m_d \bar{\psi}_d \gamma_5 \psi_d) \right] \\ & - \xi \frac{m_W}{v_\pi} \left[(W_\mu^- h \overleftrightarrow{\partial}^\mu \pi_D^+) + (W_\mu^+ h \overleftrightarrow{\partial}^\mu \pi_D^-) + \frac{1}{\cos \theta_W} (Z_\mu h \overleftrightarrow{\partial}^\mu \pi_D^0) \right] \end{aligned} \quad (11)$$

where $\psi_{u,d}$ are SM fermions. There are several important features of this Lagrangian. First, while we have used the language that the decay interactions ‘break the flavor symmetry’, this is slightly sloppy. Stated more correctly, we have married the $SU(2)_V$ symmetry of the dark pions to part of the $O(4)$ symmetry group of the Higgs potential. Both the dark pions and the SM fields transform under the shared symmetry, so we can write down single pion interactions of the form $\pi^a \mathcal{O}^a$ where \mathcal{O}^a is some triplet of SM fields.

The overall scale of the operators is set by $1/v_\pi$ for the fermions and ξ/v_π for the gauge/Higgs bosons. The fact that the interactions do not further distinguish the fermions (i.e., one overall coupling for the first four terms) nor the gauge/Higgs interactions (one coupling for the last three terms) is due to the the dark sector’s preservation of custodial symmetry. However, since custodial $SU(2)$ is broken in the SM by differences of Yukawa couplings as well as hypercharge, there is a residual differentiation of the interactions by $m_u - m_d$ as well as $g' \neq 0$.

This form is convenient, since coupling π_D to the SM fields requires breaking electroweak symmetry and hence the coupling strengths must be proportional to the mass of a SM field. The primary role of the $1/v_\pi$ parameter is to set the total width of the π_D . In this paper our main focus is on scenarios where the π_D decay promptly. This sets a lower bound on m_{SM}/v_π , where m_{SM} is the mass of the mass of the SM particle(s) in the dominant π_D decay. Scenarios where π_D is displaced or long-lived

are also interesting to study. The main search methodologies are well-known from other displaced/long-lived searches (for a review, see e.g. [173]).

The remaining model-dependent parameter is the relative strength of the coupling to fermions versus the gauge/Higgs sector that we have parameterized by ξ .

We will consider two possibilities for ξ :

$$\begin{array}{ll} \xi = 1 & \text{“gaugephilic”} \\ \xi = c_\xi \frac{v^2}{m_{\pi_D}^2} \ll 1 & \text{“gaugephobic”} \end{array} \quad (3.12)$$

The scaling of the gaugephobic parameter with the electroweak scale and the dark pion mass scale deserves some discussion. The origin of this scaling is found from an analysis of the strongly-coupled effective theories that we have discussed in detail in Ref. [120]. In essence, there are higher dimensional operators involving additional Higgs fields, suppressed by at least the scale of the dark pions, that can regenerate couplings to the gauge/Higgs sector even if they don’t exist at leading order. As we show in Ref. [120], the Stealth Dark Matter model is gaugephobic with $\xi = m_h^2/(m_{K_D}^2 - m_h^2) \simeq m_h^2/m_{K_D}^2$ where K_D is another dark pion that is at least slightly heavier than π_D . Since the dark kaon scales with the parameters of the ultraviolet theory in exactly the same way as the dark pion, in our phenomenological study we take $c_\xi = \lambda_h$ and do not distinguish between the dark pion and kaon masses.

In the limit that the dark pion mass scale is taken large, $\xi \rightarrow 0$, and the dark pions can only decay back to fermions. However, when the dark pions are near to the electroweak scale, ξ can be “smallish” but, importantly, nonzero. This implies $\pi_D \rightarrow f\bar{f}'$ dominate so long as there is no small coupling. For the specific case of π_D^0 in the mass range $m_h + m_Z < m_{\pi_D^0} < 2m_t$, the decay $\pi_D^0 \rightarrow Z + h$ dominates despite being gaugephobic. This is because the Zh mode is longitudinally enhanced, while the competing fermionic mode $\pi_D^0 \rightarrow b\bar{b}$ is suppressed by the small Yukawa coupling

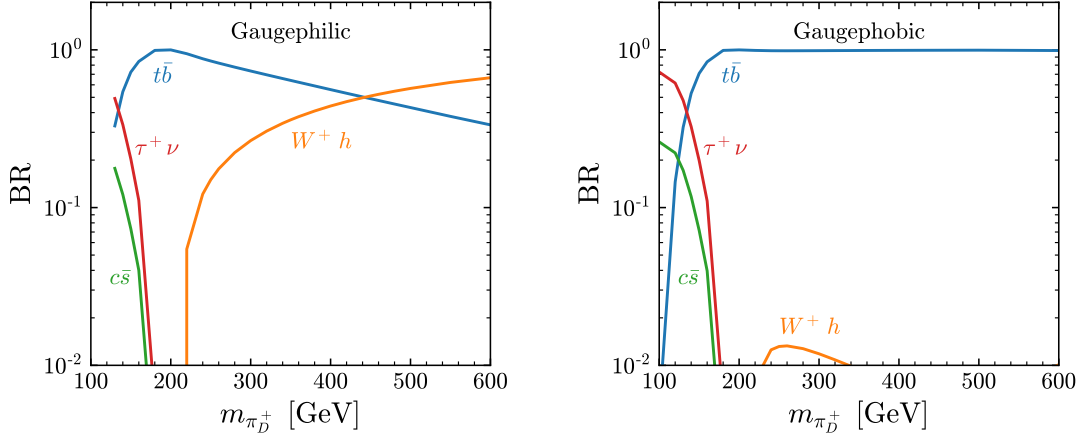


Figure 2. Branching ratios of the charged pions

y_b . For all other ranges of dark pion masses (both charged and neutral), $\pi_D \rightarrow f\bar{f}'$ dominates. By contrast, in the gaugephilic case $\pi_D \rightarrow W + h$, $Z + h$ dominate once they are kinematically open.

While the two choices in Eq. (3.12) may seem arbitrary at first, a large class of strongly-coupled models can be mapped into this categorization (see Ref. [120] for more details). Specifically, the Stealth Dark Matter model [106, 107, 117] and others similar to it are gaugephobic. By contrast, models of bosonic technicolor / induced symmetry breaking [24], as well as the triplet state in Georgi-Machacek models [174] have gaugephilic interactions.

In our taxonomy, the gaugephilic case only occurs for the $SU(2)_L$ model. This is not immediately obvious from our discussion thus far. Essentially the gauge/Higgs interactions on the last line of Eq. (2.14) is permitted with order one ξ when π_D^a is in the same representation as W_μ^a , i.e., an $SU(2)_L$ triplet. The reader may then immediately wonder why the $SU(2)_R$ case does not have $\xi = 0$. At leading order it does, but at higher orders one finds gauge/Higgs interactions are generated albeit with a suppression typically of order $m_h^2/m_{\pi_D}^2$. This is parametrically the suppression we

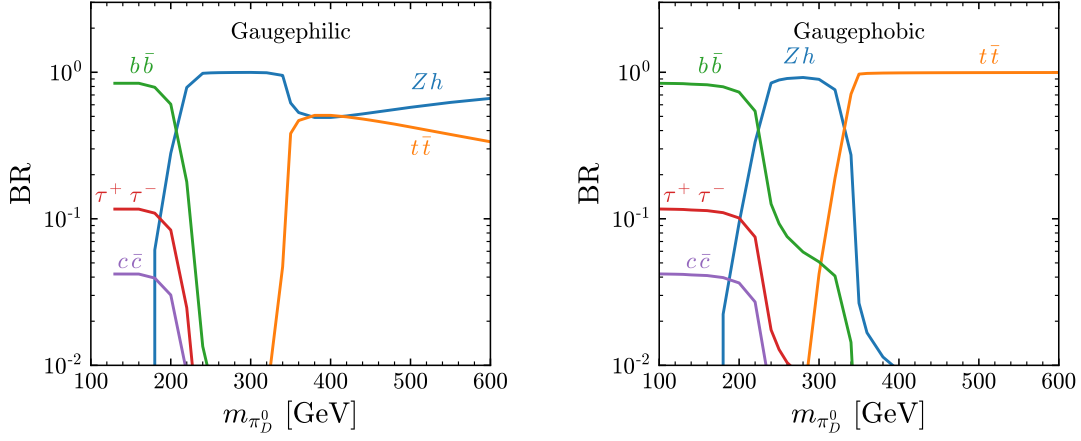


Figure 3. Branching ratios of the neutral pions

find in the Stealth Dark Matter model [120], and is similar to what we find in generic 2-flavor custodially-symmetric models. More details can be found in Ref. [120].

Any given model may or may not permit arbitrary choices for v_π and ξ ; for instance, induced electroweak symmetry breaking requires v_π fixed (up to order one coefficients) and $\xi = 1$ due to the requirements of proper electroweak symmetry breaking. However, as we detail in [120], there are models that span a wide range of $(v_\pi, \xi \lesssim 1)$.

Given ξ , the branching fractions of the π_D are fully specified as a function of the pion mass. As π_D decay couplings are proportional to mass, they decay to the heaviest kinematically available SM particles. The branching ratios for the gaugephilic and gaugephobic scenarios are compared side by side in Fig 2 (charged π_D) and 3 (neutral π_D).²

²We have omitted the anomaly-induced decay $\pi_D^0 \rightarrow \gamma\gamma$ from Fig. 3. In models with a $SU(2)$ flavor symmetry that becomes custodial $SU(2)$ after Higgs interactions, the dark sector is anomaly-free. The decay mode does reappear due to SM interactions violating custodial $SU(2)$, but is highly suppressed so as to be phenomenologically irrelevant [120].

For the charged π_D , the branching ratios in the two cases are similar at small masses. However, the unsuppressed gauge/Higgs couplings in the gaugephilic scenario imply $\pi_D \rightarrow W^+ h$ quickly dominates once it is kinematically allowed (due to the kinematic enhancement of decays to longitudinal W), while the $\pi_D \rightarrow t\bar{b}$ mode always dominates at heavy mass for the gaugephobic case. There is a similar pattern in the branching ratio of the neutral pions. Again, when the pion is light, the decay modes between the two categories are similar and are dominated by the $b\bar{b}$ mode. This similarity persists after π_D passes the Zh threshold. However, as π_D is further increased past the $t\bar{t}$ threshold we can spot the difference, as the $\pi_D \rightarrow t\bar{t}$ branching ratio dominates at large π_D masses in the gaugephobic case but stays subdominant to Zh in the gaugephilic case.

Constraints from single production

Having established the dark meson phenomenological Lagrangian and fleshed out the relevant parameters, we now move on to LHC production, sensitivities, and constraints.

The phenomenology of the dark meson sector that we pursue in this paper clearly bifurcates at $\eta = 0.5$ as evident from the branching fractions of the dark pions in Fig. 1. For $\eta > 0.5$, the ρ_D is kinematically forbidden to decay to a pair of on-shell dark pions, and thus decays to SM fermions dominate.³ The decays into SM fermions are determined solely by the gauge and color charges of the fermions, so the ρ_D phenomenology is essentially independent of the details of how the pions interact with the SM.

When $\eta < 0.5$, $\rho_D \rightarrow \pi_D \pi_D$ is open, and generally dominates so long as the number of dark colors, N_D , is not large (we'll be more precise below). In this case,

³Fig. 1 includes three-body decays through an off-shell dark pion, but the rates for these decay modes are always small compared to what is shown in the figure.

the most promising way to search for dark mesons is dark pion pair production. The largest contribution to dark pion pair production is resonant production $pp \rightarrow \rho_D \rightarrow \pi_D \pi_D$ through the dark rho, so long as it is not very heavy. Dark pions can also be pair-produced through Drell-Yan production, though this tends to give a smaller cross section due to the W or Z exchange being off-shell. We find that resonant production through ρ_D dominates for $\eta \gtrsim 0.2$ for $N_D = 4$.

The final states populated by dark pion pairs depends on how the dark pions decay, which in turn depends on whether we are in a gaugephilic or gaugephobic scenario. We have chosen 9 benchmarks spanning the phenomenology possibilities that we believe give a solid idea of the differing phenomenology, shown in Table 4. We provide the `FeynRules` [175] model files and corresponding UFO files on GitHub.⁴

We used `MadGraph5_aMC@NLO` [176] to simulate the events. When studying constraints directly on the ρ_D , we simulated $pp \rightarrow \rho_D$ and then allowed for any decay mode. For the constraints on π_D , we simulated $pp \rightarrow \pi_D \pi_D$ which then had resonant and Drell-Yan production. In all cases, showering and hadronization was performed by `Pythia 8` [177] and `Delphes 3` [178] was used for fast detector simulation. We used the default detector card because we recast both ATLAS and CMS results. Within `Delphes`, jets were calculated with `FastJet` [179] using the anti- k_t algorithm [180]

For each of the benchmark scenarios in Table 4, the mass of the π_D was scanned with variable spacing in order to capture the different decay mode transitions. We take the lower limit of dark pion mass to be 100 GeV, coming from the bound on BSM charged particles from LEP II. At each mass point, 500k events were produced for pair production of dark pions (all allowable modes). This was done for both

⁴<https://github.com/bostdiek/HeavyDarkMesons>

Model	$\eta \equiv m_{\pi_D}/m_{\rho_D}$	ξ
$SU(2)_L^{55}$	0.55	gaugephilic ($\xi = 1$)
$SU(2)_L^{45}$	0.45	
$SU(2)_L^{25}$	0.25	
$SU(2)_L^{55}$	0.55	gaugephobic ($\xi = m_h^2/m_{\pi_D}^2$)
$SU(2)_L^{45}$	0.45	
$SU(2)_L^{25}$	0.25	
$SU(2)_R^{55}$	0.55	gaugephobic ($\xi = m_h^2/m_{\pi_D}^2$)
$SU(2)_R^{45}$	0.45	
$SU(2)_R^{25}$	0.25	

Table 4. Benchmark models and parameters used in our study. Note that the gaugephilic case only occurs for the $SU(2)_L$ model, as discussed in Sec. III in the text.

$\sqrt{s} = 8$ TeV and $\sqrt{s} = 13$ TeV collisions. The π_D are decayed in the narrow width approximation using `Pythia`.

There is no dedicated search for dark mesons at the LHC. We therefore estimate the existing bounds by recasting a vast set of potentially constraining searches using Monte Carlo methods. We will present our results first, followed by a more detailed description of our recasting methods and a summary of why several searches which look promising at first glance fail to set strong bounds.

ρ_D constraints. We first consider ρ_D production and decay. The ρ_D dark vector mesons kinetically mix with electroweak gauge bosons, shown in Eq. (3.6), giving direct couplings to SM fermions, shown in Eq. (3.9). In both the $SU(2)_L$ and $SU(2)_R$ models, there is a neutral ρ_D^0 , better known as a new Z' gauge boson. Via kinetic mixing, this ρ_D^0 acquires a coupling to leptons.

The strongest constraints on generic Z' gauge bosons (with masses near or above the electroweak scale) is from the absence of resonances in the the $\ell^+\ell^-$ invariant

mass spectrum [181, 182]. Using the ATLAS 13 TeV search with 36.1 fb^{-1} of integrated luminosity [181], we have recast the dilepton searches for the combined electron and muon channels into a limit on ρ_D cross section times branching fraction to leptons. This is accomplished by simulating the production of ρ_D and decaying them according to the branching ratios shown in Fig 1. After passing through a parton shower, hadronization, and detector simulation, we select events which contain same-flavor opposite-sign leptons within the ATLAS selection criteria. The combined efficiency (branching ratio times the detector efficiencies) multiplied by the cross section can then be compared against the exclusion limits provided by the ATLAS HEPData [183].

In Fig. 4, we illustrate the bounds that we have obtained by determining the largest coupling of the ρ_D^0 to the SM for any choice of m_{ρ_D} within the range of interest in this paper. The coupling is completely determined by the model-independent quantity $\epsilon^2 \times BR(\rho_D^0 \rightarrow \ell^+ \ell^-)$, that is shown as a black line in both panels of Fig. 4. Also superimposed on the panels are the predicted sizes of $\epsilon^2 \times BR(\rho_D^0 \rightarrow \ell^+ \ell^-)$ for a given m_{π_D}/m_{ρ_D} and number of dark colors N_D in the $SU(2)_L$ model. It is important to note that ϵ is the kinetic mixing parameter and not the detector efficiency. (Similar but weaker constraints are found in the $SU(2)_R$ model.) The right panel clearly shows that the neutral dark vector meson is strongly constrained by the dilepton data when $m_{\pi_D}/m_{\rho_D} > 0.5$.

The dependence on the number of dark colors is nontrivial:

$$\sigma(pp \rightarrow \rho_D^0 \rightarrow \ell^+ \ell^-) \propto \epsilon^2 \times BR(\rho_D^0 \rightarrow \ell^+ \ell^-) \propto \begin{cases} N_D & \eta > 0.5 \\ N_D^3 & \eta < 0.5. \end{cases} \quad (3.13)$$

In the case $\eta > 0.5$, the one power of N_D comes from ϵ^2 while in the branching fraction the N_D dependence cancels. Contrast this with the case $\eta < 0.5$, where the branching

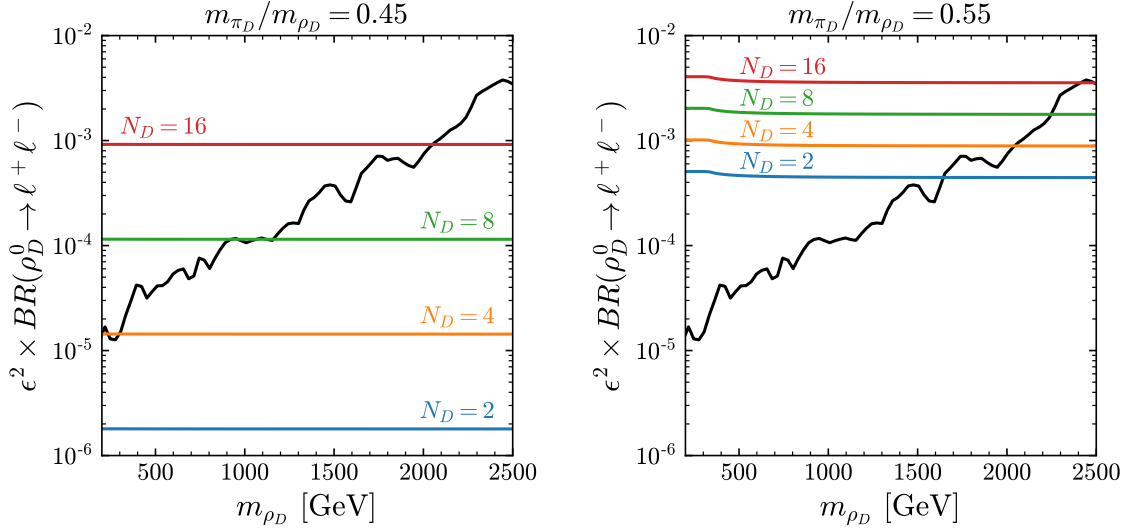


Figure 4. Constraints on the kinetic mixing between the the SM and ρ_D^0 (times the leptonic branching fraction of ρ_D^0) from the non-observation of a dilepton resonance near m_{ρ_D} . The black line is the model-independent limit. To illustrate the impact of this bound on the model space, we have superimposed the predicted $\epsilon^2 \times \text{BR}(\rho_D^0 \rightarrow \ell^+ \ell^-)$ for the $SU(2)_L$ model, varying the number of colors between 2 to 16. On the right, the 2-body decay $\rho_D^0 \rightarrow \pi_d^+ \pi_d^-$ is kinematically forbidden, leading to strong constraints: $m_{\rho_D} > 1.5\text{-}2.5$ TeV. On the left, the 2-body decay $\rho_D^0 \rightarrow \pi_d^+ \pi_d^-$ is open, and we see that when $N_D \lesssim 4$, there is no constraint from resonant ρ_D^0 production and decay to dileptons.

fraction $\text{BR}(\rho_D^0 \rightarrow \ell^+ \ell^-)|_{\eta < 0.5} \simeq \Gamma(\rho_D^0 \rightarrow \ell^+ \ell^-)/\Gamma(\rho_D^0 \rightarrow \pi_D \pi_D) \propto N_D^2$. The left panel clearly shows that when $\rho_D \rightarrow \pi_D \pi_D$ is both kinematically open ($\eta < 0.5$) and dominates ($N_D \lesssim 4$), there are virtually no LHC constraints on neutral dark vector meson production and decay. (The very narrow region near $m_{\rho_D} \sim 300$ GeV is, as we will see, also constrained by other searches).

The bounds we have obtained from the ATLAS searches for dilepton resonances assumed the width of the new resonance is relatively narrow, $\Gamma(Z')/M_{Z'} \lesssim 0.03$ [181]. In all of the cases with $\eta = 0.55$, where the ρ_D^0 can only two-decay into SM states, the width is narrow, $\Gamma_{\text{tot}}(\rho_D^0)/m_{\rho_D^0} < 10^{-3}$. Once $\rho_D \rightarrow \pi_D \pi_D$ is open, we can estimate

this partial width [35]

$$\frac{\Gamma(\rho_D \rightarrow \pi_D \pi_D)}{m_{\rho_D}} = \frac{\pi}{3N_D} \left(1 - \frac{4m_{\pi_D}^2}{m_{\rho_D}^2}\right)^{3/2} \simeq \frac{4}{N_D} \times \begin{cases} 0.02 & \eta = 0.45 \\ 0.16 & \eta = 0.25, \end{cases} \quad (3.14)$$

where we have evaluated the result for the two values $\eta = 0.45, 0.25$ used in our benchmarks for the paper. Despite the relative strong-coupling among mesons ($g_{\rho_D \pi_D \pi_D} = 4\pi/\sqrt{N_D} \gg 1$), the kinematic suppression of taking $\eta = 0.45$ suppresses the width of the ρ_D^0 to a few percent, and so the ATLAS bounds are fully applicable. For $\eta = 0.25$, the width is now tens of percent that is large enough requiring a re-analysis of the dilepton data to set precise bounds on the ρ_D^0 . For $\eta = 0.25, N < 4$, the ρ_D width to mass ratio reaches \sim tens of percent, so a simple recast of the ATLAS bounds is not completely precise. However, given that i.) the bounds on a wide resonance will be weaker than on a narrow resonance, and ii.) the narrow resonance bounds for $N < 4$ are already weak, we conclude that there is no bound on ρ_D^0 for $\eta = 0.25, N < 4$.

There is one additional constraint on the kinetic mixing of ρ_D with SM gauge bosons from LEP constraints on four-fermion effective operators [184]. Integrating out ρ_D^0 results in four-fermion operators of the form

$$\frac{4\pi}{\Lambda^2} \bar{e} e \bar{f} f, \quad (3.15)$$

where we have used the operator normalization of Ref. [184]. Matching the coefficient,

$$\begin{aligned} \frac{4\pi}{\Lambda^2} &= \frac{1}{m_{\rho_D}^2} \times \begin{cases} \epsilon^2 g^2 & SU(2)_L \text{ model} \\ \epsilon'^2 g'^2 & SU(2)_R \text{ model} \end{cases} \\ &= \frac{N_D}{16\pi^2 m_{\rho_D}^2} \times \begin{cases} g^4 & SU(2)_L \text{ model} \\ g'^4 & SU(2)_R \text{ model} \end{cases}. \end{aligned} \quad (3.16)$$

The strongest constraints from the LEP data suggest $\Lambda \gtrsim 20$ TeV [184]. For the $SU(2)_R$ model, there is no constraint due to the smallness of g' . For the $SU(2)_L$

model, the bound on $m_{\rho_D^0}$ varies from about 250–750 GeV for $N_D = 2$ –16. Given the order one uncertainties in the large N_D estimate for the kinetic mixing, this bound is not any stronger than what we have already found from Fig. 4.

Constraints on the dark pion coupling to SM. Throughout the paper, we will generally work in the “vector-like” limit (See Ref. [120]) where $\frac{m_{SM}}{v_\pi}$ is small and thus single production of π_D is suppressed. This limit is automatically safe from constraints from electroweak precision observables as well as Higgs coupling measurements, and coincides with the demarcation of our model space into the two categories $SU(2)_L$ and $SU(2)_R$. If, however, $\frac{m_{SM}}{v_\pi}$ is not so small, single production of dark pions is possible and relevant to the phenomenology. In the model of bosonic technicolor / induced electroweak symmetry breaking, this sets the strongest constraints [24].

We can also characterize the parameter space of our effective theory by determining the constraints on $1/v_\pi$ of Eq. (2.14). In Fig. 5, we consider several processes⁵ where single dark pion production can set upper bounds on $1/v_\pi$. One process is top decay, $t \rightarrow \pi_D^+ \bar{b}$. In this process the π_D^+ must be somewhat lighter than the top quark, and thus $\pi_D^+ \rightarrow \tau^+ \nu_\tau$ dominates for the charged pions, leading to an excess of τ 's in top decay. LHC analyses of top decay, however, are consistent with lepton universality [185, 186]. For values of the pion mass slightly less than the top quark mass, the pion branching ratio to τ is similar to the SM branching ratio of the W to tau. Thus, in this region the branching ratio alone is not enough to constrain the coupling. Instead, we use the total width of the top quark [7, 187, 188] as a secondary constraint, and exclude any region where the BSM additions to the

⁵Note that we only consider processes involving fermions so that we have ξ -independent constraints on $1/v_\pi$. Larger ξ , e.g., $\xi \sim 1$, there can be stronger constraints from couplings to the gauge/Higgs sector [24]. We thank Ennio Salvioni for discussions on this point.

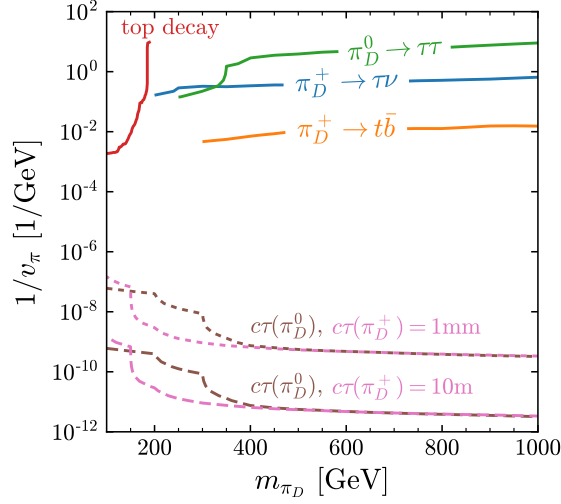


Figure 5. Constraints on the value of $1/v_\pi$ as a function of the dark pion mass. Precise measurements of the top quark exclude regions above the red line. The green, blue, and orange lines come from collider searches for heavy Higgs particles (mainly in 2HDM). Lastly, the brown and pink dashed lines are not constraints, but show at what point the phenomenology changes. Below these lines, the pions start to travel an appreciable distance in the detector, either leading to displaced vertices or disappearing tracks. The lower of these lines are around the scale when the particles leave the detector either as missing energy or look like stable charged particles.

top decay change either the width or the tauonic branching ratio by more than two standard deviations away from the measured values. This constraint is shown in red in Fig. 5.

There are also many searches for the heavy Higgs particles of two-Higgs doublet models that can be recast into searches for single production of the charged or neutral dark pions. In Refs. [189, 190], ATLAS searches for a charged Higgs produced association with $t\bar{b}$. The two searches consist of one looking for $H^+ \rightarrow \tau^+ \nu_\tau$ while the other looks for $H^+ \rightarrow t\bar{b}$. The limits are presented in terms of $\sigma(t\bar{b}H^+) \times BR$, but unfortunately HEPData is not given. We therefore take the limits from plots in Refs. [189, 190] and reinterpret them by replacing π_D^+ for the charged Higgs boson. The upper bounds on $1/v_\pi$ we obtain are shown in orange and blue in Fig. 5. Finally,

in a similar approach, Ref. [191] performed searches for a heavy neutral Higgs boson produced in association with $b\bar{b}$ and decaying to $\tau^+\tau^-$. Upon recasting this search for neutral dark pions, we find somewhat weaker constraints – shown in green in Fig. 5 – compared with the bounds from charged dark pions.

Finally, while this is not a constraint on the parameter space per se, it is interesting to determine when $1/v_\pi$ is small enough that the decays of the dark pions are no longer prompt in colliders. As a rough guide, we can use

$$\Gamma = \left(\frac{2 \text{ mm}}{c\tau} \right) \times 10^{-13} \text{ GeV} \quad (3.17)$$

and estimate that if $c\tau = 1 \text{ mm}$, then the neutral pions would lead to displaced tracks, or the charged pions would lead to kinked (or disappearing) tracks when they decay. If $c\tau > 10 \text{ m}$, then the pions can escape the detectors before decaying, leading to missing energy or long-lived charged tracks. Search strategies for both of these types of signals are interesting but best explored through existing dedicated strategies for long-lived charged or neutral particles [192, 193, 194, 195]. The smallness that $1/v_\pi$ needs to be to lead to these long-lived signals is shown in Fig. 5.

There can also be a contribution to the S parameter as a result of the interactions in Eq. (2.14). However, in the ultraviolet strongly-coupled theories considered in Ref. [120], we find the contributions depend on the spectrum of the heavier mesons, and so there is no useful translation into bounds on $1/v_\pi$. Suffice to say that there are no bounds from the S parameter when the contributions to the dark fermion masses are mostly vector-like with only smaller contributions arising from electroweak symmetry breaking [16, 196].

Clearly, there is a huge range in $1/v_\pi$ – roughly values larger than 10^{-7} and smaller than 10^{-2} , with some slight variation depending on m_{π_D} – where dark pion decays are prompt but the rate for single dark pion production is too small to

be detected. Our goal for the remainder of this paper is to explore how prompt LHC searches constrain paired dark pion production in this otherwise open region of parameter space.

Resonant Dark Pion Pair-Production at LHC

The rate for dark pion pair-production depends on the model – $SU(2)_L$ versus $SU(2)_R$, and the NDA estimates for the kinetic mixing as well as the meson self-interactions. It does *not* depend on how the dark pions decay (gaugephilic versus gaugephobic) because the production rate is independent of $1/v_\pi$ and ξ/v_π from Eq. (2.14). However, the different decay modes require different search strategies. In Table 5, we have denoted different mass regions for each of the categories defined by which decay modes are dominant. The intermediate SM particles, which may subsequently decay, are listed for both the charged ($\pi_D^\pm \pi_D^0$) and the neutral ($\pi_D^+ \pi_D^-$) currents. Note that the symmetries do not allow for neutral currents of the type $\pi_D^0 \pi_D^0$, so the $SU(2)_R$ model does not contain a resonantly enhanced charged current.

Table 5 shows that there are many Standard Model particles in the final states, with possibly exotic combinations. We analyzed 13 searches (in addition to the ones already discussed), broken down into 6 searches at 8 TeV and 7 searches at 13 TeV. Surprisingly, we find that many of the searches are not sensitive to our benchmark models. The searches with sensitivity are further detailed here, while we save a discussion of the non sensitive searches for Sec. III.

The results of our recasting are summarized in Fig. 6. This is the main result of our paper. The top line of each plot (colored in blue) shows the constraints on the model coming from searches for resonant dilepton production. As discussed in the previous section, this depends only on if the ρ_D can decay to leptons or not, and is

	Mass	Charged Current	Neutral Current
gaugephilic	$m_{\pi_D} \lesssim 150 \text{ GeV}$	$b\bar{b}\tau\nu$	$\tau^+\tau^-\nu\bar{\nu}$
	$150 \text{ GeV} \lesssim m_{\pi_D} \lesssim 200 \text{ GeV}$	$b\bar{b}t\bar{b}$	$t\bar{t}b\bar{b}$
	$200 \text{ GeV} \lesssim m_{\pi_D} \lesssim 450 \text{ GeV}$	$Z h t\bar{b}$	$t\bar{t}b\bar{b}$
	$m_{\pi_D} \gtrsim 450 \text{ GeV}$	$h h Z W^+$	$h h W^+ W^-$
gaugephobic	$m_{\pi_D} \lesssim 150 \text{ GeV}$	$b\bar{b}\tau\nu$	$\tau^+\tau^-\nu\bar{\nu}$
	$150 \text{ GeV} \lesssim m_{\pi_D} \lesssim 220 \text{ GeV}$	$b\bar{b}t\bar{b}$	$t\bar{t}b\bar{b}$
	$220 \text{ GeV} \lesssim m_{\pi_D} \lesssim 350 \text{ GeV}$	$Z h t\bar{b}$	$t\bar{t}b\bar{b}$
	$m_{\pi_D} \gtrsim 350 \text{ GeV}$	$t\bar{t}t\bar{b}$	$t\bar{t}b\bar{b}$

Table 5. Phenomenological regions for collider signatures. The charged and neutral current columns show the SM particles for the dominant branching ratios.

independent of how the π_D decay. The x axis for the plots is m_{π_D} , so the results are obtained from Fig. 4 by scaling the x axis by the ratio m_{π_D}/m_{ρ_D} .

The next two lines in the Fig. 6 display the best constraints we could find for 13 TeV searches. The first of these is a search for supersymmetry in final states with either same-sign leptons or three leptons. Recasted in terms of dark pions, it excludes m_{π_D} in the 200-300 GeV range for the gaugephilic and slightly worse for the gaugephobic categories when $\eta = 0.45$. This search does not work when $\eta = 0.25$ because for fixed m_{π_D} , smaller η implies a heavier ρ and therefore a smaller resonant contribution to pion pair production. The other 13 TeV search with moderate sensitivity is a supersymmetry search with final states of tau leptons. The bounds from this search limit the dark pion mass in all models with $\eta < 0.5$ that we examined to be $\gtrsim 130 \text{ GeV}$, the mass above which $\pi_D^+ \rightarrow \tau^+\nu$ ceases to be the dominant decay mode.

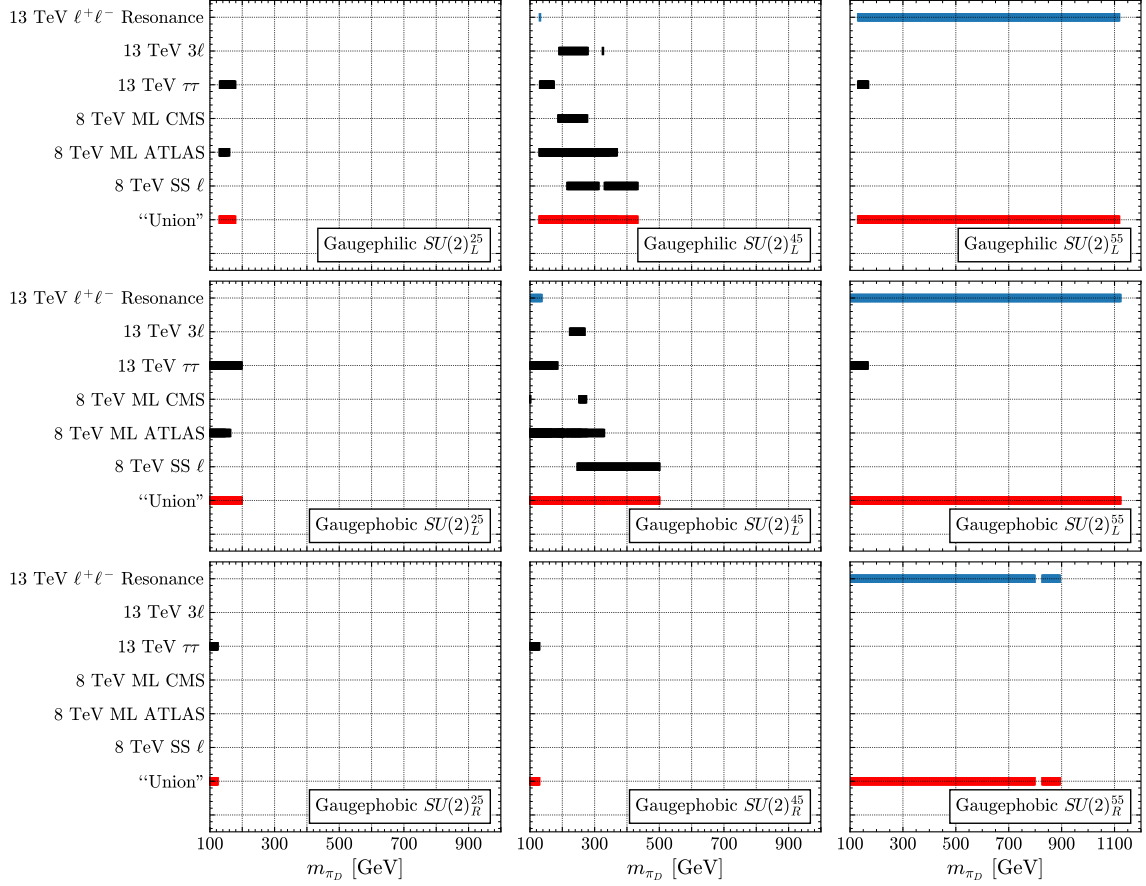


Figure 6. Summary of the dark meson exclusions for the benchmark scenarios and values of the π_D and ρ_D masses. The scenarios are labeled by the type of kinetic mixing, the ratio of the dark pion to dark rho mass $\eta = m_{\pi_D}/m_{\rho_D}$, and the relative strength of the fermionic versus bosonic dark pion decay modes. All of the dark pions decay promptly. The top line indicates the bound on ρ_D^0 inferred from recasting the latest dilepton bounds and interpreted in terms of m_{π_D} . The next five lines (in black) show the π_D mass bound from the most constraining 8 and 13 TeV searches we could find. The union of the exclusions from all of the searches is shown in the last line.

The remaining lines in Fig. 6 come from the 8 TeV searches which have sensitivity to π_D . Two are multilepton searches from ATLAS and CMS, which are general searches counting the numbers of events for many signal regions. These work well for the models at low masses, and are slightly better for the gaugephilic models. The other exclusion comes from a search for supersymmetry in states with same

sign leptons. In particular, one of the signal regions trades the usual missing energy requirement for more b-jets, which works well for the gaugephobic models.

Finally, the last line (shown in red) combines all of the previous constraints in the most naive method. The models where the ρ_D *cannot* decay to π_D are excluded to over $m_{\pi_D} = 1100$ GeV for $SU(2)$ kinetic mixing and to 900 GeV for $U(1)$ ($SU(2)_R$ model). If the mass ratio allows for decays to pions, the exclusion limits are drastically reduced. For $m_{\pi_D}/m_{\rho_D} = 0.45$, the gaugephilic limits are to around 425 GeV while the gaugephobic limits are at 500 GeV for $SU(2)$ mixing. This corresponds to 13 TeV cross sections of 600 fb and 300 fb, respectively. It is surprising that processes with such distinct final states are still allowed with these large of rates at the LHC. The $SU(2)_R$ model limits are $m_{\pi_D} \gtrsim 130$ GeV, with a cross section of a few pb. As the mass ratio is further extended, the decay products become more energetic, boosting some of the search efficiencies. However, the resulting decrease in the cross section from the heavier ρ_D compensates for this and leads to reduced limits. All of the models with $m_{\pi_D}/m_{\rho_D} = 0.25$ have limits at or below $m_{\pi_D} = 200$ GeV, corresponding to a (13 TeV) cross section of around a pb.

The rates that are still allowed are much larger than one would expect, especially given the exotic combinations of final state particles. In the next subsections, we examine the constraining searches in more detail, looking at why the searches work and what the deficiencies are. The details we expose, combined with the information in Sec. III, will help us identify important elements that future searches should incorporate in order to improve sensitivity to dark pion scenarios.

Searching for taus. Working from the bottom up of the dark pion mass range, $\mathcal{O}(100\text{--}150)$ GeV dark pions in all of our benchmark models decay primarily as

$\pi_D^+ \rightarrow \tau^+ \nu_\tau$. Therefore, we begin our survey of experimental searches with searches that explicitly look for taus.

ATLAS searches for supersymmetry in electroweak production of supersymmetric particles with final states with τ leptons using 14.8 fb^{-1} of $\sqrt{s} = 13 \text{ TeV}$ data [1]. They interpret the search in terms of the leptons coming from the decays of charginos or neutralinos. As this search is aimed at a supersymmetric model with a neutralino also in the final state, they require a large amount of missing energy, which limits the sensitivity to our benchmarks. The general search strategy is:

1. Trigger on events with two hadronically decaying τ s with $p_T > 35(25) \text{ GeV}$ and have $E_T^{\text{miss}} > 50 \text{ GeV}$.
2. Require opposite sign taus with $m_{\tau\tau} > 12 \text{ GeV}$.
3. Veto any event with a b-jet to suppress top-quark backgrounds.
4. Suppress SM backgrounds with a Z boson by removing events with $|m_{\tau\tau} - 79 \text{ GeV}| < 10 \text{ GeV}$.⁶
5. Large missing energy cut, $E_T^{\text{miss}} > 150 \text{ GeV}$.
6. Large *stransverse* mass $m_{T2} > 70 \text{ GeV}$.

The stransverse mass is defined as

$$m_{T2} = \min_{\mathbf{q}_T} \left[\max \left(m_{T,\tau1}(\mathbf{p}_{T,\tau1}, \mathbf{q}_T), m_{T,\tau2}(\mathbf{p}_{T,\tau2}, \mathbf{p}_T^{\text{miss}} - \mathbf{q}_T) \right) \right], \quad (3.18)$$

where the transverse momenta of the two taus are $\mathbf{p}_{T,\tau1(2)}$ and \mathbf{q}_T is the transverse vector which minimizes the larger of the two transverse masses. The transverse mass

⁶79 GeV is the “visible” mass of the Z for tau decays which have inherent missing energy.

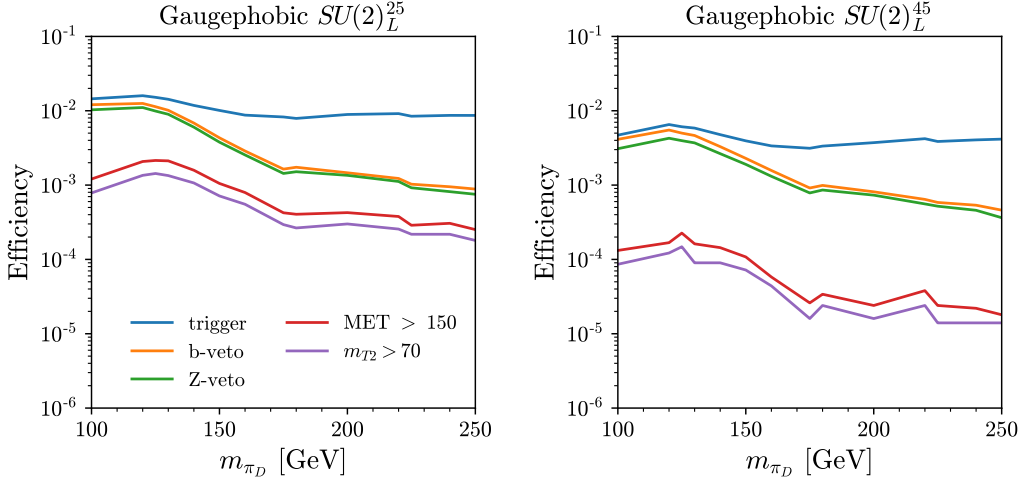


Figure 7. Cut flow for the search for hadronically decaying taus, optimized for electroweak production of supersymmetric particles [1]. The efficiency is much larger for the $\eta = 0.25$ benchmarks than the $\eta = 0.45$ models because the larger ρ_D mass leads to more energetic π_D . This increase in efficiency is offset by the decrease in resonant production cross section.

is defined as,

$$m_T(\mathbf{p}_T, \mathbf{q}_T) = \sqrt{2(p_T q_T - \mathbf{p}_T \cdot \mathbf{q}_T)} . \quad (3.19)$$

Figure 7 shows the efficiency of the signal as the various cuts are being made, and exemplifies the kinematic differences between models with different value of η . There is very little loss in efficiency from the b- and Z-vetos for masses less than 150 GeV. Additionally, the figure shows that at this stage, there is very little difference between the η values. However, there is a huge drop in efficiency when requiring large amounts of missing energy. This is not as dramatic in the $\eta = 0.25$ models, which produce more energetic π_D because of the heavier ρ_D .

The exclusions from this search are plotted in Fig. 8, where the y -axis is the cross section times search efficiency. The expected number of events in the signal region from standard model backgrounds was 5.9 ± 2.1 , while only three events were actually

observed. As fewer events were seen than expected, the observed limits of 0.32 fb is more stringent than the expected $0.43_{-0.12}^{+0.21}$ fb. Both the gaugephilic and gaugephobic models with $SU(2)$ kinetic mixing and $\eta = 0.25$ or $\eta = 0.45$ are excluded from this search if $m_{\pi_D} \lesssim 170 - 180$ GeV. Surprisingly, this search also constrains the $SU(2)$ models with $\eta = 0.55$ even though the π_D are not produced through a resonant ρ_D . These are only allowed if $m_{\pi_D} > 160$ GeV.⁷

Additionally, the $SU(2)_R$ models [that kinetically mix through $U(1)_Y$] with $\eta = 0.25, 0.45$ are also constrained to be above $m_{\pi_D} \gtrsim 130$ GeV. As shown in the summary plot of Fig. 6, this is the only search we examined which had sensitivity to the $SU(2)_R^{25,45}$ models.

The reason these limits are not stronger is because the branching ratio to taus is decreasing rapidly as the mass of the pions increases. This is compensated by an increase in the expected number of W s, Z s, and bs . The next sections examine searches which exploit these particles.

Generic multilepton searches. Examining Table 5, once $m_{\pi_D} \gtrsim 150$ GeV, pair produced dark pions decay to lots of bottom and top quarks, along with Z and W . It should be expected that searches utilizing bs and leptons could place strong constraints on the benchmark models. While we studied many model driven searches and found no limits (see Sec. III), model-independent searches proved useful. Both ATLAS and CMS have a generic search at 8 TeV based on final states with multiple leptons. (Neither collaboration has repeated the analysis at 13 TeV).

⁷While all of our signal numbers were determined using `Delphes` tagging and identification efficiencies, we derive limits by comparing them with ATLAS/CMS background numbers computed with their own dedicated programs and setting. As the identification and tagging efficiencies in `Delphes` are only an approximation to the true ATLAS/CMS numbers, our signal vs. background comparison is not totally genuine. To quantify the effect of the mismatch, we have checked the ramifications of changing the `Delphes` lepton identification efficiency by $\pm 10\%$ and find that this variation only leads to very minor shifts in the derived m_{π_D} limits.

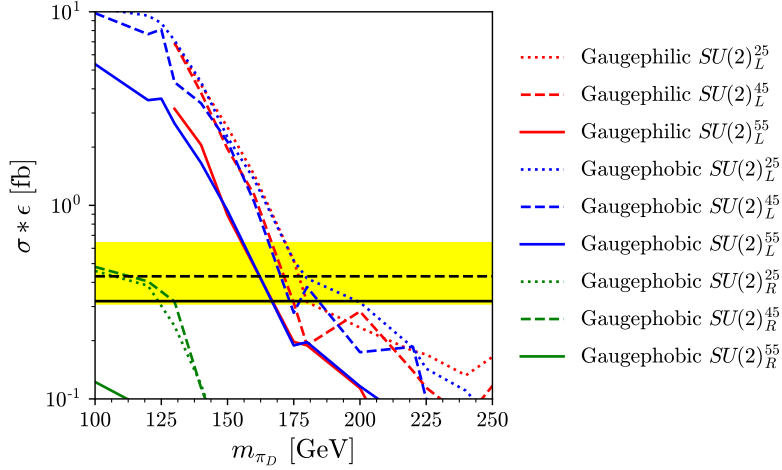


Figure 8. Exclusions from the ATLAS search for supersymmetry in final states with tau leptons [1]. The dark mesons on the lighter side of our spectrum predominately decay to taus, and the cross sections are large. The $SU(2)_L$ type models are excluded if $m_{\pi_D} \lesssim 180$ GeV while the $SU(2)_R$ models limits are around 130 GeV. This is the only search which limits the $SU(2)_R$ models where the ρ_D can decay to $\pi_D \pi_D$.

The inclusive ATLAS search looks for 3^+ leptons [2]. The basic search requirements are: 1 electron or muon for triggering purposes ($p_T > 26$ GeV, $|\eta| < 2.5$), a second electron or muon with slightly looser requirements, and a third e/μ or hadronic τ . The events are broken into further sub-categories according to several kinematic variables, such as the b -jet multiplicity, or whether or not the event contains a same-flavor-opposite-sign lepton anti-lepton pair. The signal regions are not orthogonal, and they set bounds on the BSM cross section of roughly a few fb.

Applied to π_D production, we find the most constraining signal regions are those containing a hadronic τ and that contain ≥ 1 b -jet or have low $H_{T,L}$, defined as the scalar sum of the p_T of the three leading leptons (or τ) in the event. The limits depends strongly on the lepton and tau identification. In particular, the ATLAS study used only single-prong hadronic taus⁸ in the analysis and a benchmark identification

⁸Also, there was no dedicated τ trigger in place for this analysis.

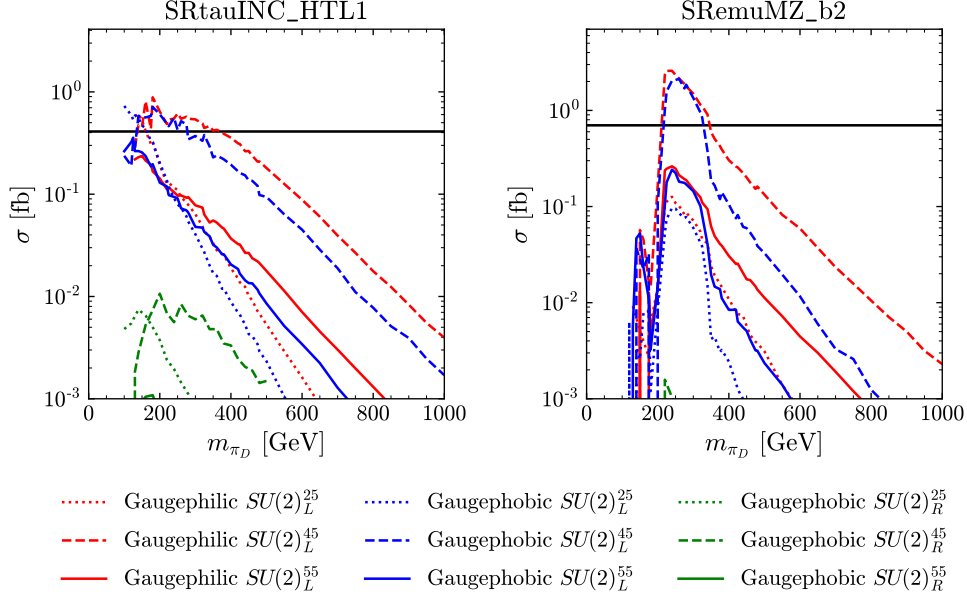


Figure 9. Expected signal cross section in two different signal regions of the ATLAS multilepton search [2] as a function of dark pion mass.

efficiency of 0.5. Compared to more recent τ reconstruction numbers [197] (which are in the default `Delphes` card), the ATLAS values are worse by a factor of ~ 2 . We artificially imposed the reduced tau reconstruction numbers for consistency.

The shape of the exclusion curves for two of the signal regions are shown in Fig. 9, and exemplify the difference between gaugephilic and gaugephobic models which were not observed in the ditau search discussed in Sec. III. The shapes show that the exclusions closely follow the π_D the branching ratios.

Out of the 144 signal regions defined in the ATLAS search, we find that 16 provide some level of constraint. These are summarized in Fig. 10. Picking the strongest limit from the signal regions, we find $\pi_D > 370$ GeV in the gaugephilic, $m_{\pi_D}/m_{\rho_D} = 0.45$ case and $\pi_D > 330$ GeV in the gaugephobic, $m_{\pi_D}/m_{\rho_D} = 0.45$ case. For $m_{\pi_D}/m_{\rho_D} = 0.25$ the bounds are looser, due to the fact that smaller m_{π_D}/m_{ρ_D} for fixed m_{π_D} implies a heavier ρ_D , and therefore a smaller resonant contribution to the

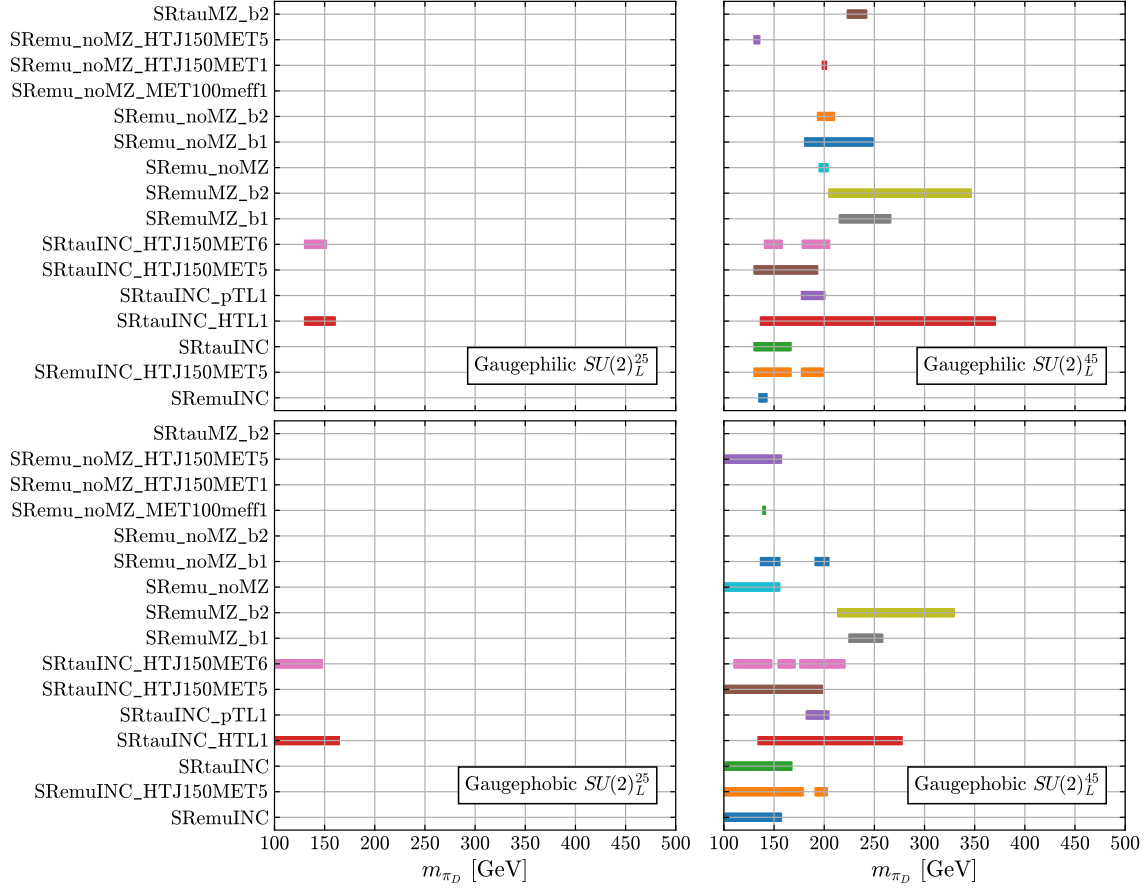


Figure 10. Out of the 144 signal regions defined in Ref. [2], 16 regions constrain some portion of the dark meson parameter space. The mass ranges which are colored are excluded. The gaugephilic models have larger branching ratios to Zh and Wh than the gaugephobic models, which leads to greater search efficiency and larger bounds.

$pp \rightarrow \pi_D \pi_D$ cross section. The difference between the limits in the gaugephilic and gaugephobic can be traced to the presence of more Higgs bosons in the gaugephilic π_D decays, since more Higgs bosons leads to more events with τ s or b -jets.

The CMS generic multilepton search is similar, but contains some important differences. It is based on 19.5 fb^{-1} of $\sqrt{s} = 8 \text{ TeV}$ data [3] and looks for events with either three or four reconstructed leptons. In this case, the definition of leptons includes electrons with $p_T > 10 \text{ GeV}$ and $|\eta| < 2.4$, muons with $p_T > 20 \text{ GeV}$ and

$|\eta| < 2.4$, or hadronically decaying taus with $p_T > 20$ GeV and $|\eta| < 2.3$. To trigger, events must contain either an electron or muon with at least $p_T > 20$ GeV and events are only allowed to have one hadronic tau.

The events are divided into 192 independent bins (96 for each of the three or four lepton cases). The bins are split based whether there are same-flavor-opposite-sign (OSSF) pairs of leptons, the invariant mass of existing OSSF pair, the presence of tagged b jets, the number of hadronic τ leptons, the amount of missing energy, and the scalar sum of accepted jet transverse momenta. When CMS combines their signal regions, they are able to set bounds on new physics on the order of $\sigma \times Br \lesssim 100$ fb.

While it would in principle be possible to combine signal regions within our study, CMS does not provide the correlation information. Therefore, we are forced to examine each bin individually. This is in contrast to the method used in the ATLAS search, which used overlapping signal regions, such that some of the regions were more inclusive. Because of this, we find that the exclusions on the benchmarks from the CMS search are not as strong as the ATLAS ones. They are summarized in Fig. 11 for the signal regions which provide a limit. While the limits are not as strong, we find that the pattern is similar to the ATLAS result, in that the gaugephilic modes have tighter constraints than the gaugephobic models.

To date, there is no 13 TeV multi-lepton analysis. Given the success we see in the 8 TeV versions at catching models that fall through the cracks in dedicated searches (see Sec. III), we encourage ATLAS and CMS to pursue similar model-independent, inclusive searches in the future.

Same sign lepton searches. The last type of search that we find has sensitivity to pair produced dark pions is also fairly generic. The main difference is that instead of looking for three or four leptons, they look for multiple leptons of

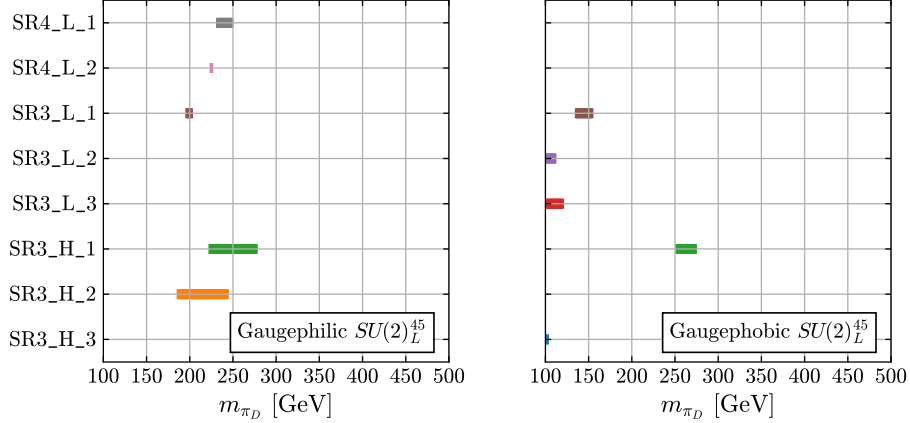


Figure 11. Out of the 192 signal regions defined in the CMS multilepton search [3], 8 regions constrain some part of the dark meson parameter space. The excluded mass ranges are colored according to the denoted signal region. The regions labeled SR3 and SR4 regions contain either 3 or 4 leptons, respectively. The L or H denotes whether the scalar sum of the p_T of the selected jets is less than 200 GeV or greater than 200 GeV. While there are different cuts concerning the number of b -jets or taus, all of the constraining regions require either $E_T^{\text{miss}} < 50$ GeV or $50 \text{ GeV} < E_T^{\text{miss}} \leq 100$ GeV.

the same electric charge. Frustratingly, the limits we find from these scenarios are stronger from an 8 TeV ATLAS search than the follow-up using a similar analysis strategy at 13 TeV with more integrated luminosity.

The ATLAS search for supersymmetry using 20.7 fb^{-1} of $\sqrt{s} = 8$ TeV collisions in final states with two same sign leptons [4] is a particularly powerful search. The search requires two leptons of the same electric charge. For electrons to be reconstructed, they must have $p_T > 20$ GeV and $|\eta| < 2.47$, while reconstructed muons have $p_T > 20$ GeV and $|\eta| < 2.4$. Jets are reconstructed with the anti- k_t algorithm with a radius parameter of 0.4 and are required to have $p_T > 40$ GeV and $|\eta| < 2.8$. In defining the signal regions, the search makes use of the transverse mass, defined as $m_T = \sqrt{2p_T^\ell E_T^{\text{miss}} (1 - \cos \Delta\phi(\ell, E_T^{\text{miss}}))}$. In addition, the effective mass is defined as the scalar sum of the transverse momentum of the leading two leptons, the selected jets, and the missing energy.

Three different signal regions are defined. The first signal region has a veto on b -jets, which severely restricts the efficiency for higher mass π_D . For lower masses, there is not enough missing energy in the events to pass the cut of $E_T^{\text{miss}} > 150$ GeV, so this signal region does not offer constraints on the model.

The next signal region looks for ≥ 1 b -jet. In addition, there must be at least three jets (can include the b jets), missing transverse momentum > 150 GeV, transverse mass > 100 GeV, and an effective mass > 700 GeV. There are no limits from this region as well, due to the large amount of missing energy required.

The third signal region takes an different approach. In addition to the two same sign leptons, at least three b jets and at least 4 jets overall are required as well. In order to be statistically independent of the other regions, this region looks for events with small amounts of missing energy or transverse mass. The dark pions have no intrinsic missing energy (other than leptonic W decays), but do produce a lot of b quarks, making this an ideal signal region.

In the gaugephobic model, the fraction of decays to $W^\pm h$ (Zh) grows with increasing charged (neutral) π_D mass, while dark pions in the gaugephobic case predominantly decays to $t\bar{b}$ ($t\bar{t}$). The difference in branching fractions leads to a smaller average b -jet multiplicity in the gaugephilic case which results in a slightly lower efficiency and, as a consequence, weaker bounds.

To obtain the number of expected signal events, we multiply the cross section and luminosity by the efficiency derived from the analysis cuts. These are then compared to the limits set by ATLAS. In the signal region, 4 events were observed against an expected background of 3.1 ± 1.6 . With this, models which would produce 7.0 expected signal events are excluded at the 95% CL. The left panel of Fig. 12 shows the results of this signal region with number of expected events for the different

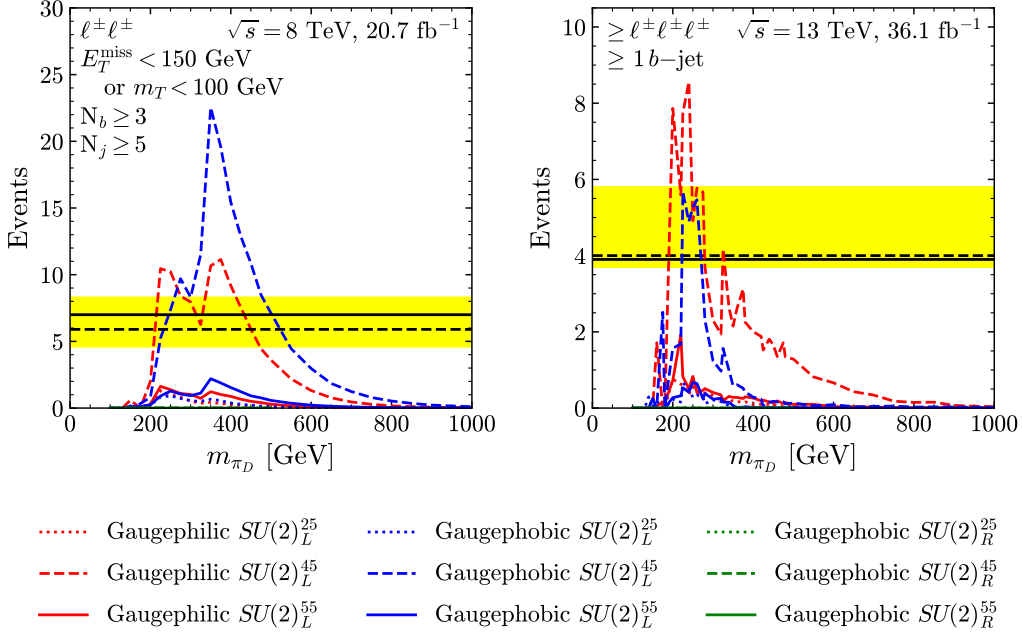


Figure 12. Signal regions of ATLAS searches for three leptons or same sign leptons which have sensitivity to our benchmarks. The left panel shows the limits from the 8 TeV analysis [4] and the right panel has the limits for the 13 TeV analysis [5]. The 8 TeV analysis has bounds to the largest values of m_{π_D} for all of the 8 and 13 TeV analysis which we studied. The 13 TeV search does not do as well because the focus of the analysis shifted to search for higher mass objects.

models are shown in the red, blue, and green lines. The regions where the expected events extends above the black line are excluded. The only benchmarks which are limited by this search are the $SU(2)_L^{45}$ models. The gaugephilic version is excluded for $210 \text{ GeV} \lesssim m_{\pi_D} \lesssim 420 \text{ GeV}$, while the gaugephobic model is ruled out if m_{π_D} is between 250 GeV and 500 GeV. These are the strongest limits that we obtained for all of the searches.

With the success of the 8 TeV analysis, there was hope that when the search was extended to 13 TeV, the limits would greatly improve. However, this is not that case. Using 36 fb^{-1} of $\sqrt{s} = 13 \text{ TeV}$ collisions, ATLAS searched for supersymmetry in final states with two same-sign leptons or three leptons [5]. The basic requirements

are nearly the same for the lepton reconstruction, however, the η cut is tightened to $|\eta| < 2.0$ for electrons and loosened to $|\eta| < 2.5$ for muons.

The signal regions are more complicated in the 13 TeV analysis. There are 19 non-exclusive signal regions defined in terms of the number of leptons required; the number of b -jets; the number of jets harder than 25, 40 or 50 GeV, regardless of flavor; the missing energy and effective mass, and the charge of the leptons.

Unlike the previous search at 8 TeV, the 13 TeV search does not have any signal regions which require at least three b -jets. Instead, to cut down on background, the signal regions either require more than 6 jets or large effective mass. This combination is aimed at TeV scale colored particles and does not bode well for searching for pair produced particles with masses in the hundreds of GeV.

The only one of the 19 regions that has sensitivity to heavy dark mesons is the one that does not have requirements on the number of jets, the effective mass, or the missing energy. Instead, it requires at least three leptons of the same-sign and one b -jet. In addition, it requires that no combination of same-sign leptons has an invariant mass around the Z pole (veto $81 < m_{e^\pm e^\pm} < 101$ GeV).

The limits from this region for the different models are shown in the right panel of Fig. 12. The efficiency is largest in the mass region where $\pi_D^+ \rightarrow t\bar{b}$ and $\pi_D^0 \rightarrow Zh$ dominate. The $\pi_D^0 \rightarrow Zh$ mode is suppressed in the gaugephobic models, hence the limits are not quite as strong as the gaugephilic case. From Fig. 12, we see that this search only excludes $m_{\pi_D} \sim 200\text{-}400$ GeV for $\eta = 0.45$, while $\eta = 0.25$ models are not constrained at all. Thus, while we expected that updating the best 8 TeV search would yield impressive bounds, it was unable to extend the limits above the 500 GeV bound set at $\sqrt{s} = 8$ TeV.

This result highlights a troubling trend. We found the strongest limits from the 8 TeV analysis, pushing the mass of the dark pion to 500 GeV for the most excluded model. However, that search was designed with supersymmetry in mind, and using a supersymmetric interpretation of the 8 TeV search excluded sparticles (stops, specifically) up to 1 TeV. In the supersymmetry interpretation, it makes sense to harden the cuts and focus on particles heavier than 1 TeV. As we have seen in this analysis, however, imposing harder cuts as done with the 13 TeV analyses is detrimental to the signals in our benchmark models, with the result that the older, 8 TeV analyses yielded the strongest constraints. In the next subsection, we discuss other searches which have been thwarted in a similar way.

Additional searches. According to Table 5 (or the branching ratios in Figs. 2 and 3), we expect pair produced dark pions to result in lots of third generation fermions or gauge/Higgs bosons. However, this is not a unique feature of heavy dark mesons. Many BSM scenarios involve new particles that couple predominantly to gauge/Higgs bosons and third generation fermions, and as a result there are numerous LHC searches (underway, or already done) looking for characteristic signals of, e.g. multiple b -jets, multiple τ s, multiple e/μ in association with b -jets or τ , etc. of this type of final states. Based on energy and luminosity alone, the expectation is that one of these 13 TeV searches should be the most constraining. Our results strikingly show this is *not* the case – we find only a few searches constrain dark pions, with the strongest searches coming from 8 TeV.

Our main result, Fig. 6 came from considering a wide array of BSM searches. While the details of the most successful five searches have been provided in the previous sections, we summarize the other, un-constraining searches in Table. 6. In

Search	\sqrt{s} [TeV]	Comments
ATLAS search for a CP-odd Higgs boson decaying to Zh [198]	8	Veto events with more than 2 b-tagged jets kills efficiency
ATLAS search for $t\bar{t}$ resonances [199]	8	Must have exactly one lepton. We have too many jets, confuses search
CMS Pair produced leptoquark [200]	8	Looking for $b\bar{b}\tau^+\tau^-$. Has minor sensitivity to overall rates, would do better with shape analysis but not enough data is provided to recast this.
ATLAS search for SUSY in final states with multiple b-jets [201]	13	Looking for heavy states, so demands large E_T^{miss} and m_{eff}
CMS search for Vh [202]	13	Looking for single production. Needs very boosted hard object.
CMS Di-Higgs $\rightarrow \tau\tau b\bar{b}$ [203]	13	Neutral pions decay through mixing with the Higgs. Measurement uses BDTs and is not recastable.
CMS Low mass vector resonances $\rightarrow q\bar{q}$ [204]	13	Looks for a bump on the falling soft-drop jet mass spectrum. Not enough information to recast the designed decorrelated tagger. Only sensitive to $\sigma \gtrsim 10^3$ pb.
CMS Vector-like $T \rightarrow th$ [205]	13	Looking for th resonance, only very heavy and needs QCD production.

Table 6. Possible search strategies which seem like they should set bounds, but have limited-to-no sensitivity.

addition to the search channel, we provide a short explanation of why dark pions were so inefficiently captured by the search strategy.

While there are varying reasons the searches in Table 6 are not sensitive, there are a few common themes:

1. Searches expect single production. This is especially true for scalars which decay to the Higgs and gauge bosons. To cut down backgrounds, events are vetoed if there are too many objects to be only Vh .
2. Searches assume large E_T^{miss} . The searches which allow for pair production assume that pair production comes from a sector preserving a Z_2 symmetry and that therefore result in an invisible/dark matter particle at the end of the decay chain. While dark pions in the parameter space we are interested are predominantly pair-produced, they only decay back to SM particles.
3. Searches at 13 TeV have their sights set on heavier new physics. As a result, their cuts are too high to capture lighter dark pions. Heavier dark pions do have higher efficiency, but are not produced at rates the ATLAS and CMS are sensitive to, especially given that there are no leading order QCD-mediated production modes.
4. Data is not presented in a way that is recast-friendly. For instance, the CMS pair produced leptoquark search actually has some minor sensitivity when only using the total number of events. The search then uses the shape of the scalar sum of the p_T of the light lepton, the hadronic τ , and the two jets to set limits, but they do not provide a fit of the shape. Similarly, experiments trying to measure standard model processes (such as $hh \rightarrow b\bar{b}\tau^+\tau^-$) may potentially be sensitive to some π_D parameter space, but they rely on machine learning techniques which cannot be reproduced.

We encourage the experiments to continue to push the limits of the LHC searches using all of the techniques they have available. However, as it is not possible for them to test every theory model, it is important that the results be presented in such a way that they can be reproduced without insider knowledge.

CHAPTER IV

SMEFT WITH CUSTODIAL SYMMETRY

From previous two chapters, we have learned that custodial symmetry has the potential of affecting the leading interactions of BSM sectors with the Higgs sector of the SM, and further determining the phenomenology of that BSM new physics. The focus of this chapter is to uncover the “fingerprint” of custodial symmetric UV physics in low energy precision observables. In this chapter, UV physics is said to be “custodial symmetric” when an $SU(2)_R$ global symmetry is preserved by all UV interactions with the Higgs sector of the SM. In order to explore the impact of custodial symmetric UV physics onto precision observables, we start from a thorough analysis of the structure of $SU(2)$ symmetries in the Standard Model.

$SU(2)$ Symmetries of the Standard Model

We first begin our discussion of the $SU(2)$ global symmetries of the SM. The Higgs sector’s $SO(4)$ flavor symmetry

$$SO(4) \sim SU(2)_L \times SU(2)_{RH}, \quad (4.1)$$

is spontaneously broken to $SO(3) \sim SU(2)_V$. In the SM, the t_V^3 generator of $SU(2)_V$ is gauged, explicitly breaking $SU(2)_V$ to just $U(1)$ that is the usual gauged $U(1)_Y$.

In the flavor sector, it is well-known that in the absence of Yukawa couplings the global flavor symmetries are enlarged to

$$U(3)_q \times U(3)_u \times U(3)_d \times U(3)_l \times U(3)_e. \quad (4.2)$$

Once hypercharge is also ungauged, the down-type quark sector flavor symmetries become $U(3)_u \times U(3)_d \rightarrow U(6)_{qR}$. In a one-generation theory, this is simply $U(1)_u \times U(1)_d \rightarrow U(2)_{qR} = U(1)_B \times SU(2)_{RqR}$, baryon number and a global $SU(2)$ isospin symmetry, that we’ll call $SU(2)_{RqR}$. This $SU(2)_{RqR}$ is exactly what would be gauged

as $SU(2)_R$ in theories that extend the SM electroweak gauge symmetry to $SU(2)_L \times SU(2)_R \times U(1)_{B-L}$ (as well as the $U(1)$ part being gauged into $U(1)_{B-L}$), however we emphasize that we are *not* imposing the larger gauge symmetry on the SM (or SMEFT) in this discussion.

There is no analogous $SU(2)$ symmetry in the SM with the lepton field content of just l and e . However, when the SM is extended to include three right-handed neutrinos, what we refer to as ν SM, the lepton sector contains a larger global flavor symmetry

$$U(3)_l \times U(3)_\nu \times U(3)_e. \quad (4.3)$$

Following the same logic for the quarks, in a one-generation theory we see that the lepton flavor symmetry is enlarged $U(1)_\nu \times U(1)_e \rightarrow U(2)_{lR} = U(1)_L \times SU(2)_{RlR}$, lepton number and lepton isospin. Again, just like for the quarks, if the SM gauge symmetry were extended to $SU(2)_L \times SU(2)_R \times U(1)_{B-L}$, the right-handed neutrinos would be required, and the global flavor symmetry $SU(2)_{RlR}$ would be gauged as $SU(2)_R$.

With three generations, the global flavor symmetries are:

$$\text{SM} : SU(2)_{RH} \times U(6)_{RqR} \supset SU(2)_{RH} \times [SU(2)_{RqR}]^3 \quad (4.4a)$$

$$\nu\text{SM} : SU(2)_{RH} \times U(6)_{RqR} \times U(6)_{RlR} \supset SU(2)_{RH} \times [SU(2)_{RqR}]^3 \times [SU(2)_{RlR}]^3 \quad (4.4b)$$

where we have identified the $SU(2)$ subgroups for convenience. The sources of global $SU(2)$ symmetry breakings in the SM are thus:

- Gauging hypercharge, which corresponds to gauging the t_R^3 generator of every global $SU(2)_R$ in 4.4a or 4.4b, simultaneously breaking all of the $SU(2)_R$'s down to $U(1)_Y$.

- $SU(2)$ -preserving Yukawa couplings, in which for each generation $SU(2)_{RH} \times SU(2)_{RI} \rightarrow SU(2)$, with $I = (q_R, l_R)$. The sum of the up-type and down-type Yukawa couplings causes this breaking pattern.
- $SU(2)$ -violating Yukawa couplings, in which for each generation $SU(2)_{RH} \times SU(2)_{RI} \rightarrow U(1)$, where the $U(1)$ becomes hypercharge once it is gauged. The *difference* between the up-type and down-type Yukawa couplings causes this breaking pattern.

We are now in a position to precisely define custodial symmetry:

UV physics is said to be **custodial symmetric** when an $SU(2)_R$ global symmetry is preserved by all UV interactions with the Higgs sector of the SM.

This is a property of a restricted set of UV theories, not a constraint on our effective field theory. Having $SU(2)_R$ gaugeable is certainly a sufficient (but not necessary) condition. As we will see, in some cases the $SU(2)_R$ that survives after integrating out UV physics is a diagonal subgroup of $SU(2)_{RH} \times SU(2)_{Rq_R} \times SU(2)_{Rl_R}$, while in other cases all three $SU(2)$ s are present.

In order to explicitly identify the $SU(2)_R$ symmetric and non-symmetric structures, we formally promote each $SU(2)_R$ symmetry of ν SM [4.4b] to be manifest, and then re-write the interactions as $SU(2)_R$ -preserving and $SU(2)_R$ -violating couplings. This is what we refer to as the “custodial basis” of the ν SM that we then extend to ν SMEFT.

The Custodial Basis

Notation and Definitions. The custodial basis of the ν SM promotes all of the $SU(2)_R$'s in Eq. (4.4b) to global symmetries that are explicitly violated by Yukawa couplings and the gauging of hypercharge. To accomplish this, we first establish

notation for the relevant group theory as well as the field content for both the standard basis as well as the custodial basis.

We use $\tau^a = \tau_R^a = \sigma^a$ with $a = 1, 2, 3$ to denote Pauli matrices. The $SU(2)_L$ and $SU(2)_R$ generators in the fundamental representation are hence $t^a = \frac{1}{2}\tau^a$ and $t_R^a = \frac{1}{2}\tau_R^a$ respectively. The $SU(3)_c$ generators in the fundamental representation are denoted by T^A with $A = 1, \dots, 8$. The SM covariant derivative is

$$D_\mu = \partial_\mu - ig_3 G_\mu^A T^A - ig_2 W_\mu^a t^a - ig_1 B_\mu \mathcal{Y}, \quad (4.5)$$

with \mathcal{Y} denoting the hypercharge, G_μ^A, W_μ^a, B_μ denoting the gauge fields, and g_3, g_2, g_1 denoting the gauge couplings. A general field strength is denoted as $X_{\mu\nu} \in \{G_{\mu\nu}^A, W_{\mu\nu}^a, B_{\mu\nu}\}$. For the dual, we adopt the convention $\tilde{X}_{\mu\nu} \equiv \frac{1}{2}\epsilon_{\mu\nu\alpha\beta}X^{\alpha\beta}$, with $\epsilon_{0123} = +1$. We use the usual Dirac matrices γ^μ , and $\sigma^{\mu\nu} \equiv \frac{i}{2}[\gamma^\mu, \gamma^\nu]$.

The Higgs doublet of the SM is

$$H = \begin{pmatrix} G^+ \\ (v + h + iG^0)/\sqrt{2} \end{pmatrix}, \quad (4.6)$$

and we also often encounter the following Higgs field currents

$$H^\dagger i \overleftrightarrow{D}_\mu H \equiv H^\dagger (iD_\mu H) - (iD_\mu H^\dagger) H, \quad (4.7a)$$

$$H^\dagger i \overleftrightarrow{D}_\mu^a H \equiv H^\dagger \tau^a (iD_\mu H) - (iD_\mu H^\dagger) \tau^a H. \quad (4.7b)$$

Our convention for the $SU(2)$ invariant tensor $\epsilon_{ij} = -\epsilon_{ji}$ is that $\epsilon_{12} = +1$. For convenience, we also define the field $\tilde{H} \equiv i\sigma^2 H^* = \epsilon H^*$, which transforms in the same way as H itself under the $SU(2)_L$ symmetry.

We can re-express the Higgs field in terms of a $(\mathbf{2}, \mathbf{2})$ bifundamental scalar field under $SU(2)_L \times SU(2)_{RH}$ as

$$\Sigma \equiv \begin{pmatrix} \tilde{H} & H \end{pmatrix} = \begin{pmatrix} (v + h - iG^0)/\sqrt{2} & G^+ \\ -G^- & (v + h + iG^0)/\sqrt{2} \end{pmatrix}, \quad (4.8)$$

In principle, all custodial symmetric interactions can be written in terms of powers of Σ with suitable $SU(2)_L$ and $SU(2)_R$ contractions. However, the notation becomes much more compact when we utilize the definition

$$\Sigma_{i_R i_L}^\dagger \equiv \epsilon_{i_R j_R} \epsilon_{i_L j_L} \Sigma_{i_L i_R} \quad (4.9)$$

which matches the complex conjugation and transpose of the 2×2 matrix definition in Eq. (4.8). For example, the SM Higgs potential becomes

$$V = \frac{\lambda}{4} [\text{tr}(\Sigma^\dagger \Sigma) - v^2]^2. \quad (4.10)$$

The matter content of the SM is rewritten as

$$q \longrightarrow q \quad (4.11)$$

$$\begin{array}{l} u \\ d \end{array} \longrightarrow q_R \equiv \begin{pmatrix} u \\ d \end{pmatrix} \quad (4.12)$$

$$l \longrightarrow l \quad (4.13)$$

$$\begin{array}{l} \nu \\ e \end{array} \longrightarrow l_R \equiv \begin{pmatrix} \nu \\ e \end{pmatrix}, \quad (4.14)$$

where we follow the notation of Ref. [127] in which q is the left-handed quark doublet, l is the left-handed lepton doublet, and we denote the right-handed doublets as q_R and l_R . As an example, the quark Yukawa couplings of the SM are re-written as

$$\frac{1}{2} y_{ij}^u \bar{q}_i \Sigma (P_+ + P_-) q_{Rj} - \frac{1}{2} y_{ij}^d \bar{q}_i \Sigma (P_+ - P_-) q_{Rj} + h.c. \quad (4.15)$$

where we have introduced the convenient shorthand

$$P_+ \equiv \mathbb{1}_{2 \times 2} \quad , \quad P_- \equiv \tau_R^3, \quad (4.16)$$

for contractions in the $SU(2)_R$ space. Exactly which $SU(2)_R$ contraction is being done will be made clear as we explain in the next section.

The Custodial Basis of (ν)SMEFT Operators. Having established our notation, we now turn our attention to constructing the custodial basis for

higher dimensional operators. Our presentation largely follows [206] extended to include right-handed neutrinos [207]. We first present all of the independent baryon-preserving operators in the Warsaw basis for ν SMEFT (suppressing flavor indices) in .1. In addition to the $76 = 42 + (17 + \text{h.c.})$ SMEFT operators, there are $25 = 7 + (9 + \text{h.c.})$ new operators involving right-handed neutrinos ν that we show in brown color for easy reference.

Next, using the notation and definitions from Sec. IV, we re-express all of the operators from the Warsaw basis in .1 into our custodial basis in .2. Our notation is

$$\text{Warsaw basis operators} \quad \left\{ \begin{array}{ll} Q_i & \text{SMEFT} \\ Q_i & \text{additional operators in } \nu\text{SMEFT} \end{array} \right. \quad (4.17)$$

$$\text{custodial basis operators} \quad \left\{ \begin{array}{ll} O_i & SU(2)\text{-invariant} \\ O_i & SU(2)_{RH}\text{-violating} \\ O_i & SU(2)_{Rq_R}\text{-violating} \\ O_i & SU(2)_{Rl_R}\text{-violating} \end{array} \right. \quad (4.18)$$

Here we distinguish among operators generated by the UV physics that preserve or violate combinations of the global $SU(2)_{RH}$ symmetry and the global isospin symmetries $SU(2)_{Rq_R}$ and $SU(2)_{Rl_R}$. Our convention is:

- If an operator is invariant under $SU(2)_{RH} \times SU(2)_{Rq_R} \times SU(2)_{Rl_R}$, or if it breaks $SU(2)_{RH} \times SU(2)_{Rq_R, Rl_R} \rightarrow SU(2)_R$, we call this custodial preserving and use black color to denote these operators.
- If an operator breaks $SU(2)_{RH} \rightarrow U(1)$ or $SU(2)_{RH} \times SU(2)_{Rq_R, Rl_R} \rightarrow U(1)$, we call this $SU(2)_{RH}$ violating (recognizing that isospin is also violated) and use blue color to denote these operators.

- If an operator preserves $SU(2)_{RH}$ but violates $SU(2)_{RqR}$ or $SU(2)_{RlR}$, we use red or green color to denote these operators. There are a few operators in which $SU(2)_{RqR} \times SU(2)_{RlR}$ may be simultaneously broken, and these appears with both red and green colors together.

Our definition of custodial symmetry – UV physics preserves an $SU(2)_R$ global symmetry in all UV interactions with the Higgs sector of the SM – is satisfied by the operators in black by construction, as well as the operators in red and green at leading matching order. The presence of new isospin violation in isolation from the Higgs sector does not affect our (tree-level) results, as we will see. We also note that four operators of type $\bar{\psi}\psi H^2 D$ categorized as custodial preserving have a possible custodial violating piece from the gauging of hypercharge. Since custodial symmetry requires the UV physics be neutral under hypercharge, we do not need to concern ourselves with this additional potential custodial violation.

An explicit translation dictionary between the two operator bases is given in .3. From this translation dictionary, one can easily determine the corresponding relations between the Wilson coefficients in the two bases through

$$\mathcal{L}_{\text{EFT}} = \sum_i a_i O_i = \sum_i C_i Q_i. \quad (4.19)$$

We provide explicit translation dictionaries between the operator coefficients in ??.

Several highlights of the results in the tables include:

- Some operators are invariants under custodial symmetry, and so the translation is trivial, such as the operators of type X^3 , H^6 , $X^2 H^2$, and $(\bar{L}L)(\bar{L}L)$.
- Operators involving $B_{\mu\nu}$ or covariant derivatives that involve B_μ violate custodial symmetry due to the gauging of hypercharge, including O_{HB} , $O_{H\tilde{B}}$, O_{HWB} , $O_{H\tilde{W}B}$, O_{lB}^\pm and O_{qB}^\pm .

- Some custodial basis operators involve a single $SU(2)_R$ contraction with P_+ (custodial symmetric) or P_- (custodial violating), formed from simple linear combinations of Warsaw basis operators, such as $\bar{\psi}\psi H^3$ and $\bar{\psi}\psi XH$. The custodial preserving (violating) operators are denoted with a superscript, as in O^\pm .
- Some custodial basis operators involve a two $SU(2)$ contractions, which is the maximum number that appear at dimension-6. These operators involve two projectors P_\pm in the same operator, and have a slightly more complicated translation, such as $(\bar{R}R)(\bar{R}R)$. These operators have two superscripts, as in $O^{\pm\pm}$. The colors of the superscripts denote whether the operator breaks quark and/or lepton isospin.
- Some operators have no explicit B_μ or P_- and yet can break custodial symmetry through the appearance of a covariant derivative that implicitly includes B_μ , such as $O_{Hl}^{(3)}$ and $O_{Hq}^{(3)}$. These operators contain two parts: a custodial preserving part from the gauging of $SU(2)_L$, i.e. the $W_\mu^a t_L^a$ term, and a custodial violating part has the hypercharge term $B_\mu t_R^3$. Note that the Wilson coefficients of these two parts are proportional to the electroweak couplings g and g' , and so lead to correlated phenomenological predictions.
- Finally, there are three operators at dimension-6 that separately break three different linear combinations of $SU(2)_{RH}$, $SU(2)_{RqR}$, $SU(2)_{RlR}$: $O_{HqR}^{(3)+}$ breaks $SU(2)_{RH} \times SU(2)_{RqR} \rightarrow SU(2)_R$; $O_{HlR}^{(3)+}$ breaks $SU(2)_{RH} \times SU(2)_{RlR} \rightarrow SU(2)_R$; $O_{lRqR}^{(3)+}$ breaks $SU(2)_{RqR} \times SU(2)_{RlR} \rightarrow SU(2)_R$. One example where these operators appear is when $SU(2)_R$ is gauged, as we will see in Sec. IV.

ν SMEFT \rightarrow SMEFT in Warsaw basis	ν SMEFT \rightarrow SMEFT in custodial basis
$C_{\nu H} = 0$	$a_{lH}^+ = -a_{lH}^-$
$C_{\nu W} = 0$	$a_{lW}^+ = -a_{lW}^-$
$C_{\nu B} = 0$	$a_{lB}^+ = -a_{lB}^-$
$C_{H\nu e} = C_{H\nu e}^* = 0$	$a_{Hl_R}^{(3)+} = a_{Hl_R}^{(3)-} = 0$
$C_{H\nu} = 0$	$a_{Hl_R}^{(1)+} = -a_{Hl_R}^{(1)-}$
$C_{\nu\nu} = C_{\nu e} = 0$	$a_{l_R l_R}^{++} = a_{l_R l_R}^{--} = -\frac{1}{2} a_{l_R l_R}^{+-}$
$C_{\nu edu} = C_{\nu edu}^* = 0$	$a_{l_R q_R}^{(3)++} = a_{l_R q_R}^{(3)+-} = 0$
$C_{\nu u} = C_{\nu d} = 0$	$a_{l_R q_R}^{(1)++} = -a_{l_R q_R}^{(1)-+}$ $a_{l_R q_R}^{(1)+-} = -a_{l_R q_R}^{(1)--}$
$C_{l\nu} = 0$	$a_{ll_R}^+ = -a_{ll_R}^-$
$C_{q\nu} = 0$	$a_{ql_R}^+ = -a_{ql_R}^-$
$C_{l\nu uq} = 0$	$a_{ll_R q_R q}^+ = -a_{ll_R q_R q}^-$
$C_{l\nu le} = 0$	$a_{ll_R ll_R} = 0$
$C_{l\nu qd}^{(1)} = 0$	$a_{ll_R qq_R}^{(1)+} = -a_{ll_R qq_R}^{(1)-}$
$C_{l\nu qd}^{(3)} = 0$	$a_{ll_R qq_R}^{(3)+} = -a_{ll_R qq_R}^{(3)-}$

Table 7. Recovering SMEFT from ν SMEFT: the left (right) column shows the constraints on the Wilson coefficients in Warsaw (custodial) basis.

Recovering SMEFT from ν SMEFT. It is straightforward to recover the dim-6 operators of SMEFT from ν SMEFT by setting the appropriate Wilson coefficients to zero. We have shown this in Table 7, along with the translation into the constraints on the custodial basis Wilson coefficients.

Flavor Indices of the Wilson Coefficients. In Tables .1-5, we have suppressed all the flavor indices, but it should be understood that each fermion field actually comes with a generation index, so are the corresponding Wilson coefficients. For example, the two-fermion operator $Q_{Hl}^{(3)}$ and four-fermion operator Q_U should

actually read

$$Q_{pr}^{(3)} = \left(H^\dagger i \overleftrightarrow{D}_\mu^a H \right) \left(\bar{l}_p \gamma^\mu \tau^a l_r \right) , \quad (4.20a)$$

$$Q_{prst} = \left(\bar{l}_p \gamma_\mu l_r \right) \left(\bar{l}_s \gamma^\mu l_t \right) . \quad (4.20b)$$

The EFT Lagrangian therefore has a sum over these generation indices:

$$\mathcal{L}_{\text{EFT}} \supset \sum_{p,r=1}^3 C_{pr}^{(3)} Q_{pr}^{(3)} + \sum_{p,r,s,t=1}^3 C_{prst} Q_{prst} = \sum_{p,r=1}^3 a_{pr}^{(3)} O_{pr}^{(3)} + \sum_{p,r,s,t=1}^3 a_{prst} O_{prst} . \quad (4.21)$$

Our convention is that Wilson coefficients without explicit flavor indices are assumed to be flavor-universal.

As we will see, most four-fermion operators are irrelevant for the phenomenology to be discussed in IV. However, one exception is that the mixed first and second generation four-lepton operator will feed into \hat{G}_F . Let us give it a special name, $a_{12} = C_{12}$, for future convenience:

$$\mathcal{L}_{\text{EFT}} \supset a_{12} \left(\bar{l}_1 \gamma_\mu l_2 \right) \left(\bar{l}_2 \gamma^\mu l_1 \right) . \quad (4.22)$$

Note that its relation to our general notation is¹

$$a_{12} = a_{1221} + a_{2112} = C_{1221} + C_{2112} = C_{12} . \quad (4.23)$$

Observables of Custodial Symmetry in (ν)SMEFT

In this section, we map (ν)SMEFT at dim-6 onto the following set of observables

$$\left\{ \hat{\alpha}, \hat{G}_F, \hat{m}_Z^2, \hat{m}_W^2, \hat{\Gamma}_{Z\nu_L \bar{\nu}_L}, \hat{\Gamma}_{Ze_L \bar{e}_L}, \hat{\Gamma}_{Ze\bar{e}}, \hat{\Gamma}_{W\nu_L e_L} \right\} . \quad (4.24)$$

In order, these are denoting the fine structure constant, the Fermi constant, the pole masses of W and Z bosons, the partial decay widths of the Z boson to left-handed neutrinos, left-handed electrons, and right-handed electrons, the partial decay widths of the W boson to left-handed neutrinos and left-handed electrons.

¹Operators involving flavor indices 2112 and 1221 we abbreviate the ‘‘Rush’’ and ‘‘Shru’’ contractions.

We have chosen a restricted set of observables that illustrate the effects of integrating out custodial symmetric UV physics. Some of them can be directly measured, for example $\hat{\alpha}$, \hat{m}_Z^2 , \hat{m}_W^2 , while others require multiple measurements or need to be inferred from other measurements. That is, we have explicitly made the choice to present observables that most easily illustrate our theoretical results. Later in Sec. IV we will discuss how to map experimental measurements to these observables and a subset of their hadronic counterpart observables in B.15. For example, while we present our results below in terms of $\{\hat{\Gamma}_{Ze_L\bar{e}_L}, \hat{\Gamma}_{Ze\bar{e}}\}$, it is much more straightforward to utilize different combinations to enable comparison with experiment, namely $\{\hat{\Gamma}_{Ze_L\bar{e}_L} + \hat{\Gamma}_{Ze\bar{e}}, \hat{A}_{FB}^{0,e}\}$, the sum of the partial widths of the Z boson into left- and right-handed electrons and the forward-backward asymmetries for the $e^+e^- \rightarrow e^+e^-$ scattering on Z resonance.

Observables in the SM. In SM, these observables are given by the three Lagrangian parameters g_1, g_2, v as²

$$\hat{\alpha}_{\text{SM}} = \frac{g_1^2 g_2^2}{4\pi (g_1^2 + g_2^2)}, \quad (4.25a)$$

$$\hat{G}_{F, \text{SM}} = \frac{1}{\sqrt{2}v^2}, \quad (4.25b)$$

$$\hat{m}_{Z, \text{SM}}^2 = \frac{1}{4} (g_1^2 + g_2^2) v^2, \quad (4.25c)$$

$$\hat{m}_{W, \text{SM}}^2 = \frac{1}{4} g_2^2 v^2. \quad (4.25d)$$

²We are neglecting the lepton masses in the decay widths.

$$\hat{\Gamma}_{Z\nu_L\bar{\nu}_L, \text{SM}} = \frac{\hat{m}_{Z, \text{SM}} g_2^2}{96\pi c_\theta^2}, \quad (4.26a)$$

$$\hat{\Gamma}_{Ze_L\bar{e}_L, \text{SM}} = \frac{\hat{m}_{Z, \text{SM}} g_2^2}{96\pi c_\theta^2} (1 - 2s_\theta^2)^2, \quad (4.26b)$$

$$\hat{\Gamma}_{Ze\bar{e}, \text{SM}} = \frac{\hat{m}_{Z, \text{SM}} g_2^2}{24\pi c_\theta^2} s_\theta^4, \quad (4.26c)$$

$$\hat{\Gamma}_{W\nu_Le_L, \text{SM}} = \frac{\hat{m}_{W, \text{SM}}}{48\pi} g_2^2, \quad (4.26d)$$

where θ denotes the Weinberg angle

$$c_\theta \equiv \frac{g_2}{\sqrt{g_1^2 + g_2^2}}, \quad s_\theta \equiv \frac{g_1}{\sqrt{g_1^2 + g_2^2}}. \quad (4.27)$$

It is also convenient to rewrite the observables $\{\hat{\Gamma}_{Ze_L\bar{e}_L}, \hat{\Gamma}_{Ze\bar{e}}\}$ in terms of $\{\hat{\Gamma}_{Ze_L\bar{e}_L} + \hat{\Gamma}_{Ze\bar{e}}, \hat{A}_{FB}^{0,e}\}$ as

$$\hat{\Gamma}_{Ze_L\bar{e}_L, \text{SM}} + \hat{\Gamma}_{Ze\bar{e}, \text{SM}} = \frac{\hat{m}_{Z, \text{SM}} g_2^2}{96\pi c_\theta^2} (1 - 4s_\theta^2 + 8s_\theta^4), \quad (4.28a)$$

$$\hat{A}_{FB, \text{SM}}^{0,e} = \frac{3}{4} \left(\frac{1 - 4s_\theta^2}{1 - 4s_\theta^2 + 8s_\theta^4} \right)^2 \quad (4.28b)$$

Observables in the SMEFT. Clearly, once the first three observables in 4.26 are measured, SM predicts the values of the other five as functions of $\{\hat{\alpha}, \hat{G}_F, \hat{m}_Z^2\}$. However, once we consider SMEFT, these predictions will be modified, as the Wilson coefficients C_i feed into every equation in 4.26.

We work in the Warsaw basis, and restrict our mapping analysis to tree-level. Because we are only interested in the leading corrections from SMEFT at dim-6 level, we only need to keep up to the linear terms in the Wilson coefficients C_i (see .1 for definitions of Warsaw basis operators extended to ν SMEFT).

In the following we present five observables corresponding to the deviations of $\{\hat{\rho}, \hat{\Gamma}_{Z\nu_L\bar{\nu}_L}, \hat{\Gamma}_{Ze_L\bar{e}_L}, \hat{\Gamma}_{Ze\bar{e}}, \hat{\Gamma}_{W\nu_Le_L}\}$ from the SM predictions:

$$\hat{\rho} \equiv \frac{\hat{m}_W^2}{\hat{m}_Z^2} \frac{2}{\hat{x}} \left(1 - \sqrt{1 - \hat{x}}\right), \quad (4.29a)$$

$$\hat{r}_{Z\nu_L\bar{\nu}_L} \equiv \frac{24\pi}{\sqrt{2}\hat{G}_F\hat{m}_Z^3} \hat{\Gamma}_{Z\nu_L\bar{\nu}_L}, \quad (4.29b)$$

$$\hat{r}_{Ze_L\bar{e}_L} \equiv \frac{24\pi}{\sqrt{2}\hat{G}_F\hat{m}_Z^3(1 - \hat{x})} \hat{\Gamma}_{Ze_L\bar{e}_L}, \quad (4.29c)$$

$$\hat{r}_{Ze\bar{e}} \equiv \frac{24\pi}{\sqrt{2}\hat{G}_F\hat{m}_Z^3(1 - \sqrt{1 - \hat{x}})^2} \hat{\Gamma}_{Ze\bar{e}}, \quad (4.29d)$$

$$\hat{r}_{W\nu_Le_L} \equiv \frac{24\pi}{\hat{G}_F\hat{m}_Z^3(1 + \sqrt{1 - \hat{x}})^{\frac{3}{2}}} \hat{\Gamma}_{W\nu_Le_L}. \quad (4.29e)$$

Here, we have introduced a convenient combination

$$\hat{x} \equiv \frac{2\sqrt{2}\pi\hat{\alpha}}{\hat{G}_F\hat{m}_Z^2}. \quad (4.30)$$

These five observables are unity in SM, but are modified in SMEFT due to nonzero Wilson coefficients. Using Warsaw basis and assuming universality among fermion generations, we calculate their dim-6 SMEFT predictions as

$$\hat{\rho} = 1 + \frac{v^2}{1 - 2s_\theta^2} \left[-\frac{1}{2}c_\theta^2 C_{HD} - 2s_\theta c_\theta C_{HWB} - 2s_\theta^2 C_{Hl}^{(3)} + \frac{1}{2}s_\theta^2 C_{12} \right], \quad (4.31a)$$

$$\hat{r}_{Z\nu_L\bar{\nu}_L} = 1 + v^2 \left[-\frac{1}{2}C_{HD} - 2C_{Hl}^{(1)} + \frac{1}{2}C_{12} \right], \quad (4.31b)$$

$$\hat{r}_{Ze_L\bar{e}_L} = 1 + \frac{v^2}{(1 - 2s_\theta^2)^2} \left[-\frac{1}{2}C_{HD} - 4s_\theta c_\theta C_{HWB} + 2(1 - 2s_\theta^2)C_{Hl}^{(1)} - 4s_\theta^2 C_{Hl}^{(3)} + \frac{1}{2}C_{12} \right], \quad (4.31c)$$

$$\hat{r}_{Ze\bar{e}} = 1 + \frac{v^2}{1 - 2s_\theta^2} \left[\frac{1}{2}C_{HD} + \frac{2c_\theta}{s_\theta} C_{HWB} + 2C_{Hl}^{(3)} - \frac{1 - 2s_\theta^2}{s_\theta^2} C_{He} - \frac{1}{2}C_{12} \right], \quad (4.31d)$$

$$\hat{r}_{W\nu_Le_L} = 1 + \frac{v^2}{1 - 2s_\theta^2} \left[-\frac{3}{4}c_\theta^2 C_{HD} - 3s_\theta c_\theta C_{HWB} - 3s_\theta^2 C_{Hl}^{(3)} + \frac{2 - s_\theta^2}{4} C_{12} \right]. \quad (4.31e)$$

We show more details of deriving these results in B. We have explicitly checked that our results agree with Ref. [122]. From 4.31, we see that in generic dim-6 SMEFT, there are nearly as many Wilson coefficients as the observables listed, so there is enough freedom for them to be modified almost freely. However, if we restrict to dim-6 operators that are custodial and flavor conserving, then many operator coefficients vanish and there will be stronger correlations among these six observables.

Observables in the Custodial Basis. To see this, we first rewrite the expressions for the observables into the custodial basis given in .2 using the translation relations provided in .5 to obtain

$$\hat{\rho} = 1 + \frac{v^2}{1 - 2s_\theta^2} \left[-2c_\theta^2 a_{HD} + 4s_\theta c_\theta a_{HWB} - 2s_\theta^2 a_{Hl}^{(3)} + \frac{1}{2} s_\theta^2 a_{12} \right], \quad (4.32a)$$

$$\hat{r}_{Z\nu_L\bar{\nu}_L} = 1 + v^2 \left[-2a_{HD} + 2a_{Hl}^{(1)} + \frac{1}{2} a_{12} \right], \quad (4.32b)$$

$$\hat{r}_{Ze_L\bar{e}_L} = 1 + \frac{v^2}{(1 - 2s_\theta^2)^2} \left[-2a_{HD} + 8s_\theta c_\theta a_{HWB} - 2(1 - 2s_\theta^2) a_{Hl}^{(1)} - 4s_\theta^2 a_{Hl}^{(3)} + \frac{1}{2} a_{12} \right], \quad (4.32c)$$

$$\begin{aligned} \hat{r}_{Ze\bar{e}} = 1 + \frac{v^2}{1 - 2s_\theta^2} & \left[2a_{HD} - \frac{4c_\theta}{s_\theta} a_{HWB} + 2a_{Hl}^{(3)} \right. \\ & \left. + \frac{1 - 2s_\theta^2}{s_\theta^2} \left(a_{Hl_R}^{(1)+} - a_{Hl_R}^{(1)-} - a_{Hl_R}^{(3)+} + a_{Hl_R}^{(3)-} \right) - \frac{1}{2} a_{12} \right], \end{aligned} \quad (4.32d)$$

$$\hat{r}_{W\nu_L e_L} = 1 + \frac{v^2}{1 - 2s_\theta^2} \left[-3c_\theta^2 a_{HD} + 6s_\theta c_\theta a_{HWB} - 3s_\theta^2 a_{Hl}^{(3)} + \frac{2 - s_\theta^2}{4} a_{12} \right]. \quad (4.32e)$$

Now if we restrict to only operators that are flavor and custodial symmetric, we obtain

$$\hat{\rho} = 1 - \frac{v^2 s_\theta^2}{1 - 2s_\theta^2} \left[2a_{Hl}^{(3)} - \frac{1}{2}a_{12} \right], \quad (4.33a)$$

$$\hat{r}_{Z\nu_L\bar{\nu}_L} = 1 + \frac{1}{2}v^2 a_{12}, \quad (4.33b)$$

$$\hat{r}_{Ze_L\bar{e}_L} = 1 - \frac{v^2}{(1 - 2s_\theta^2)^2} \left[4s_\theta^2 a_{Hl}^{(3)} - \frac{1}{2}a_{12} \right], \quad (4.33c)$$

$$\hat{r}_{Ze\bar{e}} = 1 + \frac{v^2}{1 - 2s_\theta^2} \left[2a_{Hl}^{(3)} - \frac{1}{2}a_{12} \right] - \frac{v^2}{s_\theta^2} a_{HlR}^{(3)+}, \quad (4.33d)$$

$$\hat{r}_{W\nu_L e_L} = 1 - \frac{v^2}{1 - 2s_\theta^2} \left[3s_\theta^2 a_{Hl}^{(3)} - \frac{2 - s_\theta^2}{4} a_{12} \right]. \quad (4.33e)$$

These five observables only depend on three Wilson coefficients as free parameters.

An interesting question is the robustness of the predictions in 4.33. One way to investigate this is to consider if there is any nontrivial solution, other than the custodial symmetric one above, in which the general result in 4.31 with custodial preserving and custodial violating operators can conspire to masquerade as 4.33. We find the only nontrivial solution to be

$$C_{Hl}^{(3)} + \frac{c_\theta}{s_\theta} C_{HWB} = a_{Hl}^{(3)} \quad (4.34a)$$

$$C_{He} = a_{HlR}^{(3)+} \quad (4.34b)$$

$$C_{12} = a_{12} \quad (4.34c)$$

$$C_{HD} = 0 \quad (4.34d)$$

$$C_{Hl}^{(1)} = 0. \quad (4.34e)$$

The only way custodial preserving and violating operators could conspire to reproduce 4.33 is for a custodial preserving operator coefficient $C_{Hl}^{(3)}$ to be equal and opposite to the custodial violating coefficient $\cot\theta C_{HWB}$. (All of the other relations

are consistent with custodial symmetry.) Since C_{HWB} is only generated at one-loop leading matching level, this seems extremely contrived. It is gratifying to see that any tree-level custodial violation arising C_{HD} necessarily implies a different set of correlated predictions for our observables.

We have presented our results in 4.31 that apply to SMEFT and ν SMEFT alike, since we did not consider observables involving right-handed neutrinos. Nevertheless, the conversation from 4.31 to 4.32 to 4.33 implicitly assumes that right-handed neutrinos are in the spectrum at the scale where the UV physics is integrated out. Hence, in ν SMEFT, one could construct an (at least in principle) observable involving $\hat{\Gamma}_{Z\nu_R\nu_R}$. However, we cannot construct the ratio $\hat{r}_{Z\nu_R\nu_R}$, because of course $\hat{\Gamma}_{Z\nu_R\nu_R}$ is zero in (ν) SM. One can show that $\hat{\Gamma}_{Z\nu_R\nu_R}$ receives a correction from just one ν SMEFT operator, $C_{H\nu}$. In the case where there are no flavor or custodial violating observables generated by integrating out the UV physics, i.e., the same assumptions that led to our result 4.33, the custodial symmetric part of $C_{H\nu}$ is just $a_{Hl_R}^{(3)+}$, and so there is no additional dependence on custodial preserving operators of ν SMEFT. While it is possible to construct observables that involve $\hat{\Gamma}_{Z\nu_R\nu_R}$, they are necessarily dependent on the masses of the right-handed neutrinos. For example, if the right-handed neutrino masses were above the electroweak symmetry breaking scale, but below the scale of the UV physics, there would be no new (Z pole) observables to consider. For this reason, we do not consider further observables that rely on assuming the scale of the right-handed neutrinos is below the electroweak scale.

EOM Redundancies

From the argument we made in the section above, one may naively think that the EFT of a custodial preserving UV sector would be fully captured by the subset of

those operators in our custodial basis (.2) that do not contain any type of custodial violation. Interestingly, this is not the case.

After integrating out UV physics, the resulted EFT operators may lie outside of an arbitrarily chosen operator basis. In order to present the entire EFT in the custodial basis, one can apply integrating by parts (IBP) and equation of motion (EOM) redundancies to trade these operators into linear combinations of operators within the custodial basis. Most redundancy relations, such as integration by parts (IBP) and Fierz identities, will not change the custodial-preserving nature of these operators. However, the Standard Model EOMs mix operators that are custodial preserving with custodial violating ones because the gauging of hypercharge and the presence of Yukawa couplings explicitly breaks custodial symmetry. As a result, even if the original operators from integrating out heavy physics preserve custodial symmetry, the linear combinations they are traded into may contain custodial violating operators.

This means that, to fully capture the EFT from integrating out a custodial-preserving UV sector one may need both custodial-preserving operators and custodial-violating ones in a particular basis. To better illustrate this issue, we take a closer look at a specific example that we will encounter later in our discussion of UV theory examples.

Consider the operator $Q_R = |H|^2|DH|^2$ that preserves custodial symmetry. It can be generated at tree-level by integrating out a heavy W' gauge boson as we see in Secs. IV,IV. Although Q_R is not an operator in the Warsaw basis, it can be traded into Warsaw operators by IBP and the EOM of Higgs field in the Standard Model, which reads as

$$(D^2H)^j = (m_H^2 - \lambda|H|^2) H^j + \left(\epsilon_{jk} \bar{l}^k \Gamma_{\nu\nu} - \bar{e} \Gamma_e^\dagger l^j + \epsilon_{jk} \bar{q}^k \Gamma_{uu} - \bar{d} \Gamma_d^\dagger q^j \right) \quad (4.35)$$

Combine this using EOM and IBP, and we convert Q_R into

$$\begin{aligned}
|H|^2|DH|^2 &= \frac{1}{2}Q_{H\Box} + 2\lambda Q_H - \lambda v^2|H|^4 \\
&+ \frac{1}{2}(Y_u Q_{uH} + Y_d Q_{dH} + Y_\nu Q_{\nu H} + Y_e Q_{eH} + \text{h.c.}) , \quad (4.36)
\end{aligned}$$

While $Q_{H\Box}$ and Q_H are custodial preserving operators, the appearance of $Y_f Q_{fH}$ violates custodial symmetry. This is a consequence of the implementation of EOM because the Standard Model EOM explicitly breaks custodial symmetry via the Yukawa couplings. Therefore, integrating out custodial symmetric UV physics may generate both custodial-preserving and custodial violating operators in a particular basis.

Implications of EOM Redundancies for our Observables. We now consider implications of the EOM redundancies which a custodial invariant outside of Warsaw basis can become a custodial violating operator in the Warsaw basis. Our observables given in 4.33 assumed the presence of only custodial preserving operators in our custodial basis. Given that using EOM can generate custodial violating operators in our basis, our analysis in Sec. IV is potentially incomplete. In this section we show that this EOM subtlety does not affect our results in 4.33 if we restrict to tree-level matching.

Let us first identify which EOMs in ν SM lead to custodial symmetry violating operators. Clearly, the EOM for gluons and W bosons do not break custodial symmetry, and hence do not cause this problem. The EOM for B boson is irrelevant, since operators containing factors of $\partial^\mu B_{\mu\nu}$ are considered custodial violating operators already, which would not be generated at the matching scale. Therefore, the only potentially problematic EOMs are those for the Higgs H and the fermions ψ .

Total	$H^4 D^2$	$\bar{\psi}\psi H^2 D$	$H^2 D^4$	$\bar{\psi}\psi D^3$	$\bar{\psi}\psi X D$	$\bar{\psi}\psi H D^2$
38	1	8	1	4	8	16

Table 8. Custodial invariants outside of Warsaw basis that yield custodial violating operators in Warsaw basis upon using H and ψ EOM redundancies.

Next, let us find all the ν SMEFT dim-6 custodial preserving operators containing an EOM factor of H or ψ , i.e. containing $D^2 H$, $\not{D}\psi$, or $\not{D}\bar{\psi}$. Using the Hilbert series technique [130, 131, 132, 133, 134], with the EOM redundancy relation relaxed,³ we find that there are 38 additional independent custodial preserving operators outside of Warsaw basis.⁴ They can be divided into six classes according to the field content, as listed in 8.

In general, these custodial invariant operators will yield, upon trading via EOM, a variety of custodial violating operators in the Warsaw basis. However, if we focus on tree-level matching, then the situation is much simpler. As was originally worked out in [208, 209], and recently emphasized and generalized by [210], only a small subset of SMEFT operators can be generated by tree-level matching.⁵ Among the operators listed in 8, only the first two classes, $H^4 D^2$ and $\bar{\psi}\psi H^2 D$ belong to this subset. They contain nine operators, which are nothing but the ν SMEFT “kinetic terms” multiplied

³This can be achieved by taking H , ψ , and $\bar{\psi}$ (and their descendants) as “long representations” of the conform group, as opposed to “short representations”. See [134] for details.

⁴Here we are counting the number of real Wilson coefficients.

⁵For completeness, we repeat the derivation of this result in B, following the method used in [210].

by $|H|^2$:

$$|H|^2 |DH|^2, \quad (4.37a)$$

$$|H|^2 \bar{\psi} i \not{D} \psi + \text{h.c.}, \quad \text{with } \psi = q, l, q_R, l_R. \quad (4.37b)$$

We already encountered the first operator above, and showed the result of transforming it into the Warsaw basis through EOM in 4.36. The second operator transformed into the Warsaw basis becomes

$$|H|^2 \bar{q} i \not{D} q = Y_u Q_{uH} + Y_d Q_{dH}, \quad \text{for } \psi = q. \quad (4.38)$$

We see that the custodial violating operators obtained through this procedure are all in class 5, $\bar{\psi}\psi H^3$, as given in .1. However, it is clear from 4.31 that none of these custodial violating operators feeds into the observables discussed in Sec. IV. Therefore, our results in 4.33 stand, provided that we limit ourselves to tree-level matching of a custodial symmetric UV theory onto our custodial basis of ν SMEFT.

Observables of UV Theories with Custodial Symmetry

In this section, we calculate the predictions for our observables in four different custodial symmetric UV theories as simple examples that demonstrate our results. We consider in Sec. IV a real singlet scalar; in Sec. IV a heavy Z' from a spontaneously broken $U(1)_{B-L}$ theory; in Sec. IV heavy W' 's and Z' 's from embedding the electroweak group into $SU(2)_L \times SU(2)_R \times U(1)_{B-L}$; in Sec. IV a heavy W'_L from embedding $SU(2)_L$ into $SU(2)_A \times SU(2)_B$. The real singlet scalar theory is well-known to produce a small number of higher dimensional operators making it straightforward to study. The $U(1)_{B-L}$ theory is interesting because there are only four-fermion interactions generated at the matching scale, which is distinct from many SMEFT analyses that consider, for example, just bosonic operators. The $SU(2)_L \times SU(2)_R \times U(1)_{B-L}$ theory is nontrivial and quite interesting because

it effectively gauges custodial symmetry in the UV. Once $SU(2)_R \times U(1)_{B-L}$ is spontaneously broken to $U(1)_Y$, however, custodial symmetry is spontaneously broken and custodial violating operators are generated at the matching scale. However, in the formal limit in which the gauge coupling of the $U(1)_{B-L}$ group vanishes, custodial symmetry is restored, and we find nontrivial tree-level contributions to two of our observables arising from $O_{HlR}^{(3)+}$. Finally, the heavy W'_L from embedding $SU(2)_L$ into $SU(2)_A \times SU(2)_B$ is interesting because it leads to contributions to all of our observables. In particular, this custodial symmetric UV theory leads to both vertex corrections as well as four-fermion operators that result in $\hat{\rho} \neq 1$ at tree-level.

Singlet scalar extension. We consider a real singlet scalar ϕ at some heavy scale M as a first example of UV-completion of SMEFT with custodial symmetry. This model has been studied in detail by Jiang *et al.* in [211].

At the renormalizable level, this scalar is only allowed to couple to the Standard Model exclusively through the SM Higgs doublet H due to Lorentz invariance and Gauge invariance. We parameterize the ϕ part of the Lagrangian (up to tadpoles) as

$$\mathcal{L} \supset \frac{1}{2} (\partial\phi)^2 - \frac{1}{2} M^2 \phi^2 - A |H|^2 \phi - \frac{1}{2} \kappa |H|^2 \phi^2 - \frac{1}{3!} \mu \phi^3 - \frac{1}{4!} \lambda_\phi \phi^4. \quad (4.39)$$

After integrating out ϕ , we get a SMEFT. At tree-level, there are only two nonzero Wilson coefficients at dim-6 in the Warsaw basis [211]:

$$C_H = -\frac{\kappa A^2}{2M^4} + \frac{\mu A^3}{6M^6}, \quad (4.40a)$$

$$C_{H\Box} = -\frac{A^2}{2M^4}. \quad (4.40b)$$

Now transforming to our custodial basis defined in .2 (by applying our dictionary in .4), we get the nonzero Wilson coefficients as

$$a_H = -\frac{\kappa A^2}{16M^4} + \frac{\mu A^3}{48M^6}, \quad (4.41a)$$

$$a_{H\Box} = -\frac{A^2}{2M^4}. \quad (4.41b)$$

As both O_H and $O_{H\Box}$ are custodial invariants (shown in .2), we see that this SMEFT is indeed custodial symmetric. Applying our result 4.33 to this EFT, we get the prediction on the observables at tree-level as

$$\hat{\rho} = \hat{r}_{Z\nu_L\bar{\nu}_L} = \hat{r}_{Ze_L\bar{e}_L} = \hat{r}_{Ze\bar{e}} = \hat{r}_{W\nu_L e_L} = 1. \quad (4.42)$$

Z' associated with a $U(1)_{B-L}$ symmetry. Another example highlighted in this section is a Z'_{B-L} model, where the heavy Z' is the gauge boson of a $U(1)_{B-L}$ symmetry in the UV (see, e.g., Ref. [212]). This classical symmetry can be broken at the quantum level through triangle anomalies. To consistently gauge the symmetry, one has to ensure that the triangle anomaly contributions from different fermion species are canceled. In the case of $U(1)_{B-L}$, the anomaly cancellation can be simply achieved by introducing three SM-singlet right-handed neutrinos ν , a requirement that is automatically by enforcing $SU(2)_{Rl_R}$ isospin on the right-handed lepton sector.

Assuming that this $U(1)_{B-L}$ gauge boson Z' couples to the $B-L$ current $j_{B-L} \equiv j_B - j_L$ through a coupling $\frac{1}{2}g_Z$, then our UV Lagrangian is

$$\mathcal{L}_{\text{UV}} = -\frac{1}{4}Z'_{\mu\nu}Z'^{\mu\nu} + \frac{1}{2}M^2Z'_\mu Z'^\mu + g_Z Z'_\mu \sum_{\psi=q,u,d,l,\nu,e} \bar{\psi}\gamma^\mu Y_{Z,\psi}\psi. \quad (4.43)$$

Here the charge $Y_{Z,\psi} = \frac{1}{2}(B-L)$ for each type of fermion is summarized in 9. We have also assumed that the Z' has a large mass M . This can be acquired through the

Higgsing from a heavy scalar in the UV which only couples to Z' , or via a *Stüeckelberg* mechanism which allows M to be a free parameter in the model. In principle, a generic Z'_{B-L} can mix with the hypercharge gauge boson B through a coupling $\frac{1}{2}\epsilon B^{\mu\nu} Z'_{\mu\nu}$. As we have pointed out previously, hypercharge is one of the two sources in the Standard Model which break custodial symmetry (the other is the Yukawa coupling). The mixing of Z' with hypercharge will break custodial symmetry in the UV. Because of that, we have taken ϵ to vanish, $\epsilon = 0$. This is a requirement that follows once we impose the UV theory preserve custodial symmetry, which was after all the purpose of this section.

ψ	q	u	d	l	ν	e
$Y_{Z,\psi}$	$\frac{1}{6}$	$\frac{1}{6}$	$\frac{1}{6}$	$-\frac{1}{2}$	$-\frac{1}{2}$	$-\frac{1}{2}$

Table 9. Fermion charges Y_Z under the Z' gauge interaction.

Now integrating out Z' at tree-level, we obtain the EFT Lagrangian

$$\mathcal{L}_{\text{EFT}} = -\frac{g_Z^2}{2M^2} \left(\sum_{\psi=q,u,d,l,\nu,e} \bar{\psi} \gamma_\mu Y_{Z,\psi} \psi \right) \left(\sum_{\psi=q,u,d,l,\nu,e} \bar{\psi} \gamma^\mu Y_{Z,\psi} \psi \right). \quad (4.44)$$

We see that only four-fermion operators of the type $(\bar{L}L)(\bar{L}L)$, $(\bar{R}R)(\bar{R}R)$, and $(\bar{L}L)(\bar{R}R)$ are generated. In Warsaw basis, the Wilson coefficients can be summarized as

$$C_{ud}^{(1)} = C_{qu}^{(1)} = C_{qd}^{(1)} = 2C_{qq}^{(1)} = 2C_{uu} = 2C_{dd} = -\frac{g_Z^2}{2M^2} 2Y_1^2, \quad (4.45a)$$

$$C_{\nu e} = C_{l\nu} = C_{le} = 2C_{ll} = 2C_{\nu\nu} = 2C_{ee} = -\frac{g_Z^2}{2M^2} 2Y_2^2, \quad (4.45b)$$

$$C_{lq}^{(1)} = C_{\nu u} = C_{\nu d} = C_{e u} = C_{e d} = C_{lu} = C_{ld} = C_{q\nu} = C_{qe} = -\frac{g_Z^2}{2M^2} 2Y_1 Y_2, \quad (4.45c)$$

where we have defined $Y_1 \equiv \frac{1}{6}$ and $Y_2 \equiv -\frac{1}{2}$ for convenience. Transforming to our custodial basis defined in .2 (again by applying the dictionary in .4), we see that the

only nonzero Wilson coefficients are those of the custodial invariants:

$$\left\{ \begin{array}{l} a_{ll} = -\frac{g_Z^2}{2M^2} Y_2^2 \\ a_{qq}^{(1)} = -\frac{g_Z^2}{2M^2} Y_1^2 \\ a_{lq}^{(1)} = -\frac{g_Z^2}{2M^2} 2Y_1 Y_2 \end{array} \right\}, \quad \left\{ \begin{array}{l} a_{l_R l_R}^{++} = -\frac{g_Z^2}{2M^2} Y_2^2 \\ a_{q_R q_R}^{(1)++} = -\frac{g_Z^2}{2M^2} Y_1^2 \\ a_{l_R q_R}^{(1)++} = -\frac{g_Z^2}{2M^2} 2Y_1 Y_2 \end{array} \right\}, \quad \left\{ \begin{array}{l} a_{l_R}^+ = -\frac{g_Z^2}{2M^2} 2Y_2^2 \\ a_{l q_R}^+ = -\frac{g_Z^2}{2M^2} 2Y_1 Y_2 \\ a_{q l_R}^+ = -\frac{g_Z^2}{2M^2} 2Y_1 Y_2 \\ a_{q q_R}^{(1)+} = -\frac{g_Z^2}{2M^2} 2Y_1^2 \end{array} \right\}. \quad (4.46)$$

This is the manifestation of the UV physics preserving custodial symmetry.

Now to apply our observable results in 4.33, we also need to figure out the Wilson coefficient a_{12} defined in 4.22. We can restore the generation indices in Q_{ll} from 4.44:

$$\mathcal{L}_{\text{EFT}} \supset -\frac{g_Z^2}{2M^2} Y_2^2 \sum_{p,r=1}^3 (\bar{l}_p \gamma_\mu l_p) (\bar{l}_r \gamma^\mu l_r). \quad (4.47)$$

We see that

$$a_{prst}^{ll} = -\frac{g_Z^2}{2M^2} Y_2^2 \delta_{pr} \delta_{st}. \quad (4.48)$$

Therefore, using 4.23 we get

$$a_{12} = a_{1221}^{ll} + a_{2112}^{ll} = 0. \quad (4.49)$$

Now plugging everything into 4.33, we finally get for this EFT

$$\hat{\rho} = \hat{r}_{Z\nu_L \bar{\nu}_L} = \hat{r}_{Ze_L \bar{e}_L} = \hat{r}_{Ze\bar{e}} = \hat{r}_{W\nu_L e_L} = 1. \quad (4.50)$$

Heavy W 's and Z 's from a UV theory with $SU(2)_L \times SU(2)_R \times U(1)_{B-L}$.

In this section, we consider a minimum custodial symmetric UV embedding of the

electroweak sector, by promoting the electroweak gauge symmetry to $SU(2)_L \times SU(2)_R \times U(1)_{B-L}$. The covariant derivative is now

$$D_\mu = \partial_\mu - igW_\mu^a t^a - ig_R R_\mu^a t_R^a - ig_K Y_K K_\mu. \quad (4.51)$$

with R_μ^a, K_μ the gauge bosons and t_R^a, Y_K the corresponding generators for $SU(2)_R$ and $U(1)_{B-L}$. In order to break this enlarged symmetry down to electroweak symmetry at low energy, we introduce a new heavy scalar field Φ , which is an $SU(2)_R$ doublet with $Y_{K,\Phi} = \frac{1}{2}$ and $SU(2)_L$ singlet. Upon acquiring a vev

$$\Phi = \frac{1}{\sqrt{2}} \begin{pmatrix} 0 \\ v_\phi + \phi \end{pmatrix}, \quad (4.52)$$

it breaks $SU(2)_R \times U(1)_{B-L}$ to $U(1)_Y$, with the hypercharge $\mathbf{y} = t_R^3 + Y_K$.⁶ In this example, the custodial symmetry is an exact symmetry respected by the UV theory at the high energy scale. However, it is spontaneously broken at the scale v_ϕ . Once we integrate out the heavy gauge bosons and Φ , this v_ϕ gives rise to all the custodial violating effects in the resulting SMEFT, putting the hypercharge part of the dim-4 custodial violations and those at higher mass dimensions onto the same footing. This is in analogy with the case of MFV [144].⁷

The UV Lagrangian in this example is

$$\mathcal{L}_{\text{UV}} = -\frac{1}{4}W_{\mu\nu}^a W^{a,\mu\nu} - \frac{1}{4}R_{\mu\nu}^a R^{a,\mu\nu} - \frac{1}{4}K_{\mu\nu} K^{\mu\nu} + |D\Phi|^2 - V_\Phi + |DH|^2 - V_H + \bar{\psi}i\not{D}\psi. \quad (4.53)$$

Here we have switched off any possible interactions between Φ and H for simplicity, and hence focus on the effects of integrating out the heavy gauge bosons. After the

⁶The story is completely in parallel with how the SM Higgs H breaks $SU(2)_L \times U(1)_Y$ to $U(1)_{EM}$, with electric charge $Q = t^3 + y$.

⁷Note that this example would not account for the Yukawa custodial violation in SM.

symmetry breaking, we can identify the mass eigenstates of the gauge bosons

$$(R_\mu^a, K_\mu) \rightarrow (R_\mu^\pm, X_\mu, B_\mu) , \quad (4.54)$$

among which B_μ remains massless, but R_μ^\pm and X_μ obtain masses

$$m_R^2 = \frac{1}{4} g_R^2 v_\phi^2 , \quad (4.55a)$$

$$m_X^2 = \frac{1}{4} (g_R^2 + g_K^2) v_\phi^2 . \quad (4.55b)$$

We then integrate out these heavy gauge bosons (together with the heavy scalar Φ) at the tree-level, and obtain the EFT Lagrangian

$$\begin{aligned} \mathcal{L}_{\text{EFT}} = & \mathcal{L}_{\text{SM}} + \frac{g_R^2}{2m_R^2} \left[\left(iD_{\text{SM}}^\mu \tilde{H}^\dagger \right) H + \sum_{\psi=q_R, l_R} \bar{\psi} \gamma^\mu t_R^- \psi \right] \left[H^\dagger \left(iD_{\text{SM}, \mu} \tilde{H} \right) - \sum_{\psi=q_R, l_R} \bar{\psi} \gamma_\mu t_R^+ \psi \right] \\ & - \frac{g_R^2}{2m_X^2 c_R^2} \left[\frac{c_R^2}{2} \left(H^\dagger i \overleftrightarrow{D}_{\text{SM}}^\mu H \right) + \sum_{\psi=q_R, l_R} \bar{\psi} \gamma^\mu (t_R^3 - s_R^2 \mathcal{Y}) \psi \right] \\ & \times \left[\frac{c_R^2}{2} \left(H^\dagger i \overleftrightarrow{D}_{\text{SM}, \mu} H \right) + \sum_{\psi=q_R, l_R} \bar{\psi} \gamma_\mu (t_R^3 - s_R^2 \mathcal{Y}) \psi \right] \\ & + \mathcal{O}(\text{dim-8}) . \end{aligned} \quad (4.56)$$

Here the mixing angle is defined as usual

$$c_R = \cos \theta_R \equiv \frac{g_R}{\sqrt{g_R^2 + g_K^2}} . \quad (4.57)$$

We see that as expected, this EFT spontaneously breaks custodial symmetry, and thus custodial violating operators are generated at the matching scale v_ϕ , such as the combination

$$\left(H^\dagger i \overleftrightarrow{D}_{\text{SM}, \mu} H \right) \left(H^\dagger i \overleftrightarrow{D}_{\text{SM}}^\mu H \right) = Q_{H\Box} + 4Q_{HD} , \quad (4.58)$$

in which Q_{HD} is a custodial violating operator. However, the Wilson coefficients of these custodial violating operators (as one can check) are proportional to the

hypercharge gauge coupling

$$g_1^2 = \frac{g_R^2 g_K^2}{g_R^2 + g_K^2}. \quad (4.59)$$

This is just a reflection that the dim-6 custodial violations have the same source as that of dim-4. From this point of view, we see that there are two interesting limits in which the UV theory could preserve custodial symmetry: $g_K \rightarrow 0$ and $g_R \rightarrow 0$, both of which will yield a vanishing $g_1 \rightarrow 0$. Let us now explore both of them in detail below.

The Limit $g_K \rightarrow 0$. In this limit, $c_R \rightarrow 1$ and $s_R \rightarrow 0$. The result in 4.56 simplifies to

$$\begin{aligned} \mathcal{L}_{\text{EFT}}(g_K \rightarrow 0) = \mathcal{L}_{\text{SM}}(g_1 \rightarrow 0) - \frac{1}{2v_\phi^2} & \left[\text{tr}(\Sigma^\dagger i D_{\text{SM},\mu} \Sigma \tau_R^a) - \sum_{\psi=q_R, l_R} \bar{\psi}_R \gamma_\mu \tau_R^a \psi_R \right] \\ & \times \left[\text{tr}(\Sigma^\dagger i D_{\text{SM}}^\mu \Sigma \tau_R^a) - \sum_{\psi=q_R, l_R} \bar{\psi}_R \gamma^\mu \tau_R^a \psi_R \right]. \end{aligned} \quad (4.60)$$

Clearly, this is a custodial symmetric Lagrangian. Focusing on the dim-6 part, we find

$$\begin{aligned} \mathcal{L}_c & \equiv \mathcal{L}_{\text{EFT}}(g_K \rightarrow 0) - \mathcal{L}_{\text{SM}}(g_1 \rightarrow 0) \\ & = -\frac{1}{2v_\phi^2} \left[4Q_R + O_{H\Box} - 2 \left(O_{Hl_R}^{(3)+} + O_{Hq_R}^{(3)+} \right) + \left(O_{l_R l_R}^{++} + 2O_{l_R q_R}^{(3)++} + O_{q_R q_R}^{(3)++} \right) \right]. \end{aligned} \quad (4.61)$$

We see the appearance of

$$Q_R \equiv |H|^2 |DH|^2, \quad (4.62)$$

a custodial symmetric operator (upon taking $g_1 = 0$) that is outside of the Warsaw basis. We now can apply our results from IV to transform it into Warsaw basis

operators using the Higgs EOM redundancy relation:

$$Q_R \equiv |H|^2 |DH|^2 = 2\lambda Q_H + \frac{1}{2} Q_{H\Box} + \frac{1}{2} Q_Y - \lambda v^2 |H|^4. \quad (4.63)$$

Since this EOM relation does not respect custodial symmetry, a custodial violating operator in Warsaw basis Q_Y have been generated:⁸

$$Q_Y \equiv Y_u Q_{uH} + Y_d Q_{dH} + Y_\nu Q_{\nu H} + Y_e Q_{eH} + \text{h.c.} \quad (4.64)$$

Now putting everything together, we can identify the Wilson coefficients in our custodial basis:

$$\left\{ \begin{array}{l} a_H = -\frac{\lambda}{2v_\phi^2} \\ a_{H\Box} = -\frac{3}{2v_\phi^2} \end{array} \right\}, \quad \left\{ \begin{array}{l} a_{Hl_R}^{(3)+} = a_{Hq_R}^{(3)+} = -a_{l_R q_R}^{(3)++} = \frac{1}{v_\phi^2} \\ a_{l_R l_R}^{++} = a_{q_R q_R}^{(3)++} = -\frac{1}{2v_\phi^2} \end{array} \right\}, \quad \left\{ \begin{array}{l} a_{lH}^\pm = -\frac{Y_\nu \pm Y_e}{4v_\phi^2} \\ a_{qH}^\pm = -\frac{Y_u \pm Y_d}{4v_\phi^2} \end{array} \right\}. \quad (4.65)$$

These are mostly custodial preserving operators. The only exceptions are a_{lH}^- and a_{qH}^- . As explained, this is a consequence of implementing the SM EOM, which mediates the custodial violation at dim-4 ($Y_u \neq Y_d$ and $Y_\nu \neq Y_e$) to dim-6. We also notice the appearance of the three operators: $O_{Hl_R}^{(3)+}$, $O_{Hq_R}^{(3)+}$ and $O_{l_R q_R}^{(3)++}$. They are generated because in the 2-2-1 model, the gauging of $SU(2)_R$ reduces the three independent global $SU(2)_{RH} \times SU(2)_{Rq_R} \times SU(2)_{Rl_R}$ down to one single gauged $SU(2)_R$.

Now let us turn to the predictions on the observables discussed in IV. Because we do have custodial violating operators generated in this example, we should in principle use 4.32. However, our custodial violating Wilson coefficients are a_{qH}^- and a_{lH}^- , belonging to class 5: $\bar{\psi}\psi H^3$ in .2, which do not feed into these observables, as demonstrated by 4.32. Therefore, our result in 4.33 still holds, as we expect by

⁸Note that this operator violates custodial symmetry due to Yukawa mismatch $Y_u \neq Y_d$ and $Y_\nu \neq Y_e$.

the general argument given in IV. Plugging in 4.65, we find that the only nontrivial contribution to the observables is from $a_{Hl_R}^{(3)+}$:

$$\hat{\rho} = 1, \quad (4.66a)$$

$$\hat{r}_{Z\nu_L\bar{\nu}_L} = 1, \quad (4.66b)$$

$$\hat{r}_{Ze_L\bar{e}_L} = 1, \quad (4.66c)$$

$$\hat{r}_{Ze\bar{e}} = 1 - s_\theta^2 \frac{v^2}{v_\phi^2}, \quad (4.66d)$$

$$\hat{r}_{W\nu_L e_L} = 1. \quad (4.66e)$$

The Limit $g_R \rightarrow 0$. Now let us consider the other limit, $g_R \rightarrow 0$, that also yields $g_1 \rightarrow 0$. In this limit, we have $c_R \rightarrow 0$ and $s_R \rightarrow 1$. However, simplifying the result in 4.56 is not as naive as plugging these values in. The subtlety of this limit that the “heavy” gauge bosons R_μ^\pm become massless $m_R \rightarrow 0$ (see 4.55), if v_ϕ (and hence m_X) is kept finite. In this case, truncating the EFT expansion at $\frac{1}{m_R^2}$ is no longer a good approximation, namely that some higher mass dimension terms in 4.56 actually become *more* important. Correctly summing over these contributions turns out to be simply removing the first line in 4.56, and yields the EFT Lagrangian

$$\mathcal{L}_{\text{EFT}}(g_R \rightarrow 0) = \mathcal{L}_{\text{SM}}(g_1 \rightarrow 0) - \frac{g_K^2}{2m_X^2} (\bar{\psi}\gamma^\mu Y_K \psi) (\bar{\psi}\gamma_\mu Y_K \psi) + \mathcal{O}(\text{dim}-8). \quad (4.67)$$

This EFT Lagrangian is precisely 4.44.

The above derivation of 4.67 through summing over all the important higher mass dimension terms, and then canceling the first line in 4.56 seems somewhat mysterious. This awkwardness is merely a reflection of the EFT not being a convenient framework anymore when $m_R \rightarrow 0$. The story is actually quite simple if we take the limit $g_R \rightarrow 0$ in the UV theory instead, i.e. in 4.53. It is then clear that $g_R \rightarrow 0$ decouples the gauge bosons R_μ^a from the rest of the theory, and only K_μ will acquire mass from v_ϕ , which

then works precisely as the Z' boson in 4.43. So there is no doubt that we will obtain precisely the same EFT as in 4.44.

A Heavy W'_L Gauge Boson. In this section, we consider an example of integrating out a heavy W'_L gauge boson. Specifically, we consider a symmetry breaking $SU(2)_A \times SU(2)_B \rightarrow SU(2)_L$. The covariant derivative is

$$D_\mu = \partial_\mu - ig_A W_{A\mu}^a t_A^a - ig_B W_{B\mu}^a t_B^a. \quad (4.68)$$

The gauge sector Lagrangian is

$$\mathcal{L} \supset -\frac{1}{4} W_{A\mu\nu}^a W_A^{a\mu\nu} - \frac{1}{4} W_{B\mu\nu}^a W_B^{a\mu\nu} + \frac{1}{2} \text{tr} \left[(D^\mu \Phi)^\dagger (D_\mu \Phi) \right], \quad (4.69)$$

where the heavy scalar field Φ is a 2×2 matrix that transforms as a fundamental bilinear under the $SU(2)_A \times SU(2)_B$:

$$\Phi \rightarrow U_A \Phi U_B^\dagger. \quad (4.70)$$

Therefore, the concrete form of its covariant derivative is

$$D_\mu \Phi = \partial_\mu \Phi - ig_A W_{A\mu}^a t^a \Phi + ig_B \Phi W_{B\mu}^a t^a, \quad (4.71)$$

with $t^a = \frac{1}{2} \sigma^a$ the $SU(2)$ generators in the fundamental representation. The symmetry is spontaneously broken by the vev of the heavy scalar field Φ :

$$\Phi \supset \frac{1}{\sqrt{2}} v_\Phi \begin{pmatrix} 1 & 0 \\ 0 & 1 \end{pmatrix}. \quad (4.72)$$

The unbroken group is an $SU(2)$ formed by the generators $t_A^a + t_B^a$, which we identify as our $SU(2)_L$ group in the SM. The corresponding gauge boson is the W

boson. For the broken generators, the corresponding gauge boson W'_L acquire mass from v_Φ :

$$\begin{aligned} \frac{1}{2} \text{tr} \left[(D^\mu \Phi)^\dagger (D_\mu \Phi) \right] &\supset \frac{1}{8} v_\Phi^2 (g_A W_A^{a\mu} - g_B W_B^{a\mu}) (g_A W_{A\mu}^a - g_B W_{B\mu}^a) \\ &= \frac{1}{8} v_\Phi^2 (g_A^2 + g_B^2) W'_L{}^{a\mu} W_{L\mu}{}^a. \end{aligned} \quad (4.73)$$

We see that $m_{W'_L}^2 = \frac{1}{4} (g_A^2 + g_B^2) v_\Phi^2$, and

$$W'_{L\mu}{}^a \equiv \frac{1}{\sqrt{g_A^2 + g_B^2}} (g_A W_{A\mu}^a - g_B W_{B\mu}^a), \quad (4.74a)$$

$$W_\mu^a \equiv \frac{1}{\sqrt{g_A^2 + g_B^2}} (g_B W_{A\mu}^a + g_A W_{B\mu}^a). \quad (4.74b)$$

With the above rotation, we can write the covariant derivative as

$$D_\mu = \partial_\mu - i g_2 W_\mu^a (t_A^a + t_B^a) - i W'_{L\mu}{}^a \left(\frac{g_A^2}{\sqrt{g_A^2 + g_B^2}} t_A^a - \frac{g_B^2}{\sqrt{g_A^2 + g_B^2}} t_B^a \right), \quad (4.75)$$

with the SM gauge coupling $g_2 = \frac{g_A g_B}{\sqrt{g_A^2 + g_B^2}}$.

For the interactions between the above gauge sector and the SM fields, we assume that W_A plays the role of W before the symmetry breaking, namely that the SM fields couple to W_A exactly the way they couple to the W boson, and do not couple to W_B at all. This means that for nontrivially charged fields $t_A^a \neq 0$ but $t_B^a = 0$. From 4.75, we see that after the symmetry breaking, the SM fields couple to both W and W'_L . Up to linear power in W'_L , this interaction is

$$\mathcal{L} \supset \frac{g_A^2}{\sqrt{g_A^2 + g_B^2}} W'_{L\mu}{}^a J_W^{a\mu}. \quad (4.76)$$

Here $J_W^{a\mu}$ denotes the SM $SU(2)_L$ current:

$$J_{W\mu}^a = \frac{1}{2} \left(H^\dagger i \overleftrightarrow{D}_{\text{SM}, \mu}^a H + \sum_{\psi} \bar{\psi} \gamma_{\mu} \tau^a \psi \right). \quad (4.77)$$

Integrating out W' at tree-level, we obtain an EFT up to dim-6 as

$$\mathcal{L}_{\text{EFT}} = -\frac{g_A^4}{g_A^2 + g_B^2} \frac{1}{2m_{W'_L}^2} J_{W\mu}^a J_W^{a\mu} = -\frac{2c_A^4}{v_{\Phi}^2} J_{W\mu}^a J_W^{a\mu}, \quad (4.78)$$

where we have defined the mixing angle $c_A \equiv \frac{g_A}{\sqrt{g_A^2 + g_B^2}}$. Clearly, this EFT Lagrangian is custodial symmetric. Plugging in 4.77, we get

$$\begin{aligned} \mathcal{L}_{\text{EFT}} &= -\frac{c_A^4}{v_{\Phi}^2} \left[\frac{1}{2} Q_R + \frac{1}{8} Q_{H\Box} + Q_{Hl}^{(3)} + Q_{Hq}^{(3)} + \frac{1}{2} Q_{ll} + \frac{1}{2} Q_{qq}^{(3)} + Q_{lq}^{(3)} \right] \\ &= -\frac{c_A^4}{v_{\Phi}^2} \left[\lambda Q_H + \frac{3}{8} Q_{H\Box} + \frac{1}{4} (Y_u Q_{uH} + Y_d Q_{dH} + Y_{\nu} Q_{\nu H} + Y_e Q_{eH} + \text{h.c.}) \right. \\ &\quad \left. + Q_{Hl}^{(3)} + Q_{Hq}^{(3)} + \frac{1}{2} Q_{ll} + \frac{1}{2} Q_{qq}^{(3)} + Q_{lq}^{(3)} \right]. \end{aligned} \quad (4.79)$$

From the first line above, we see that all the effective operators are custodial invariants, as expected from 4.78. In the second line, we trade the operator Q_R for operators in the Warsaw Basis. As explained before, this procedure yields custodial violating operators, due to the use of SM equations of motion. We can now identify the Wilson coefficients in Warsaw Basis

$$\left\{ \begin{array}{l} C_H = -\frac{c_A^4}{v_{\Phi}^2} \lambda \\ C_{H\Box} = -\frac{c_A^4}{v_{\Phi}^2} \frac{3}{8} \end{array} \right\}, \left\{ \begin{array}{l} (C_{uH}, C_{dH}, C_{\nu H}, C_{eH}) = -\frac{c_A^4}{v_{\Phi}^2} \frac{1}{4} (Y_u, Y_d, Y_{\nu}, Y_e) \\ C_{Hl}^{(3)} = C_{Hq}^{(3)} = 2C_{ll} = 2C_{qq}^{(3)} = C_{lq}^{(3)} = -\frac{c_A^4}{v_{\Phi}^2} \end{array} \right\}. \quad (4.80)$$

Using the translation relations provided in .4, we get the Wilson coefficients in the Custodial Basis:

$$\left\{ \begin{array}{l} a_H = -\frac{c_A^4}{v_\Phi^2} \frac{1}{8} \lambda \\ a_{H\Box} = -\frac{c_A^4}{v_\Phi^2} \frac{3}{8} \end{array} \right\}, \quad \left\{ \begin{array}{l} a_{lH}^\pm = -\frac{c_A^4}{v_\Phi^2} \frac{1}{16} (Y_\nu \pm Y_e) \\ a_{qH}^\pm = -\frac{c_A^4}{v_\Phi^2} \frac{1}{16} (Y_u \pm Y_d) \end{array} \right\}, \quad (4.81a)$$

$$a_{Hl}^{(3)} = a_{Hq}^{(3)} = 2a_{ll} = 2a_{qq}^{(3)} = a_{lq}^{(3)} = -\frac{c_A^4}{v_\Phi^2}. \quad (4.81b)$$

As expected, we find the appearance of a_{lH}^- and a_{qH}^- , due to use of SM equations of motion. However, as generally argued in IV, as well as concretely shown in 4.32, these custodial violating Wilson coefficients do not feed into our benchmark observables discussed in IV, and our results in 4.33 still hold. To use this result, however, we also need to compute the a_{12} defined in 4.22 to compute the observables discussed in IV. To do so, we restore the generation indices in Q_{ll} from 4.78:

$$\mathcal{L}_{\text{EFT}} \supset -\frac{c_A^4}{2v_\Phi^2} \sum_{p,r=1}^3 (\bar{l}_p \gamma_\mu \tau^a l_p) (\bar{l}_r \gamma^\mu \tau^a l_r). \quad (4.82)$$

To make this into the form of Q_{ll} , we need to also restore the $SU(2)_L$ indices being contracted, and use the group identity:

$$\tau_{ij}^a \tau_{kl}^a = 4 \left(\frac{1}{2} \delta_{il} \delta_{jk} - \frac{1}{4} \delta_{ij} \delta_{kl} \right). \quad (4.83)$$

Substituting this in, we get

$$\begin{aligned}
\mathcal{L}_{\text{EFT}} &\supset -\frac{c_A^4}{2v_\Phi^2} \sum_{p,r=1}^3 (\bar{l}_p^\mu \gamma_\mu \tau_{ij}^a l_p^j) (\bar{l}_r^k \gamma^\mu \tau_{kl}^a l_r^l) \\
&= -\frac{c_A^4}{2v_\Phi^2} \sum_{p,r=1}^3 [2 (\bar{l}_p^\mu \gamma_\mu l_p^j) (\bar{l}_r^j \gamma^\mu l_r^i) - (\bar{l}_p^\mu \gamma_\mu l_p^i) (\bar{l}_r^j \gamma^\mu l_r^j)] \\
&= -\frac{c_A^4}{2v_\Phi^2} \sum_{p,r=1}^3 [2 (\bar{l}_p \gamma_\mu l_r) (\bar{l}_r \gamma^\mu l_p) - (\bar{l}_p \gamma_\mu l_p) (\bar{l}_r \gamma^\mu l_r)] . \tag{4.84}
\end{aligned}$$

To obtain the last line above, we have used Fierz identity for the first term in the square bracket, and then suppressed the $SU(2)_L$ indices as usual. Now we can read off the Wilson coefficient with generation indices:

$$a_{prst}^{ll} = -\frac{c_A^4}{2v_\Phi^2} (2\delta_{pt}\delta_{rs} - \delta_{pr}\delta_{st}) . \tag{4.85}$$

Now using 4.23 we get

$$a_{12} = a_{1221}^{ll} + a_{2112}^{ll} = -2\frac{c_A^4}{v_\Phi^2} . \tag{4.86}$$

Plugging all the relevant Wilson coefficients into 4.33, we obtain the pseudo observables

$$\hat{\rho} = 1 + \left[\frac{s_\theta^2}{1 - 2s_\theta^2} \right] \frac{c_A^4 v^2}{v_\Phi^2} , \tag{4.87a}$$

$$\hat{r}_{Z\nu_L \bar{\nu}_L} = 1 - \frac{c_A^4 v^2}{v_\Phi^2} , \tag{4.87b}$$

$$\hat{r}_{Ze_L \bar{e}_L} = 1 - \left[\frac{1 - 4s_\theta^2}{(1 - 2s_\theta^2)^2} \right] \frac{c_A^4 v^2}{v_\Phi^2} , \tag{4.87c}$$

$$\hat{r}_{Ze\bar{e}} = 1 - \left[\frac{1}{1 - 2s_\theta^2} \right] \frac{c_A^4 v^2}{v_\Phi^2} , \tag{4.87d}$$

$$\hat{r}_{W\nu_L e_L} = 1 - \left[\frac{2 - 7s_\theta^2}{2(1 - 2s_\theta^2)} \right] \frac{c_A^4 v^2}{v_\Phi^2} . \tag{4.87e}$$

In particular, note that the observable $\hat{\rho} \neq 1$, even though the UV sector integrated out is custodial symmetric.

Custodial Symmetry vis-a-vis Flavor Symmetry

As we discussed in Sec. IV, there are several $SU(2)_R$ global symmetries in the SM. The one we associate with custodial symmetry arises in the Higgs sector $SU(2)_{RH}$ is, however, explicitly broken by Yukawa interactions that cause $SU(2)_{RH} \times SU(2)_{RqR}$ to be broken down to just $U(1)_Y$. Thus, even a “minimal flavor violating” extension to the SM has custodial violation. Most of the Yukawa couplings are numerically small, and so the explicit custodial violation is similarly small. However, the near maximal difference between the top and bottom Yukawas implies the top quark is able to induce substantial custodial violation in many operators of (ν) SMEFT at both tree-level and loop level. The observables we considered in 4.31 are precisely constructed to *not* have custodial violation from the top quark Yukawa coupling appear at tree-level. This is obvious because there is no dependence of our observables on y_t . This is the central reason we have focused on exploring observables that are sensitive to *tree-level* violations of custodial symmetry. Put another way, our results are fundamentally limited by top-quark induced radiative corrections of additional ν SMEFT operators feeding into our observables.

One can also probe the possibilities in which the UV theory has non-trivial flavor structure. In our UV theory examples, the singlet scalar theory is trivially flavor-symmetric. The $U(1)_{B-L}$ theory is also necessarily flavor-symmetric, since after all what is being gauged is the residual $U(1)$ global flavor symmetry that remains in ν SM after all of the SM Yukawa couplings have broken $U(3)^6 \rightarrow U(1)_B \times U(1)_L$. Finally, the $SU(2)_L \times SU(2)_R \times U(1)_{B-L}$ theory is flavor-symmetric assuming all of

the $SU(2)_R$ global symmetries are gauged. This is essentially automatic once one permits custodial symmetric 3×3 Yukawa couplings.

For the W'_L model, however, if some of the left-handed quark doublets transformed under $SU(2)_A$ while others transformed under $SU(2)_B$, this would also lead to flavor-nonuniversality. The flavor nonuniversalities would show up as flavor-dependent deviations to our observables, i.e., one would need to generalize beyond the flavor-universal corrections to the observables that we have calculated.

Experimental Measurements of our Observables

We have presented our results in terms of the observables

$$\left\{ \hat{\rho}, \hat{\Gamma}_{Z\nu_L\bar{\nu}_L}, \hat{\Gamma}_{Ze_L\bar{e}_L}, \hat{\Gamma}_{Ze\bar{e}}, \hat{\Gamma}_{W\nu_L e_L} \right\}, \quad (4.88)$$

and an additional set of hadronic observables in Appendix B. Observable in this context is by definition basis independent, but that does not necessarily imply that it can be directly measured.

First consider what is required to make tree-level predictions for our observables, and then we consider how they would be modified to account for SM loop corrections. We have used as our inputs $\hat{\alpha}$, \hat{G}_F , \hat{m}_Z^2 , and so the observable $\hat{\rho}$ requires in addition a measurement of \hat{m}_W^2 . The widths $\left\{ \hat{\Gamma}_{Ze_L\bar{e}_L}, \hat{\Gamma}_{Ze\bar{e}} \right\}$ are most easily measured by rewriting them in the linear combinations $\left\{ \hat{\Gamma}_{Ze_L\bar{e}_L} + \hat{\Gamma}_{Ze\bar{e}}, \hat{A}_{FB}^{0,e} \right\}$. Here, direct measurements of the angular distributions of $e^+e^- \rightarrow e^+e^-$ on Z resonance can determine $\hat{A}_{FB}^{0,e}$ [213]. The partial width into electrons $\hat{\Gamma}_{Ze_L\bar{e}_L} + \hat{\Gamma}_{Ze\bar{e}}$ is not directly measured, and instead one uses measurements of the total rate $e^+e^- \rightarrow e^+e^-$ on Z resonance as well as the total width of Z boson, Γ_Z , that was determined by separate measurements scanning the lineshape of $e^+e^- \rightarrow$ hadrons [213].

The partial width of Z into neutrinos must be inferred by subtracting the measured contributions of the Z partial widths from the measured total width [213].

For this presentation, we assume flavor universality and neglect the masses of the quarks and leptons. The Z partial width into neutrinos is

$$3\hat{\Gamma}_{Z\nu_L\bar{\nu}_L} = \Gamma_{\text{tot}} - \hat{\Gamma}_{Zll} - \hat{\Gamma}_{Zqq} \quad (4.89)$$

where we emphasize the observable we have used throughout this paper, $\hat{\Gamma}_{Z\nu_L\bar{\nu}_L}$, is the width into just one generation, and

$$\hat{\Gamma}_{Zll} = 3 \left(\hat{\Gamma}_{Ze_L\bar{e}_L} + \hat{\Gamma}_{Ze\bar{e}} \right), \quad (4.90a)$$

$$\hat{\Gamma}_{Zqq} = 2 \left(\hat{\Gamma}_{Zu_L\bar{u}_L} + \hat{\Gamma}_{Zu\bar{u}} \right) + 3 \left(\hat{\Gamma}_{Zd_L\bar{d}_L} + \hat{\Gamma}_{Zd\bar{d}} \right). \quad (4.90b)$$

Notice that it is not possible to determine the width into neutrinos without taking into account the corrections to the hadronic observables given in Appendix B. Since the hadronic observables in B.15 depend on additional ν SMEFT quark operators, we must also measure a restricted set of hadronic observables in order to remove the dependence on those quark operator Wilson coefficients. This is accomplished by enlarging our set of observables to include $\hat{\Gamma}_{Zqq}$. This depends on one specific linear combination of quark operator Wilson coefficients that can be read off from B.15. (It also depends on $a_{Hl}^{(3)}$ and a_{12} , but this poses no ambiguity since the observables in Sec. IV already depend on the same quantities.) Hence, once this Z to hadrons width is measured, any deviation is ascribed to the otherwise unknown quark level operators, and thus Z hadronic observables do not provide any additional information. But, they do allow us to obtain a measurement of $\hat{\Gamma}_{Z\nu_L\bar{\nu}_L}$ using Eq. (4.89).

Finally, we turn to the W partial widths. Similar to the discussion for Z partial widths, separate measurements must be combined to obtain an experimental determination of the partial widths: the branching fraction of W into $l\nu$ or hadrons, multiplied by the measured W total width. This can be accomplished using LEP II data that simultaneously measures the W mass and width by doing a global

fit to $e^+e^- \rightarrow \bar{f}f\bar{f}f$ rates and distributions [214]. Care must be taken to extract these quantities given that there are additional operators in SMEFT that induces corrections such as to the triple gauge boson vertex that also must be disentangled [122]. This is beyond the scope of our work.

Tables of Operators, Coefficients, and Translations

1 : X^3		2 : H^6		3 : $H^4 D^2$		5 : $\bar{\psi}\psi H^3 + \text{h.c.}$	
Q_G	$f^{ABC} G_\mu^{A\nu} G_\nu^{B\rho} G_\rho^{C\mu}$	Q_H	$ H ^6$	$Q_{H\Box}$	$-(\partial_\mu H ^2) (\partial^\mu H ^2)$	$Q_{\nu H}$	$ H ^2 (\bar{l}\tilde{H}\nu)$
$Q_{\tilde{G}}$	$f^{ABC} \tilde{G}_\mu^{A\nu} \tilde{G}_\nu^{B\rho} \tilde{G}_\rho^{C\mu}$			Q_{HD}	$[(D_\mu H^\dagger) H] [H^\dagger (D^\mu H)]$	Q_{eH}	$ H ^2 (\bar{l}H e)$
Q_W	$\epsilon^{abc} W_\mu^{a\nu} W_\nu^{b\rho} W_\rho^{c\mu}$					Q_{uH}	$ H ^2 (\bar{q}\tilde{H}u)$
$Q_{\tilde{W}}$	$\epsilon^{abc} \tilde{W}_\mu^{a\nu} \tilde{W}_\nu^{b\rho} \tilde{W}_\rho^{c\mu}$					Q_{dH}	$ H ^2 (\bar{q}H d)$
4 : $X^2 H^2$		6 : $\bar{\psi}\psi XH + \text{h.c.}$		7 : $\bar{\psi}\psi H^2 D$			
Q_{HG}	$ H ^2 G_{\mu\nu}^A G^{A\mu\nu}$	$Q_{\nu W}$	$(\bar{l}\sigma^{\mu\nu}\nu)\tau^a \tilde{H}W_{\mu\nu}^a$	$Q_{Hl}^{(1)}$			$(H^\dagger i \overleftrightarrow{D}_\mu H)(\bar{l}\gamma^\mu l)$
$Q_{H\tilde{G}}$	$ H ^2 \tilde{G}_{\mu\nu}^A G^{A\mu\nu}$	Q_{eW}	$(\bar{l}\sigma^{\mu\nu}e)\tau^a H W_{\mu\nu}^a$	$Q_{Hl}^{(3)}$			$(H^\dagger i \overleftrightarrow{D}_\mu^a H)(\bar{l}\gamma^\mu \tau^{a l})$
Q_{HW}	$ H ^2 W_{\mu\nu}^a W^{a\mu\nu}$	$Q_{\nu B}$	$(\bar{l}\sigma^{\mu\nu}\nu)\tilde{H}B_{\mu\nu}$	$Q_{Hq}^{(1)}$			$(H^\dagger i \overleftrightarrow{D}_\mu H)(\bar{q}\gamma^\mu q)$
$Q_{H\tilde{W}}$	$ H ^2 \tilde{W}_{\mu\nu}^a W^{a\mu\nu}$	Q_{eB}	$(\bar{l}\sigma^{\mu\nu}e)HB_{\mu\nu}$	$Q_{Hq}^{(3)}$			$(H^\dagger i \overleftrightarrow{D}_\mu^a H)(\bar{q}\gamma^\mu \tau^a q)$
Q_{HB}	$ H ^2 B_{\mu\nu} B^{\mu\nu}$	Q_{uG}	$(\bar{q}\sigma^{\mu\nu}T^A u)\tilde{H}G_{\mu\nu}^A$	$Q_{H\nu}$			$(H^\dagger i \overleftrightarrow{D}_\mu H)(\bar{\nu}\gamma^\mu \nu)$
$Q_{H\tilde{B}}$	$ H ^2 \tilde{B}_{\mu\nu} B^{\mu\nu}$	Q_{dG}	$(\bar{q}\sigma^{\mu\nu}T^A d)HG_{\mu\nu}^A$	Q_{He}			$(H^\dagger i \overleftrightarrow{D}_\mu H)(\bar{e}\gamma^\mu e)$
Q_{HWB}	$H^\dagger \tau^a H W_{\mu\nu}^a B^{\mu\nu}$	Q_{uW}	$(\bar{q}\sigma^{\mu\nu}u)\tau^a \tilde{H}W_{\mu\nu}^a$	$Q_{H\nu e} + \text{h.c.}$			$(\tilde{H}^\dagger i D_\mu H)(\bar{\nu}\gamma^\mu e)$
$Q_{H\tilde{W}B}$	$H^\dagger \tau^a H \tilde{W}_{\mu\nu}^a B^{\mu\nu}$	Q_{dW}	$(\bar{q}\sigma^{\mu\nu}d)\tau^a H W_{\mu\nu}^a$	Q_{Hu}			$(H^\dagger i \overleftrightarrow{D}_\mu H)(\bar{u}\gamma^\mu u)$
		Q_{uB}	$(\bar{q}\sigma^{\mu\nu}u)\tilde{H}B_{\mu\nu}$	Q_{Hd}			$(H^\dagger i \overleftrightarrow{D}_\mu H)(\bar{d}\gamma^\mu d)$
		Q_{dB}	$(\bar{q}\sigma^{\mu\nu}d)HB_{\mu\nu}$	$Q_{Hud} + \text{h.c.}$			$(\tilde{H}^\dagger i D_\mu H)(\bar{u}\gamma^\mu d)$
8 : $(\bar{L}L)(\bar{L}L)$		8 : $(\bar{R}R)(\bar{R}R)$		8 : $(\bar{L}L)(\bar{R}R)$			
Q_{ll}	$(\bar{l}\gamma_\mu l)(\bar{l}\gamma^\mu l)$	$Q_{\nu\nu}$	$(\bar{\nu}\gamma_\mu \nu)(\bar{\nu}\gamma^\mu \nu)$	$Q_{l\nu}$			$(\bar{l}\gamma_\mu l)(\bar{\nu}\gamma^\mu \nu)$
$Q_{qq}^{(1)}$	$(\bar{q}\gamma_\mu q)(\bar{q}\gamma^\mu q)$	Q_{ee}	$(\bar{e}\gamma_\mu e)(\bar{e}\gamma^\mu e)$	Q_{le}			$(\bar{l}\gamma_\mu l)(\bar{e}\gamma^\mu e)$
$Q_{qq}^{(3)}$	$(\bar{q}\gamma_\mu \tau^a q)(\bar{q}\gamma^\mu \tau^a q)$	$Q_{\nu e}$	$(\bar{\nu}\gamma_\mu \nu)(\bar{e}\gamma^\mu e)$	Q_{lu}			$(\bar{l}\gamma_\mu l)(\bar{u}\gamma^\mu u)$
$Q_{lq}^{(1)}$	$(\bar{l}\gamma_\mu l)(\bar{q}\gamma^\mu q)$	Q_{uu}	$(\bar{u}\gamma_\mu u)(\bar{u}\gamma^\mu u)$	Q_{ld}			$(\bar{l}\gamma_\mu l)(\bar{d}\gamma^\mu d)$
$Q_{lq}^{(3)}$	$(\bar{l}\gamma_\mu \tau^a l)(\bar{q}\gamma^\mu \tau^a q)$	Q_{dd}	$(\bar{d}\gamma_\mu d)(\bar{d}\gamma^\mu d)$	$Q_{q\nu}$			$(\bar{q}\gamma_\mu q)(\bar{\nu}\gamma^\mu \nu)$
		$Q_{ud}^{(1)}$	$(\bar{u}\gamma_\mu u)(\bar{d}\gamma^\mu d)$	Q_{qe}			$(\bar{q}\gamma_\mu q)(\bar{e}\gamma^\mu e)$
		$Q_{ud}^{(8)}$	$(\bar{u}\gamma_\mu T^A u)(\bar{d}\gamma^\mu T^A d)$	$Q_{qu}^{(1)}$			$(\bar{q}\gamma_\mu q)(\bar{u}\gamma^\mu u)$
		$Q_{\nu u}$	$(\bar{\nu}\gamma_\mu \nu)(\bar{u}\gamma^\mu u)$	$Q_{qd}^{(1)}$			$(\bar{q}\gamma_\mu q)(\bar{d}\gamma^\mu d)$
		$Q_{\nu d}$	$(\bar{\nu}\gamma_\mu \nu)(\bar{d}\gamma^\mu d)$	$Q_{qu}^{(8)}$			$(\bar{q}\gamma_\mu T^A q)(\bar{u}\gamma^\mu T^A u)$
		Q_{eu}	$(\bar{e}\gamma_\mu e)(\bar{u}\gamma^\mu u)$	$Q_{qd}^{(8)}$			$(\bar{q}\gamma_\mu T^A q)(\bar{d}\gamma^\mu T^A d)$
		Q_{ed}	$(\bar{e}\gamma_\mu e)(\bar{d}\gamma^\mu d)$				
		$Q_{\nu e d u} + \text{h.c.}$	$(\bar{\nu}\gamma_\mu e)(\bar{d}\gamma^\mu u)$				
8 : $(\bar{L}R)(\bar{R}L) + \text{h.c.}$		8 : $(\bar{L}R)(\bar{L}R) + \text{h.c.}$					
$Q_{l\nu u q}$	$(\bar{l}^i \nu)(\bar{u} q^i)$	$Q_{l\nu l e}$	$(\bar{l}^i \nu)\epsilon_{ij}(\bar{l}^j e)$	$Q_{quqd}^{(1)}$	$(\bar{q}^i u)\epsilon_{ij}(\bar{q}^j d)$		
Q_{ledq}	$(\bar{l}^i e)(\bar{d} q^i)$	$Q_{quqd}^{(8)}$	$(\bar{q}^i T^A u)\epsilon_{ij}(\bar{q}^j T^A d)$	$Q_{l\nu qd}^{(1)}$	$(\bar{l}^i \nu)\epsilon_{ij}(\bar{q}^j d)$		
		$Q_{lequ}^{(1)}$	$(\bar{l}^i e)\epsilon_{ij}(\bar{q}^j u)$	$Q_{l\nu qd}^{(3)}$	$(\bar{l}^i \sigma_{\mu\nu} \nu)\epsilon_{ij}(\bar{q}^j \sigma^{\mu\nu} d)$		
		$Q_{l\nu qd}^{(3)}$	$(\bar{l}^i \sigma_{\mu\nu} \nu)\epsilon_{ij}(\bar{q}^j \sigma^{\mu\nu} d)$	$Q_{lequ}^{(3)}$	$(\bar{l}^i \sigma_{\mu\nu} e)\epsilon_{ij}(\bar{q}^j \sigma^{\mu\nu} u)$		

Table .1. ν SMEFT dim-6 baryon-preserving operators in Warsaw basis. In addition to the $76 = 42 + (17 + \text{h.c.})$ SMEFT operators, there are $25 = 7 + (9 + \text{h.c.})$ new operators involving right-handed neutrinos ν , which are colored in brown.

	1 : X^3	2 : H^6	3 : $H^4 D^2$	5 : $\bar{\psi}\psi H^3 + \text{h.c.}$
O_G	$f^{ABC} G_\mu^{A\nu} G_\nu^{B\rho} G_\rho^{C\mu}$	O_H	$[\text{tr}(\Sigma^\dagger \Sigma)]^3$	O_{iH}^\pm
$O_{\tilde{G}}$	$f^{ABC} \tilde{G}_\mu^{A\nu} G_\nu^{B\rho} G_\rho^{C\mu}$		$O_{H\Box}$	O_{qH}^\pm
O_W	$\epsilon^{abc} W_\mu^{a\nu} W_\nu^{b\rho} W_\rho^{c\mu}$			
$O_{\tilde{W}}$	$\epsilon^{abc} \tilde{W}_\mu^{a\nu} W_\nu^{b\rho} W_\rho^{c\mu}$			
	4 : $X^2 H^2$	6 : $\bar{\psi}\psi XH + \text{h.c.}$	7 : $\bar{\psi}\psi H^2 D$	
O_{HG}	$\text{tr}(\Sigma^\dagger \Sigma) G_{\mu\nu}^A G^{A\mu\nu}$	O_{lW}^\pm	$(\bar{l}\sigma^{\mu\nu}\tau^a \Sigma P_\pm l_R) W_{\mu\nu}^a$	$O_{Hl}^{(1)}$
$O_{H\tilde{G}}$	$\text{tr}(\Sigma^\dagger \Sigma) \tilde{G}_{\mu\nu}^A G^{A\mu\nu}$	O_{lB}^\pm	$(\bar{l}\sigma^{\mu\nu} \Sigma P_\pm l_R) B_{\mu\nu}$	$O_{Hl}^{(3)}$
O_{HW}	$\text{tr}(\Sigma^\dagger \Sigma) W_{\mu\nu}^a W^{a\mu\nu}$	O_{qG}^\pm	$(\bar{q}\sigma^{\mu\nu} T^A \Sigma P_\pm q_R) G_{\mu\nu}^A$	$O_{Hq}^{(1)}$
$O_{H\tilde{W}}$	$\text{tr}(\Sigma^\dagger \Sigma) \tilde{W}_{\mu\nu}^a W^{a\mu\nu}$	O_{qW}^\pm	$(\bar{q}\sigma^{\mu\nu} \tau^a \Sigma P_\pm q_R) W_{\mu\nu}^a$	$O_{Hq}^{(3)}$
O_{HB}	$\text{tr}(\Sigma^\dagger \Sigma) B_{\mu\nu} B^{\mu\nu}$	O_{qB}^\pm	$(\bar{q}\sigma^{\mu\nu} \Sigma P_\pm q_R) B_{\mu\nu}$	$O_{HlR}^{(1)\pm}$
$O_{H\tilde{B}}$	$\text{tr}(\Sigma^\dagger \Sigma) \tilde{B}_{\mu\nu} B^{\mu\nu}$			$O_{HlR}^{(3)\pm}$
O_{HWB}	$\text{tr}(\Sigma^\dagger \tau^a \Sigma \tau_R^3) W_{\mu\nu}^a B^{\mu\nu}$			$O_{HqR}^{(1)\pm}$
$O_{H\tilde{W}B}$	$\text{tr}(\Sigma^\dagger \tau^a \Sigma \tau_R^3) \tilde{W}_{\mu\nu}^a B^{\mu\nu}$			$O_{HqR}^{(3)\pm}$
	8 : $(\bar{L}L)(\bar{L}L)$	8 : $(\bar{R}R)(\bar{R}R)$	8 : $(\bar{L}L)(\bar{R}R)$	
O_{ll}	$(\bar{l}\gamma_\mu l)(\bar{l}\gamma^\mu l)$	$O_{lR}^{\pm\pm}$	$(\bar{l}_R \gamma_\mu P_\pm l_R)(\bar{l}_R \gamma^\mu P_\pm l_R)$	O_{llR}^\pm
$O_{qq}^{(1)}$	$(\bar{q}\gamma_\mu q)(\bar{q}\gamma^\mu q)$	O_{lR}^{+-}	$(\bar{l}_R \gamma_\mu P_+ l_R)(\bar{l}_R \gamma^\mu P_- l_R)$	O_{lqR}^\pm
$O_{qq}^{(3)}$	$(\bar{q}\gamma_\mu \tau^a q)(\bar{q}\gamma^\mu \tau^a q)$	$O_{qR}^{(1)\pm\pm}$	$(\bar{q}_R \gamma_\mu P_\pm q_R)(\bar{q}_R \gamma^\mu P_\pm q_R)$	O_{qlR}^\pm
$O_{lq}^{(1)}$	$(\bar{l}\gamma_\mu l)(\bar{q}\gamma^\mu q)$	$O_{qR}^{(1)+-}$	$(\bar{q}_R \gamma_\mu P_+ q_R)(\bar{q}_R \gamma^\mu P_- q_R)$	$O_{qqR}^{(1)\pm}$
$O_{lq}^{(3)}$	$(\bar{l}\gamma_\mu \tau^a l)(\bar{q}\gamma^\mu \tau^a q)$	$O_{qR}^{(3)++}$	$(\bar{q}_R \gamma_\mu \tau_R^a q_R)(\bar{q}_R \gamma^\mu \tau_R^a q_R)$	$O_{qqR}^{(8)\pm}$
		$O_{lRqR}^{(1)\pm\pm}$	$(\bar{l}_R \gamma_\mu P_\pm l_R)(\bar{q}_R \gamma^\mu P_\pm q_R)$	
		$O_{lRqR}^{(1)\pm\mp}$	$(\bar{l}_R \gamma_\mu P_\pm l_R)(\bar{q}_R \gamma^\mu P_\mp q_R)$	
		$O_{lRqR}^{(3)++}$	$(\bar{l}_R \gamma_\mu \tau_R^a l_R)(\bar{q}_R \gamma^\mu \tau_R^a P_\pm q_R)$	
	8 : $(\bar{L}R)(\bar{R}L) + \text{h.c.}$	8 : $(\bar{L}R)(\bar{L}R) + \text{h.c.}$		
O_{lRqRq}^\pm	$(\bar{l}^i l_R^j) P_\pm^{jk} (\bar{q}_R^k q^i)$	O_{llRlR}	$(\bar{l}^i l_R^k) \epsilon_{ij} \epsilon_{kl} (\bar{l}^j l_R^l)$	
		$O_{qqRqR}^{(1)}$	$(\bar{q}^i q_R^k) \epsilon_{ij} \epsilon_{kl} (\bar{q}^j q_R^l)$	
		$O_{qqRqR}^{(8)}$	$(\bar{q}^i T^A q_R^k) \epsilon_{ij} \epsilon_{kl} (\bar{q}^j T^A q_R^l)$	
		$O_{lRqqR}^{(1)\pm}$	$(\bar{l}^i l_R^k) \epsilon_{ij} (\epsilon P_\pm)_{kl} (\bar{q}^j q_R^l)$	
		$O_{lRqqR}^{(3)\pm}$	$(\bar{l}^i \sigma_{\mu\nu} l_R^k) \epsilon_{ij} (\epsilon P_\pm)_{kl} (\bar{q}^j \sigma^{\mu\nu} q_R^l)$	

Table .2. ν SMEFT dim-6 baryon-preserving operators in our custodial basis. Operators are colored black (custodial preserving), blue (custodial violating), red (quark isospin violating), or green (lepton isospin violating). For example, O^+ is custodial preserving while O^- is custodial violating, since the former involves P_+ while the latter involves P_- . The notation O^- implies the operator violates both quark and lepton isospin. See text for details.

1 : X^3		2 : H^6		3 : $H^4 D^2$		5 : $\bar{\psi}\psi H^3 + \text{h.c.}$			
O_G	Q_G	O_H	$8Q_H$	$O_{H\Box}$	$Q_{H\Box}$	O_{lH}^\pm	$2(Q_{\nu H} \pm Q_{eH})$		
$O_{\tilde{G}}$	$Q_{\tilde{G}}$			O_{HD}	$Q_{H\Box} + 4Q_{HD}$	O_{qH}^\pm	$2(Q_{uH} \pm Q_{dH})$		
O_W	Q_W								
$O_{\tilde{W}}$	$Q_{\tilde{W}}$								
4 : $X^2 H^2$		6 : $\bar{\psi}\psi XH + \text{h.c.}$		7 : $\bar{\psi}\psi H^2 D$					
O_{HG}	$2Q_{HG}$	O_{lW}^\pm	$Q_{\nu W} \pm Q_{eW}$	$O_{Hl}^{(1)}$	$-Q_{Hl}^{(1)}$				
$O_{H\tilde{G}}$	$2Q_{H\tilde{G}}$	O_{lB}^\pm	$Q_{\nu B} \pm Q_{eB}$	$O_{Hl}^{(3)}$	$Q_{Hl}^{(3)}$				
O_{HW}	$2Q_{HW}$	O_{qG}^\pm	$Q_{uG} \pm Q_{dG}$	$O_{Hq}^{(1)}$	$-Q_{Hq}^{(1)}$				
$O_{H\tilde{W}}$	$2Q_{H\tilde{W}}$	O_{qW}^\pm	$Q_{uW} \pm Q_{dW}$	$O_{Hq}^{(3)}$	$Q_{Hq}^{(3)}$				
O_{HB}	$2Q_{HB}$	O_{qB}^\pm	$Q_{uB} \pm Q_{dB}$	$O_{HlR}^{(1)\pm}$	$-(Q_{H\nu} \pm Q_{He})$				
$O_{H\tilde{B}}$	$2Q_{H\tilde{B}}$			$O_{HlR}^{(3)\pm}$	$\pm 2(Q_{H\nu e} \pm \text{h.c.}) - Q_{H\nu} \pm Q_{He}$				
O_{HWB}	$-2Q_{HWB}$			$O_{HqR}^{(1)\pm}$	$-(Q_{Hu} \pm Q_{Hd})$				
$O_{H\tilde{W}B}$	$-2Q_{H\tilde{W}B}$			$O_{HqR}^{(3)\pm}$	$\pm 2(Q_{Hud} \pm \text{h.c.}) - Q_{Hu} \pm Q_{Hd}$				
8 : $(\bar{L}L)(\bar{L}L)$			8 : $(\bar{R}R)(\bar{R}R)$			8 : $(\bar{L}L)(\bar{R}R)$			
O_{ll}	Q_{ll}	$O_{l_R l_R}^{\pm\pm}$	$Q_{\nu\nu} + Q_{ee} \pm 2Q_{\nu e}$			$O_{l_R}^\pm$	$Q_{l\nu} \pm Q_{le}$		
$O_{qq}^{(1)}$	$Q_{qq}^{(1)}$	$O_{l_R l_R}^{+-}$	$Q_{\nu\nu} - Q_{ee}$			O_{lqR}^\pm	$Q_{l\nu} \pm Q_{ld}$		
$O_{qq}^{(3)}$	$Q_{qq}^{(3)}$	$O_{qRqR}^{(1)\pm\pm}$	$Q_{uu} + Q_{dd} \pm 2Q_{ud}^{(1)}$			O_{qlR}^\pm	$Q_{q\nu} \pm Q_{qe}$		
$O_{lq}^{(1)}$	$Q_{lq}^{(1)}$	$O_{qRqR}^{(1)+-}$	$Q_{uu} - Q_{dd}$			$O_{qqR}^{(1)\pm}$	$Q_{qu}^{(1)} \pm Q_{qd}^{(1)}$		
$O_{lq}^{(3)}$	$Q_{lq}^{(3)}$	$O_{qRqR}^{(3)++}$	$8Q_{ud}^{(8)} - \frac{2N_c - 4}{N_c} Q_{ud}^{(1)} + Q_{uu} + Q_{dd}$			$O_{qqR}^{(8)\pm}$	$Q_{qu}^{(8)} \pm Q_{qd}^{(8)}$		
		$O_{l_R qR}^{(1)\pm\pm}$	$(Q_{\nu u} + Q_{ed}) \pm (Q_{\nu d} + Q_{eu})$						
		$O_{l_R qR}^{(1)\pm\mp}$	$(Q_{\nu u} - Q_{ed}) \mp (Q_{\nu d} - Q_{eu})$						
		$O_{l_R qR}^{(3)\pm\pm}$	$2(Q_{\nu e d u} \pm \text{h.c.}) + (Q_{\nu u} - Q_{eu}) \mp (Q_{\nu d} - Q_{ed})$						
8 : $(\bar{L}R)(\bar{R}L) + \text{h.c.}$			8 : $(\bar{L}R)(\bar{L}R) + \text{h.c.}$						
		$O_{l_R qRq}^\pm$	$Q_{l\nu u q} \pm Q_{ledq}$			$O_{l_R l_R}$	$2Q_{l\nu le}$		
					$O_{qqRqqR}^{(1)}$	$2Q_{quqd}^{(1)}$			
					$O_{qqRqqR}^{(8)}$	$2Q_{quqd}^{(8)}$			
					$O_{l_R qqR}^{(1)\pm}$	$-Q_{lequ}^{(1)} \pm Q_{l\nu qd}^{(1)}$			
					$O_{l_R qqR}^{(3)\pm}$	$-Q_{lequ}^{(3)} \pm Q_{l\nu qd}^{(3)}$			

Table .3. A dictionary of the custodial basis in terms of Warsaw basis. The color scheme is the same as given in Table .1 and Table .2.

1 : X^3		2 : H^6		3 : $H^4 D^2$		5 : $\bar{\psi}\psi H^3 + \text{h.c.}$	
a_G	C_G	a_H	$\frac{1}{8}C_H$	$a_{H\Box}$	$C_{H\Box} - \frac{1}{4}C_{HD}$	a_{lH}^\pm	$\frac{1}{4}(C_{\nu H} \pm C_{eH})$
$a_{\tilde{G}}$	$C_{\tilde{G}}$			a_{HD}	$\frac{1}{4}C_{HD}$	a_{qH}^\pm	$\frac{1}{4}(C_{uH} \pm C_{dH})$
a_W	C_W						
$a_{\tilde{W}}$	$C_{\tilde{W}}$						
4 : $X^2 H^2$		6 : $\bar{\psi}\psi XH + \text{h.c.}$		7 : $\bar{\psi}\psi H^2 D$			
a_{HG}	$\frac{1}{2}C_{HG}$	a_{lW}^\pm	$\frac{1}{2}(C_{\nu W} \pm C_{eW})$	$a_{Hl}^{(1)}$	$-C_{Hl}^{(1)}$		
$a_{H\tilde{G}}$	$\frac{1}{2}C_{H\tilde{G}}$	a_{lB}^\pm	$\frac{1}{2}(C_{\nu B} \pm C_{eB})$	$a_{Hl}^{(3)}$	$C_{Hl}^{(3)}$		
a_{HW}	$\frac{1}{2}C_{HW}$	a_{qG}^\pm	$\frac{1}{2}(C_{uG} \pm C_{dG})$	$a_{Hq}^{(1)}$	$-C_{Hq}^{(1)}$		
$a_{H\tilde{W}}$	$\frac{1}{2}C_{H\tilde{W}}$	a_{qW}^\pm	$\frac{1}{2}(C_{uW} \pm C_{dW})$	$a_{Hq}^{(3)}$	$C_{Hq}^{(3)}$		
a_{HB}	$\frac{1}{2}C_{HB}$	a_{qB}^\pm	$\frac{1}{2}(C_{uB} \pm C_{dB})$	$a_{HlR}^{(1)\pm}$	$-\frac{1}{2}(C_{H\nu} \pm C_{He}) + \frac{1}{4}(\pm C_{H\nu e} - C_{H\nu e}^*)$		
$a_{H\tilde{B}}$	$\frac{1}{2}C_{H\tilde{B}}$			$a_{HlR}^{(3)\pm}$	$\frac{1}{4}(\pm C_{H\nu e} + C_{H\nu e}^*)$		
a_{HWB}	$-\frac{1}{2}C_{HWB}$			$a_{HqR}^{(1)\pm}$	$-\frac{1}{2}(C_{Hu} \pm C_{Hd}) + \frac{1}{4}(\pm C_{Hud} - C_{Hud}^*)$		
$a_{H\tilde{W}B}$	$-\frac{1}{2}C_{H\tilde{W}B}$			$a_{HqR}^{(3)\pm}$	$\frac{1}{4}(\pm C_{Hud} + C_{Hud}^*)$		
8 : $(\bar{L}L)(\bar{L}L)$			8 : $(\bar{R}R)(\bar{R}R)$			8 : $(\bar{L}L)(\bar{R}R)$	
a_{ll}	C_{ll}	$a_{lRlR}^{\pm\pm}$	$\frac{1}{4}(C_{\nu\nu} + C_{ee} \pm C_{\nu e})$			a_{lR}^\pm	$\frac{1}{2}(C_{l\nu} \pm C_{le})$
$a_{qq}^{(1)}$	$C_{qq}^{(1)}$	a_{lRlR}^{+-}	$\frac{1}{2}(C_{\nu\nu} - C_{ee})$			a_{lqR}^\pm	$\frac{1}{2}(C_{l\nu} \pm C_{ld})$
$a_{qq}^{(3)}$	$C_{qq}^{(3)}$	$a_{qRqR}^{(1)\pm\pm}$	$\frac{1}{4}[(C_{uu} + C_{dd}) \pm C_{ud}^{(1)} - \frac{1}{4}C_{ud}^{(8)} \pm (\frac{1}{4} - \frac{1}{2N_c})C_{ud}^{(8)}]$			a_{qlR}^\pm	$\frac{1}{2}(C_{q\nu} \pm C_{qe})$
$a_{lq}^{(1)}$	$C_{lq}^{(1)}$	$a_{qRqR}^{(1)+-}$	$\frac{1}{2}(C_{uu} - C_{dd})$			$a_{qqR}^{(1)\pm}$	$\frac{1}{2}[C_{qu}^{(1)} \pm C_{qd}^{(1)}]$
$a_{lq}^{(3)}$	$C_{lq}^{(3)}$	$a_{qRqR}^{(3)++}$	$\frac{1}{8}C_{ud}^{(8)}$			$a_{qqR}^{(8)\pm}$	$\frac{1}{2}[C_{qu}^{(8)} \pm C_{qd}^{(8)}]$
		$a_{lRqR}^{(1)\pm\pm}$	$\frac{1}{4}[(C_{\nu u} + C_{eu}) \pm (C_{\nu d} + C_{ed})]$				
		$a_{lRqR}^{(1)-\pm}$	$\frac{1}{4}[(C_{\nu u} - C_{eu}) \pm (C_{\nu d} - C_{ed}) + (-C_{\nu edu} \pm C_{\nu edu}^*)]$				
		$a_{lRqR}^{(3)\pm\pm}$	$\frac{1}{4}(C_{\nu edu} \pm C_{\nu edu}^*)$				
8 : $(\bar{L}R)(\bar{R}L) + \text{h.c.}$			8 : $(\bar{L}R)(\bar{L}R) + \text{h.c.}$				
		a_{lRqRq}^\pm	$\frac{1}{2}(C_{l\nu uq} \pm C_{ledq})$		a_{llRlR}	$\frac{1}{2}C_{l\nu le}$	
					$a_{qqRqR}^{(1)}$	$\frac{1}{2}C_{quqd}^{(1)}$	
					$a_{qqRqR}^{(8)}$	$\frac{1}{2}C_{quqd}^{(8)}$	
					$a_{llRqR}^{(1)\pm}$	$\frac{1}{2}[-C_{lequ}^{(1)} \pm C_{lvqd}^{(1)}]$	
					$a_{llRqR}^{(3)\pm}$	$\frac{1}{2}[-C_{lequ}^{(3)} \pm C_{lvqd}^{(3)}]$	

Table .4. A translation dictionary from the Warsaw basis Wilson Coefficients C_i to Custodial basis Wilson Coefficients a_i .

1 : X^3		2 : H^6		3 : $H^4 D^2$		5 : $\bar{\psi}\psi H^3 + \text{h.c.}$	
$C_G, C_{\tilde{G}}$	$a_G, a_{\tilde{G}}$	C_H	$8 a_H$	$C_{H\Box}$	$a_{H\Box} + a_{HD}$	$C_{\nu H}, C_{eH}$	$2(a_{lH}^+ \pm a_{lH}^-)$
$C_W, C_{\tilde{W}}$	$a_W, a_{\tilde{W}}$			C_{HD}	$4 a_{HD}$	C_{uH}, C_{dH}	$2(a_{qH}^+ \pm a_{qH}^-)$
4 : $X^2 H^2$		6 : $\bar{\psi}\psi XH + \text{h.c.}$		7 : $\bar{\psi}\psi H^2 D$			
C_{HG}	$2 a_{HG}$	$C_{\nu W}, C_{eW}$	$a_{lW}^+ \pm a_{lW}^-$	$C_{Hl}^{(1)}$			$-a_{Hl}^{(1)}$
$C_{H\tilde{G}}$	$2 a_{H\tilde{G}}$	$C_{\nu B}, C_{eB}$	$a_{lB}^+ \pm a_{lB}^-$	$C_{Hl}^{(3)}$			$a_{Hl}^{(3)}$
C_{HW}	$2 a_{HW}$	C_{uG}, C_{dG}	$a_{qG}^+ \pm a_{qG}^-$	$C_{Hq}^{(1)}$			$-a_{Hq}^{(1)}$
$C_{H\tilde{W}}$	$2 a_{H\tilde{W}}$	C_{uW}, C_{dW}	$a_{qW}^+ \pm a_{qW}^-$	$C_{Hq}^{(3)}$			$a_{Hq}^{(3)}$
C_{HB}	$2 a_{HB}$	C_{uB}, C_{dB}	$a_{qB}^+ + a_{qB}^-$	$C_{H\nu}, C_{He}$			$-a_{HlR}^{(1)+} \mp a_{HlR}^{(1)-} \mp a_{HlR}^{(3)+} - a_{HlR}^{(3)-}$
$C_{H\tilde{B}}$	$2 a_{H\tilde{B}}$			$C_{H\nu e}$			$2[a_{HlR}^{(3)+} - a_{HlR}^{(3)-}]$
C_{HWB}	$-2 a_{HWB}$			C_{Hu}, C_{Hd}			$-a_{HqR}^{(1)+} \mp a_{HqR}^{(1)-} \mp a_{HqR}^{(3)+} - a_{HqR}^{(3)-}$
$C_{H\tilde{W}B}$	$-2 a_{H\tilde{W}B}$			C_{Hud}			$2[a_{HqR}^{(3)+} - a_{HqR}^{(3)-}]$
8 : $(\bar{L}L)(\bar{L}L)$			8 : $(\bar{R}R)(\bar{R}R)$			8 : $(\bar{L}L)(\bar{R}R)$	
C_{ll}	a_{ll}	$C_{\nu\nu}$	$a_{lR}^{++} + a_{lR}^{--} + a_{lR}^{+-}$	$C_{l\nu}$	$a_{llR}^+ + a_{llR}^-$		
$C_{qq}^{(1)}$	$a_{qq}^{(1)}$	C_{ee}	$a_{lR}^{++} + a_{lR}^{--} - a_{lR}^{+-}$	C_{le}	$a_{llR}^+ - a_{llR}^-$		
$C_{qq}^{(3)}$	$a_{qq}^{(3)}$	$C_{\nu e}$	$2(a_{lR}^{++} - a_{lR}^{--})$	C_{lu}	$a_{lqR}^+ + a_{lqR}^-$		
$C_{lq}^{(1)}$	$a_{lq}^{(1)}$	C_{uu}	$a_{qRqR}^{(1)++} + a_{qRqR}^{(1)--} + a_{qRqR}^{(1)+-} + a_{qRqR}^{(3)++}$	C_{ld}	$a_{lqR}^+ - a_{lqR}^-$		
$C_{lq}^{(3)}$	$a_{lq}^{(3)}$	C_{dd}	$a_{qRqR}^{(1)++} + a_{qRqR}^{(1)--} - a_{qRqR}^{(1)+-} + a_{qRqR}^{(3)++}$	$C_{q\nu}$	$a_{qlR}^+ + a_{qlR}^-$		
		$C_{ud}^{(1)}$	$2[a_{qRqR}^{(1)++} - a_{qRqR}^{(1)--}] + \left(\frac{4}{N_c} - 2\right)a_{qRqR}^{(3)++}$	C_{qe}	$a_{qlR}^+ - a_{qlR}^-$		
		$C_{ud}^{(8)}$	$8a_{qRqR}^{(3)++}$	$C_{qu}^{(1)}$	$a_{qqR}^{(1)+} + a_{qqR}^{(1)-}$		
		$C_{\nu u}$	$a_{lRqR}^{(1)++} + a_{lRqR}^{(1)--} + a_{lRqR}^{(1)+-} + a_{lRqR}^{(1)-+} + a_{lRqR}^{(3)++} + a_{lRqR}^{(3)+-}$	$C_{qd}^{(1)}$	$a_{qqR}^{(1)+} - a_{qqR}^{(1)-}$		
		$C_{\nu d}$	$a_{lRqR}^{(1)++} - a_{lRqR}^{(1)--} - a_{lRqR}^{(1)+-} + a_{lRqR}^{(1)-+} - a_{lRqR}^{(3)++} + a_{lRqR}^{(3)+-}$	$C_{qu}^{(8)}$	$a_{qqR}^{(8)+} + a_{qqR}^{(8)-}$		
		C_{eu}	$a_{lRqR}^{(1)++} - a_{lRqR}^{(1)--} + a_{lRqR}^{(1)+-} - a_{lRqR}^{(1)-+} - a_{lRqR}^{(3)++} - a_{lRqR}^{(3)+-}$	$C_{qd}^{(8)}$	$a_{qqR}^{(8)+} - a_{qqR}^{(8)-}$		
		C_{ed}	$a_{lRqR}^{(1)++} + a_{lRqR}^{(1)--} - a_{lRqR}^{(1)+-} - a_{lRqR}^{(1)-+} + a_{lRqR}^{(3)++} - a_{lRqR}^{(3)+-}$				
		$C_{\nu edu}$	$2[a_{lRqR}^{(3)++} + a_{lRqR}^{(3)+-}]$				
8 : $(\bar{L}R)(\bar{R}L) + \text{h.c.}$			8 : $(\bar{L}R)(\bar{L}R) + \text{h.c.}$				
$C_{l\nu uq}, C_{ledq}$	$a_{lRqRq}^+ \pm a_{lRqRq}^-$		C_{lvle}	$2 a_{llR} ll_R$			
			$C_{quqd}^{(1)}, C_{quqd}^{(8)}$	$2 a_{qqRqqR}^{(1)}, 2 a_{qqRqqR}^{(8)}$			
			$C_{lvqd}^{(1)}, C_{lequ}^{(1)}$	$\mp a_{llRqqR}^{(1)+} - a_{llRqqR}^{(1)-}$			
			$C_{lvqd}^{(3)}, C_{lequ}^{(3)}$	$\mp a_{llRqqR}^{(3)+} - a_{llRqqR}^{(3)-}$			

Table .5. A translation dictionary from the Custodial basis Wilson Coefficients a_i to Warsaw basis Wilson Coefficients C_i .

CHAPTER V

CONCLUSIONS

Effective Theories of Dark Mesons

In Chapter II we have studied dark sectors that arise from a new, strongly-coupled confining gauge group $SU(N_D)$ with dark fermions transforming under the electroweak part of the SM. In dark sectors that preserve custodial $SU(2)$ in their interactions with the SM, a custodial triplet of dark pions appears in the low energy effective theory. The low energy effective interactions with the SM can be classified by the custodial symmetry, leading to two distinct possibilities: “Gaugephilic”: where $\pi_D^0 \rightarrow Zh$, $\pi_D^\pm \rightarrow Wh$ dominate once kinematically open, and “Gaugephobic”: where $\pi_D^0 \rightarrow \bar{f}f$, $\pi_D^\pm \rightarrow \bar{f}'f$ dominate. These classifications assume the only sources of custodial $SU(2)$ breaking are from the SM: the gauging of hypercharge, $g'Y$, and the difference between the up-type and down-type Yukawa couplings, \mathcal{Y}_{ij}^ϕ .

The simplest theories that exhibited the gaugephobic and gaugephilic classifications contained two-flavors, and we examined one chiral theory and two vector-like theories. The chiral theory is familiar from bosonic technicolor/strongly-coupled induced electroweak symmetry breaking. There, the dominant source of dark pion interactions with the SM is from Goldstone-pion mixing and leads to a gaugephilic decay pattern. In the vector-like theories, dark pion interactions with the SM arise through higher dimensional operators. If we demand custodial $SU(2)$ invariance in these higher dimensional operators, we find that interactions between the π_D and gauge bosons first occur at dimension-9 (in the UV) while $\pi_D \bar{f}f$ operators can be written at dimension-7. The mismatch in operator dimension means the vector-like theories are gaugephobic.

Next, we examined a four-flavor theory. With the proper electroweak charge assignment, this scenario can have both vector-like and chiral masses among its dark fermions, and is therefore a hybrid of the chiral and vector scenarios. The most phenomenologically interesting limit is when the chiral mass is small compared to the vector-like mass. In this case, we find the lightest custodial $SU(2)$ triplet of dark pions have gaugephobic interactions with the SM in which $\pi^0 \rightarrow Zh$, $\pi^\pm \rightarrow Wh$ are suppressed by $\simeq m_h^2/m_K^2$ relative to fermionic decays. In the chiral lagrangian for the full multiplet of 15 dark pions, this arises through a cancellation between the dark pion mixing with the Goldstones of the SM and dark pion mixing with the Higgs boson of the SM. Decoupling the heavier dark pion multiplets such that only the lightest triplet remains, the four-flavor theory maps into a two-flavor theory with higher dimensional operators that preserve custodial $SU(2)$ and are minimally flavor violating. The custodial $SU(2)$ symmetry of these interactions automatically leads to the operator suppression $\simeq v^2/\Lambda^2$, in agreement with what we found by explicit calculation of the four-flavor theory.

In theories that preserve custodial $SU(2)$, the neutral dark pion decays to the SM through “gaugephobic” or “gaugephilic” interactions with a suppressed rate of $\pi^0 \rightarrow \gamma\gamma$. In each of the theories considered, there is no axial anomaly contribution to the decay. However, since the dark pions do have interactions with SM, and the SM fermions have an anomalous axial-vector current, the decay $\pi^0 \rightarrow \gamma\gamma$ does occur, but is suppressed by the same $1/v_\pi$ that suppresses the direct decay $\pi^0 \rightarrow \text{SM SM}$. In the Standard Model, the analogy would be to imagine that the up and down quarks have an exact custodial $SU(2)$ symmetry, i.e., $Q_u = -Q_d = 1/2$ and $y_u = y_d$. In this case, the anomaly contribution to $\pi^0 \rightarrow \gamma\gamma$ in the Standard Model would vanish. However, even without the anomaly, the SM π^0 decays through the mode $\pi^0 \rightarrow e^+e^-$

proportional to the electron Yukawa coupling. This interaction has the same form as the two-flavor chiral theory we considered in this paper. Now there remains a one-loop suppressed contribution $\pi^0 \rightarrow \gamma\gamma$ through the electron Yukawa coupling, but this is highly suppressed compared with the fermionic decay, which is precisely what happens with the π^0 of the custodial $SU(2)$ symmetric dark sector theories that we have considered in this paper.

Finally, the astute reader may have noticed that all of the vector-like dark sector theories with custodially symmetric interactions with the SM were gaugephobic. The only gaugephilic case presented in the paper is the two-flavor chiral theory, which might give the reader the impression that vector-like theories are automatically gaugephobic. This is not the case. As an explicit counter-example, the custodial triplets in Georgi-Machacek models have gaugephilic couplings (e.g. [174]). It will come as no surprise that we have already constructed strongly-coupled models based on coset theories that generate the scalar sector of Georgi-Machacek theories as dark pions with gaugephilic couplings with the SM. The details will be left to further investigations.

LHC Phenomenology of Dark Mesons

In Chapter III we have examined the phenomenology of dark pions – composite states with electroweak and Higgs interactions that may lurk at the electroweak scale. Dark pion - like states are a component of many BSM scenarios with new strong dynamics near the electroweak scale.

- In addition to electroweak interactions, dark pions are also resonantly produced via dark rhos that kinetically mix with SM gauge bosons and decay through interactions with SM fermions or into hV . The overall size of the single-pion to

SM coupling and the relative strength of the fermionic versus Vh decay modes encodes some information about the symmetry structure of the strong sector and is the subject of Ref. [120].

- Taken more abstractly, dark pions represent a type of new physics that is predominantly pair produced, is uncolored, and decays back to SM final states. This is a particularly tricky combination for the LHC, since the lack of strong interactions means the BSM cross sections are small and the fact that the final states are pure SM leaves few easy handles to separate signal from background.
- The phenomenology of the dark pions is governed largely by a few parameters; the relative strength of the dark pion decays to fermionic versus gauge bosons, the type of kinetic mixing [whether with $SU(2)_L$ or $U(1)_Y$], and the mass of π_D relative to ρ_D . Setting up nine benchmark models with different values for these key parameters, we explored the constraints on dark mesons from 8 and 13 TeV LHC searches.
- The only scenario where we find constraints in the TeV range is when the ρ_D^0 is kinematically forbidden from decaying to dark pions and therefore decays with significant branching ratio into leptons, the $SU(2)_{L,R}^{55}$ cases. For all other cases, $\rho_D \rightarrow \pi_D \pi_D$ is kinematically accessible so the dilepton bounds are negligible and the best avenue is to look for signals of π_D pairs. Depending on the type of kinetic mixing and the relative mass of the ρ_D mesons, the bounds on m_{π_D} from π_D pair production signals vary from slightly above the LEP II charged particle bound to ~ 500 GeV. The strongest bounds come when the mass of ρ_D is not too much heavier than $2m_{\pi_D}$, and kinetically mix with the $SU(2)_L$, while the weakest bounds come when the kinetic mixing only involves $U(1)_Y$. As the most

extreme example of how light these particles can be while remaining undetected, consider the $SU(2)_R^{45}$ model. There, dark pions as light as ~ 130 GeV are still viable; perhaps more surprising, the vector ρ_D in this scenario sits at ~ 300 GeV!

- In our survey of LHC searches, we found the most useful features for bounding dark mesons to be signal regions with high multiplicity of leptons and/or b-jets *without* strong requirements on the energy (of the individual objects, or summed) or missing energy. As model-specific searches march towards higher masses in the 13 TeV era, this type of signal region has become rarer and rarer. For scenarios without a dedicated search, such as the dark meson explored here – or, more generally, for types of BSM physics that is pair produced with sub-QCD rates and does not bring a non-SM source of missing energy – the net result is that 13 TeV searches can be less sensitive than 8 TeV versions. Generic searches based on multiple leptons served as a catch-all for this type of “non-standard” BSM at 8 TeV, and we encourage ATLAS and CMS to repeat similar studies with 13 TeV.

SMEFT with Custodial Symmetry

The robust way to uncover the details of UV physics is to measure all (ν)SMEFT operators in complete generality. This requires measurements to constrain the coefficients of over 3000 operators at dimension-6. Even restricting to one generation, measurements would be required for nearly 100 coefficients of dimension-6 operators. This is a daunting task.

In Chapter IV, we have proposed a much smaller set of operators to probe specific information: is the UV physics consistent (or not) with custodial symmetry. We have identified a set of observables, in Sec. IV:

$$\{ \hat{\rho}, \hat{r}_{Z\nu_L\bar{\nu}_L}, \hat{r}_{Ze_L\bar{e}_L}, \hat{r}_{Ze\bar{e}}, \hat{r}_{W\nu_L e_L} \}, \quad (5.1)$$

[as well as corresponding hadronic pseudo-observables, see Eq. (B.19)] in which *if* experimental measurements *do not* match the custodial symmetric pattern of predictions, c.f. Eq. (4.33), then the UV physics does not respect custodial symmetry at tree-level. Our result generalizes the commonly used observable $\rho \neq 1$ at tree-level implying custodial symmetry violation, which only occurs when the leading matching corrections to (ν) SMEFT operators are purely oblique.

The observables Eq. (5.1) depend on on just three custodial symmetric operators with Wilson coefficients $a_{Hl}^{(3)}$, $a_{HlR}^{(3)+}$ and a_{12} . The $\hat{\rho}$ observable, for instance, does not receive a correction from either \hat{m}_Z^2 or \hat{m}_W^2 , and instead it arises purely from the corrections to \hat{G}_F from vertex corrections and four-fermion interactions. As a result, the deviation of $\hat{\rho}$ from 1 is proportional to just the linear combination of Wilson coefficients $2a_{Hl}^{(3)} - a_{12}/2$. The same linear combination also appears in other observables such as $\hat{r}_{Ze\bar{e}}$ in Eq. (4.33). This is because the vertex correction $V_{Ze\bar{e}}$ only receives a correction from $a_{HlR}^{(3)+}$, a Wilson coefficient related to right-handed leptons, instead of $a_{Hl}^{(3)}$, which is left-handed. Given these two different operators are independent, the corrections to $\hat{r}_{Ze\bar{e}}$ happen to be a simple sum of these two different effects. Notice also that the same linear combination from \hat{G}_F , namely $2a_{Hl}^{(3)} - a_{12}/2$, appears in all five predictions of the hadronic pseudo-observables, Eq. (B.19) for the same reason as explained in more detail at the end of App. B.

We demonstrated the utility of our results by calculating the corrections to our observables in four distinct custodial symmetric UV theory examples. In two UV

theory examples, a singlet scalar [Sec. IV] and a heavy Z' associated with $U(1)_{B-L}$ [Sec. IV], the predictions are

$$\hat{\rho} = \hat{r}_{Z\nu_L\bar{\nu}_L} = \hat{r}_{Ze_L\bar{e}_L} = \hat{r}_{Ze\bar{e}} = \hat{r}_{W\nu_L e_L} = 1. \quad (5.2)$$

By itself, this is entirely uninformative, since predicting these observables do not deviate from unity is indistinguishable from the what the SM predicts (again, at tree-level). However, when combined with other observables that deviate from the SM prediction, e.g., a modified Higgs trilinear coupling (in the case of the singlet model) or a new/modified four-fermion interaction (in the case of the $U(1)_{B-L}$ model), our observables provide a way to distinguish among UV theory possibilities. In the case of these two particular models, the prediction for our observables is no deviation from the SM which is fully consistent with the UV theories having custodial symmetry.

We also calculated the corrections in two custodial symmetric UV theory examples in which there *are* contributions to our observables. The first example of this type is embedding the SM into a larger gauge symmetry, $SU(2)_L \times SU(2)_R \times U(1)_{B-L}$ in which custodial symmetry is effectively gauged as $SU(2)_R$ [Sec. IV]. The spontaneous breaking of $SU(2)_R \times U(1)_{B-L} \rightarrow U(1)_Y$ in general also spontaneously breaks custodial symmetry, leading to tree-level contributions to custodial violating operators. However, in a particular limit in which the gauge coupling of $U(1)_{B-L}$ is taken to vanish, custodial symmetry is restored. In this specific version of this UV theory, $O_{Hl_R}^{(3)+}$, $O_{Hq_R}^{(3)+}$ and $O_{l_R q_R}^{(3)++}$ are generated by the gauging of $SU(2)_R$ that explicitly breaks three independent global symmetries $SU(2)_{RH} \times SU(2)_{Rq_R} \times SU(2)_{Rl_R}$ down to one single gauged $SU(2)_R$. The leptonic operator $O_{Hl_R}^{(3)+}$, in particular, contributes only to the observable $\hat{r}_{Ze\bar{e}}$, that leads to the predictions

$$\hat{r}_{Ze\bar{e}} = 1 - s_\theta^2 \frac{v^2}{v_\phi^2}, \quad \hat{\rho} = \hat{r}_{Z\nu_L\bar{\nu}_L} = \hat{r}_{Ze_L\bar{e}_L} = \hat{r}_{W\nu_L e_L} = 1. \quad (5.3)$$

This pattern of deviation of our observables is a telltale sign of the custodial symmetric UV theory in which gauged $SU(2)_R \times U(1)_{B-L}$ is spontaneously broken to $U(1)_Y$.

Finally, we considered a UV theory with a heavy W'_L that arises from a gauged $SU(2)_A \times SU(2)_B$ spontaneously breaking to $SU(2)_L$ [Sec. IV]. In this theory, the left-handed quarks and leptons of the SM transformed under $SU(2)_A$, and after $SU(2)_A \times SU(2)_B \rightarrow SU(2)_L$, couple to the SM W boson. However, there remains a residual coupling of the left-handed quarks and leptons to the heavy W'_L due to the mixing among $W_{A,B}$, and this leads to both vertex corrections of W couplings, $C_{Hl}^{(3)}$, $C_{Hq}^{(3)}$, as well as four-fermion couplings C_{ll} , $C_{qq}^{(3)}$, $C_{lq}^{(3)}$ among other corrections shown in Eq. (4.80). The vertex corrections and four-fermion operators lead to deviations from the SM for all of our observables, shown in Eq. (4.87), that depend on only one quantity from the UV physics, c_A^4/v_Φ^4 , the heavy W' mixing angle c_A divided by the vev of the scalar field v_Φ that breaks $SU(2)_A \times SU(2)_B \rightarrow SU(2)_L$. In particular, in this model the ρ observable is

$$\hat{\rho} = 1 + \left[\frac{s_\theta^2}{1 - 2s_\theta^2} \right] \frac{c_A^4 v^2}{v_\Phi^2}, \quad (5.4)$$

that has a tree-level deviation from 1 due to the non-oblique corrections arising in this custodial symmetric UV theory. By itself, observing the deviation in $\hat{\rho}$ from the SM in Eq. (5.4) is insufficient to conclude anything about the symmetry structure of the UV theory. Once we combine this deviation with the other predictions shown in Eq. (4.87), we could uncover whether the UV theory is (or is not) consistent with custodial symmetry.

Alas, our results have limitations. We have already emphasized that if experimental measurements do not match the custodial symmetric pattern of predictions then the UV physics does not respect custodial symmetry at tree-level. The converse is not true. If experimental measurements follow our pattern of

predictions, this is a necessary but not sufficient condition for custodial symmetry of the UV theory. In particular, there are a few operators in which custodial symmetry can be violated that do not contribute to our observables, specifically those of the form $\psi^2 H^3$. We argued in Sec. IV they do not affect our observables, which was a good thing since they are generated by under the EOM redundancy used to rewrite custodial symmetric operators that are generated not in our custodial basis back into our custodial basis. If custodial violating contributions were generated to just these operators by a UV theory, our observables would not be sensitive. Our results are also not sensitive to custodial violation that appears only at loop level at leading matching order. Here we should distinguish between two possibilities: there are well-known loop corrections to our observables purely from the SM physics, such as the contribution to $\hat{\rho}$ from the custodial-violating difference between the top and bottom quark Yukawa couplings. These effects could be easily incorporated into framework by redefining our observables to include the SM loop effects. However, additional contributions to our observables that arise from radiative corrections from (ν) SMEFT operators are not included. For some theories, radiative corrections are known, for example the singlet scalar model [211, 215]. It would be interesting to investigate if there are persistent patterns that bely a UV theory with custodial symmetry even after radiative corrections are included.

APPENDIX A

EFFECTIVE THEORIES OF DARK MESON

Gaugephobic 2HDMs

We review the application of the $(\mathbf{2}, \mathbf{2})$ custodial symmetry formalism in the context of general two-Higgs doublet models (2HDM) [216, 217, 218, 219]. We'll focus on a general CP-conserving 2HDM.

The most general 2HDM potential can be written as [220, 121]

$$\begin{aligned}
 V_{2HDM} = & m_{11}^2(\phi_1^\dagger\phi_1) + m_{22}^2(\phi_2^\dagger\phi_2) \\
 & - m_{12}^2(\phi_1^\dagger\phi_2) - (m_{12}^2)^*(\phi_2^\dagger\phi_1) \\
 & + \frac{1}{2}\lambda_1(\phi_1^\dagger\phi_1)^2 + \frac{1}{2}\lambda_2(\phi_2^\dagger\phi_2)^2 + \lambda_3(\phi_1^\dagger\phi_1)(\phi_2^\dagger\phi_2) \\
 & + \lambda_4(\phi_1^\dagger\phi_2)(\phi_2^\dagger\phi_1) + \frac{1}{2}[\lambda_5(\phi_1^\dagger\phi_2)^2 + \lambda_5^*(\phi_2^\dagger\phi_1)^2] \\
 & + [\lambda_6(\phi_1^\dagger\phi_2) + \lambda_6^*(\phi_2^\dagger\phi_1)](\phi_1^\dagger\phi_1) \\
 & + [\lambda_7(\phi_1^\dagger\phi_2) + \lambda_7^*(\phi_2^\dagger\phi_1)](\phi_2^\dagger\phi_2)
 \end{aligned} \tag{A.1}$$

where m_{11}^2 , m_{22}^2 , $\lambda_{1,2,3,4}$ are real parameters and m_{12}^2 , $\lambda_{5,6,7}$ complex. And ϕ_1 and ϕ_2 are two complex scalar doublets

$$\phi_1 = \begin{pmatrix} \phi_1^+ \\ \phi_1^0 \end{pmatrix}, \quad \phi_2 = \begin{pmatrix} \phi_2^+ \\ \phi_2^0 \end{pmatrix}, \tag{A.2}$$

In general, m_{11}^2 , m_{22}^2 , and $\lambda_{1,2,3,4}$ are real parameters while m_{12}^2 and $\lambda_{5,6,7}$ can be complex. Nevertheless, in this study we restrict our discussion to CP-conserving models, by assuming all the parameters of V_{2HDM} are real [121]. And we also assume the parameters are chosen to make V_{2HDM} bounded below so that each of the ϕ_i acquires a VEV, denoted as v_1 and v_2 which satisfy

$$v_1^2 + v_2^2 = v^2 = (246 \text{ GeV})^2 \tag{A.3}$$

and we define

$$t_\beta \equiv \tan \beta \equiv \frac{v_2}{v_1} \quad (\text{A.4})$$

The goal of this section is to demonstrate explicitly that it's possible to write a general 2HDM potential in terms of a $(\mathbf{2}, \mathbf{2})$ custodial symmetry formalism, by introducing matrices M_{ij} similar to Eq. (2.2)

$$M_{ij} \equiv (\tilde{\phi}_i, \phi_j) = \begin{pmatrix} \phi_i^{0*} & \phi_j^+ \\ -\phi_i^- & \phi_j^0 \end{pmatrix} \quad (\text{A.5})$$

where $i, j = 1, 2$

It is crucial to our approach that we define the following \mathbf{K} -terms [216, 217, 218]

$$\mathbf{K} = \begin{pmatrix} K_0 \\ K_1 \\ K_2 \\ K_3 \end{pmatrix} = \begin{pmatrix} \phi_1^\dagger \phi_1 + \phi_2^\dagger \phi_2 \\ \phi_1^\dagger \phi_2 + \phi_2^\dagger \phi_1 \\ i(\phi_2^\dagger \phi_1 - \phi_1^\dagger \phi_2) \\ \phi_1^\dagger \phi_1 - \phi_2^\dagger \phi_2 \end{pmatrix} \quad (\text{A.6})$$

Given Eqs. (A.5-A.6), we may write \mathbf{K} in two different ways, with either M_{11} and M_{22} , or M_{21} alone

$$\begin{aligned} K_0 &= \frac{1}{2} \text{tr} \left(M_{11}^\dagger M_{11} + M_{22}^\dagger M_{22} \right) = \text{tr} \left(M_{21}^\dagger M_{21} \right) \\ K_1 &= \text{tr} \left(M_{11}^\dagger M_{22} \right) = 2 \text{Re}(\det M_{21}^\dagger) \\ K_2 &= (-i) \text{tr} \left(M_{11} \tau_3 M_{22}^\dagger \right) = -2 \text{Im}(\det M_{21}) \\ K_3 &= \frac{1}{2} \text{tr} \left(M_{11}^\dagger M_{11} - M_{22}^\dagger M_{22} \right) = -\text{tr} \left(M_{21} \tau_3 M_{21}^\dagger \right) \end{aligned} \quad (\text{A.7})$$

Then it is straightforward to verify that V_{2HDM} can be written in terms of \mathbf{K} in a compact form of

$$V_{2HDM} = \boldsymbol{\xi}^T \mathbf{K} + \mathbf{K}^T \mathbf{E} \mathbf{K} \quad (\text{A.8})$$

where the mass parameter vector $\boldsymbol{\xi}$ and the coupling parameter matrix \mathbf{E} are [218]

$$\boldsymbol{\xi} = \begin{pmatrix} \frac{1}{2}(m_{11}^2 + m_{22}^2) \\ -\text{Re}(m_{12}^2) \\ \text{Im}(m_{12}^2) \\ \frac{1}{2}(m_{11}^2 - m_{22}^2) \end{pmatrix} \quad (\text{A.9})$$

$$\mathbf{E} = \frac{1}{4} \begin{pmatrix} \frac{1}{2}(\lambda_1 + \lambda_2) + \lambda_3 & \text{Re}(\lambda_6 + \lambda_7) & -\text{Im}(\lambda_6 + \lambda_7) & \frac{1}{2}(\lambda_1 - \lambda_2) \\ \text{Re}(\lambda_6 + \lambda_7) & \lambda_4 + \text{Re}(\lambda_5) & -\text{Im}(\lambda_5) & \text{Re}(\lambda_6 - \lambda_7) \\ -\text{Im}(\lambda_6 + \lambda_7) & -\text{Im}(\lambda_5) & \lambda_4 - \text{Re}(\lambda_5) & -\text{Im}(\lambda_6 - \lambda_7) \\ \frac{1}{2}(\lambda_1 - \lambda_2) & \text{Re}(\lambda_6 - \lambda_7) & -\text{Im}(\lambda_6 - \lambda_7) & \frac{1}{2}(\lambda_1 + \lambda_2) - \lambda_3 \end{pmatrix} \quad (\text{A.10})$$

As a consequence of Eq. (A.7), there are actually two types of custodial transformations to the potential [221]: Type I: M_{11} and M_{22} transform as

$$M_{ii} \longrightarrow LM_{ii}R^\dagger \quad \text{for } i = 1, 2 \quad (\text{A.11})$$

where L and R are $SU(2)_L$ and $SU(2)_R$ matrices. Type II: In this case, it's M_{21} which transforms as

$$M_{21} \longrightarrow LM_{21}R^\dagger \quad (\text{A.12})$$

The potential V_{2HDM} preserves custodial symmetry if it is invariant under either type of the custodial transformations.

Nevertheless, recall that there is an explicit τ_3 in Eq. (A.7). In fact, it's a $(\tau_3)_R$ which appears either in the K_2 term under the Type I custodial transformation, or in the K_3 term for the Type II. Since $(\tau_3)_R$ breaks custodial symmetry explicitly, K_2 term should be absent from V_{2HDM} with Type I custodial symmetry, same as K_3 term for Type II. Apparently, to meet this requirement the corresponding entries in $\boldsymbol{\xi}$ and \mathbf{E} must vanish.

With the argument above, the conditions for a custodial symmetric 2HDM potential can be summarized as:

Type I:

$$\boldsymbol{\xi}_I = \begin{pmatrix} \cdot \\ \cdot \\ 0 \\ \cdot \end{pmatrix}, \quad \mathbf{E}_I = \begin{pmatrix} \cdot & \cdot & 0 & \cdot \\ \cdot & \cdot & 0 & \cdot \\ 0 & 0 & 0 & 0 \\ \cdot & \cdot & 0 & \cdot \end{pmatrix} \quad (\text{A.13})$$

Type II:

$$\boldsymbol{\xi}_{II} = \begin{pmatrix} \cdot \\ \cdot \\ \cdot \\ 0 \end{pmatrix}, \quad \mathbf{E}_{II} = \begin{pmatrix} \cdot & \cdot & \cdot & 0 \\ \cdot & \cdot & \cdot & 0 \\ \cdot & \cdot & \cdot & 0 \\ 0 & 0 & 0 & 0 \end{pmatrix} \quad (\text{A.14})$$

For a CP -conserving 2HDM:

$$\boldsymbol{\xi}_{CP} = \begin{pmatrix} \frac{1}{2}(m_{11}^2 + m_{22}^2) \\ -m_{12}^2 \\ 0 \\ \frac{1}{2}(m_{11}^2 - m_{22}^2) \end{pmatrix} \quad (\text{A.15})$$

$$\mathbf{E}_{CP} = \frac{1}{4} \begin{pmatrix} \frac{1}{2}(\lambda_1 + \lambda_2) + \lambda_3 & \lambda_6 + \lambda_7 & 0 & \frac{1}{2}(\lambda_1 - \lambda_2) \\ \lambda_6 + \lambda_7 & \lambda_4 + \lambda_5 & 0 & \lambda_6 - \lambda_7 \\ 0 & 0 & \lambda_4 - \lambda_5 & 0 \\ \frac{1}{2}(\lambda_1 - \lambda_2) & \lambda_6 - \lambda_7 & 0 & \frac{1}{2}(\lambda_1 + \lambda_2) - \lambda_3 \end{pmatrix} \quad (\text{A.16})$$

Compare Eqs. (A.15-A.16) to (A.13), we see that to preserve Type-I custodial symmetry, the condition required is

$$\lambda_4 = \lambda_5 \quad (\text{A.17})$$

Similarly, the conditions for a Type-II custodial symmetry are

$$\begin{aligned}
m_{11}^2 &= m_{22}^2 \\
\lambda_1 &= \lambda_2 \\
\lambda_6 &= \lambda_7 \\
\lambda_3 &= \frac{1}{2}(\lambda_1 + \lambda_2) = \lambda_1
\end{aligned}
\tag{A.18}$$

As is well-known, the observable that measures custodial violation is the ρ -parameter. Assuming the first three conditions of Eq. (A.18), the one-loop contributions to $\Delta\rho$ [174] from either Type-I or Type-II models can be calculated to the leading order in v^2 as

$$\Delta\rho = \frac{1}{192\pi^2} \left(\frac{v^2}{m_A^2} \right) (\lambda_4 - \lambda_5)(\lambda_1 - \lambda_3)
\tag{A.19}$$

where m_A is the mass of the heavy pseudoscalar Higgs state A^0 in 2HDM. We explicitly see that $\Delta\rho$ is proportional to $(\lambda_4 - \lambda_5)$ and $(\lambda_1 - \lambda_3)$, which can be identified with the contribution from Type-I and Type-II, correspondingly.

We can also map the general Type II 2HDM model onto the the minimal supersymmetric model (MSSM) where the λ_i are [121]

$$\begin{aligned}
\lambda_1 &= \lambda_2 = \frac{1}{4}(g^2 + g'^2) \\
\lambda_3 &= \frac{1}{4}(g^2 - g'^2) \\
\lambda_4 &= -\frac{1}{2}g^2 \\
\lambda_5 &= \lambda_6 = \lambda_7 = 0.
\end{aligned}
\tag{A.20}$$

The contribution to $\Delta\rho$ is then

$$\Delta\rho = \frac{1}{192\pi^2} \left(\frac{v^2}{m_A^2} \right) \left(-\frac{1}{2}g^2 \right) \left(\frac{1}{2}g'^2 \right).
\tag{A.21}$$

The 2HDM potential of the MSSM contains custodial symmetry violation with a small but non-zero correction to the ρ -parameter. The correct is, nevertheless, proportional to g'^2 that is precisely the SM violation of custodial symmetry by gauging hypercharge.

Phenomenologically, the heavy Higgs states in a 2HDM may decay into SM particles if kinematically allowed. Comparing to our study of dark mesons, we are particularly interested in the branching fractions of the charged Higgs H^\pm and the pseudoscalar A^0 decaying into SM fermion pairs or gauge boson and Higgs pairs, especially in the decoupling limit $m_A \gg v$. In this limit, Eq. (A.19) indicates that $\Delta\rho$ is always suppressed by two powers of the heavy mass scale m_A , which means the amount of possible custodial symmetry violation is restricted to be relatively small. As a result, one can say that 2HDM becomes custodially symmetric in the decoupling limit.

As for the decay branching fractions, though the couplings of H^\pm and A^0 to SM fermions are usually model dependent, their values are proportional to $\tan\beta$ or $\cot\beta$ [174]

$$C_{ff} \propto g \frac{m_f}{m_W} (\tan\beta \text{ or } \cot\beta) \quad (\text{A.22})$$

On the other hand, the couplings to SM gauge bosons and SM Higgs are proportional to $\cos(\beta - \alpha)$ [174]

$$C_{Wh} \propto g \cos(\beta - \alpha) \quad (\text{A.23})$$

where α is the CP-even scalar mixing angle, and in the decoupling limit,

$$\cos(\beta - \alpha) = \mathcal{O}\left(\frac{v^2}{m_A^2}\right) \quad (\text{A.24})$$

Compare Eq. (A.22) to Eq. (A.23), we see that to the leading order in v^2 ,

$$\frac{C_{Wh}}{C_{ff}} \propto \cos(\beta - \alpha) \propto \mathcal{O}\left(\frac{v^2}{m_A^2}\right) \quad (\text{A.25})$$

Therefore, in the decoupling limit a 2HDM becomes custodially symmetric, and the decays of its heavy states to SM particle in this limit are gaugephobic.

APPENDIX B

SMEFT WITH CUSTODIAL SYMMETRY

Details of Mapping onto Observables

In this appendix, we provide some details on the intermediate steps that lead to our results in 4.31. We work with the Warsaw basis of dim-6 ν SMEFT shown in .1, restricted to one fermion generation. We will perform tree-level mapping, and only up to dim-6.

First, we find the corrections to the two-point functions of electroweak gauge bosons

$$\Pi_{WW}(p^2) = 2p^2v^2C_{HW}, \quad (\text{B.1a})$$

$$\Pi_{ZZ}(p^2) = \frac{1}{2}\hat{m}_{Z, \text{SM}}^2C_{HD} + 2p^2v^2(c_\theta^2C_{HW} + s_\theta^2C_{HB} + c_\theta s_\theta C_{HWB}), \quad (\text{B.1b})$$

$$\Pi_{\gamma\gamma}(p^2) = 2p^2v^2(s_\theta^2C_{HW} + c_\theta^2C_{HB} - c_\theta s_\theta C_{HWB}), \quad (\text{B.1c})$$

$$\Pi_{\gamma Z}(p^2) = p^2v^2[2c_\theta s_\theta(C_{HW} - C_{HB}) - (c_\theta^2 - s_\theta^2)C_{HWB}], \quad (\text{B.1d})$$

where as usual $\Pi_{VV}(p^2)$ denotes the transverse part of the full two-point function of the gauge bosons:

$$i\Pi_{VV}^{\mu\nu}(p^2) = i\Pi_{VV}(p^2)\left(\eta^{\mu\nu} - \frac{p^\mu p^\nu}{p^2}\right) + \left(i\frac{p^\mu p^\nu}{p^2}\text{term}\right). \quad (\text{B.2})$$

Next, we move on to the three-point vertices. For the observables considered in IV, the relevant vertex corrections between the electroweak gauge bosons and the leptons are

$$V_{Z\nu_L\bar{\nu}_L} = 1 - v^2 \left(C_{Hl}^{(1)} - C_{Hl}^{(3)} \right), \quad (\text{B.3a})$$

$$V_{Ze_L\bar{e}_L} = 1 + \frac{v^2}{1 - 2s_\theta^2} \left(C_{Hl}^{(1)} + C_{Hl}^{(3)} \right), \quad (\text{B.3b})$$

$$V_{Ze\bar{e}} = 1 - \frac{v^2}{2s_\theta^2} C_{He}, \quad (\text{B.3c})$$

$$V_{Wl\bar{l}} = 1 + v^2 C_{Hl}^{(3)}. \quad (\text{B.3d})$$

Note that corrections to the four-fermion vertices would not feed into $\hat{\alpha}$ due to lack of pole structure. The only corrections to the four-point vertices (or more) needs to be considered in our analysis is C_{12} we mentioned in IV. It is the only four-fermion correction that would feed into \hat{G}_F .

With the above, we would like to find the modifications to 4.26. The first four observables are relatively simpler:

$$\begin{aligned} \hat{\alpha} &= \frac{g_1^2 g_2^2}{4\pi (g_1^2 + g_2^2)} \left[\frac{p^2}{p^2 - \Pi_{\gamma\gamma}(p^2)} \Big|_{p^2 \rightarrow 0} \right] \\ &= \hat{\alpha}_{\text{SM}} \left[1 + 2v^2 (s_\theta^2 C_{HW} + c_\theta^2 C_{HB} - c_\theta s_\theta C_{HWB}) \right], \end{aligned} \quad (\text{B.4a})$$

$$\begin{aligned} \hat{G}_F &= \frac{\sqrt{2}g_2^2}{8} V_{Wl\bar{l}}^2 \left[\frac{-1}{p^2 - \hat{m}_{W, \text{SM}}^2 - \Pi_{WW}(p^2)} \Big|_{p^2 \rightarrow 0} \right] - \frac{C_{12}}{2\sqrt{2}} \\ &= \hat{G}_{F, \text{SM}} \left[1 + 2v^2 C_{Hl}^{(3)} - \frac{1}{2} v^2 C_{12} \right], \end{aligned} \quad (\text{B.4b})$$

$$\begin{aligned} \hat{m}_Z^2 &= \hat{m}_{Z, \text{SM}}^2 + \Pi_{ZZ}(\hat{m}_{Z, \text{SM}}^2) \\ &= \hat{m}_{Z, \text{SM}}^2 \left[1 + \frac{1}{2} v^2 C_{HD} + 2v^2 (c_\theta^2 C_{HW} + s_\theta^2 C_{HB} + c_\theta s_\theta C_{HWB}) \right], \end{aligned} \quad (\text{B.4c})$$

$$\hat{m}_W^2 = \hat{m}_{W, \text{SM}}^2 + \Pi_{WW}(\hat{m}_{W, \text{SM}}^2) = \hat{m}_{W, \text{SM}}^2 (1 + 2v^2 C_{HW}). \quad (\text{B.4d})$$

These will lead us to the $\hat{\rho}$ part in 4.31.

For the decay widths corrections in 4.26, we need a bit more setup. We define the amplitude $i\hat{M}$ as the strength $\hat{\kappa}$ multiplied by the polarization kinematics:

$$i\hat{M}_{Z\psi\bar{\psi}} \equiv i\hat{\kappa} (\epsilon_\mu \bar{u}_\psi \gamma^\mu P_{L/R} v_{\bar{\psi}}) , \quad (\text{B.5})$$

with ϵ_μ denoting the polarization vectors for Z boson, u and v denoting the Dirac spinors for the fermion legs, and $P_{L/R} = \frac{1\mp\gamma^5}{2}$ denoting the projector depending on the chirality of the fermion ψ . The $\hat{\kappa}$ for W boson decay is defined similarly. With this, one can compute the decay width

$$\hat{\Gamma}_{Z\psi\bar{\psi}} = \frac{1}{16\pi\hat{m}_Z} \overline{|\hat{M}_{Z\psi\bar{\psi}}|^2} = \frac{\hat{m}_Z}{24\pi} \hat{\kappa}^2 . \quad (\text{B.6})$$

So our \hat{r} defined in 4.29 can be expressed as

$$\hat{r}_{Z\nu_L\bar{\nu}_L} = \frac{\hat{\kappa}_{Z\nu_L\bar{\nu}_L}^2}{\sqrt{2}\hat{G}_F\hat{m}_Z^2} , \quad (\text{B.7a})$$

$$\hat{r}_{Ze_L\bar{e}_L} = \frac{\hat{\kappa}_{Ze_L\bar{e}_L}^2}{\sqrt{2}\hat{G}_F\hat{m}_Z^2(1-\hat{x})} , \quad (\text{B.7b})$$

$$\hat{r}_{Ze\bar{e}} = \frac{\hat{\kappa}_{Ze\bar{e}}^2}{\sqrt{2}\hat{G}_F\hat{m}_Z^2(1-\sqrt{1-\hat{x}})^2} , \quad (\text{B.7c})$$

$$\hat{r}_{W\nu_Le_L} \equiv \frac{\hat{m}_W\hat{\kappa}_{W\nu_Le_L}^2}{\hat{G}_F\hat{m}_Z^3(1+\sqrt{1-\hat{x}})^{\frac{3}{2}}} . \quad (\text{B.7d})$$

In SM, these strengths are

$$\hat{\kappa}_{Z\nu_L\bar{\nu}_L, \text{SM}}^2 = \frac{g_2^2}{4c_\theta^2} = \sqrt{2}\hat{G}_{F, \text{SM}}\hat{m}_Z^2 , \quad (\text{B.8a})$$

$$\hat{\kappa}_{Ze_L\bar{e}_L, \text{SM}}^2 = \frac{g_2^2}{4c_\theta^2} (1-2s_\theta^2)^2 = \sqrt{2}\hat{G}_{F, \text{SM}}\hat{m}_Z^2 (1-\hat{x}_{\text{SM}}) , \quad (\text{B.8b})$$

$$\hat{\kappa}_{Ze\bar{e}, \text{SM}}^2 = \frac{g_2^2}{c_\theta^2} s_\theta^4 = \sqrt{2}\hat{G}_{F, \text{SM}}\hat{m}_Z^2 \left(1-\sqrt{1-\hat{x}_{\text{SM}}}\right)^2 , \quad (\text{B.8c})$$

$$\hat{\kappa}_{W\nu_Le_L, \text{SM}}^2 = \frac{g_2^2}{2} = \hat{G}_{F, \text{SM}} \frac{\hat{m}_Z^3}{\hat{m}_W} \left(1+\sqrt{1-\hat{x}_{\text{SM}}}\right)^{\frac{3}{2}} . \quad (\text{B.8d})$$

In SMEFT dim-6 Warsaw basis, these become

$$\begin{aligned}
\hat{\kappa}_{Z\nu_L\bar{\nu}_L} &= \hat{\kappa}_{Z\nu_L\bar{\nu}_L, \text{SM}}(R_Z)^{1/2}V_{Z\nu_L\bar{\nu}_L} \\
&= \hat{\kappa}_{Z\nu_L\bar{\nu}_L, \text{SM}} \left[1 + v^2 (c_\theta^2 C_{HW} + s_\theta^2 C_{HB} + c_\theta s_\theta C_{HWB}) - v^2 (C_{HI}^{(1)} - C_{HI}^{(3)}) \right], \tag{B.9a}
\end{aligned}$$

$$\begin{aligned}
\hat{\kappa}_{Ze_L\bar{e}_L} &= \hat{\kappa}_{Ze_L\bar{e}_L, \text{SM}}(R_Z)^{1/2} \left[V_{Ze_L\bar{e}_L} + \frac{2c_\theta s_\theta}{1-2s_\theta^2} \frac{1}{p^2} \Pi_{\gamma Z}(p^2) \right] \\
&= \hat{\kappa}_{Ze_L\bar{e}_L, \text{SM}} \left[1 + v^2 (c_\theta^2 C_{HW} + s_\theta^2 C_{HB} + c_\theta s_\theta C_{HWB}) + v^2 \frac{1}{1-2s_\theta^2} (C_{HI}^{(1)} + C_{HI}^{(3)}) \right. \\
&\quad \left. + v^2 \frac{4c_\theta^2 s_\theta^2}{1-2s_\theta^2} (C_{HW} - C_{HB}) - 2v^2 c_\theta s_\theta C_{HWB} \right], \tag{B.9b}
\end{aligned}$$

$$\begin{aligned}
\hat{\kappa}_{Ze\bar{e}} &= \hat{\kappa}_{Ze\bar{e}, \text{SM}}(R_Z)^{1/2} \left[V_{Ze\bar{e}} - \frac{c_\theta}{s_\theta} \frac{1}{p^2} \Pi_{\gamma Z}(p^2) \right] \\
&= \hat{\kappa}_{Ze\bar{e}, \text{SM}} \left[1 + v^2 (c_\theta^2 C_{HW} + s_\theta^2 C_{HB} + c_\theta s_\theta C_{HWB}) - v^2 \frac{1}{2s_\theta^2} C_{He} \right. \\
&\quad \left. - v^2 2c_\theta^2 (C_{HW} - C_{HB}) + v^2 \frac{c_\theta}{s_\theta} (1-2s_\theta^2) C_{HWB} \right], \tag{B.9c}
\end{aligned}$$

$$\begin{aligned}
\hat{\kappa}_{W\nu_L e_L} &= \hat{\kappa}_{W\nu_L e_L, \text{SM}}(R_W)^{1/2}V_{W\nu_L e_L} \\
&= \hat{\kappa}_{W\nu_L e_L, \text{SM}} \left[1 + v^2 C_{HW} + v^2 C_{HI}^{(3)} \right]. \tag{B.9d}
\end{aligned}$$

These are the corresponding corrections to the last three expressions in 4.26, where

R_W and R_Z are the residues of the W and Z boson at the pole mass:

$$R_W = 1 + \left[\frac{d}{dp^2} \Pi_{WW}(p^2) \right] \Big|_{p^2=\hat{m}_W^2, \text{SM}} = 1 + 2v^2 C_{HW}, \tag{B.10a}$$

$$R_Z = 1 + \left[\frac{d}{dp^2} \Pi_{ZZ}(p^2) \right] \Big|_{p^2=\hat{m}_Z^2, \text{SM}} = 1 + 2v^2 (c_\theta^2 C_{HW} + s_\theta^2 C_{HB} + c_\theta s_\theta C_{HWB}). \tag{B.10b}$$

Plugging B.9 as well as B.4 into B.7 leads us to the expressions in 4.31. In particular, after obtaining $\hat{r}_{Ze_L\bar{e}_L}$ and $\hat{r}_{Ze\bar{e}}$, the last line of 4.31, namely the forward-backward asymmetry of $e^+e^- \rightarrow e^+e^-$ scattering on Z resonance can be calculated straightforwardly as

$$\hat{A}_{FB}^{0,e} = \frac{3}{4} \left[\frac{\hat{\Gamma}_{Ze_L\bar{e}_L} - \hat{\Gamma}_{Ze\bar{e}}}{\hat{\Gamma}_{Ze_L\bar{e}_L} + \hat{\Gamma}_{Ze\bar{e}}} \right]^2. \quad (\text{B.11})$$

Recall 4.26 and 4.29, we may express the decay widths in terms of our pseudo-observables,

$$\hat{\Gamma}_{Ze_L\bar{e}_L} = \left[\frac{\hat{m}_{Z, \text{SM}} g_2^2}{96\pi c_\theta^2} \right] \times \left[(1 - 2s_\theta^2)^2 \hat{r}_{Ze_L\bar{e}_L} \right], \quad (\text{B.12a})$$

$$\hat{\Gamma}_{Ze\bar{e}} = \left[\frac{\hat{m}_{Z, \text{SM}} g_2^2}{96\pi c_\theta^2} \right] \times \left[(4s_\theta^4) \hat{r}_{Ze\bar{e}} \right]. \quad (\text{B.12b})$$

Substitute B.12 back into B.11, we have

$$\begin{aligned} \hat{A}_{FB}^{0,e} &= \frac{3}{4} \left[\frac{\hat{\Gamma}_{Ze_L\bar{e}_L} - \hat{\Gamma}_{Ze\bar{e}}}{\hat{\Gamma}_{Ze_L\bar{e}_L} + \hat{\Gamma}_{Ze\bar{e}}} \right]^2 \\ &= \frac{3}{4} \left[\frac{(1 - 2s_\theta^2)^2 \hat{r}_{Ze_L\bar{e}_L} - (4s_\theta^4) \hat{r}_{Ze\bar{e}}}{(1 - 2s_\theta^2)^2 \hat{r}_{Ze_L\bar{e}_L} + (4s_\theta^4) \hat{r}_{Ze\bar{e}}} \right]^2. \end{aligned} \quad (\text{B.13})$$

Finally, putting the expressions of $\hat{r}_{Ze_L\bar{e}_L}$ and $\hat{r}_{Ze\bar{e}}$ we obtained in 4.31 back into B.13, with further simplification this provides us the last line of 4.31, i.e. the tree-level SMEFT prediction of the pseudo-observable $\hat{r}_{FB}^{0,e}$ at dim-6.

It is worth mentioning that if we restrict to operators that are flavor and custodial symmetric, then the corrections we have calculated here are substantially simplified. First, the corrections to the two-point functions of electroweak gauge bosons in B.1 vanish because they are all custodial violating operators except C_{HW} , which

nevertheless cannot be generated at tree-level. As a consequence, the corrections to $\hat{\alpha}$, \hat{m}_Z^2 and \hat{m}_W^2 in B.4 also vanish, as well as the residue corrections R_W and R_Z in B.10. The only surviving non-zero corrections are the vertex corrections in B.3 and the correction to \hat{G}_F ,

$$V_{Z\nu_L\bar{\nu}_L} = 1 + v^2 C_{Hl}^{(3)} = 1 + v^2 a_{Hl}^{(3)}, \quad (\text{B.14a})$$

$$V_{Ze_L\bar{e}_L} = 1 + \frac{v^2}{1 - 2s_\theta^2} C_{Hl}^{(3)} = 1 + \frac{v^2}{1 - 2s_\theta^2} a_{Hl}^{(3)}, \quad (\text{B.14b})$$

$$V_{Ze\bar{e}} = 1 - \frac{v^2}{2s_\theta^2} C_{He} = 1 - \frac{v^2}{2s_\theta^2} a_{Hl_R}^{(3)+}, \quad (\text{B.14c})$$

$$V_{W\bar{u}} = 1 + v^2 C_{Hl}^{(3)} = 1 + v^2 a_{Hl}^{(3)}, \quad (\text{B.14d})$$

$$\frac{\hat{G}_F}{\hat{G}_{F, \text{SM}}} = 1 + v^2 \left[2C_{Hl}^{(3)} - \frac{1}{2}C_{12} \right] = 1 + v^2 \left[2a_{Hl}^{(3)} - \frac{1}{2}a_{12} \right]. \quad (\text{B.14e})$$

This explains why the observables in 4.33 demonstrate correlated predictions when arising from operators that are custodial and flavor preserving, with only three Wilson coefficients $a_{Hl}^{(3)}$, $a_{Hl_R}^{(3)+}$ and a_{12} involved.

Hadronic Observables

In this Appendix, we consider a set of five quark pseudo-observables in addition to those listed in Sec. IV:

$$\left\{ \hat{\Gamma}_{Zu_L\bar{u}_L}, \hat{\Gamma}_{Zu\bar{u}}, \hat{\Gamma}_{Zd_L\bar{d}_L}, \hat{\Gamma}_{Zd\bar{d}}, \hat{\Gamma}_{Wu_Ld_L} \right\} \quad (\text{B.15})$$

In order, these denote the partial decay widths of the Z boson to left-handed up-type quarks, left-handed down-type quarks, right-handed up-type quarks, right-handed down-type quarks, and the partial decay widths of the W boson to left-handed up-type and down-type quarks.

We present our results in terms of definite parity hadronic final states in order to most easily compare with the results we showed in Sec. IV. In Z decay measurements,

however, the first two generations of quarks are essentially indistinguishable, and so in practice the measurable observables are $\hat{\Gamma}_{Zqq}$ and $\hat{\Gamma}_{Wqq}$ as well as measurements involving the b -quark. This is why, in this section, we refer to these as (pseudo)-observables instead of simply observables. With these caveats in mind, let's proceed to determine the pseudo-observables leaving an interpretation of their use with respect to measurements to Sec. IV. In terms of the three Lagrangian parameters g_1, g_2, v , the hadronic (pseudo)-observables are

$$\hat{\Gamma}_{Zu_L\bar{u}_L, \text{SM}} = \frac{\hat{m}_{Z, \text{SM}} g_2^2}{288\pi c_\theta^2} (3 - 4s_\theta^2)^2, \quad (\text{B.16a})$$

$$\hat{\Gamma}_{Zu\bar{u}, \text{SM}} = \frac{\hat{m}_{Z, \text{SM}} g_2^2}{18\pi c_\theta^2} s_\theta^4, \quad (\text{B.16b})$$

$$\hat{\Gamma}_{Zd_L\bar{d}_L, \text{SM}} = \frac{\hat{m}_{Z, \text{SM}} g_2^2}{288\pi c_\theta^2} (3 - 2s_\theta^2)^2, \quad (\text{B.16c})$$

$$\hat{\Gamma}_{Zd\bar{d}, \text{SM}} = \frac{\hat{m}_{Z, \text{SM}} g_2^2}{72\pi c_\theta^2} s_\theta^4, \quad (\text{B.16d})$$

$$\hat{\Gamma}_{Wu_Ld_L, \text{SM}} = \frac{\hat{m}_{W, \text{SM}}}{16\pi} g_2^2. \quad (\text{B.16e})$$

We can then construct the ratios of the new correction pseudo-observables with respect to the SM ones as:

$$\hat{r}_{Zu_L\bar{u}_L} \equiv \frac{72\pi}{\sqrt{2}\hat{G}_F\hat{m}_Z^3(1+2\sqrt{1-\hat{x}})^2} \hat{\Gamma}_{Zu_L\bar{u}_L}, \quad (\text{B.17a})$$

$$\hat{r}_{Zu\bar{u}} \equiv \frac{18\pi}{\sqrt{2}\hat{G}_F\hat{m}_Z^3(1-\sqrt{1-\hat{x}})^2} \hat{\Gamma}_{Zu\bar{u}}, \quad (\text{B.17b})$$

$$\hat{r}_{Zd_L\bar{d}_L} \equiv \frac{72\pi}{\sqrt{2}\hat{G}_F\hat{m}_Z^3(2+\sqrt{1-\hat{x}})^2} \hat{\Gamma}_{Zd_L\bar{d}_L}, \quad (\text{B.17c})$$

$$\hat{r}_{Zd\bar{d}} \equiv \frac{72\pi}{\sqrt{2}\hat{G}_F\hat{m}_Z^3(1-\sqrt{1-\hat{x}})^2} \hat{\Gamma}_{Zd\bar{d}}, \quad (\text{B.17d})$$

$$\hat{r}_{Wu_Ld_L} \equiv \frac{8\pi}{\hat{G}_F\hat{m}_Z^3(1+\sqrt{1-\hat{x}})^{\frac{3}{2}}} \hat{\Gamma}_{Wu_Ld_L}, \quad (\text{B.17e})$$

where x is defined as before by 4.30.

These five pseudo-observables are unity in SM, but are modified in SMEFT due to nonzero Wilson coefficients. Nevertheless, in a generic SMEFT at dim-6 there are 8 Wilson coefficients related to these 5 pseudo-observables. Here we list them in the Warsaw basis:

$$\hat{r}_{Zu_L\bar{u}_L} = 1 + \frac{v^2}{(1-2s_\theta^2)(3-4s_\theta^2)} \left[-\frac{1}{2}(3-2s_\theta^2)C_{HD} - 8s_\theta c_\theta C_{HWB} - 6(1-2s_\theta^2)C_{Hq}^{(1)} - 2(3-2s_\theta^2)C_{Hl}^{(3)} + 6(1-2s_\theta^2)C_{Hq}^{(3)} + \frac{1}{2}(3-2s_\theta^2)C_{12} \right], \quad (\text{B.18a})$$

$$\hat{r}_{Zu\bar{u}} = 1 + \frac{v^2}{1-2s_\theta^2} \left[\frac{1}{2}C_{HD} + \frac{2c_\theta}{s_\theta}C_{HWB} + 2C_{Hl}^{(3)} + \frac{3(1-2s_\theta^2)}{2s_\theta^2}C_{Hu} - \frac{1}{2}C_{12} \right], \quad (\text{B.18b})$$

$$\hat{r}_{Zd_L\bar{d}_L} = 1 + \frac{v^2}{(1-2s_\theta^2)(3-2s_\theta^2)} \left[-\frac{1}{2}(3-4s_\theta^2)C_{HD} - 4s_\theta c_\theta C_{HWB} + 6(1-2s_\theta^2)C_{Hq}^{(1)} - 2(3-4s_\theta^2)C_{Hl}^{(3)} + 6(1-2s_\theta^2)C_{Hq}^{(3)} + \frac{1}{2}(3-4s_\theta^2)C_{12} \right], \quad (\text{B.18c})$$

$$\hat{r}_{Zd\bar{d}} = 1 + \frac{v^2}{1-2s_\theta^2} \left[\frac{1}{2}C_{HD} + \frac{2c_\theta}{s_\theta}C_{HWB} + 2C_{Hl}^{(3)} - \frac{3(1-2s_\theta^2)}{s_\theta^2}C_{Hd} - \frac{1}{2}C_{12} \right], \quad (\text{B.18d})$$

$$\hat{r}_{Wu_L d_L} = 1 + \frac{v^2}{1-2s_\theta^2} \left[-\frac{3}{4}c_\theta^2 C_{HD} - 3s_\theta c_\theta C_{HWB} - (2-s_\theta^2)C_{Hl}^{(3)} + 2(1-2s_\theta^2)C_{Hq}^{(3)} + \frac{1}{4}(2-s_\theta^2)C_{12} \right]. \quad (\text{B.18e})$$

Now consider the UV physics respects flavor and custodial symmetry. Many operators are absent and there are stronger correlations among these observables. To see this, we go to the custodial basis given in .2 and restrict to those that are flavor

and custodial symmetric:

$$\hat{r}_{Zu_L\bar{u}_L} = 1 - \frac{v^2(3 - 2s_\theta^2)}{(1 - 2s_\theta^2)(3 - 4s_\theta^2)} \left[2a_{Hl}^{(3)} - \frac{1}{2}a_{12} \right] + \frac{6v^2}{3 - 4s_\theta^2} a_{Hq}^{(3)}, \quad (\text{B.19a})$$

$$\hat{r}_{Zu\bar{u}} = 1 + \frac{v^2}{1 - 2s_\theta^2} \left[2a_{Hl}^{(3)} - \frac{1}{2}a_{12} \right] - \frac{3v^2}{2s_\theta^2} a_{HqR}^{(3)+}, \quad (\text{B.19b})$$

$$\hat{r}_{Zd_L\bar{d}_L} = 1 - \frac{v^2(3 - 4s_\theta^2)}{(1 - 2s_\theta^2)(3 - 2s_\theta^2)} \left[2a_{Hl}^{(3)} - \frac{1}{2}a_{12} \right] + \frac{6v^2}{3 - 2s_\theta^2} a_{Hq}^{(3)}, \quad (\text{B.19c})$$

$$\hat{r}_{Zd\bar{d}} = 1 + \frac{v^2}{1 - 2s_\theta^2} \left[2a_{Hl}^{(3)} - \frac{1}{2}a_{12} \right] - \frac{3v^2}{s_\theta^2} a_{HqR}^{(3)+}, \quad (\text{B.19d})$$

$$\hat{r}_{Wu_L d_L} = 1 - \frac{v^2(2 - s_\theta^2)}{2(1 - 2s_\theta^2)} \left[2a_{Hl}^{(3)} - \frac{1}{2}a_{12} \right] + 2v^2 a_{Hq}^{(3)}. \quad (\text{B.19e})$$

As we have mentioned at the end of App. B, these predictions of the five hadronic observables are determined somewhat surprisingly by only three free parameters: two hadronic Wilson coefficients $a_{Hq}^{(3)}$ and $a_{HqR}^{(3)+}$, and the aforementioned linear combination from the correction to \hat{G}_F , namely $\left[2a_{Hl}^{(3)} - \frac{1}{2}a_{12} \right]$. If we combine all of these results into Z and W partial decay widths into hadrons, then incorporate the five leptonic observables in 4.33, these two hadronic partial decay widths do not add any additional information but could still be used as cross-check information at least with respect to specific UV theories.

Tree-level Dim-6 Operators

In this appendix, we show that for the operators types listed in 8, only $H^4 D^2$ and $\bar{\psi}\psi H^2 D$ can be possibly generated at tree-level when matching with a renormalizable UV theory. In below, our derivation follows the argument given in Section 3 of [210].

We parameterize a generic renormalizable UV theory as

$$\mathcal{L}_{\text{UV}} = \frac{1}{2}\Omega^T K \Omega - \Omega^T J + \mathcal{O}(\Omega^3). \quad (\text{B.20})$$

Here Ω denotes a collection of heavy particles that we will integrate out when performing the matching:

$$\Omega = \begin{pmatrix} \Phi \\ \Psi \\ \bar{\Psi} \\ V_\mu \end{pmatrix}, \quad (\text{B.21})$$

with Φ a set of real scalars, $\Psi, \bar{\Psi}$ a set of Weyl fermions, and V_μ a set of vector bosons.

The matrix K captures the quadratic piece in Ω :

$$K = \begin{pmatrix} -D^2 - M^2 & -y\psi & -y\bar{\psi} & 0 \\ -y\psi & -M - y\phi & -(\bar{\sigma} \cdot iD)^T & 0 \\ -y\bar{\psi} & \bar{\sigma} \cdot iD & -M - y\phi & 0 \\ 0 & 0 & 0 & \eta^{\mu\nu} (D^2 + M^2 + g\phi^2) - D^\nu D^\mu + [D^\mu, D^\nu] \end{pmatrix}. \quad (\text{B.22})$$

Here $\phi, \psi, \bar{\psi}$ denote the light scalars and Weyl fermions that we are going to keep in the EFT. Similarly, the covariant derivative D^μ contains only the light gauge bosons in the EFT. Note that our masses and couplings M, λ, y, g etc. here are all schematic. If there is a nonzero tree-level matching result, then we also need a term linear in Ω in the UV Lagrangian. This is parameterized by the second term in B.20, with

$$J = \begin{pmatrix} y\psi\psi + y\bar{\psi}\bar{\psi} + \lambda\phi^3 \\ y\phi\psi \\ y\phi\bar{\psi} \\ g\bar{\psi}\sigma^\mu\psi + g\phi\overleftrightarrow{D}^\mu\phi \end{pmatrix}. \quad (\text{B.23})$$

To match at tree-level, we solve the equations of motion for Ω to get

$$\Omega_v [\phi, \psi, \bar{\psi}] = K^{-1} J. \quad (\text{B.24})$$

We then substitute this solution back into \mathcal{L}_{UV} to obtain the EFT:

$$\mathcal{L}_{\text{EFT}} = \mathcal{L}_{\text{UV}}(\Omega = \Omega_v) = -\frac{1}{2}J^T K^{-1} J. \quad (\text{B.25})$$

Now expanding K^{-1} gives us a tower of effective operators, which we can truncated according to the desired mass dimension. At dim-6, this expansion is fairly simple because the factors J^T and J have already mostly saturated the mass dimension, allowing for at most one mass dimension (from the fields) to keep in K^{-1} . Therefore we get

$$K^{-1} \supset -\frac{1}{M^2} \begin{pmatrix} 1 & 0 & 0 & 0 \\ 0 & M - y\phi & -(\bar{\sigma} \cdot iD)^T & 0 \\ 0 & \bar{\sigma} \cdot iD & M - y\phi & 0 \\ 0 & 0 & 0 & -\eta^{\mu\nu} \end{pmatrix}, \quad (\text{B.26})$$

and

$$\mathcal{L}_{\text{EFT}} \supset \frac{1}{2M^2} J^T \begin{pmatrix} 1 & 0 & 0 & 0 \\ 0 & M - y\phi & -(\bar{\sigma} \cdot iD)^T & 0 \\ 0 & \bar{\sigma} \cdot iD & M - y\phi & 0 \\ 0 & 0 & 0 & -\eta^{\mu\nu} \end{pmatrix} J. \quad (\text{B.27})$$

From this we can easily enumerate all the possible types of field content in the dim-6 matching result, which is summarized by Figure 1 in [210]. In particular, we note that the presence of the covariant derivative D^μ is very limited. First, there will be no field strength factor, which are commutators of the covariant derivatives $X^{\mu\nu} \sim [D^\mu, D^\nu]$. In addition, there is no operator with three or higher powers of D^μ . Furthermore, at the second power of D^μ , the only possible operators are of the type $\phi^4 D^2$; and at the first power of D^μ , the only possible operators are of the type $\bar{\psi}\psi\phi^2 D$. Applying this conclusion to our 8, we see that only $H^4 D^2$ and $\bar{\psi}\psi H^2 D$ can be possibly generated at tree-level.

EOM Equivalence Example

We know that predictions on physical observables are invariant under a basis change in an EFT. One way of performing a basis change is to trade operators through their redundancy relations due to the Equations of Motion (EOM) at the *leading order* (see e.g. Ref. [222] for detailed explanation). Such a basis change yields equivalent physical predictions up to the order of the EFT expansion. This intuitive fact, however, brings complications for characterizing models with “minimal” custodial violation. Since custodial symmetry is broken by ν SM interactions, it is violated by ν SM equations of motion, namely the leading order EOM in ν SMEFT. This means that when changing basis through EOM redundancy in ν SMEFT, one can trade custodial preserving operators into custodial violating operators and vice versa. But they give the same predictions on physical observables. This point is potentially confusing. In this appendix, we give a simple example, demonstrating how custodial preserving and violating operators could yield the same physical predictions.

In this example, the physical observables that we will focus on are the Higgs decay widths $\Gamma_{h \rightarrow WW^*}$, $\Gamma_{h \rightarrow ZZ^*}$, and $\Gamma_{h \rightarrow f\bar{f}}$, with f denoting the Dirac fields for ν SM fermions $f \in \{f_u, f_d, f_\nu, f_e\}$ and ¹

$$f_u \equiv \begin{pmatrix} u_L \\ u_R \end{pmatrix}, \quad f_d \equiv \begin{pmatrix} d_L \\ d_R \end{pmatrix}, \quad f_\nu \equiv \begin{pmatrix} \nu_L \\ \nu_R \end{pmatrix}, \quad f_e \equiv \begin{pmatrix} e_L \\ e_R \end{pmatrix}. \quad (\text{B.28})$$

For our purpose, it is actually sufficient to study the corresponding amplitudes iM_{hWW} , iM_{hZZ} , and $iM_{hf\bar{f}}$ as “pseudo” observables. In fact, as we shall see in below, we will also strip off the external polarization vectors, spinors, etc. from these amplitudes, because the corrections we will study have trivial momentum dependence.

¹For simplicity, we work with only one generation of fermions, and assume real Yukawa couplings.

In the following, we will pick a simple basis change through EOM redundancy, and show how the two bases give the same predictions on these amplitudes. In particular, we consider the operator

$$Q_R \equiv |H|^2 |DH|^2, \quad (\text{B.29})$$

which is outside the Warsaw basis in .1. Using the Higgs EOM in ν SM, one can write this operator as a linear combination of those included in the Warsaw basis. Concretely, the Higgs sector of the ν SM Lagrangian is

$$\mathcal{L}_{\text{SM}\nu} \supset |DH|^2 - \lambda \left(|H|^2 - \frac{1}{2}v^2 \right)^2 - \left(Y_u \bar{q} \tilde{H} u + Y_d \bar{q} H d + Y_\nu \bar{l} \tilde{H} \nu + Y_e \bar{l} H e + \text{h.c.} \right). \quad (\text{B.30})$$

The resulting Higgs EOM (together with integration by parts redundancy) gives the following redundancy relation

$$Q_R \equiv |H|^2 |DH|^2 = \frac{1}{2} Q_{H\Box} + 2\lambda Q_H + \frac{1}{2} Q_Y - \lambda v^2 |H|^4, \quad (\text{B.31})$$

where we have defined the custodial violating (due to Yukawa mismatch $Y_u \neq Y_d$ and $Y_\nu \neq Y_e$) operator Q_Y as

$$Q_Y \equiv Y_u Q_{uH} + Y_d Q_{dH} + Y_\nu Q_{\nu H} + Y_e Q_{eH} + \text{h.c.} \quad (\text{B.32})$$

Rearranging B.31, we get

$$Q_{H\Box} = 2Q_R - 4\lambda Q_H - Q_Y + 2\lambda v^2 |H|^4 \quad \rightarrow \quad 2Q_R - Q_Y. \quad (\text{B.33})$$

In the last expression here, we have dropped operators not contributing to the aforementioned amplitudes. This equivalence relation means that for the corrections on iM_{hWW} , iM_{hZZ} , and $iM_{hf\bar{f}}$, the custodial preserving operator $Q_{H\Box}$ in the Warsaw basis is equivalent to the combination $2Q_R - Q_Y$, with Q_Y a custodial violating operator in the Warsaw basis and Q_R a custodial preserving operator outside the Warsaw basis. In the rest of this appendix, we will demonstrate this equivalence,

i.e.between the following two toy EFT Lagrangians

$$\mathcal{L}_{\text{Warsaw}} = C_{H\Box} Q_{H\Box}, \quad (\text{B.34a})$$

$$\mathcal{L}_{\text{Alternative}} = C_R Q_R + C_Y Q_Y, \quad (\text{B.34b})$$

with $C_R = 2C_{H\Box}$ and $C_Y = -C_{H\Box}$.

ν SM Predictions. Before studying the EFT corrections, let us first work out the predictions in ν SM as a warm up. To compute the gauge boson amplitudes, we examine the Higgs sector:

$$\begin{aligned} \mathcal{L}_{\text{SM}\nu} \supset |DH|^2 &= \frac{1}{2}(\partial h)^2 + \frac{g_2^2}{4}(v+h)^2 W_\mu^+ W^{-\mu} + \frac{1}{2} \frac{g_2^2}{4c_\theta^2} (v+h)^2 Z_\mu Z^\mu \\ &\supset \frac{1}{2}(\partial h)^2 + \frac{g_2^2 v^2}{4} W_\mu^+ W^{-\mu} + \frac{1}{2} \frac{g_2^2 v^2}{4c_\theta^2} Z_\mu Z^\mu + \frac{g_2^2}{4} 2vh W_\mu^+ W^{-\mu} + \frac{1}{2} \frac{g_2^2}{4c_\theta^2} 2vh Z_\mu Z^\mu. \end{aligned} \quad (\text{B.35})$$

In order to determine the free parameters g_2^2 , c_θ^2 , and v , we take the observables \hat{m}_W^2 , \hat{m}_Z^2 , and \hat{G}_F .² From the above, we see that these are related to the ν SM parameters as

$$\hat{m}_W^2 = \frac{g_2^2 v^2}{4}, \quad \hat{m}_Z^2 = \frac{g_2^2 v^2}{4c_\theta^2}, \quad \hat{G}_F = \frac{\sqrt{2}g_2^2}{8\hat{m}_W^2} = \frac{1}{\sqrt{2}v^2}. \quad (\text{B.36})$$

Solving these, we get the ν SM parameters

$$v^2 = \frac{1}{\sqrt{2}\hat{G}_F}, \quad g_2^2 = \frac{4\hat{m}_W^2}{v^2} = 4\sqrt{2}\hat{G}_F\hat{m}_W^2, \quad \frac{g_2^2}{c_\theta^2} = \frac{4\hat{m}_Z^2}{v^2} = 4\sqrt{2}\hat{G}_F\hat{m}_Z^2. \quad (\text{B.37})$$

Now we can obtain the ν SM predictions on the amplitudes $h \rightarrow WW$ and $h \rightarrow ZZ$:

$$iM_{hWW} = \frac{g_2^2}{4} 2v = 2\hat{m}_W^2 \sqrt{\sqrt{2}\hat{G}_F}, \quad (\text{B.38a})$$

$$iM_{hZZ} = \frac{g_2^2}{4c_\theta^2} 2v = 2\hat{m}_Z^2 \sqrt{\sqrt{2}\hat{G}_F}. \quad (\text{B.38b})$$

As noted before, we have stripped off the polarization vector part of these amplitudes, since they are irrelevant for our current analysis.

²We use \hat{m}_W^2 here for simplicity. In real analysis (see e.g.[140]), one typically uses the more accurately measured quantity $\hat{\alpha}$ — the fine structure constant in place of \hat{m}_W^2 .

To compute the fermion amplitudes, we examine the Yukawa sector:

$$\begin{aligned} \mathcal{L}_{\text{SM}\nu} \supset & - \left(Y_u \bar{q} \tilde{H} u + Y_d \bar{q} H d + Y_\nu \bar{l} \tilde{H} \nu + Y_e \bar{l} H e + \text{h.c.} \right) \\ & = - \sum_f \frac{1}{\sqrt{2}} Y_f (v + h) \bar{f} f = - \sum_f \frac{1}{\sqrt{2}} Y_f v \bar{f} f - \sum_f \frac{1}{\sqrt{2}} Y_f h \bar{f} f. \end{aligned} \quad (\text{B.39})$$

Again, we need to first determine the new free parameter Y_f . For this we can pick \hat{m}_f :

$$\hat{m}_f = \frac{1}{\sqrt{2}} Y_f v, \quad (\text{B.40})$$

which gives

$$\frac{1}{\sqrt{2}} Y_f = \frac{\hat{m}_f}{v} = \hat{m}_f \sqrt{\sqrt{2} \hat{G}_F}. \quad (\text{B.41})$$

Now the $h \rightarrow f \bar{f}$ amplitudes are predicted as

$$iM_{h\bar{f}f} = -i \frac{1}{\sqrt{2}} Y_f = -i \hat{m}_f \sqrt{\sqrt{2} \hat{G}_F}. \quad (\text{B.42})$$

Similar to the case of gauge boson amplitudes, the spinor part of the fermion amplitude is irrelevant for us and has been stripped off.

Correction in Warsaw Basis. Let us now check the prediction of the aforementioned amplitudes by our Warsaw basis toy EFT Lagrangian in B.34a. For this, we need to work out the effects of the operator $Q_{H\Box}$. As is well-known (see e.g.[223]), this operator corrects the Higgs amplitudes of the type $h \rightarrow XX$ (with XX denoting WW , ZZ , or $f\bar{f}$) by a universal residue effect. Specifically, we have

$$Q_{H\Box} \equiv - (\partial_\mu |H|^2) (\partial^\mu |H|^2) = -(v + h)^2 (\partial h)^2 \supset \frac{1}{2} (-2v^2) (\partial h)^2. \quad (\text{B.43})$$

This yields a nontrivial residue for the Higgs field

$$R_h = (1 - 2v^2 C_{H\Box})^{-1} = 1 + 2v^2 C_{H\Box}, \quad (\text{B.44})$$

which feeds into the amplitudes of our interests as

$$iM_{hXX} \rightarrow R_h^{1/2} iM_{hXX} = (1 + v^2 C_{H\Box}) iM_{hXX}. \quad (\text{B.45})$$

Note that in above calculations, we are only keeping up to the linear power in the EFT expansion parameter $\frac{v^2}{\Lambda^2}$. This is because the EOM equivalence is supposed to hold only up to this order.

Correction in the Alternative Basis. Now let us check the prediction by the same toy EFT Lagrangian written in the alternative basis i.e.B.34b. For this we need to work out the effects of the operators Q_R and Q_Y .

For Q_R , we use B.35 to get

$$\begin{aligned}
Q_R &= |H|^2 |DH|^2 = \frac{1}{2}(v+h)^2 |DH|^2 \\
&= \frac{1}{4}(v+h)^2 (\partial h)^2 + \frac{g_2^2}{4} \frac{1}{2}(v+h)^4 W_\mu^+ W^{-\mu} + \frac{1}{2} \frac{g_2^2}{4c_\theta^2} \frac{1}{2}(v+h)^4 Z_\mu Z^\mu \\
&\supset \frac{1}{2} v^2 \left[\frac{1}{2} (\partial h)^2 + \frac{g_2^2 v^2}{4} W_\mu^+ W^{-\mu} + \frac{1}{2} \frac{g_2^2 v^2}{4c_\theta^2} Z_\mu Z^\mu \right] \\
&\quad + v^2 \frac{g_2^2}{4} 2vh W_\mu^+ W^{-\mu} + v^2 \frac{1}{2} \frac{g_2^2}{4c_\theta^2} 2vh Z_\mu Z^\mu.
\end{aligned} \tag{B.46}$$

We see that now with a Wilson coefficient C_R , the observables \hat{m}_W^2 , \hat{m}_Z^2 , and \hat{G}_F become

$$\hat{m}_W^2 = \frac{g_2^2 v^2}{4} \left(1 + \frac{1}{2} v^2 C_R \right), \tag{B.47a}$$

$$\hat{m}_Z^2 = \frac{g_2^2 v^2}{4c_\theta^2} \left(1 + \frac{1}{2} v^2 C_R \right), \tag{B.47b}$$

$$\hat{G}_F = \frac{\sqrt{2} g_2^2}{8\hat{m}_W^2} = \frac{1}{\sqrt{2} v^2} \left(1 + \frac{1}{2} v^2 C_R \right)^{-1}. \tag{B.47c}$$

Solving these we obtain

$$v^2 = \frac{1}{\sqrt{2} \hat{G}_F} \left(1 + \frac{1}{2} v^2 C_R \right)^{-1} = \frac{1}{\sqrt{2} \hat{G}_F} \left(1 - \frac{1}{2} v^2 C_R \right), \tag{B.48a}$$

$$g_2^2 = \frac{4\hat{m}_W^2}{v^2} \left(1 + \frac{1}{2} v^2 C_R \right)^{-1} = 4\sqrt{2} \hat{G}_F \hat{m}_W^2, \tag{B.48b}$$

$$\frac{g_2^2}{c_\theta^2} = \frac{4\hat{m}_Z^2}{v^2} \left(1 + \frac{1}{2} v^2 C_R \right)^{-1} = 4\sqrt{2} \hat{G}_F \hat{m}_Z^2. \tag{B.48c}$$

Comparing with B.37, we see that the parameters g_2^2 and c_θ^2 are unchanged, but v^2 receives a modification. Note that we now also have a nontrivial Higgs residue as well

$$R_h = \left(1 + \frac{1}{2}v^2 C_R\right)^{-1}. \quad (\text{B.49})$$

It is interesting to note that the following combination is unaffected

$$R_h^{1/2} \frac{1}{v} = \sqrt{\sqrt{2}\hat{G}_F}. \quad (\text{B.50})$$

This is a reflection that the part $\frac{1}{2}v^2 |DH|^2$ in Q_R is just rescaling the whole field H (namely v and h together in the same way), and hence has no physical observable effects. Therefore, all the physical effects of Q_R come from the rest of it $\frac{1}{2}(2vh + h^2) |DH|^2$. For $h \rightarrow XX$ amplitudes, it is obvious that this part can only modify $h \rightarrow WW$ and $h \rightarrow ZZ$, which are given by

$$iM_{hWW} = R_h^{1/2} \frac{g_2^2}{4} 2v (1 + v^2 C_R) = 2\hat{m}_W^2 \sqrt{\sqrt{2}\hat{G}_F} \left(1 + \frac{1}{2}v^2 C_R\right), \quad (\text{B.51a})$$

$$iM_{hZZ} = R_h^{1/2} \frac{g_2^2}{4c_\theta^2} 2v (1 + v^2 C_R) = 2\hat{m}_Z^2 \sqrt{\sqrt{2}\hat{G}_F} \left(1 + \frac{1}{2}v^2 C_R\right). \quad (\text{B.51b})$$

Next, we check the effects of the operator Q_Y .

$$\begin{aligned} Q_Y &\equiv Y_u Q_{uH} + Y_d Q_{dH} + Y_\nu Q_{\nu H} + Y_e Q_{eH} + \text{h.c.} \\ &= |H|^2 \left(Y_u \bar{q} \tilde{H} u + Y_d \bar{q} H d + Y_\nu \bar{l} \tilde{H} \nu + Y_e \bar{l} H e + \text{h.c.} \right) \\ &= \sum_f \frac{1}{2\sqrt{2}} Y_f (v+h)^3 \bar{f} f \supset \sum_f \frac{1}{2\sqrt{2}} Y_f v^3 \bar{f} f + \sum_f \frac{1}{2\sqrt{2}} Y_f 3v^2 h \bar{f} f. \end{aligned} \quad (\text{B.52})$$

We see that now with a Wilson coefficient C_Y , the parameter-fixing observable \hat{m}_f becomes

$$\hat{m}_f = \frac{1}{\sqrt{2}} Y_f v \left(1 - \frac{1}{2}v^2 C_Y\right). \quad (\text{B.53})$$

With this, we can compute the fermion amplitude as

$$\begin{aligned} iM_{h\bar{f}f} &= R_h^{1/2} \left[-i \frac{1}{\sqrt{2}} Y_f \left(1 - \frac{3}{2}v^2 C_Y\right) \right] = -i R_h^{1/2} \frac{\hat{m}_f}{v} (1 - v^2 C_Y) \\ &= -i \hat{m}_f \sqrt{\sqrt{2}\hat{G}_F} (1 - v^2 C_Y). \end{aligned} \quad (\text{B.54})$$

Note that in getting the second line, we have used the fact that the ratio $R_h^{1/2} \frac{1}{v}$ is unmodified by Q_R , as we have seen in B.50. This manifests our general argument that Q_R would not modify $iM_{h\bar{f}f}$.

Finally, using B.51 and B.54 with $C_R = 2C_{H\Box}$ and $C_Y = -C_{H\Box}$, we get

$$iM_{hWW} = 2\hat{m}_W^2 \sqrt{\sqrt{2}\hat{G}_F} \left(1 + \frac{1}{2}v^2 C_R \right) = 2\hat{m}_W^2 \sqrt{\sqrt{2}\hat{G}_F} (1 + v^2 C_{H\Box}) , \quad (\text{B.55a})$$

$$iM_{hZZ} = 2\hat{m}_Z^2 \sqrt{\sqrt{2}\hat{G}_F} \left(1 + \frac{1}{2}v^2 C_R \right) = 2\hat{m}_Z^2 \sqrt{\sqrt{2}\hat{G}_F} (1 + v^2 C_{H\Box}) , \quad (\text{B.55b})$$

$$iM_{h\bar{f}f} = -i\hat{m}_f \sqrt{\sqrt{2}\hat{G}_F} (1 - v^2 C_Y) = -i\hat{m}_f \sqrt{\sqrt{2}\hat{G}_F} (1 + v^2 C_{H\Box}) . \quad (\text{B.55c})$$

Clearly, these agree with the Warsaw basis results we obtained in B.45.

REFERENCES CITED

- [1] **ATLAS Collaboration** Collaboration, “Search for electroweak production of supersymmetric particles in final states with tau leptons in $\sqrt{s} = 13\text{TeV}$ pp collisions with the ATLAS detector,” Tech. Rep. ATLAS-CONF-2016-093, CERN, Geneva, Aug, 2016. <http://cds.cern.ch/record/2211437>.
- [2] **ATLAS** Collaboration, G. Aad *et al.*, “Search for new phenomena in events with three or more charged leptons in pp collisions at $\sqrt{s} = 8\text{ TeV}$ with the ATLAS detector,” *JHEP* **08** (2015) 138, [arXiv:1411.2921](https://arxiv.org/abs/1411.2921) [hep-ex].
- [3] **CMS** Collaboration, S. Chatrchyan *et al.*, “Search for anomalous production of events with three or more leptons in pp collisions at $\sqrt{s} = 8\text{ TeV}$,” *Phys. Rev. D* **90** (2014) 032006, [arXiv:1404.5801](https://arxiv.org/abs/1404.5801) [hep-ex].
- [4] **ATLAS** Collaboration, “Search for strongly produced superpartners in final states with two same sign leptons with the ATLAS detector using 21 fb-1 of proton-proton collisions at $\sqrt{s}=8\text{ TeV}$,” Tech. Rep. ATLAS-CONF-2013-007, 2013.
- [5] **ATLAS** Collaboration, M. Aaboud *et al.*, “Search for supersymmetry in final states with two same-sign or three leptons and jets using 36 fb^{-1} of $\sqrt{s} = 13\text{ TeV}$ pp collision data with the ATLAS detector,” *JHEP* **09** (2017) 084, [arXiv:1706.03731](https://arxiv.org/abs/1706.03731) [hep-ex].
- [6] B. Carr, F. Kuhnel, and M. Sandstad, “Primordial Black Holes as Dark Matter,” *Phys. Rev. D* **94** (2016) no. 8, 083504, [arXiv:1607.06077](https://arxiv.org/abs/1607.06077) [astro-ph.CO].
- [7] **Particle Data Group** Collaboration, M. Tanabashi *et al.*, “Review of Particle Physics,” *Phys. Rev. D* **98** (2018) no. 3, 030001.
- [8] A. D. Sakharov, “Violation of CP invariance, C asymmetry, and baryon asymmetry of the universe,” *Soviet Physics Uspekhi* **34** (may, 1991) 392–393. <https://doi.org/10.1070%2Fpu1991v034n05abeh002497>.
- [9] J. M. Cline, “Baryogenesis,” in *Les Houches Summer School - Session 86: Particle Physics and Cosmology: The Fabric of Spacetime*. 9, 2006. [arXiv:hep-ph/0609145](https://arxiv.org/abs/hep-ph/0609145).
- [10] T. Cohen, “As Scales Become Separated: Lectures on Effective Field Theory,” *PoS TASI2018* (2019) 011, [arXiv:1903.03622](https://arxiv.org/abs/1903.03622) [hep-ph].
- [11] E. H. Simmons, “Phenomenology of a Technicolor Model With Heavy Scalar Doublet,” *Nucl. Phys.* **B312** (1989) 253–268.

- [12] S. Samuel, “BOSONIC TECHNICOLOR,” *Nucl. Phys.* **B347** (1990) 625–650.
- [13] M. Dine, A. Kagan, and S. Samuel, “Naturalness in Supersymmetry, or Raising the Supersymmetry Breaking Scale,” *Phys. Lett.* **B243** (1990) 250–256.
- [14] A. Kagan and S. Samuel, “The Family mass hierarchy problem in bosonic technicolor,” *Phys. Lett.* **B252** (1990) 605–610.
- [15] A. Kagan and S. Samuel, “Renormalization group aspects of bosonic technicolor,” *Phys. Lett.* **B270** (1991) 37–44.
- [16] C. D. Carone and E. H. Simmons, “Oblique corrections in technicolor with a scalar,” *Nucl. Phys.* **B397** (1993) 591–615, [arXiv:hep-ph/9207273 \[hep-ph\]](#).
- [17] C. D. Carone and H. Georgi, “Technicolor with a massless scalar doublet,” *Phys. Rev.* **D49** (1994) 1427–1436, [arXiv:hep-ph/9308205 \[hep-ph\]](#).
- [18] B. A. Dobrescu and J. Terning, “Negative contributions to S in an effective field theory,” *Phys. Lett.* **B416** (1998) 129–136, [arXiv:hep-ph/9709297 \[hep-ph\]](#).
- [19] M. Antola, M. Heikinheimo, F. Sannino, and K. Tuominen, “Unnatural Origin of Fermion Masses for Technicolor,” *JHEP* **03** (2010) 050, [arXiv:0910.3681 \[hep-ph\]](#).
- [20] A. Azatov, J. Galloway, and M. A. Luty, “Superconformal Technicolor,” *Phys. Rev. Lett.* **108** (2012) 041802, [arXiv:1106.3346 \[hep-ph\]](#).
- [21] A. Azatov, J. Galloway, and M. A. Luty, “Superconformal Technicolor: Models and Phenomenology,” *Phys. Rev.* **D85** (2012) 015018, [arXiv:1106.4815 \[hep-ph\]](#).
- [22] T. Gherghetta and A. Pomarol, “A Distorted MSSM Higgs Sector from Low-Scale Strong Dynamics,” *JHEP* **12** (2011) 069, [arXiv:1107.4697 \[hep-ph\]](#).
- [23] J. Galloway, M. A. Luty, Y. Tsai, and Y. Zhao, “Induced Electroweak Symmetry Breaking and Supersymmetric Naturalness,” *Phys. Rev.* **D89** (2014) no. 7, 075003, [arXiv:1306.6354 \[hep-ph\]](#).
- [24] S. Chang, J. Galloway, M. Luty, E. Salvioni, and Y. Tsai, “Phenomenology of Induced Electroweak Symmetry Breaking,” *JHEP* **03** (2015) 017, [arXiv:1411.6023 \[hep-ph\]](#).
- [25] H. Beauchesne, K. Earl, and T. Gregoire, “The spontaneous Z2 breaking Twin Higgs,” *JHEP* **01** (2016) 130, [arXiv:1510.06069 \[hep-ph\]](#).

- [26] R. Harnik, K. Howe, and J. Kearney, “Tadpole-Induced Electroweak Symmetry Breaking and pNGB Higgs Models,” *JHEP* **03** (2017) 111, [arXiv:1603.03772 \[hep-ph\]](#).
- [27] T. Alanne, M. T. Frandsen, and D. Buarque Franzosi, “Testing a dynamical origin of Standard Model fermion masses,” *Phys. Rev.* **D94** (2016) 071703, [arXiv:1607.01440 \[hep-ph\]](#).
- [28] J. Galloway, A. L. Kagan, and A. Martin, “A UV complete partially composite-pNGB Higgs,” *Phys. Rev.* **D95** (2017) no. 3, 035038, [arXiv:1609.05883 \[hep-ph\]](#).
- [29] A. Agugliaro, O. Antipin, D. Becciolini, S. De Curtis, and M. Redi, “UV complete composite Higgs models,” *Phys. Rev.* **D95** (2017) no. 3, 035019, [arXiv:1609.07122 \[hep-ph\]](#).
- [30] D. Barducci, S. De Curtis, M. Redi, and A. Tesi, “An almost elementary Higgs: Theory and Practice,” *JHEP* **08** (2018) 017, [arXiv:1805.12578 \[hep-ph\]](#).
- [31] B. Bellazzini, C. Csáki, and J. Serra, “Composite Higgses,” *Eur. Phys. J.* **C74** (2014) no. 5, 2766, [arXiv:1401.2457 \[hep-ph\]](#).
- [32] P. W. Graham, D. E. Kaplan, and S. Rajendran, “Cosmological Relaxation of the Electroweak Scale,” *Phys. Rev. Lett.* **115** (2015) no. 22, 221801, [arXiv:1504.07551 \[hep-ph\]](#).
- [33] O. Antipin and M. Redi, “The Half-composite Two Higgs Doublet Model and the Relaxion,” *JHEP* **12** (2015) 031, [arXiv:1508.01112 \[hep-ph\]](#).
- [34] B. Batell, M. A. Fedderke, and L.-T. Wang, “Relaxation of the Composite Higgs Little Hierarchy,” *JHEP* **12** (2017) 139, [arXiv:1705.09666 \[hep-ph\]](#).
- [35] C. Kilic, T. Okui, and R. Sundrum, “Vectorlike Confinement at the LHC,” *JHEP* **02** (2010) 018, [arXiv:0906.0577 \[hep-ph\]](#).
- [36] G. D. Kribs, T. S. Roy, J. Terning, and K. M. Zurek, “Quirky Composite Dark Matter,” *Phys. Rev.* **D81** (2010) 095001, [arXiv:0909.2034 \[hep-ph\]](#).
- [37] C. Kilic and T. Okui, “The LHC Phenomenology of Vectorlike Confinement,” *JHEP* **04** (2010) 128, [arXiv:1001.4526 \[hep-ph\]](#).
- [38] R. Harnik, G. D. Kribs, and A. Martin, “Quirks at the Tevatron and Beyond,” *Phys. Rev.* **D84** (2011) 035029, [arXiv:1106.2569 \[hep-ph\]](#).
- [39] R. Fok and G. D. Kribs, “Chiral Quirkonium Decays,” *Phys. Rev.* **D84** (2011) 035001, [arXiv:1106.3101 \[hep-ph\]](#).

- [40] M. R. Buckley and E. T. Neil, “Thermal Dark Matter from a Confining Sector,” *Phys.Rev.* **D87** (2013) no. 4, 043510, [arXiv:1209.6054 \[hep-ph\]](#).
- [41] Y. Bai and P. Schwaller, “Scale of dark QCD,” *Phys. Rev.* **D89** (2014) no. 6, 063522, [arXiv:1306.4676 \[hep-ph\]](#).
- [42] J. Brod, J. Drobnak, A. L. Kagan, E. Stamou, and J. Zupan, “Stealth QCD-like strong interactions and the $t\bar{t}$ asymmetry,” *Phys. Rev.* **D91** (2015) no. 9, 095009, [arXiv:1407.8188 \[hep-ph\]](#).
- [43] Z. Chacko, D. Curtin, and C. B. Verhaaren, “A Quirky Probe of Neutral Naturalness,” *Phys. Rev.* **D94** (2016) no. 1, 011504, [arXiv:1512.05782 \[hep-ph\]](#).
- [44] K. Agashe, P. Du, S. Hong, and R. Sundrum, “Flavor Universal Resonances and Warped Gravity,” *JHEP* **01** (2017) 016, [arXiv:1608.00526 \[hep-ph\]](#).
- [45] S. Matsuzaki, K. Nishiwaki, and R. Watanabe, “Phenomenology of flavorful composite vector bosons in light of B anomalies,” *JHEP* **08** (2017) 145, [arXiv:1706.01463 \[hep-ph\]](#).
- [46] D. Buttazzo, D. Redigolo, F. Sala, and A. Tesi, “Fusing Vectors into Scalars at High Energy Lepton Colliders,” [arXiv:1807.04743 \[hep-ph\]](#).
- [47] P. Schwaller, D. Stolarski, and A. Weiler, “Emerging Jets,” *JHEP* **05** (2015) 059, [arXiv:1502.05409 \[hep-ph\]](#).
- [48] T. Cohen, M. Lisanti, and H. K. Lou, “Semivisible Jets: Dark Matter Undercover at the LHC,” *Phys. Rev. Lett.* **115** (2015) no. 17, 171804, [arXiv:1503.00009 \[hep-ph\]](#).
- [49] M. Freytsis, S. Knapen, D. J. Robinson, and Y. Tsai, “Gamma-rays from Dark Showers with Twin Higgs Models,” *JHEP* **05** (2016) 018, [arXiv:1601.07556 \[hep-ph\]](#).
- [50] M. Kim, H.-S. Lee, M. Park, and M. Zhang, “Examining the origin of dark matter mass at colliders,” [arXiv:1612.02850 \[hep-ph\]](#).
- [51] T. Cohen, M. Lisanti, H. K. Lou, and S. Mishra-Sharma, “LHC Searches for Dark Sector Showers,” *JHEP* **11** (2017) 196, [arXiv:1707.05326 \[hep-ph\]](#).
- [52] H. Beauchesne, E. Bertuzzo, G. Grilli Di Cortona, and Z. Tabrizi, “Collider phenomenology of Hidden Valley mediators of spin 0 or 1/2 with semivisible jets,” *JHEP* **08** (2018) 030, [arXiv:1712.07160 \[hep-ph\]](#).
- [53] S. Renner and P. Schwaller, “A flavoured dark sector,” *JHEP* **08** (2018) 052, [arXiv:1803.08080 \[hep-ph\]](#).

- [54] R. Mahbubani, P. Schwaller, and J. Zurita, “Closing the window for compressed Dark Sectors with disappearing charged tracks,” *JHEP* **06** (2017) 119, [arXiv:1703.05327 \[hep-ph\]](#). [Erratum: *JHEP*10,061(2017)].
- [55] O. Buchmueller, A. De Roeck, K. Hahn, M. McCullough, P. Schwaller, K. Sung, and T.-T. Yu, “Simplified Models for Displaced Dark Matter Signatures,” *JHEP* **09** (2017) 076, [arXiv:1704.06515 \[hep-ph\]](#).
- [56] Y. Hochberg, E. Kuflik, and H. Murayama, “SIMP Spectroscopy,” *JHEP* **05** (2016) 090, [arXiv:1512.07917 \[hep-ph\]](#).
- [57] N. Daci, I. De Bruyn, S. Lowette, M. H. G. Tytgat, and B. Zaldivar, “Simplified SIMPs and the LHC,” *JHEP* **11** (2015) 108, [arXiv:1503.05505 \[hep-ph\]](#).
- [58] Y. Hochberg, E. Kuflik, and H. Murayama, “Dark spectroscopy at lepton colliders,” *Phys. Rev.* **D97** (2018) no. 5, 055030, [arXiv:1706.05008 \[hep-ph\]](#).
- [59] T. Han, Z. Si, K. M. Zurek, and M. J. Strassler, “Phenomenology of hidden valleys at hadron colliders,” *JHEP* **07** (2008) 008, [arXiv:0712.2041 \[hep-ph\]](#).
- [60] J. Kang and M. A. Luty, “Macroscopic Strings and ‘Quirks’ at Colliders,” *JHEP* **11** (2009) 065, [arXiv:0805.4642 \[hep-ph\]](#).
- [61] R. Harnik and T. Wizansky, “Signals of New Physics in the Underlying Event,” *Phys. Rev.* **D80** (2009) 075015, [arXiv:0810.3948 \[hep-ph\]](#).
- [62] S. Knapen, S. Pagan Griso, M. Papucci, and D. J. Robinson, “Triggering Soft Bombs at the LHC,” *JHEP* **08** (2017) 076, [arXiv:1612.00850 \[hep-ph\]](#).
- [63] A. Pierce, B. Shakya, Y. Tsai, and Y. Zhao, “Searching for confining hidden valleys at LHCb, ATLAS, and CMS,” *Phys. Rev.* **D97** (2018) no. 9, 095033, [arXiv:1708.05389 \[hep-ph\]](#).
- [64] S. Nussinov, “TECHNOCOSMOLOGY: COULD A TECHNIBARYON EXCESS PROVIDE A ‘NATURAL’ MISSING MASS CANDIDATE?,” *Phys.Lett.* **B165** (1985) 55.
- [65] R. S. Chivukula and T. P. Walker, “TECHNICOLOR COSMOLOGY,” *Nucl.Phys.* **B329** (1990) 445.
- [66] S. M. Barr, R. S. Chivukula, and E. Farhi, “Electroweak Fermion Number Violation and the Production of Stable Particles in the Early Universe,” *Phys.Lett.* **B241** (1990) 387–391.

- [67] S. M. Barr, “Baryogenesis, sphalerons and the cogeneration of dark matter,” *Phys.Rev.* **D44** (1991) 3062–3066.
- [68] D. B. Kaplan, “A Single explanation for both the baryon and dark matter densities,” *Phys.Rev.Lett.* **68** (1992) 741–743.
- [69] R. S. Chivukula, A. G. Cohen, M. E. Luke, and M. J. Savage, “A Comment on the strong interactions of color - neutral technibaryons,” *Phys.Lett.* **B298** (1993) 380–382, [arXiv:hep-ph/9210274](#) [hep-ph].
- [70] J. Bagnasco, M. Dine, and S. D. Thomas, “Detecting technibaryon dark matter,” *Phys.Lett.* **B320** (1994) 99–104, [arXiv:hep-ph/9310290](#) [hep-ph].
- [71] M. Yu. Khlopov and C. Kouvaris, “Composite dark matter from a model with composite Higgs boson,” *Phys. Rev.* **D78** (2008) 065040, [arXiv:0806.1191](#) [astro-ph].
- [72] T. A. Rytov and F. Sannino, “Ultra Minimal Technicolor and its Dark Matter TIMP,” *Phys. Rev.* **D78** (2008) 115010, [arXiv:0809.0713](#) [hep-ph].
- [73] T. Hambye and M. H. G. Tytgat, “Confined hidden vector dark matter,” *Phys. Lett.* **B683** (2010) 39–41, [arXiv:0907.1007](#) [hep-ph].
- [74] Y. Bai and R. J. Hill, “Weakly Interacting Stable Pions,” *Phys.Rev.* **D82** (2010) 111701, [arXiv:1005.0008](#) [hep-ph].
- [75] R. Lewis, C. Pica, and F. Sannino, “Light Asymmetric Dark Matter on the Lattice: SU(2) Technicolor with Two Fundamental Flavors,” *Phys.Rev.* **D85** (2012) 014504, [arXiv:1109.3513](#) [hep-ph].
- [76] M. Frigerio, A. Pomarol, F. Riva, and A. Urbano, “Composite Scalar Dark Matter,” *JHEP* **07** (2012) 015, [arXiv:1204.2808](#) [hep-ph].
- [77] S. Bhattacharya, B. Melić, and J. Wudka, “Pionic Dark Matter,” *JHEP* **02** (2014) 115, [arXiv:1307.2647](#) [hep-ph].
- [78] A. Hietanen, R. Lewis, C. Pica, and F. Sannino, “Fundamental Composite Higgs Dynamics on the Lattice: SU(2) with Two Flavors,” *JHEP* **07** (2014) 116, [arXiv:1404.2794](#) [hep-lat].
- [79] D. Marzocca and A. Urbano, “Composite Dark Matter and LHC Interplay,” *JHEP* **07** (2014) 107, [arXiv:1404.7419](#) [hep-ph].
- [80] R. Pasechnik, V. Beylin, V. Kuksa, and G. Vereshkov, “Composite scalar Dark Matter from vector-like SU(2) confinement,” *Int. J. Mod. Phys.* **A31** (2016) no. 08, 1650036, [arXiv:1407.2392](#) [hep-ph].

- [81] O. Antipin, M. Redi, and A. Strumia, “Dynamical generation of the weak and Dark Matter scales from strong interactions,” *JHEP* **01** (2015) 157, [arXiv:1410.1817 \[hep-ph\]](#).
- [82] Y. Hochberg, E. Kuflik, H. Murayama, T. Volansky, and J. G. Wacker, “Model for Thermal Relic Dark Matter of Strongly Interacting Massive Particles,” *Phys. Rev. Lett.* **115** (2015) no. 2, 021301, [arXiv:1411.3727 \[hep-ph\]](#).
- [83] A. Carmona and M. Chala, “Composite Dark Sectors,” *JHEP* **06** (2015) 105, [arXiv:1504.00332 \[hep-ph\]](#).
- [84] S. Bruggisser, F. Riva, and A. Urbano, “Strongly Interacting Light Dark Matter,” *SciPost Phys.* **3** (2017) no. 3, 017, [arXiv:1607.02474 \[hep-ph\]](#).
- [85] Y. Wu, T. Ma, B. Zhang, and G. Cacciapaglia, “Composite Dark Matter and Higgs,” *JHEP* **11** (2017) 058, [arXiv:1703.06903 \[hep-ph\]](#).
- [86] H. Davoudiasl, P. P. Giardino, E. T. Neil, and E. Rinaldi, “Unified Scenario for Composite Right-Handed Neutrinos and Dark Matter,” *Phys. Rev.* **D96** (2017) no. 11, 115003, [arXiv:1709.01082 \[hep-ph\]](#).
- [87] A. Berlin, N. Blinov, S. Gori, P. Schuster, and N. Toro, “Cosmology and Accelerator Tests of Strongly Interacting Dark Matter,” *Phys. Rev.* **D97** (2018) no. 5, 055033, [arXiv:1801.05805 \[hep-ph\]](#).
- [88] D. S. Alves, S. R. Behbahani, P. Schuster, and J. G. Wacker, “Composite Inelastic Dark Matter,” *Phys.Lett.* **B692** (2010) 323–326, [arXiv:0903.3945 \[hep-ph\]](#).
- [89] M. Lisanti and J. G. Wacker, “Parity Violation in Composite Inelastic Dark Matter Models,” *Phys. Rev.* **D82** (2010) 055023, [arXiv:0911.4483 \[hep-ph\]](#).
- [90] D. Spier Moreira Alves, S. R. Behbahani, P. Schuster, and J. G. Wacker, “The Cosmology of Composite Inelastic Dark Matter,” *JHEP* **1006** (2010) 113, [arXiv:1003.4729 \[hep-ph\]](#).
- [91] S. B. Gudnason, C. Kouvaris, and F. Sannino, “Dark Matter from new Technicolor Theories,” *Phys. Rev.* **D74** (2006) 095008, [arXiv:hep-ph/0608055 \[hep-ph\]](#).
- [92] D. D. Dietrich and F. Sannino, “Conformal window of SU(N) gauge theories with fermions in higher dimensional representations,” *Phys. Rev.* **D75** (2007) 085018, [arXiv:hep-ph/0611341 \[hep-ph\]](#).
- [93] R. Foadi, M. T. Frandsen, and F. Sannino, “Technicolor Dark Matter,” *Phys. Rev.* **D80** (2009) 037702, [arXiv:0812.3406 \[hep-ph\]](#).

- [94] J. Mardon, Y. Nomura, and J. Thaler, “Cosmic Signals from the Hidden Sector,” *Phys. Rev.* **D80** (2009) 035013, [arXiv:0905.3749 \[hep-ph\]](#).
- [95] F. Sannino, “Conformal Dynamics for TeV Physics and Cosmology,” *Acta Phys. Polon.* **B40** (2009) 3533–3743, [arXiv:0911.0931 \[hep-ph\]](#).
- [96] R. Barbieri, S. Rychkov, and R. Torre, “Signals of composite electroweak-neutral Dark Matter: LHC/Direct Detection interplay,” *Phys. Lett.* **B688** (2010) 212–215, [arXiv:1001.3149 \[hep-ph\]](#).
- [97] A. Belyaev, M. T. Frandsen, S. Sarkar, and F. Sannino, “Mixed dark matter from technicolor,” *Phys. Rev.* **D83** (2011) 015007, [arXiv:1007.4839 \[hep-ph\]](#).
- [98] **Lattice Strong Dynamics (LSD) Collaboration** Collaboration, T. Appelquist *et al.*, “Lattice calculation of composite dark matter form factors,” *Phys.Rev.* **D88** (2013) no. 1, 014502, [arXiv:1301.1693 \[hep-ph\]](#).
- [99] A. Hietanen, R. Lewis, C. Pica, and F. Sannino, “Composite Goldstone Dark Matter: Experimental Predictions from the Lattice,” [arXiv:1308.4130 \[hep-ph\]](#).
- [100] J. M. Cline, Z. Liu, G. Moore, and W. Xue, “Composite strongly interacting dark matter,” *Phys. Rev.* **D90** (2014) no. 1, 015023, [arXiv:1312.3325 \[hep-ph\]](#).
- [101] **Lattice Strong Dynamics (LSD) Collaboration** Collaboration, T. Appelquist *et al.*, “Composite bosonic baryon dark matter on the lattice: SU(4) baryon spectrum and the effective Higgs interaction,” *Phys.Rev.* **D89** (2014) no. 9, 094508, [arXiv:1402.6656 \[hep-lat\]](#).
- [102] G. Krnjaic and K. Sigurdson, “Big Bang Darkleosynthesis,” *Phys. Lett.* **B751** (2015) 464–468, [arXiv:1406.1171 \[hep-ph\]](#).
- [103] W. Detmold, M. McCullough, and A. Pochinsky, “Dark Nuclei I: Cosmology and Indirect Detection,” *Phys.Rev.* **D90** (2014) no. 11, 115013, [arXiv:1406.2276 \[hep-ph\]](#).
- [104] W. Detmold, M. McCullough, and A. Pochinsky, “Dark nuclei. II. Nuclear spectroscopy in two-color QCD,” *Phys.Rev.* **D90** (2014) no. 11, 114506, [arXiv:1406.4116 \[hep-lat\]](#).
- [105] M. Asano and R. Kitano, “Partially Composite Dark Matter,” *JHEP* **09** (2014) 171, [arXiv:1406.6374 \[hep-ph\]](#).

- [106] T. Appelquist *et al.*, “Stealth Dark Matter: Dark scalar baryons through the Higgs portal,” *Phys. Rev.* **D92** (2015) no. 7, 075030, [arXiv:1503.04203 \[hep-ph\]](#).
- [107] T. Appelquist *et al.*, “Detecting Stealth Dark Matter Directly through Electromagnetic Polarizability,” *Phys. Rev. Lett.* **115** (2015) no. 17, 171803, [arXiv:1503.04205 \[hep-ph\]](#).
- [108] V. Drach, A. Hietanen, C. Pica, J. Rantaharju, and F. Sannino, “Template Composite Dark Matter: $SU(2)$ gauge theory with 2 fundamental flavours,” *PoS LATTICE2015* (2016) 234, [arXiv:1511.04370 \[hep-lat\]](#).
- [109] R. T. Co, K. Harigaya, and Y. Nomura, “Chiral Dark Sector,” *Phys. Rev. Lett.* **118** (2017) no. 10, 101801, [arXiv:1610.03848 \[hep-ph\]](#).
- [110] K. R. Dienes, F. Huang, S. Su, and B. Thomas, “Dynamical Dark Matter from Strongly-Coupled Dark Sectors,” *Phys. Rev.* **D95** (2017) no. 4, 043526, [arXiv:1610.04112 \[hep-ph\]](#).
- [111] H. Ishida, S. Matsuzaki, and Y. Yamaguchi, “Bosonic-Seesaw Portal Dark Matter,” *PTEP* **2017** (2017) no. 10, 103B01, [arXiv:1610.07137 \[hep-ph\]](#).
- [112] A. Francis, R. J. Hudspith, R. Lewis, and S. Tulin, “Dark matter from one-flavor $SU(2)$ gauge theory,” *PoS LATTICE2016* (2016) 227, [arXiv:1610.10068 \[hep-lat\]](#).
- [113] S. J. Lonsdale, M. Schroor, and R. R. Volkas, “Asymmetric Dark Matter and the hadronic spectra of hidden QCD,” *Phys. Rev.* **D96** (2017) no. 5, 055027, [arXiv:1704.05213 \[hep-ph\]](#).
- [114] J. M. Berryman, A. de Gouvêa, K. J. Kelly, and Y. Zhang, “Dark Matter and Neutrino Mass from the Smallest Non-Abelian Chiral Dark Sector,” *Phys. Rev.* **D96** (2017) no. 7, 075010, [arXiv:1706.02722 \[hep-ph\]](#).
- [115] A. Mitridate, M. Redi, J. Smirnov, and A. Strumia, “Dark Matter as a weakly coupled Dark Baryon,” *JHEP* **10** (2017) 210, [arXiv:1707.05380 \[hep-ph\]](#).
- [116] A. Francis, R. J. Hudspith, R. Lewis, and S. Tulin, “Dark Matter from Strong Dynamics: The Minimal Theory of Dark Baryons,” [arXiv:1809.09117 \[hep-ph\]](#).
- [117] G. D. Kribs and E. T. Neil, “Review of strongly-coupled composite dark matter models and lattice simulations,” *Int. J. Mod. Phys.* **A31** (2016) no. 22, 1643004, [arXiv:1604.04627 \[hep-ph\]](#).

- [118] V. Beylin, M. Bezuglov, V. Kuksa, and N. Volchanskiy, “An analysis of a minimal vectorlike extension of the Standard Model,” *Adv. High Energy Phys.* **2017** (2017) 1765340, [arXiv:1611.06006 \[hep-ph\]](#).
- [119] G. Ecker, J. Gasser, A. Pich, and E. de Rafael, “The Role of Resonances in Chiral Perturbation Theory,” *Nucl. Phys.* **B321** (1989) 311–342.
- [120] G. D. Kribs, A. Martin, and T. Tong, “Effective Theories of Dark Mesons with Custodial Symmetry,” *JHEP* **08** (2019) 020, [arXiv:1809.10183 \[hep-ph\]](#).
- [121] J. F. Gunion and H. E. Haber, “The CP conserving two Higgs doublet model: The Approach to the decoupling limit,” *Phys. Rev.* **D67** (2003) 075019, [arXiv:hep-ph/0207010 \[hep-ph\]](#).
- [122] I. Brivio and M. Trott, “The Standard Model as an Effective Field Theory,” *Phys. Rept.* **793** (2019) 1–98, [arXiv:1706.08945 \[hep-ph\]](#).
- [123] B. Henning, X. Lu, T. Melia, and H. Murayama, “2, 84, 30, 993, 560, 15456, 11962, 261485, ...: Higher dimension operators in the SM EFT,” *JHEP* **08** (2017) 016, [arXiv:1512.03433 \[hep-ph\]](#). [Erratum: *JHEP*09,019(2019)].
- [124] C. B. Marinissen, R. Rahn, and W. J. Waalewijn, “..., 83106786, 114382724, 1509048322, 2343463290, 27410087742, ... Efficient Hilbert Series for Effective Theories,” [arXiv:2004.09521 \[hep-ph\]](#).
- [125] S. Weinberg, “Varieties of Baryon and Lepton Nonconservation,” *Phys. Rev.* **D22** (1980) 1694.
- [126] W. Buchmuller and D. Wyler, “Effective Lagrangian Analysis of New Interactions and Flavor Conservation,” *Nucl. Phys.* **B268** (1986) 621–653.
- [127] B. Grzadkowski, M. Iskrzynski, M. Misiak, and J. Rosiek, “Dimension-Six Terms in the Standard Model Lagrangian,” *JHEP* **10** (2010) 085, [arXiv:1008.4884 \[hep-ph\]](#).
- [128] G. F. Giudice, C. Grojean, A. Pomarol, and R. Rattazzi, “The Strongly-Interacting Light Higgs,” *JHEP* **06** (2007) 045, [arXiv:hep-ph/0703164 \[hep-ph\]](#).
- [129] J. Elias-Miró, C. Grojean, R. S. Gupta, and D. Marzocca, “Scaling and tuning of EW and Higgs observables,” *JHEP* **05** (2014) 019, [arXiv:1312.2928 \[hep-ph\]](#).
- [130] E. E. Jenkins and A. V. Manohar, “Algebraic Structure of Lepton and Quark Flavor Invariants and CP Violation,” *JHEP* **10** (2009) 094, [arXiv:0907.4763 \[hep-ph\]](#).

- [131] A. Hanany, E. E. Jenkins, A. V. Manohar, and G. Torri, “Hilbert Series for Flavor Invariants of the Standard Model,” *JHEP* **03** (2011) 096, [arXiv:1010.3161 \[hep-ph\]](#).
- [132] L. Lehman and A. Martin, “Hilbert Series for Constructing Lagrangians: expanding the phenomenologist’s toolbox,” *Phys. Rev.* **D91** (2015) 105014, [arXiv:1503.07537 \[hep-ph\]](#).
- [133] B. Henning, X. Lu, T. Melia, and H. Murayama, “Hilbert series and operator bases with derivatives in effective field theories,” *Commun. Math. Phys.* **347** (2016) no. 2, 363–388, [arXiv:1507.07240 \[hep-th\]](#).
- [134] B. Henning, X. Lu, T. Melia, and H. Murayama, “Operator bases, S -matrices, and their partition functions,” *JHEP* **10** (2017) 199, [arXiv:1706.08520 \[hep-th\]](#).
- [135] L. Lehman, “Extending the Standard Model Effective Field Theory with the Complete Set of Dimension-7 Operators,” *Phys. Rev.* **D90** (2014) no. 12, 125023, [arXiv:1410.4193 \[hep-ph\]](#).
- [136] L. Lehman and A. Martin, “Low-derivative operators of the Standard Model effective field theory via Hilbert series methods,” *JHEP* **02** (2016) 081, [arXiv:1510.00372 \[hep-ph\]](#).
- [137] R. Alonso, E. E. Jenkins, A. V. Manohar, and M. Trott, “Renormalization Group Evolution of the Standard Model Dimension Six Operators III: Gauge Coupling Dependence and Phenomenology,” *JHEP* **04** (2014) 159, [arXiv:1312.2014 \[hep-ph\]](#).
- [138] C. Hays, A. Martin, V. Sanz, and J. Setford, “On the impact of dimension-eight SMEFT operators on Higgs measurements,” *JHEP* **02** (2019) 123, [arXiv:1808.00442 \[hep-ph\]](#).
- [139] J. Elias-Miro, J. R. Espinosa, E. Masso, and A. Pomarol, “Higgs windows to new physics through $d=6$ operators: constraints and one-loop anomalous dimensions,” *JHEP* **11** (2013) 066, [arXiv:1308.1879 \[hep-ph\]](#).
- [140] B. Henning, X. Lu, and H. Murayama, “How to use the Standard Model effective field theory,” *JHEP* **01** (2016) 023, [arXiv:1412.1837 \[hep-ph\]](#).
- [141] R. Barbieri, A. Pomarol, R. Rattazzi, and A. Strumia, “Electroweak symmetry breaking after LEP-1 and LEP-2,” *Nucl. Phys.* **B703** (2004) 127–146, [arXiv:hep-ph/0405040 \[hep-ph\]](#).
- [142] J. D. Wells and Z. Zhang, “Effective theories of universal theories,” *JHEP* **01** (2016) 123, [arXiv:1510.08462 \[hep-ph\]](#).

- [143] J. D. Wells and Z. Zhang, “Renormalization group evolution of the universal theories EFT,” *JHEP* **06** (2016) 122, arXiv:1512.03056 [hep-ph].
- [144] G. D’Ambrosio, G. F. Giudice, G. Isidori, and A. Strumia, “Minimal flavor violation: An Effective field theory approach,” *Nucl. Phys.* **B645** (2002) 155–187, arXiv:hep-ph/0207036 [hep-ph].
- [145] P. Sikivie, L. Susskind, M. B. Voloshin, and V. I. Zakharov, “Isospin Breaking in Technicolor Models,” *Nucl. Phys.* **B173** (1980) 189–207.
- [146] C. T. Hill and E. H. Simmons, “Strong Dynamics and Electroweak Symmetry Breaking,” *Phys. Rept.* **381** (2003) 235–402, arXiv:hep-ph/0203079 [hep-ph]. [Erratum: *Phys. Rept.* 390,553(2004)].
- [147] H. Georgi and D. B. Kaplan, “Composite Higgs and Custodial SU(2),” *Phys. Lett.* **145B** (1984) 216–220.
- [148] M. J. Dugan, H. Georgi, and D. B. Kaplan, “Anatomy of a Composite Higgs Model,” *Nucl. Phys.* **B254** (1985) 299–326.
- [149] K. Agashe, R. Contino, and A. Pomarol, “The Minimal composite Higgs model,” *Nucl. Phys.* **B719** (2005) 165–187, arXiv:hep-ph/0412089 [hep-ph].
- [150] K. Agashe, R. Contino, L. Da Rold, and A. Pomarol, “A Custodial symmetry for $Zb\bar{b}$,” *Phys. Lett.* **B641** (2006) 62–66, arXiv:hep-ph/0605341 [hep-ph].
- [151] C. Csaki, J. Hubisz, G. D. Kribs, P. Meade, and J. Terning, “Big corrections from a little Higgs,” *Phys. Rev.* **D67** (2003) 115002, arXiv:hep-ph/0211124 [hep-ph].
- [152] J. L. Hewett, F. J. Petriello, and T. G. Rizzo, “Constraining the littlest Higgs,” *JHEP* **10** (2003) 062, arXiv:hep-ph/0211218 [hep-ph].
- [153] S. Chang, “A ‘Littlest Higgs’ model with custodial SU(2) symmetry,” *JHEP* **12** (2003) 057, arXiv:hep-ph/0306034 [hep-ph].
- [154] H.-C. Cheng and I. Low, “TeV symmetry and the little hierarchy problem,” *JHEP* **09** (2003) 051, arXiv:hep-ph/0308199 [hep-ph].
- [155] M.-C. Chen and S. Dawson, “One loop radiative corrections to the rho parameter in the littlest Higgs model,” *Phys. Rev.* **D70** (2004) 015003, arXiv:hep-ph/0311032 [hep-ph].
- [156] A. Delgado, M. Garcia-Pepin, B. Ostdiek, and M. Quiros, “Dark Matter from the Supersymmetric Custodial Triplet Model,” *Phys. Rev.* **D92** (2015) no. 1, 015011, arXiv:1504.02486 [hep-ph].

- [157] S.-M. Choi, H. M. Lee, Y. Mambrini, and M. Pierre, “Vector SIMP dark matter with approximate custodial symmetry,” *JHEP* **07** (2019) 049, [arXiv:1904.04109 \[hep-ph\]](#).
- [158] M. J. G. Veltman, “Limit on Mass Differences in the Weinberg Model,” *Nucl. Phys.* **B123** (1977) 89–99.
- [159] M. E. Peskin and T. Takeuchi, “Estimation of oblique electroweak corrections,” *Phys.Rev.* **D46** (1992) 381–409.
- [160] C. Grojean, W. Skiba, and J. Terning, “Disguising the oblique parameters,” *Phys. Rev.* **D73** (2006) 075008, [arXiv:hep-ph/0602154 \[hep-ph\]](#).
- [161] M. Trott, “On the consistent use of Constructed Observables,” *JHEP* **02** (2015) 046, [arXiv:1409.7605 \[hep-ph\]](#).
- [162] G. D. Kribs, A. Martin, B. Ostdiek, and T. Tong, “Dark Mesons at the LHC,” *JHEP* **07** (2019) 133, [arXiv:1809.10184 \[hep-ph\]](#).
- [163] Y. Bai and A. Martin, “Topological Pions,” *Phys. Lett.* **B693** (2010) 292–295, [arXiv:1003.3006 \[hep-ph\]](#).
- [164] P. Duka, J. Gluza, and M. Zralek, “Quantization and renormalization of the manifest left-right symmetric model of electroweak interactions,” *Annals Phys.* **280** (2000) 336–408, [arXiv:hep-ph/9910279 \[hep-ph\]](#).
- [165] G. Buchalla, O. Cata, and C. Krause, “A Systematic Approach to the SILH Lagrangian,” *Nucl. Phys.* **B894** (2015) 602–620, [arXiv:1412.6356 \[hep-ph\]](#).
- [166] N. Craig, J. A. Evans, R. Gray, C. Kilic, M. Park, S. Somalwar, and S. Thomas, “Multi-Lepton Signals of Multiple Higgs Bosons,” *JHEP* **02** (2013) 033, [arXiv:1210.0559 \[hep-ph\]](#).
- [167] A. Djouadi, “The Anatomy of electro-weak symmetry breaking. II. The Higgs bosons in the minimal supersymmetric model,” *Phys. Rept.* **459** (2008) 1–241, [arXiv:hep-ph/0503173 \[hep-ph\]](#).
- [168] T. Das, G. S. Guralnik, V. S. Mathur, F. E. Low, and J. E. Young, “Electromagnetic mass difference of pions,” *Phys. Rev. Lett.* **18** (1967) 759–761.
- [169] C. G. Callan, Jr., S. R. Coleman, J. Wess, and B. Zumino, “Structure of phenomenological Lagrangians. 2.,” *Phys. Rev.* **177** (1969) 2247–2250.
- [170] M. Bando, T. Kugo, and K. Yamawaki, “Nonlinear Realization and Hidden Local Symmetries,” *Phys. Rept.* **164** (1988) 217–314.

- [171] R. S. Chivukula, N. D. Christensen, and E. H. Simmons, “Low-energy effective theory, unitarity, and non-decoupling behavior in a model with heavy Higgs-triplet fields,” *Phys. Rev.* **D77** (2008) 035001, [arXiv:0712.0546](#) [[hep-ph](#)].
- [172] J. Alexander *et al.*, “Dark Sectors 2016 Workshop: Community Report,” 8, 2016. [arXiv:1608.08632](#) [[hep-ph](#)].
- [173] L. Lee, C. Ohm, A. Soffer, and T.-T. Yu, “Collider Searches for Long-Lived Particles Beyond the Standard Model,” *Prog. Part. Nucl. Phys.* **106** (2019) 210–255, [arXiv:1810.12602](#) [[hep-ph](#)].
- [174] J. F. Gunion, H. E. Haber, G. L. Kane, and S. Dawson, “The Higgs Hunter’s Guide,” *Front. Phys.* **80** (2000) 1–404.
- [175] A. Alloul, N. D. Christensen, C. Degrande, C. Duhr, and B. Fuks, “FeynRules 2.0 - A complete toolbox for tree-level phenomenology,” *Comput. Phys. Commun.* **185** (2014) 2250–2300, [arXiv:1310.1921](#) [[hep-ph](#)].
- [176] J. Alwall, R. Frederix, S. Frixione, V. Hirschi, F. Maltoni, O. Mattelaer, H. S. Shao, T. Stelzer, P. Torrielli, and M. Zaro, “The automated computation of tree-level and next-to-leading order differential cross sections, and their matching to parton shower simulations,” *JHEP* **07** (2014) 079, [arXiv:1405.0301](#) [[hep-ph](#)].
- [177] T. Sjöstrand, S. Ask, J. R. Christiansen, R. Corke, N. Desai, P. Ilten, S. Mrenna, S. Prestel, C. O. Rasmussen, and P. Z. Skands, “An Introduction to PYTHIA 8.2,” *Comput. Phys. Commun.* **191** (2015) 159–177, [arXiv:1410.3012](#) [[hep-ph](#)].
- [178] **DELPHES 3** Collaboration, J. de Favereau, C. Delaere, P. Demin, A. Giammanco, V. Lemaître, A. Mertens, and M. Selvaggi, “DELPHES 3, A modular framework for fast simulation of a generic collider experiment,” *JHEP* **02** (2014) 057, [arXiv:1307.6346](#) [[hep-ex](#)].
- [179] M. Cacciari, G. P. Salam, and G. Soyez, “FastJet User Manual,” *Eur. Phys. J.* **C72** (2012) 1896, [arXiv:1111.6097](#) [[hep-ph](#)].
- [180] M. Cacciari, G. P. Salam, and G. Soyez, “The Anti-k(t) jet clustering algorithm,” *JHEP* **04** (2008) 063, [arXiv:0802.1189](#) [[hep-ph](#)].
- [181] **ATLAS** Collaboration, M. Aaboud *et al.*, “Search for new high-mass phenomena in the dilepton final state using 36 fb^{-1} of proton-proton collision data at $\sqrt{s} = 13 \text{ TeV}$ with the ATLAS detector,” *JHEP* **10** (2017) 182, [arXiv:1707.02424](#) [[hep-ex](#)].

- [182] **CMS** Collaboration, A. M. Sirunyan *et al.*, “Search for high-mass resonances in dilepton final states in proton-proton collisions at $\sqrt{s} = 13$ TeV,” [arXiv:1803.06292](https://arxiv.org/abs/1803.06292) [[hep-ex](#)].
- [183] **ATLAS** Collaboration, “Search for new high-mass phenomena in the dilepton final state using 36.1 fb^{-1} of proton-proton collision data at $\sqrt{s} = 13$ TeV with the ATLAS detector,” 2017.
<http://www.hepdata.net/record/ins1609250?version=1&table=Table6>.
- [184] **ALEPH, DELPHI, L3, OPAL, LEP Electroweak** Collaboration, S. Schael *et al.*, “Electroweak Measurements in Electron-Positron Collisions at W-Boson-Pair Energies at LEP,” *Phys. Rept.* **532** (2013) 119–244, [arXiv:1302.3415](https://arxiv.org/abs/1302.3415) [[hep-ex](#)].
- [185] **CDF** Collaboration, T. A. Aaltonen *et al.*, “Study of Top-Quark Production and Decays involving a Tau Lepton at CDF and Limits on a Charged-Higgs Boson Contribution,” *Phys. Rev.* **D89** (2014) no. 9, 091101, [arXiv:1402.6728](https://arxiv.org/abs/1402.6728) [[hep-ex](#)].
- [186] **ATLAS** Collaboration, G. Aad *et al.*, “Measurements of the top quark branching ratios into channels with leptons and quarks with the ATLAS detector,” *Phys. Rev.* **D92** (2015) no. 7, 072005, [arXiv:1506.05074](https://arxiv.org/abs/1506.05074) [[hep-ex](#)].
- [187] **D0** Collaboration, V. M. Abazov *et al.*, “An Improved determination of the width of the top quark,” *Phys. Rev.* **D85** (2012) 091104, [arXiv:1201.4156](https://arxiv.org/abs/1201.4156) [[hep-ex](#)].
- [188] **CMS** Collaboration, V. Khachatryan *et al.*, “Measurement of the ratio $\mathcal{B}(t \rightarrow Wb)/\mathcal{B}(t \rightarrow Wq)$ in pp collisions at $\sqrt{s} = 8$ TeV,” *Phys. Lett.* **B736** (2014) 33–57, [arXiv:1404.2292](https://arxiv.org/abs/1404.2292) [[hep-ex](#)].
- [189] **ATLAS** Collaboration, T. A. collaboration, “Search for charged Higgs bosons in the τ +jets final state using 14.7 fb^{-1} of pp collision data recorded at $\sqrt{s} = 13$ TeV with the ATLAS experiment,”.
- [190] **ATLAS** Collaboration, T. A. collaboration, “Search for charged Higgs bosons in the $H^\pm \rightarrow tb$ decay channel in pp collisions at $\sqrt{s} = 13$ TeV using the ATLAS detector,”.
- [191] **ATLAS** Collaboration, M. Aaboud *et al.*, “Search for additional heavy neutral Higgs and gauge bosons in the ditau final state produced in 36 fb^{-1} of pp collisions at $\sqrt{s} = 13$ TeV with the ATLAS detector,” *JHEP* **01** (2018) 055, [arXiv:1709.07242](https://arxiv.org/abs/1709.07242) [[hep-ex](#)].

- [192] Z. Liu and B. Tweedie, “The Fate of Long-Lived Superparticles with Hadronic Decays after LHC Run 1,” *JHEP* **06** (2015) 042, arXiv:1503.05923 [hep-ph].
- [193] J. A. Evans and J. Shelton, “Long-Lived Staus and Displaced Leptons at the LHC,” *JHEP* **04** (2016) 056, arXiv:1601.01326 [hep-ph].
- [194] D. Curtin *et al.*, “Long-Lived Particles at the Energy Frontier: The MATHUSLA Physics Case,” *Rept. Prog. Phys.* **82** (2019) no. 11, 116201, arXiv:1806.07396 [hep-ph].
- [195] J. Liu, Z. Liu, and L.-T. Wang, “Enhancing Long-Lived Particles Searches at the LHC with Precision Timing Information,” *Phys. Rev. Lett.* **122** (2019) no. 13, 131801, arXiv:1805.05957 [hep-ph].
- [196] R. Barbieri, B. Bellazzini, V. S. Rychkov, and A. Varagnolo, “The Higgs boson from an extended symmetry,” *Phys. Rev. D* **76** (2007) 115008, arXiv:0706.0432 [hep-ph].
- [197] **ATLAS** Collaboration, “Measurement of the tau lepton reconstruction and identification performance in the ATLAS experiment using pp collisions at $\sqrt{s} = 13$ TeV,”.
- [198] **ATLAS** Collaboration, G. Aad *et al.*, “Search for a CP-odd Higgs boson decaying to Zh in pp collisions at $\sqrt{s} = 8$ TeV with the ATLAS detector,” *Phys. Lett.* **B744** (2015) 163–183, arXiv:1502.04478 [hep-ex].
- [199] **ATLAS** Collaboration, G. Aad *et al.*, “A search for $t\bar{t}$ resonances using lepton-plus-jets events in proton-proton collisions at $\sqrt{s} = 8$ TeV with the ATLAS detector,” *JHEP* **08** (2015) 148, arXiv:1505.07018 [hep-ex].
- [200] **CMS** Collaboration, V. Khachatryan *et al.*, “Search for pair production of third-generation scalar leptoquarks and top squarks in proton–proton collisions at $\sqrt{s}=8$ TeV,” *Phys. Lett.* **B739** (2014) 229–249, arXiv:1408.0806 [hep-ex].
- [201] **ATLAS** Collaboration, M. Aaboud *et al.*, “Search for Supersymmetry in final states with missing transverse momentum and multiple b -jets in proton–proton collisions at $\sqrt{s} = 13$ TeV with the ATLAS detector,” arXiv:1711.01901 [hep-ex].
- [202] **CMS** Collaboration, V. Khachatryan *et al.*, “Search for heavy resonances decaying into a vector boson and a Higgs boson in final states with charged leptons, neutrinos, and b quarks,” *Submitted to: Phys. Lett. B* (2016) , arXiv:1610.08066 [hep-ex].

- [203] CMS Collaboration, A. M. Sirunyan *et al.*, “Search for Higgs boson pair production in events with two bottom quarks and two tau leptons in proton–proton collisions at $\sqrt{s} = 13\text{TeV}$,” *Phys. Lett.* **B778** (2018) 101–127, arXiv:1707.02909 [hep-ex].
- [204] CMS Collaboration, A. M. Sirunyan *et al.*, “Search for low mass vector resonances decaying into quark-antiquark pairs in proton-proton collisions at $\sqrt{s} = 13\text{ TeV}$,” *JHEP* **01** (2018) 097, arXiv:1710.00159 [hep-ex].
- [205] CMS Collaboration, V. Khachatryan *et al.*, “Search for single production of a heavy vector-like T quark decaying to a Higgs boson and a top quark with a lepton and jets in the final state,” *Phys. Lett.* **B771** (2017) 80–105, arXiv:1612.00999 [hep-ex].
- [206] E. E. Jenkins, A. V. Manohar, and M. Trott, “Renormalization Group Evolution of the Standard Model Dimension Six Operators I: Formalism and lambda Dependence,” *JHEP* **10** (2013) 087, arXiv:1308.2627 [hep-ph].
- [207] Y. Liao and X.-D. Ma, “Operators up to Dimension Seven in Standard Model Effective Field Theory Extended with Sterile Neutrinos,” *Phys. Rev.* **D96** (2017) no. 1, 015012, arXiv:1612.04527 [hep-ph].
- [208] C. Arzt, M. B. Einhorn, and J. Wudka, “Patterns of deviation from the standard model,” *Nucl. Phys.* **B433** (1995) 41–66, arXiv:hep-ph/9405214 [hep-ph].
- [209] M. B. Einhorn and J. Wudka, “The Bases of Effective Field Theories,” *Nucl. Phys.* **B876** (2013) 556–574, arXiv:1307.0478 [hep-ph].
- [210] N. Craig, M. Jiang, Y.-Y. Li, and D. Sutherland, “Loops and trees in generic EFTs,” arXiv:2001.00017 [hep-ph].
- [211] M. Jiang, N. Craig, Y.-Y. Li, and D. Sutherland, “Complete One-Loop Matching for a Singlet Scalar in the Standard Model EFT,” *JHEP* **02** (2019) 031, arXiv:1811.08878 [hep-ph].
- [212] J. Heeck, “Unbroken B – L symmetry,” *Phys. Lett.* **B739** (2014) 256–262, arXiv:1408.6845 [hep-ph].
- [213] The ALEPH, DELPHI, L3, OPAL, SLD Collaborations, the LEP Electroweak Working Group, the SLD Electroweak and Heavy Flavour Groups, “Precision Electroweak Measurements on the Z Resonance,” *Phys. Rept.* **427** (2006) 257, hep-ex/0509008.

- [214] The ALEPH, DELPHI, L3, OPAL Collaborations, the LEP Electroweak Working Group, “Electroweak Measurements in Electron-Positron Collisions at W-Boson-Pair Energies at LEP,” *Phys. Rept.* **532** (2013) 119, [arXiv:1302.3415 \[hep-ex\]](#).
- [215] U. Haisch, M. Ruhdorfer, E. Salvioni, E. Venturini, and A. Weiler, “Singlet night in Feynman-ville: one-loop matching of a real scalar,” *JHEP* **04** (2020) 164, [arXiv:2003.05936 \[hep-ph\]](#).
- [216] F. Nagel, *New aspects of gauge-boson couplings and the Higgs sector*. PhD thesis, Heidelberg U., 2004. <http://www.ub.uni-sbheidelberg.de/archiv/4803>.
- [217] M. Maniatis, A. von Manteuffel, O. Nachtmann, and F. Nagel, “Stability and symmetry breaking in the general two-Higgs-doublet model,” *Eur. Phys. J.* **C48** (2006) 805–823, [arXiv:hep-ph/0605184 \[hep-ph\]](#).
- [218] B. Grzadkowski, M. Maniatis, and J. Wudka, “The bilinear formalism and the custodial symmetry in the two-Higgs-doublet model,” *JHEP* **11** (2011) 030, [arXiv:1011.5228 \[hep-ph\]](#).
- [219] H. E. Haber and D. O’Neil, “Basis-independent methods for the two-Higgs-doublet model III: The CP-conserving limit, custodial symmetry, and the oblique parameters S, T, U,” *Phys. Rev.* **D83** (2011) 055017, [arXiv:1011.6188 \[hep-ph\]](#).
- [220] H. E. Haber and R. Hempfling, “The Renormalization group improved Higgs sector of the minimal supersymmetric model,” *Phys. Rev.* **D48** (1993) 4280–4309, [arXiv:hep-ph/9307201 \[hep-ph\]](#).
- [221] A. Pomarol and R. Vega, “Constraints on CP violation in the Higgs sector from the rho parameter,” *Nucl. Phys.* **B413** (1994) 3–15, [arXiv:hep-ph/9305272 \[hep-ph\]](#).
- [222] S. Scherer and H. W. Fearing, “Field transformations and the classical equation of motion in chiral perturbation theory,” *Phys. Rev.* **D52** (1995) 6445–6450, [arXiv:hep-ph/9408298 \[hep-ph\]](#).
- [223] N. Craig, C. Englert, and M. McCullough, “New Probe of Naturalness,” *Phys. Rev. Lett.* **111** (2013) no. 12, 121803, [arXiv:1305.5251 \[hep-ph\]](#).